Simulation and Design Platform for Fiber Optic Communication Systems

By

Galathara L.A.U.K.S. Kahanda

A dissertation submitted to the graduate faculty in Computer Science in partial fulfillment of the requirements for the degree of Doctor of Philosophy.
The City University of New York

2008

This manuscript has been read and accepted for the Graduate Faculty in Computer Science in satisfaction of the dissertation requirement for the degree Doctor of Philosophy.

Dr. Syed V. Ahamed

Date Mentor and Chair of the committee

Dr. T. Brown

Date Executive Officer, Department of Computer Science
Graduate Center, CUNY

Dr. M. Kress

Dr. A. Levine

Dr. M. Anshal

Dr. Victor B. Lawrence

Supervisory Committee

The City University of New York

Abstract

Simulation and Design Platform for Fiber Optic Communication Systems

By

Galathara. L. A. U. K.S. Kahanda

Advisor: Professor Syed V. Ahamed

Telecommunication has the greatest impact in our daily life than any other technology. For instance, cellular phones have become necessity of every age group. In order to provide efficient service to the public, scientists, working in Telecommunication industry, are continuously searching for new technologies. The worldwide demand for bandwidth seems to double every three years.

Only optical fiber can satisfy such information capacity requirements. In recent years, it has become apparent that fiber optics is steadily replacing copper wire as the standard means of signal transmission in telecommunication. They span the long distances between local phone systems providing the backbone for many network systems. Other system users include cable television services, university campuses, office buildings, industrial plants, and electric utility companies.

In this research, I explore the traditional glass fiber, as well as, the emerging plastic fiber as a potential competitor. Modified FS* Fiber simulation package is developed to cover all aspects of fiber optic communication systems. It includes software to simulate both wavelength division multiplexing (WDM) systems and optical time division multiplexing (OTDM) systems.

With the help of the modified FS* simulation model, one can observe the behavior of fiber optic systems with noisy light emitting diodes (LED). In addition, effects of leakage in erbium doped systems and variation of signal to noise ratio (SNR), with the pulse width, as well as, the fiber characteristics, can be observed. The modified FS* simulation model also contains separate routines not only to simulate the traditional glass fiber, but also to simulate the new plastic fiber.

Keywords: Telecommunication, bandwidth, fiber optics, backbone, WDM, OTDM, Modified FS* fiber simulation model, SNR

Acknowledgements

This is the last step of a long journey. Along the way, I was taught, directed, supported and inspired by my advisor and examination committee chair, Professor Syed V. Ahamed. I have been most fortunate to be exposed to and benefit from his scientific thinking and thoughtfulness and his vast knowledge in areas of Electrical Engineering as well as Computer Science.

I am grateful to Professor Mike Kress for encouraging and supporting me with the necessary guidance. I also wish to express my sincere gratitude to Professor Alfred Levine for his enthusiasm towards my research and his invaluable guidance for the accomplishment of this study enterprise. It was my pleasure and honor to have Professor Victor Lawrence, Dean, Department Electrical Engineering, Stevens Institute of Technology, NJ, as my external examiner. I greatly appreciate his helpful comments and comprehensive encouragement given.

It is my bounden duty to remind my late father and mother with a deep debt of gratitude for bringing me up and guiding me in the correct path with all the love and care needed and in fact, if not for that parental commitment I would not be able to achieve this goal.

I have to extend my gratitude to my brothers Srikantha, Mahendra and Dhammike and to my sisters Srimathie and Priyadarshani, as all of them stood by me to give a helping hand in all my needs and that gave me the necessary confidence to face the various challenges of life, up to the present day.

I must mention with gratitude an elder sister of mine who passed away in the prime of her life. I still remember how lovingly she had raised my level of aspiration with her encouraging words.

My wife Darshani's support and encouragement through out this difficult journey is appreciated. Last but not least my sincere thanks are due to my lovely daughter Sachini who spent most of her time doing homework accompanying me while I was on my way to College of Staten Island to work on this dissertation yet never complained about missing hugs and kisses.

Dedication

This dissertation is dedicated to my late parents Mr. **L.A.G Lekamge** and Ms. **Sisuma Samarakoone**, who happened to be my first teachers and taught me invaluable lessons in life and also to my lovely daughter **Sachini Kahanda**, the most precious gift I ever had in my life.

CONTENTS

List of Figures

List of Tables

Simulation and Design Platform for Fiber Optic Communication Systems

1. 1 Introduction

The implication of telecommunication into our daily lives has been arguably the most important and surprising development of the last 25 years. There are three basic types of information to be exchanged: voice, video and data. In the recent past there were separate branches of telecommunication: The telephone and the radio provided the voice delivery, TV delivered the images, and computers processed data. Before this revolution, telephone service and its place in our lives had been largely stable for more than a generation. The growth of the industry was very slow. The distinction between oversea and domestic calls blurred with the advance in switching and transmission, undersea cable, and communication satellites. Most of the traffic on the network remained voice, largely in analog format with facsimile (Fax) beginning to make inroads. A relatively small amount of data traffic was carried by modems operating at rates up to 9600 bits per second over voice connections. Multiplexing of signals was rudimentary; most connections were point-to-point business applications. The contrast of the past with today's network is overwhelming. The conversion from analog

to digital has long since been completed. A wide range of services, each with its unique set of traffic characteristics and performance requirements, are available. At the core of the change is becoming accepted to handle all telecommunication traffic and functions. What's more, today's computers provide multimedia services (combination of music, pictures, text and voice). Thus, today's telecommunications business is a complex industry that provides delivery of any type of information throughout the world.

In order for such a great change to occur many streams needed to be converged. At the most basic level was the explosive growth of the technology. The digital switching and processing are intrinsic to the modern network but are possible only through integrated-circuit technology. There are many examples of this technology at work. One striking example is the voice-band modem. At the beginning of the era, the rule of thumb for cost was a dollar per bit per second. Integrated technology and other factors, contributed to the several orders of magnitude increase in performance, with 56 kilobits per second is now routine with less expensive modems.

The second key technological development was optical fiber, which virtually provides the perfect transmission medium. Modern techniques used in the manufacture of semiconductors brought down the loss per kilometer

of a fiber to fractions of a decibel (dB). The development of fiber led to a quantum leap in transmission rates.

A significant contribution to the advance was made by software. At the beginning, the telephone network, oriented as it was toward voice traffic, was not helpful to data traffic. Impairments, which were no problem for voice, would severely deteriorate data signals. The response to these problems was packet switching, in which data are encapsulated into packets and passed through the networks in hops between intermediate points. Error can be controlled at each hop or end-to-end as appropriate to the error conditions. The user pays only for the amount of information transmitted, not for the duration.

Packet switching is at the core of the system that contributed to the telecommunication revolution, the ARPANET, which went into service in 1971. The design objective of ARPANET was to provide reliable communication suitable for traffic between computers, over an unreliable network. The TCP/IP (Transmission Control Protocol / Internet Protocol) protocols did the job effectively and are now the standard way of organizing information flow in the telecommunication network in spite of the fact that the telephone network has improved greatly in reliability.

Another important development at the beginning of the internet era was ALOHA, which was developed at the University of Hawaii with the objective of allowing a large number of low volume users to share a wireless data network among the Hawaiian Islands. The technique is packet-oriented and employs a dispersed system of traffic control called random access. ALOHA was the ancestor of the Ethernet, which is the standard for forming networks of computers in industry, government, university, and home settings. An Ethernet, perhaps including wireless access points, can link together all the appliances in your home and all the processors in your car.

There are important legal developments that played a part in the communication revolution. Previously, the telephone network was operated as a public utility. Innovations were rare since only few companies existed in the arena. The telephone administration had a monopoly on the equipment deployed. The system served society very well, but was slow to respond to the opportunities and demands of advancing technology. The 1971 "Carterfone" decision of the United States seems to have opened a new path for telecommunication industry. The decision was to allow non-telephone equipment to be connected to the network for only safety purposes. This was followed by antitrust action taken by the U.S. government dismantle

American Telephone and Telegraph Company into number of smaller companies.

Point to Point Systems vs. Networks

Figure 1.1 shows the general block diagram of a telecommunication system. Information in its original form, that is, voice, video or data, enters a transmitter. The transmitter converts it into a form suitable for transmission (such as an electrical signal), prepares the converted signal for transmission (in other words, it modulates and multiplexes it), and transmits the signal. The signal travels through a communication link, also called a transmission medium. This link can be a copper wire, coaxial cable, air, or an optical fiber. A receiver recognizes the signal, prepares it for conversion (by demodulating and demultiplexing) and converts the signal into its required form of information. Figure 1.1 depicts a typical *point-to-point telecommunication system*.

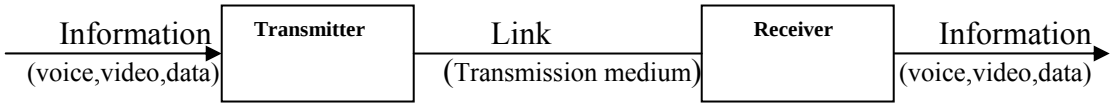

Fig. 1.1 Point-to-Point Telecommunication System

In fact, in any discussion of telecommunication, we bear in mind point-to-point telecommunication as the typical arrangement. But as soon as

three or more nodes become involved in the communication, we need to have a *network* to connect them. *A network is a combination of nodes connected by links*. Figure 1.2 shows different configurations or topologies for telecommunication networks.

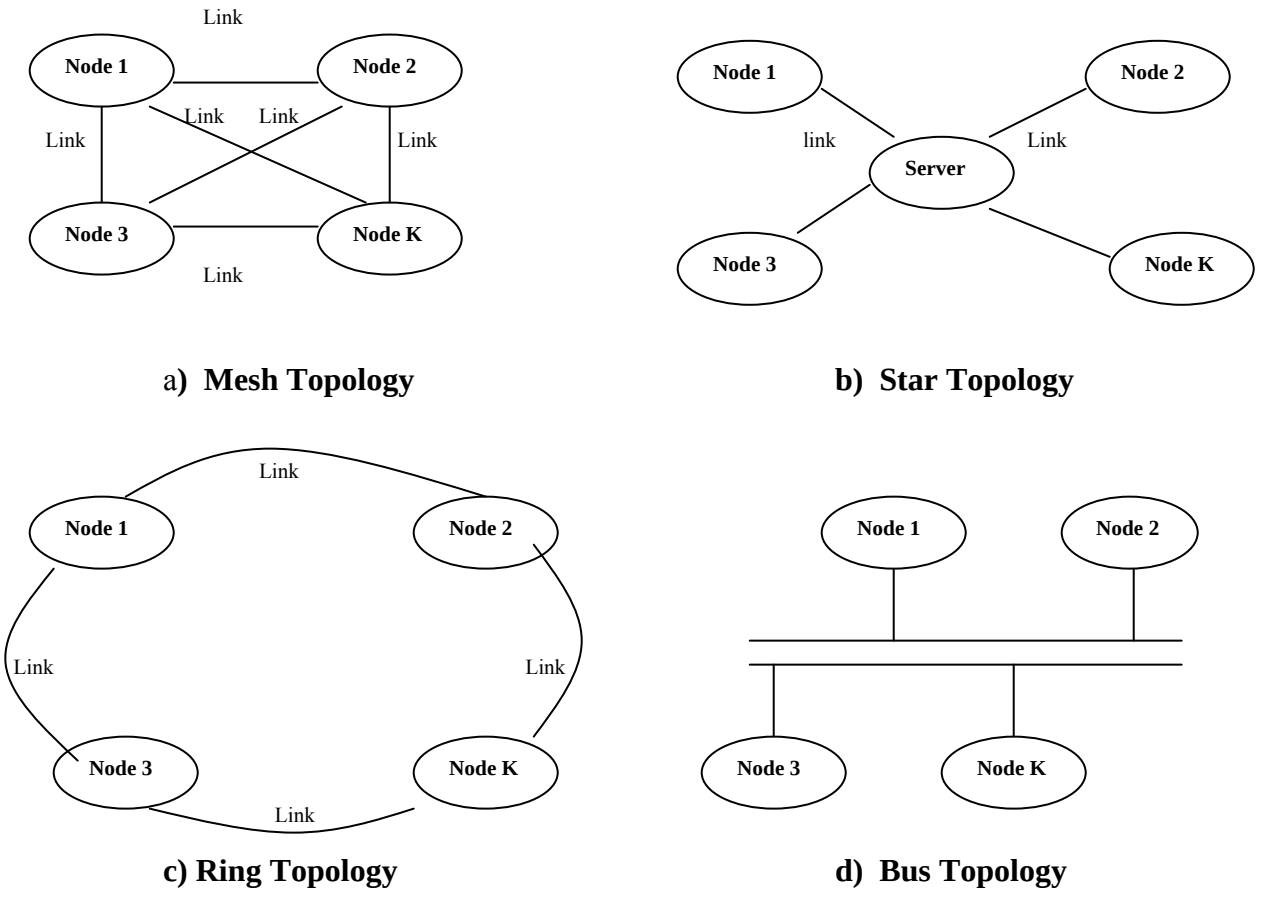

a) **Mesh Topology**

b) Star Topology

c) Ring Topology

d) Bus Topology

Fig. 1.2 Telecommunication Networks

1. 3 Information Carrying Capacity

Information carrying capacity is the ability of a communication link to transmit a certain amount of information per unit time. Demand for more capacity has increased since we produce more information and we transmit most of them in digital form.

It is well known that the developed countries have moved from the post-industrial era to the information era. These countries now produce more information than they do tangible products. The more information they produce, the greater the need for its delivery because information works only when it is delivered to the right place, at the right time and in the right form.

1.4 Analog VS. Digital Transmission

There are two basic forms of a signal: analog and digital. The analog signal carries information by means of the values of its amplitude, frequency or phase. Noise and other distortions change these values, resulting very often in misinterpretation of information. This is why analog technology is very error prone and requires great efforts to keep it working reliably. The digital signal carries information in bits, which can be either logical 1 or 0. Any distortion results in a signal amplitude change but doesn't alter the logical meaning of the signal. For example, a pulse with amplitudes between 2.0V and 3.3V means logical 1, while a pulse with amplitudes between 0

and 0.8V is still logical 0. However, if we use digital transmission, there is a price to pay. Digital transmission requires more channel capacity than that of analog transmission.

1.5 The Need for Fiber Optic Communication Systems

The major characteristic of a telecommunications system is unquestionably its information carrying capacity, but there are many other important characteristics. For instance, for a bank network, security is probably more important than capacity. For a brokerage firm, speed of transmission is the crucial feature of a network. In general, though, capacity is top priority for most system users. We cannot increase link capacity as much as we would like.

The major limit is shown by the **Shannon-Hartley theorem**:

$$\mathbf{C = BW \times \log_2 (1 + SNR)}$$

Where **C** is the information-carrying capacity (Bits/sec),

BW is the link bandwidth (Hz),

and **SNR** is the signal to noise power ratio.

The frequency of the signal carrier limits the channel bandwidth. The higher the carrier's frequency, the greater is the channel bandwidth and the higher is the information carrying capacity of the system.

A copper wire can carry a signal up to 1 MHz over a short distance. A coaxial cable can propagate a signal up to 100 MHz. Radio frequencies are in the range of 500 KHz to 100 MHz. Microwaves, including satellite channels, operate up to 100GHz. Fiber-optic communication systems use light as the signal carrier; light frequency is between 100 and 1000 THz. Therefore, one can expect much more capacity from optical systems.

To illustrate this point, consider these transmission media in terms of their capacity to carry, simultaneously, a specific number of one-way voice channels. A single coaxial cable can carry up to 13,000 channels (this value represents the order of the magnitude, not the exact value), a microwave terrestrial link can carry up to 20,000 channels and a satellite link can carry up to 100,000 channels. However, one fiber-optic communication link can carry 300,000 two-way voice channels simultaneously (ex: Transatlantic cable TAT-13). That's impressive and explains why fiber-optic communication systems form the backbone of modern telecommunication and will most certainly shape its future.

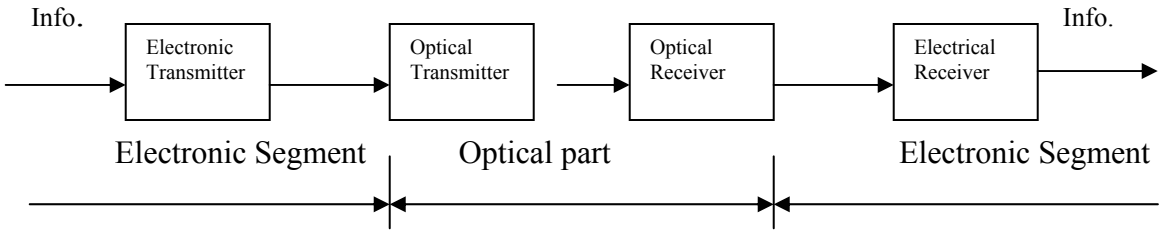

Fig 1.3 Basic Block Diagram of a present fiber-optic Communication link

Information to be conveyed using fiber optic communication system enters an electronic transmitter, where it is prepared for transmission very much in the conventional manner, that is, it is converted into electrical form, modulated and multiplexed. The signal then moves to the optical transmitter, where it is converted into optical form, and the resulting light signal is transmitted over optical fiber. At the receiver end, an optical detector converts the light back into an electrical signal, which is processed by the electronic receiver to extract the information and present it in a usable form (audio, video or data output**).**

The major function of a light source is to convert an information signal from its electrical form into light. Today fiber-optic communication systems use either light-emitting diodes (LEDs) or Laser diodes (LDs).

The transmission medium in fiber-optic communication systems is an optical fiber. The optical fiber is the transparent flexible filament that guides light from a transmitter to a receiver. Optical fiber carries signals in the form of light. The key component of an optical receiver is its photo-detector. The

major function of a photo-detector is to convert an optical information signal back into an electrical signal (photo current). Semiconductor photo- diode can be used as a photo-detector.

1.6 Optical Devices for Emerging Networks

The newest of networks blend communication and processing at the very seminal level. In the information processing environment, the five major components to consider are the processors, the memory, the input/output systems, the bus structures, and the switching devices. Conventional computing systems assume the availability of electronic power sources, detectors, and amplifiers.

1.7 The Role of Fiber-Optic Communication Technology

Fiber-optic communication technology has not already only changed the telecommunication arena, but it is still doing so. In fact, because of the telecommunication industry's increasing demand for capacity, in recent years, the bandwidth of commercial systems has increased more than a hundredfold. The potential information carrying capacity of a single fiber-optic channel is estimated at 50 Tbps. However, from a practical standpoint, commercial links have transmitted far fewer than 100 Gbps. Researchers and engineers are working continuously to develop new techniques that approach

the potential capacity limit. Two recent major technological advances, wavelength division multiplexing (WDM) and erbium-doped optical fiber amplifiers (EDFA), have boosted the capacity of the existing systems and have brought about dramatic improvements in the capacity of systems now in development. In fact, WDM is increasingly becoming the technology of choice in achieving smooth, manageable capacity expansion.

As pointed out previously, communication industry has deployed high-frequency signal carriers. The shift from radio frequency to microwaves (a thousand fold leap) allowed engineers to increase a given system's information carrying capacity at least ten times over.

This success inspired researchers to seek a solution to the problem of reliable communication by continuing to increase microwave frequency. But at a frequency of more than 100 GHz, where microwaves overlap the infrared zone, microwave attenuation in air reaches such a high level that transmission distance becomes unacceptably short.

The solution appeared to be clear, use a waveguide structure to transmit ultra high frequency (UHF) electromagnetic waves. These waveguides, in the form of steel tubes, rectangular in cross section with openings at each end, have now been in use for years in radar and other UHF

systems for delivering and distributing microwaves over very short distances.

In the late 1960s and early 1970s, scientists and engineers at Bell Laboratories achieved significant progress in designing waveguides for long distance systems. These waveguides offered a very impressive characteristic of 238,000 voice channels per unit. But the waveguides remained open-end steel tubes about several centimeters in inner diameter. However, the newer ones are now circular in cross section. They remained inefficient from cost, installation, maintenance, and other practical standpoints. Then, scientists and engineers changed their focus to increase the carrier frequency even higher than the highest microwave frequency. In other words, they decided to use the range of optical frequencies.

Once this decision was reached, the problem of how to guide the light arose. In reality, guiding light over a significant distance is a complicated problem. First, there's the matter of developing a practical waveguide that could carry light in a manner similar to the way copper wire conducts electrical current. This required developing a transmission medium which would be easy to install and maintain. This was, indeed, a complicated task since it had never before been done. In response, researchers, turned to optical fiber, a transparent, flexible filament made from glass or plastic.

Then, researchers faced another problem of figuring out how to carry light inside a bending fiber. This was an issue since light is a ray propagating along a straight line. A Dutch mathematics professor, Willebrod Van Roijen Snellius, who discovered Snell's law in 1621, provided the answer. According to Snell's law, light could travel inside a bending fiber using the phenomenon known as total *internal reflection*.

More than 200 years later, in 1870, British physicist, John Tyndall, demonstrated that light could be conducted in a curved stream of water. This was the first experiment that proved the existence of the phenomenon of total internal refection. Then, optical fiber became the light guide of choice.

However, soon another major drawback, called light attenuation, arose. This was a major turning point in the history of fiber-optic communications. It was then Charles Kao who delivered a landmark paper, "Dielectric Fiber surface waveguides for Optical Frequencies", which was considered the key to unlocking the door to the fiber optic technology as we know it today. He indicated that the major concern at the time was to reduce light attenuation. His own experiments resulted in an attenuation of more than 1000 dB/km, an unacceptably high loss under any circumstances. Such a loss level, if not significantly reduced, would make fiber optics technology

totally unusable. In fact, Kao said that the practical use of fiber optics for communications might start when attenuation would be less than 20 dB/km.

After more than 15 years of extensive work, manufacturers developed an incredibly low-loss optical fiber with attenuation of less than 0.3 dB/km. This meant that light would become weaker to about 0.933 for every kilometer it travels. Today, optical fiber with attenuation less than 0.16 dB/km are routinely available.

1.8 The Industry today and Future trends

Today, each time any communication link is activated, fiber optic communication technology gets deployed. Future trends will see this technology continue to penetrate all levels of telecommunications networks. The power of fiber optics not only meets the growing demand for information carrying capacity but also opens new avenues of future telecommunications possibilities. Today fiber optic technology defines access, transmission, signaling, switching, and networking technologies. In other words, it plays the key role in every aspect of modern telecommunication.

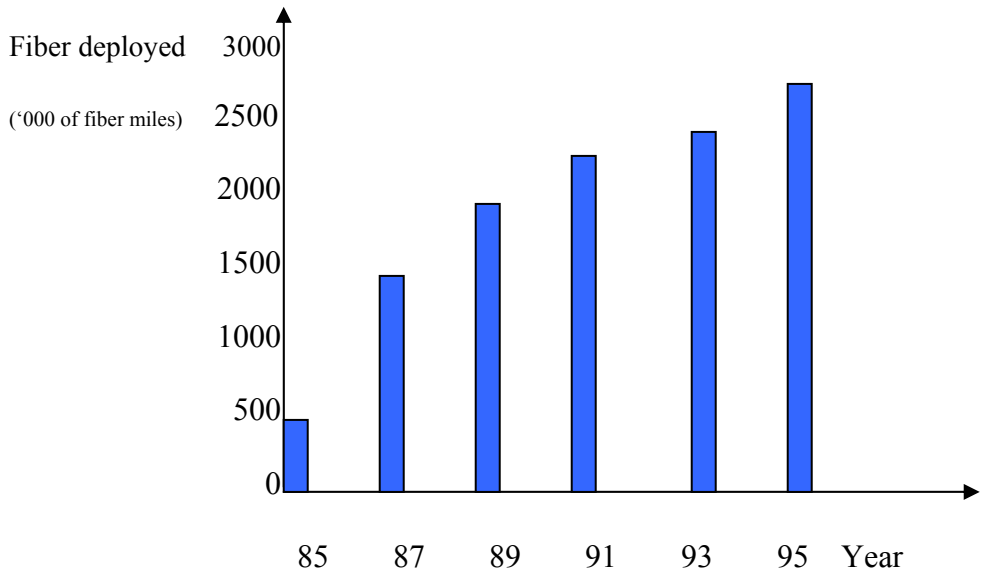

Fig. 1.4 Dynamics of deployment of telephone fiber-optic networks in USA.

Local telephone Networks

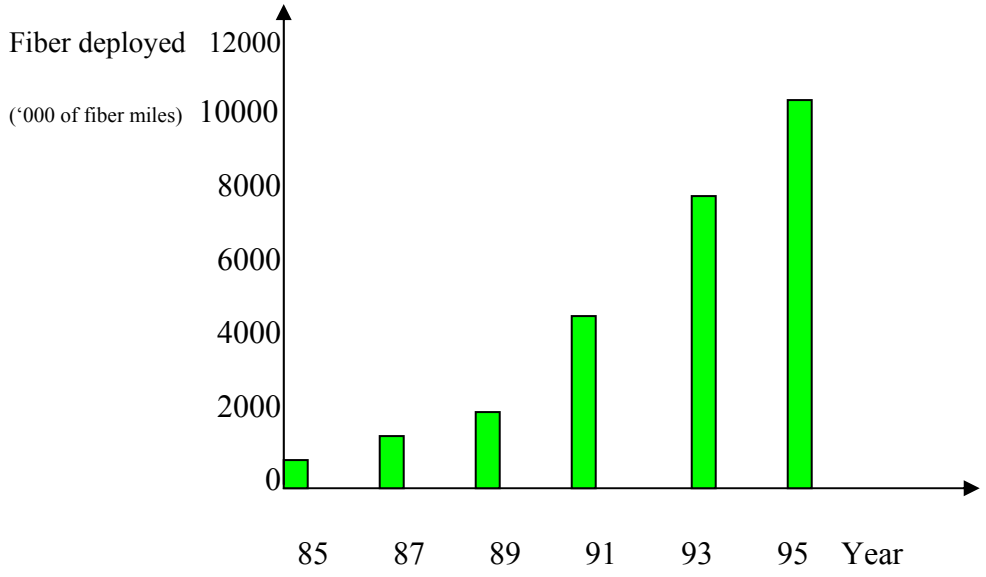

Fig. 1.5 Dynamics of deployment of telephone fiber-optic networks in USA.

Long distance telephone Networks

Figure 1.4 and 1.5 depict the statistics of fiber-optic communications networks deployed by local and long distance operating companies. We can see the exponential growth in fiber miles installed by telephone companies. The expansion is even more dynamic in the recent years.

1.9 Worldwide submarine networks

The first international undersea fiber-optic link, which linked England and Belgium, was laid on the floor of the North Sea in 1986. At the end of 1988, the first transatlantic fiber-optic cable was laid to connect the United States and Europe. This project, called TAT-8, was a mutual venture of AT&T, British Telecom, and France Telecom. The link runs 5600km from Tuckerton, New Jersey to the European shelf, where it divides into two branches. One branch travels more than 500 km to England and the other continues for more than 300 km to France.

The link used in the TAT-8 project can carry 80,000 voice channels. But this number just characterizes its information carrying capacity. The link uses a single mode fiber and operates at a wavelength of 1300 nm. Laser diodes with a mean lifetime of 10^6 hours provide the light source for the system.

To compensate signal attenuation, special devices called repeaters were installed every 50km along the cable. A repeater, also called a regenerator,

works with a digital signal. It analyzes the incoming signal, makes a decision as to whether the pulse represents logic 1 or 0, generates a new pulse based on that decision, and sends all of the pulses farther along the link. To do this job, a repeater has to convert an optical signal into an electrical signal. Then the electrical signal is processed and converts back to optical form to continue transmission over optical fiber. There is a drawback here. Optical fiber is a dielectric and consequently, it cannot directly carry an electric signal. Thus a separate conductor must be included in submarine cables to deliver electric power. The conductor in the TAT-8 project carries 1.6 amperes to feed electric power to the system's repeaters.

TAT-12 and TAT-13, which connect the United States and Europe, use the WDM technique to increase the information carrying capacity of the link. These links carry more than 300,000 voice channels, nearly four times more than the 80,000 voice channels processed by the TAT-8 link.

1.10 Satellite systems versus fiber-optic networks

The obvious question at this point is, why do we need a worldwide fiber optic network if we can reach practically any point on the globe using satellite communication systems? The answer lays in the two major advantages offered by fiber optics communication over satellite communication, namely, its higher information carrying capacity and its speed in transmitting the signal.

As for information carrying capacity, a single optical fiber has the potential to carry up to 50 Tb/s. There is no indication today that satellite communication technology will ever achieve such an information carrying capacity. Another disadvantage of satellite communication is the signal delay caused by the long distance that a signal has to travel from earth station to satellite and back. Fiber optics provide much more straight and shorter connections between transmitters and receivers, virtually eliminating this problem. The major drawback to satellite communication is its susceptibility to adverse atmospheric conditions.

On the other hand, satellite communication has the ability to reach nearly any point on the globe without wiring. The Iridium Project, based on a number of low-orbiting satellites, spans the entire globe, giving everyone a global wireless connection. It is highly unlikely that either one of these

technologies will eliminate the other. A more likely scenario is that satellite communication and fiber-optic technology will prove to be complementary rather than competitive players in the telecommunication industry.

1.11 Fiber to the Home and Fiber to the Desk

For local telephone networks, this means that all connections between central offices and all connections from remote terminals to central offices use optical-fiber cables. The only connections in place today using copper wire as a transmission medium are links between the customer premises and the nearest remote terminal. This "last mile" is the bottle neck in the modern telecommunications network only because there is no way to replace about a billion twisted wire pair connections of copper cable overnight with optical fiber all around the world. To get some idea of the gravity of this subscriber-line problem, it is suffice to say that in the United States, alone, there are more than 250 million lines that would have to be replaced.

Two trends rapidly developing in the United States relate to optical-fiber networking. One push is to use WDM, putting several signals that differ in wavelength into one fiber for more efficient use of the existing optical fiber networks. The other key trend is that nontraditional telecommunication companies enter into the arena. Today, besides the many telephone companies, a number of other telecommunication providers are on

the scene. Among them are cable TV companies, which use their fiber-optic networks to enter the business of telephone and computer connection services.

From intercontinental transmission lines to intra-device connections, we can see fiber optics in play. For example, we can find fiber-optic links inside a modern signaling machine SS7. The utility and gas-pipe line industries already are customers of fiber optics. Furthermore, automotive and avionics industries are expanding their use of fiber optics for communication.

1.12 Different Multiplexing Techniques for increasing the bandwidth

Fiber optics has become the core of our telecommunications and data networking infrastructure. Optical fiber is the preferred means of transmission for any data over a few tens of megabits per second and over anything from a kilometer and upwards. The first generation of fiber optic networks used optical fiber as a replacement for copper cable for transmission at higher bit rates over long distances. The second generation of fiber optic networks is just emerging.

These networks really exploit the capacity of fiber to achieve overall transmission capacities of several tens of gigabits per second to terabits per second. Moreover, they exploit routing and switching of signals in the

optical domain. The rapid evolution of technology, coupled with the ever growing demand for bandwidth, is resulting in a rapid transition of these networks from research laboratories into the marketplace.

The increasing demand for bandwidth, along with the fact that it is relatively expensive in many cases to lay new fiber miles, forces us to find ways to increase the capacity on existing fiber. There are fundamentally two ways of increasing the transmission capacity on a fiber. The first way is to increase the bit rate using OTDM. Many lower-speed data streams are multiplexed into a higher-speed stream at the transmission bit rate by means of Optical Time Division Multiplexing (OTDM). The OTDM approach requires the bit rate on the fiber to be increased to 10 Gb/s or beyond. The two major system impairments that these systems face are chromatic dispersion and polarization mode dispersion (PMD). Chromatic dispersion is not a problem if the link uses dispersion-shift fibers. With standard, single mode fiber, the chromatic dispersion limit is about 60 km at 10 Gb/s and about 1000 km at 2.5 Gb/s. With practical transmitters, the distances are even smaller. The 10 Gb/s limit can be further reduced in the presence of self-phase modulation. Beyond these distances, the signal must be electronically regenerated, or some form of chromatic dispersion compensation must be employed. Eventually, OTDM is limited by the

speeds that can be achieved by electronics. About 90% of the installed fiber in the United States and Europe are standard single-mode fiber. Japan has installed a significant amount of dispersion-shifted fiber. OTDM is a competitive approach for short to medium links or for links operating over dispersion shifted fiber. The other factor that may influence network operators' decision to deploy OTDM is the fact that its approach needs to be compatible with the standard network management techniques. 10 Gb/s OTDM systems are becoming commercially available from a number of vendors today and there is ongoing research to develop 20 Gb/s and 40 Gb/s OTDM systems.

The other way to increase transmission capacity is to use a technique called Wavelength Division Multiplexing (WDM). WDM is essentially the same as frequency division multiplexing, which has been used in radio systems for more than a century. The idea is to transmit data simultaneously at multiple carrier wavelengths (or equivalently, frequencies) over a fiber. WDM transmission systems, employing up to 32 wavelengths at 2.5 Gb/s, each over a single fiber, are commercially available today, and systems with fewer wavelengths at 10 Gb/s are becoming available. WDM provides a way to increase the transmission capacity by using multiple channels at different wavelengths.

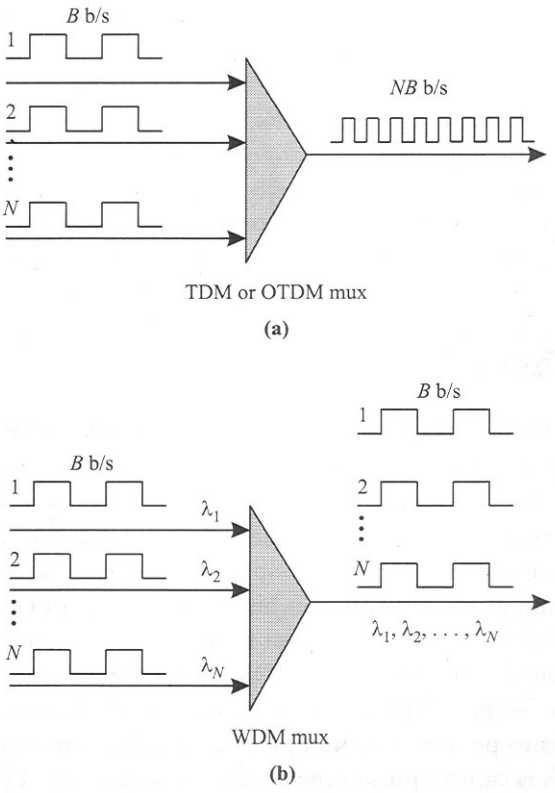

Fig 1.6 Different Multiplexing Techniques for increasing the transmission capacity on an optical fiber. **(a)** Electronic or Optical time division multiplexing. **(b)** Wavelength division multiplexing.

Both multiplexing techniques take in N data streams, each of B b/s and multiplex them into a single fiber with a total aggregate rate of NB b/s.

The WDM approach is to keep the bit rate the same, say 2.5 Gb/s, and add more wavelengths, each carrying data at this bit rate.

The advantages of WDM over OTDM are the following:

1. Because of the lower bit rates, the distance limit due to chromatic dispersion is much larger for WDM systems than for equivalent OTDM systems. Likewise polarization mode dispersion (PMD) does not impose a significant distance limitation at bit rates of 2.5 Gb/s or lower in most links.
2. The transmission capacity can be increased in a modular manner by adding additional wavelengths when capacity increases are required, as opposed to a large up-front installation in the case of OTDM. For example, in a four channel WDM system, the capacity can be modularly increased from 2.5 Gb/s all the way to 10 Gb/s in steps of 2.5 Gb/s. On the other hand, a 10 Gb/s OTDM system must be installed at once and may not be as modular.
3. WDM systems can be designed to be transparent systems. This follows the idea of using different wavelengths to carry data at different bit rates and protocol formats. This can be a major advantage in some cases.

4. WDM system may be preferred to OTDM system in designing more complicated networks. For example, if there is a network node at which most of the traffic is to be passed through and a small fraction is to be dropped and added, it may be more cost effective to use a WDM optical add/drop element than a full-blown set of OTDM terminals (or WDM terminals).

On the other hand, WDM does suffer some disadvantages as well relative to OTDM. Four such disadvantages are:

1. WDM systems are generally not suitable for deployment over dispersion-shifted fiber because of the limitation imposed by four wave mixing.
2. WDM systems require specially designed optical amplifiers that provide flat gain profiles. Moreover, their gain must be independent of the number of wavelengths in the system so as to make upgrades easy and, more importantly, to prevent a failure in one channel from causing an outage in another channel.
3. WDM systems require separate terminating equipments for each channel, including an expensive laser and a receiver. An OTDM system, on the other hand, requires one piece of terminating equipment.

However, this equipment must include the electronics necessary to multiplex and demultiplex the lower speed streams.

4. Transparent WDM systems offer less monitoring and network management capability than OTDM systems because they are unaware of the actual format and data rate on the individual channels. Thus, they cannot monitor parameters, such as, the bit error rate (BER) or frame errors in the data. Of course, the other equipment, attached to the WDM equipment, which actually terminates the data, can perform all these functions. However, this makes fault isolation somewhat tricky. In some cases, it may be difficult to determine whether a fault is in the WDM equipment or in the attached equipment.

2.0 The Fiber Optic Revolution and Information Highways

In the information age, we are seeing a growing demand for networks of higher capacities at lower costs. This demand is caused by many different factors. The tremendous growth of the Internet and the World Wide Web has brought more and more users online, consuming large amounts of bandwidth due to data transfers involving video images. Moreover, a telephone call from a user logging into Internet lasts much longer than a voice call, resulting in a significant increase in the load that the telephone network must support.

At the same time, businesses are relying increasingly on intranets and extranets, essentially, high-speed networks, for their day-to-day operations. Furthermore, the ultimate vision of the information age is that information can be located anywhere but is accessible from everywhere as if it were located locally. Networks of enormous capacity will be required to provide the infrastructure to realize this vision. All these factors are driving the need for more bandwidth in networks as well as new network services.

To fulfill the demand for bandwidth and to deploy new services, network operators must deploy new technologies. Optical networking is one such key technology. New technologies invariably result in reducing the cost of bandwidth. This reduced cost of bandwidth in turn spurs the development

of a new set of applications that make use of more and more bandwidth, which in turn drives the need for more bandwidth in the network. This positive feedback cycle shows no sign of abating in the near future.

As we are witnessing this tremendous growth in network traffic and the demand for new services, the world's telecommunications markets are being deregulated. Large telephone monopolies, that in the past could take their time to plan network upgrades, are now faced with increasing competition in local as well as long-distance services. The new entrants into this arena are actively building new networks. The old players must rapidly incorporate new technology in their networks to maintain a competitive edge. Competitive pressures are likely to result in a significant reduction in the price of bandwidth to end-users and will, at the same time, force network operators to run their networks more efficiently. All this is driving the development of high capacity optical networks and their remarkably rapid transition from the research laboratories into commercial deployment.

The impact of fiber optic systems to carry voice and data, entering the telephone plant, is akin to the impact of digital carrier systems in the early 1960s. The survey of the fiber optic systems over the last decade reveals that the systems are experiencing about two orders of magnitude enhancement in the ratio of component costs to system performance every

five years. Three typical landmarks of achievement are (a) the 45 Mbps (0.82 μm) fiber optic system in 1982 (b) the 1.7 Gbps (1.3 or 1.5μm) fiber optic system in mid 1988, and then (c) the 10 Gbps transoceanic fiber optic segment in 1994/5.

There are two major areas of the impact of both these digital systems; the trunk systems and the subscriber systems. Earlier digital carriers (T1/E1, T1C, T2/E2, etc) are now deeply entrenched in most telephone systems around the world and have literally brought the digital revolution closer to the routine telephone users: first, via the trunks and long distance, PCM (64 kbps) digitally encoded telephone voice service and second, via the subscriber loop plants and the PCM (64 kbps), the ADPCM (32 kbps) and the ADM (37.6 kbps, via the SLC-40 system) digitally encoded telephone services to the remote areas of countries.

In the wideband and broadband arenas, the impact is equally profound from inexpensive, crystal clear, and bandwidth-intensive multimedia services to every integrated digital remote terminal with optical carrier capacity. Fiber has already made deep inroads in the trunk systems. Most of the modern trunks are digital and fiber based. Fiber-switch interface is almost as prevalent as the D-channels banks of the 1970s. The rate of data transfers is much higher now and is therefore, more dependable. In fact, it is

uneconomical to think of the older copper based analog carrier systems in the 2000s. In fact, it is unrealistic to think of the plain old copper digital carrier systems for the newer networks. Digital copper systems still have a tiny niche in the modernization of services and/or maximization of the utility of the copper already installed in place.

Fiber, for the distribution of data, is used via the hybrid subscriber loop plants using the modern subscriber loop carriers (e.g., fiber optic SLC-96 or SLC-2000). It has the impact of bringing the information revolution to end users via wideband multimedia services. Multiplexed visual/picture and video information was carried at hundreds of megabits per second (at OC-N rates) in the 1990s rather than multiplexed voice information that digital carriers carried at a few megabits per second (at T1/E1, T1C and T2/E2) systems carried in the 1960s and 1970s. Whereas the plain old copper (transmission and D-channel) based carrier systems brought in digital revolution to the telephone plant, the fiber optic (transmission and DCS switches) based facilities is bringing the information revolution to the customers.

3.0 Basic Concepts in Fiber Optic Transmission Systems

As discussed before, optical Fiber is a remarkable communication medium compared to other media such as copper or free space. An optical fiber provides low-loss transmission over an enormous frequency range of about 25 THz, which is an order of magnitude higher than the bandwidth available in copper cables or any other transmission medium.

3.1 Light propagation in Optical Fiber

An optical fiber consists of a cylindrical ***core*** surrounded by a ***cladding***. The cross section of an optical fiber is shown in figure 3.1.

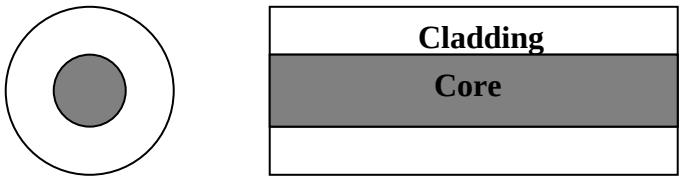

Fig 3.1 The Cross Section of an Optical Fiber

Both the core and the cladding are made primarily of silica (SiO_2), which has a refractive index of approximately 1.45. During the manufacturing of the fiber, certain impurities (or dopants) are introduced into the core and/or the cladding, so that the refractive index of the core is slightly higher than that of the cladding.

We can obtain a simplified understanding of light propagation in optical fiber using the geometrical optics approach (ray theory). This

approach is valid when the fiber used, having core radius a, is much larger than the operating wavelength λ. Such fibers are termed multimode, and first generation optical communication links were built using such fibers with the radius a in the range of 25-100 μm and λ around 0.85 μm.

In the geometrical optics approach, light can be thought of as consisted of a number of rays, propagating in straight lines within a material (or medium), and getting reflected and/or refracted at the interfaces between two materials. Figure 3.2 shows the interface between two media of refractive index n_1 and n_2. A light ray from medium 1 is incident on the interface of medium 1 with medium 2. The angle of incidence is the angle between the incident ray and the normal to the interface between two media, and is denoted by θ_1. Part of the energy is reflected into medium 1 as a *reflected ray*, and the remainder passes into medium 2 as a *refracted ray*. The angle of reflection θ_{1r} is the angle between the reflected ray and the normal to the interface. Similarly, the angle of refraction, θ_2, is the angle between the refracted ray and the normal.

The laws of geometrical optics states that:

$\theta_{1r} = \theta_1$ (for total internal reflection)

and

$n_1 \sin \theta_1 = n_2 \sin \theta_2$. (This equation is known as **Snell's law**)

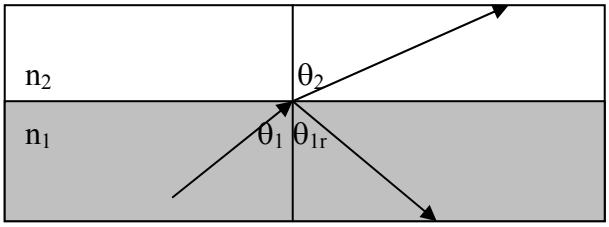

Fig 3.2. Reflection and Refraction of light rays at the interface between two media.

As the angle of incidence θ_1 increases, the angle of reflection θ_2 also increases. If $n_1 > n_2$ there comes a time when $\theta_2 = \Pi/2$ radians. This happens when $\theta_1 = \sin^{-1}(n_2/n_1)$. For larger values of θ_1, there is no refracted ray and all the energy from the incident ray is reflected. This phenomenon is called *total internal reflection*. The smallest angle of incidence, for which we get total internal reflection, is called the *critical angle* and equals $\sin^{-1}(n_2 / n_1)$.

Simply stated, from the geometrical viewpoint, light propagates in optical fiber due to a series of total internal reflections that occur at the core-cladding interface. This is depicted in figure 3.3. In this figure, coupling of light, from medium outside (taken to be air with refractive index n_0) into the fiber, is also shown. It can be shown, using Snell's law, that only those light rays that are incident at an angle

$\theta_0 < \theta_0^{max} = \sin^{-1}\sqrt{(n_1^2 - n_2^2)}/n_0$, at the air-core interface, will undergo total internal reflection at the core-cladding interface and will thus

propagate. Such rays are called guided rays. This quantity $\mathbf{n_0 \sin\theta_0^{max}}$ is a measure of the light gathering capacity of the fiber and is called the numerical aperture (NA).

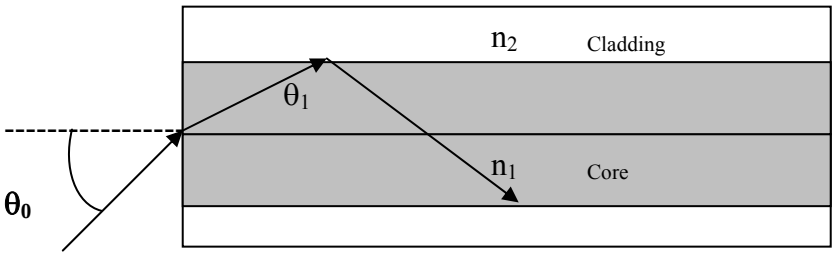

Fig 3.3. Propagation of light rays in Optical fiber by total internal reflection

3.2 Optical Properties

3.2.1 Attenuation

The loss of optical energy that a light pulse experiences as it travels down the fiber is called attenuation. Three causes for the loss of energy are scattering, absorption, and bending.

3.2.2 Scattering

In the early fabrication of fibers (mid-sixties to early seventies), impurities was the major reason for high attenuation of the optical signal. Suppose there is an imperfection in a core material, as shown in figure 3.4. A beam propagating at the critical angle or less will change direction after it meets the obstacle. In other words, light will scatter. This scattering effect

prevents attainments of total internal reflection at the core-cladding boundary, resulting in a power loss since some light will pass out of the core. This is the basic mechanism underlying scattering loss.

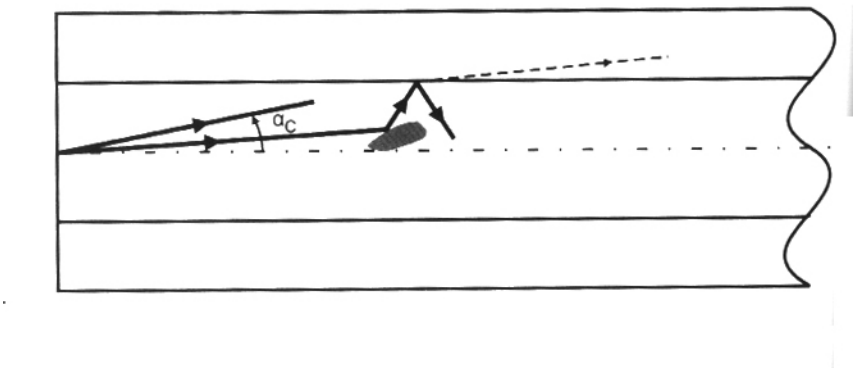

Fig 3.4 Scattering Loss

Even very small changes in the value of the core's refractive index will be seen by a traveling beam as an optical obstacle and this obstacle will change the direction of the original beam. An extremely high level of purity against some elements is necessary. For example, two parts per billion (ppb) of Cobalt can induce a 10 dB/km loss; twenty ppb of Nickel, Iron or Chromium or fifty ppb of Copper or even hundred ppb of Manganese or Vanadium can each induce 10dB/km loss through the fiber. In 1970, the quality control of the fiber manufacture process was poor enough to induce a 20 dB/km fiber. In 1972, the loss was reduced to about 4 dB/km and fiber for communication became, scientifically and economically, feasible for longer distance trunk applications.

3.2.2.1 Effects of Scattering

Scattering, as the term implies, is caused by the energy in the rays that leave the fiber due to the imperfection of the geometry of the fiber. The measure of the imperfection is its relation to the wavelength of the light through the fiber. Thus, at the imperfection, a certain amount of light leaves the fiber at the same wavelength as it reaches the imperfection. Silicon dioxide (SiO_2) is a non-crystalline material. The atoms are arranged in a somewhat random fashion where any incremental volume of the material does not hold the same number of atoms. The light through the glass does interact with the electron in the material.

Rayleigh scattering, caused by the weak interaction (absorption and re-radiation at the same wavelength, but delayed in phase) of the light with the electrons in the glass structure, represents a theoretical lower limit on the attenuation of the particular type of glass for a given wave length. A typical loss curve at various wavelengths is depicted in figure 3.5. Rayleigh scattering limit for 0.85μm wavelength (from GaAlAs light source) is about 1.6 dB/km and varies inversely with the fourth power of the wavelength. However, the lower limit of the loss is about 0.5 dB/km, at 1.3μm, and less than 0.2 dB/km, at 1.55μm. The newer sources of light and matching optical

detectors have been investigated and successfully fabricated and deployed for high quality fibers fabricated with 0.16 dB/km loss at 1.55μm.

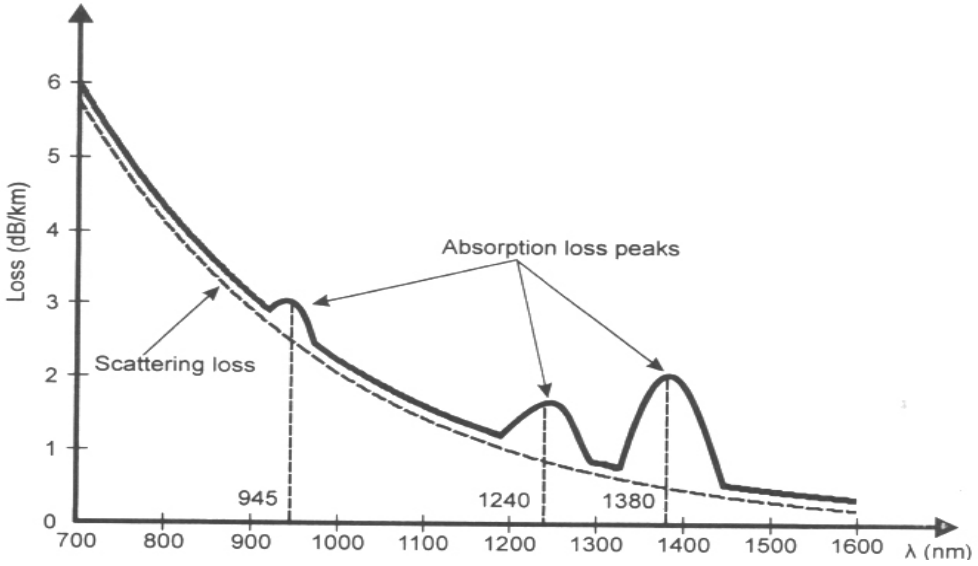

Fig 3.5 Typical Loss curve for Silica Glass Fibers

The presence of the OH radical (water) offers strong absorbing resonance at about 1.4μm wavelength. This "water peak" effect is due to the lingering presence of some of the OH radical in the fiber core material. Total eradication of this peak has not been successful and the fiber system designers, therefore, avoid the 1.4μm wavelength for silica glass fiber core material. At wavelengths in excess of 1.6μm, the absorption loss in silica glass in and by itself starts to increase rapidly and viability of optical systems using this material does not exist.

This does not mean the other materials have same restrictions (OH and Rayleigh limits) and cannot be used for other types of fibers. Some

materials (dark fibers) offer a theoretical loss limit of 0.01 dB/km, but the practical uses within a scientific and economic system have yet to be demonstrated.

3.2.3 Absorption

If an incoming photon has a frequency (f) and its energy (E_p=hf) is equal to the energy gap (ΔE) of the material, then this photon will be absorbed by the material. ΔE is the energy difference between two energy levels. It is impossible to change the energy levels of the material, since they have been predetermined by nature. However, by changing light frequency we can reduce absorption.

3.2.3.1 Effects of Absorption

Absorption is caused by the photon-electron interaction, which results as the propagating light prompts the electrons to undergo state transitions. Impurities and the silica glass material both absorb energy. However, the impurities absorb substantial amounts of energy from the pulse in the wavelength, which carries the pulse and thus, modifies its amplitude and its shape.

Silica glass, on the other hand, does absorb the energy, but in a waveband generally beyond the region of interest where the pulse energy is concentrated. The energy absorbed by the electron is eventually released as

light of the other wavelengths or heat due to mechanical vibration within the material.

3.3 Bending Losses

3.3.1 Macrobending Loss

Bending losses can be grouped into two: Macrobending loss and Microbending loss. Figure 3.6 shows two conflicting situations: (1) The beam forms a critical propagation angle with the fiber's central axis at the straightened, or flat, part of the fiber: (2) But the same beam forms a propagation angle that is more than critical when it strikes the boundary of the bent fiber. The result is failure to achieve total internal reflection in the bent fiber, which means that some portion of the beam is escaping from the core of the fiber. Hence, the power of the light arriving at its destination will be less than the power of the light emitted into the fiber from a light source.

In other words, bending an optical fiber introduces a loss in light power, or attenuation. This loss is commonly known as Macrobending loss and is one of the major causes of the total attenuation that light experiences while propagating through an optical fiber. Macrobending is loss caused by the curvature of the entire fiber axis.

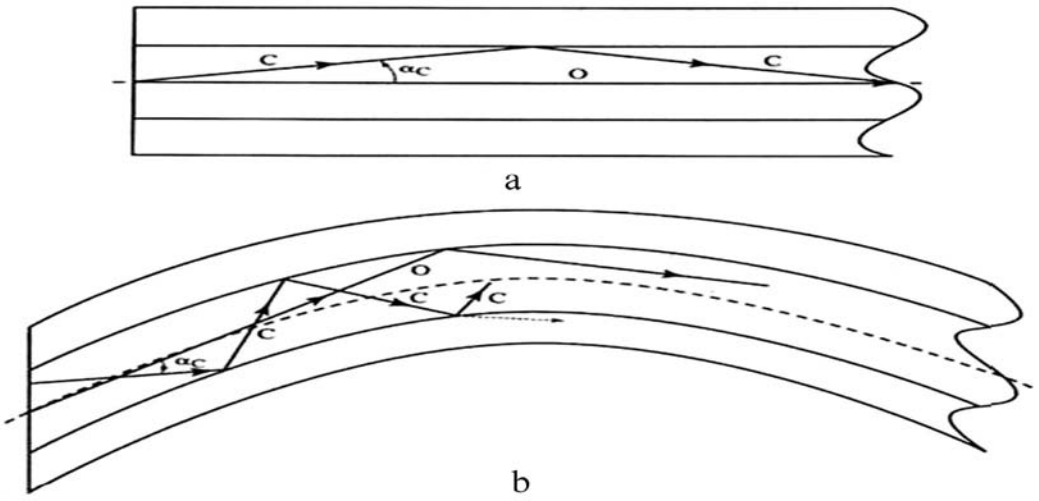

Fig 3.6 Macrobending losses for fundamental (o) and critical (c) modes

a). straight fiber b). bent fiber

Manufacturers of optical fiber have learned how to reduce a fiber's bending sensitivity by designing refractive index profiles. Unfortunately, improvement in bending sensitivity can be achieved only at the expense of the degradation of a fiber's other parameters. For example, one turn at a 32-mm diameter mandrel causes a 0.5 dB (approximately 11%) bending loss for one popular type of fiber. Sometimes manufacturers include the minimal bending radius in their data sheets. There is no straightforward method to eliminate this type of attenuation. The only thing can do is to be cautious when bending an optical fiber.

Bending can change not only the optical properties but also the mechanical characteristics of optical fibers. The rules of thumb regarding minimum bending radius are these: A bending radius should be more than 150 times the cladding diameter of the fiber for long term applications and more than 100 times the cladding diameter for short term applications.

3.3.2 Microbending loss

There is another type of bending loss in fiber, known as microbending loss. This is also caused by failure to achieve the condition of total internal reflection. Figure 3.7 shows this type of loss in an optical fiber.

Some imperfection in the geometry of the core-cladding interface might result in micro convexity or micro dent in that area. Although light travels along the straight segment of a fiber, the beam meets these imperfections and changes its direction. The beam, which initially travels at the critical propagation angle, after being reflected at these imperfection points, will change the angle of propagation. The result is that the condition of total internal reflection is not attained and portions of the light beam will be refracted; that is, they will leak out of the core. This is the mechanism of microbending loss.

In short, microbending is loss caused by microdeformation of the fiber axis. Fiber optic users can do nothing to overcome microbending loss except

ask manufactures to improve the quality of their optical fibers. Fortunately, the fiber manufacturing process is so well developed today that microbending loss is not a major problem.

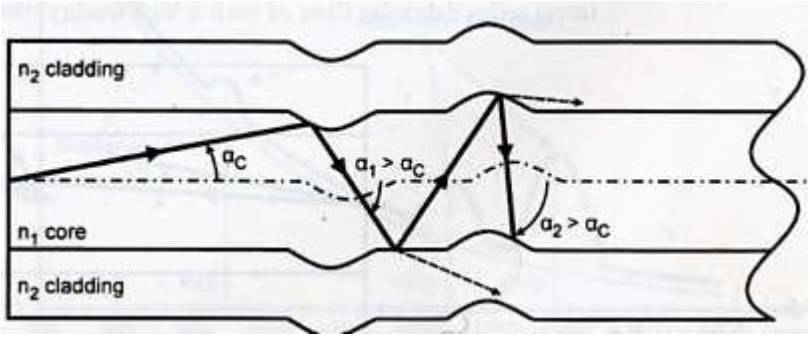

Fig 3.7 Microbending loss

3.4 Intermodal and Chromatic Dispersion

Right from the beginning, fiber optic communication technology promised the highest possible information carrying capacity of any medium simply because its signal carrier (light) has the highest frequency among all the practical carriers. But as soon as the first fiber optic communication systems appeared, it immediately became clear that the capacity of these systems was very far from theoretical expectations. The reason for this disappointment was modal or intermodal dispersion.

3.4.1 Modes

Numerical aperture is the property that characterizes the ability of a specific optical fiber to gather light. The larger the numerical aperture, the easier it is to direct light into an optical fiber. In other words, the greater the numerical aperture, the larger the amount of light that can be directed into an optical fiber. It would seem, therefore, that we would want to have a numerical aperture as large as possible. But this is not always true. There is an inherent limitation that prevents us from making numerical aperture larger. To understand this obstacle, we have to consider the modes in an optical fiber.

The fact is that light can propagate inside an optical fiber only as a set of separate beams or rays. These beams are traveling inside the fiber, at distinct propagating angles, ranging from 0 to the critical value α_c. These different beams are called modes. These modes can be ordered by their propagating angles. The smaller the mode's propagating angle, the lower the order of the mode. Thus, the mode traveling precisely along the fiber's central axis is the zero order mode and the mode traveling at the critical propagation angle is the highest order mode possible for the fiber. The number of modes in an optical fiber is determined by the normalized frequency parameter, V, which

is often called, the normalized cut-off frequency. The normalized cut-off frequency is equal to:

$$V = \frac{\pi d}{\lambda} [(n_1)^2 - (n_2)^2]^{1/2}$$

Where d is the core diameter, λ is the operating wavelength, and n_1 and n_2 are refractive indices of the core and cladding, respectively. For a large V number (>20), the following formula for a step-index fiber can be applied:

$$N = V^2/2$$

For a graded index fiber, the formula is:

$$N = V^2/4.$$

This depicts that the number of modes is directly proportional to the core diameter and the numerical aperture, and inversely proportional to the wavelength.

3.4.2 Delay distortion or Dispersion

Pulse spreading caused by delay dispersion in optical systems arises for two major reasons: *first*, the differential lengths of the paths traversed by different modes of propagation and *second*, the lack of a perfectly coherent source of optical power, which gives light at a fixed wavelength.

3.5 Incremental delays

Owing to the different lengths of the paths taken by different guided rays, the energy in a narrow (in time) pulse, at the input of the fiber, will be spread out over a larger time interval at the output of the fiber. A measure of this time spread is called **modal dispersion** and is obtained by taking the difference in time, δT, between the fastest and the slowest guided rays.

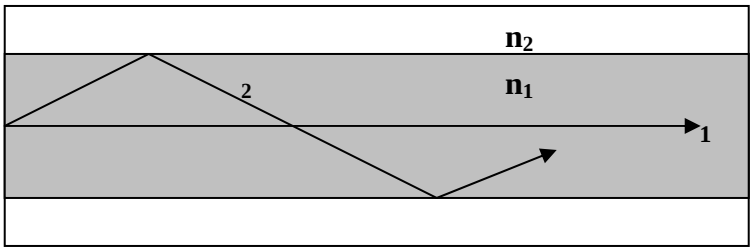

Fig 3.8 Different paths of rays through the fiber

Zero angle ray (ray 1), in fig 3.8, travels the axial length of the fiber along its axis and, thus, reaches the end of the fiber first. On the other hand, the ray (ray 2) at the critical angle, gets reflected numerous times and arrives delayed by an increment of time.

We can show that $\delta T = n_1 / c.l. [(n_1 - n_2) / n_2]$,

where l is the axial length of the fiber in meters, n_1, n_2 are refractive indices of the core and the cladding respectively, and c is the velocity of light in meters per second.

One of the standard techniques to reduce modal dispersion is to use the graded index fiber as shown in fig 3.9. This fiber has a parabolic distribution of the refractive index, being highest at the center and tapering off towards the cladding. Rays do travel different distances in the core, but the longest distance is in the region of the lowest optical density. Thus, an equalization effect takes place and all rays tend to arrive at the same time, thus, reducing the modal delay spreading that occurs in the core. In practice, the pulse spread of 50 ns/km, with step index fiber, can be reduced to about 0.5 to 2.5 ns/km or about 100 to 20 times reduced pulse spread.

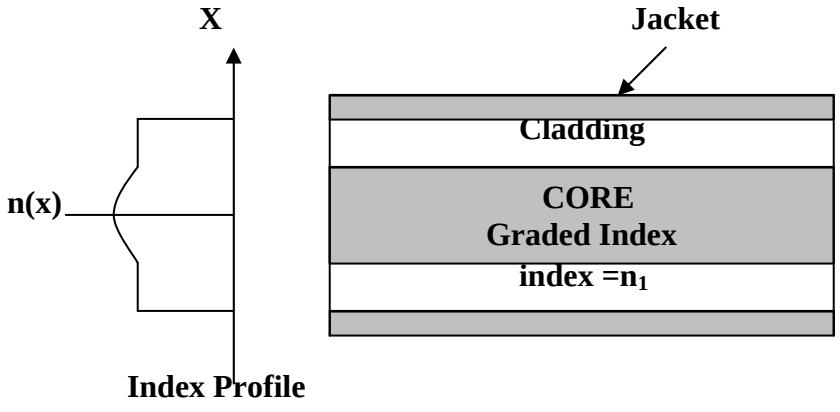

Fig 3.9 Typical Configuration of graded Index Fiber

The second solution to the modal dispersion problem is to use single mode fiber. Consider a very small diameter single mode fiber, with a core diameter D of about 6.6μm for a light source, with a wavelength of 1μm in free space and 0.66μm in silica glass. The ratio of the wavelength to the core diameter is 1/10, thus the spacing between rays is 1/10 radian or about 7.5 degrees.

This inference is based on the solution of Maxwell's equation or the laws of physical optics, which asserts that only certain discrete angles (corresponding to the discrete set of guided modes, typically the lowest four, the HE_{11}, the TE_{01}, the TM_{01}, and the HE_{21}, for the step index fiber which is, indeed, a dielectric waveguide) can propagate in the fiber. The spacing between the angles of propagation, of the individual rays in the set, corresponds to the ratio of optical wavelength of the light, λ, through the fiber, and to the fiber diameter, D.

Next consider a fiber consisting of the core and cladding with fractional difference between the refractive indices of the core and the cladding of 0.5 percent, with the first allowed ray away from the axis above the maximum angle Θ_{max}. Thus, by accurate control on the wavelength of the light that is incident at the entry into the fiber and accurate control of the refractive indices of the core and cladding only one ray (i.e single mode of

light) enters this single mode fiber and is the only one guided wave in the fiber. Though slightly harder to splice and couple to the source, single mode fibers can carry pulses of very high-speed data. There is no modal spread due to the singular presence of only one mode through the fiber.

3.5.1 Material dispersion

The second major reason for the pulse spreading is due to the presence of optical energy at numerous wavelengths in the light emitted from LEDs and perhaps a chirp in the laser source. Different optical wavelengths travel at different speeds. The range of light from LEDs and other noncoherant light sources may become quite broad. The optical density or the index of refraction of silica glass is sensitive to the wavelength and is evident as the prism effect upon white light. This effect shows up because the propagation speed will vary with wavelength if the second derivative of the index of refraction with respect to wavelength is not zero. This effect, known as, material dispersion, is measured in ns/(km-nm) and is characterized by the variation in delay with respect to the change in wavelength (nm). In fig 3.10, the typical material dispersion effect is plotted for silica glass over a range of wavelengths. It is easy to see that material dispersion effect can be sizable under certain conditions. At 0.85μm wavelength, the dispersion is about 0.1ns/km-nm. If the optical band spread

from an incoherent LED is 50 nm, then the pulse spread between the two extremes of the wavelength is 5 ns/km. When the pulse width is only 20ns at 50 Mbps, then pulse spread due to material dispersion becomes significant.

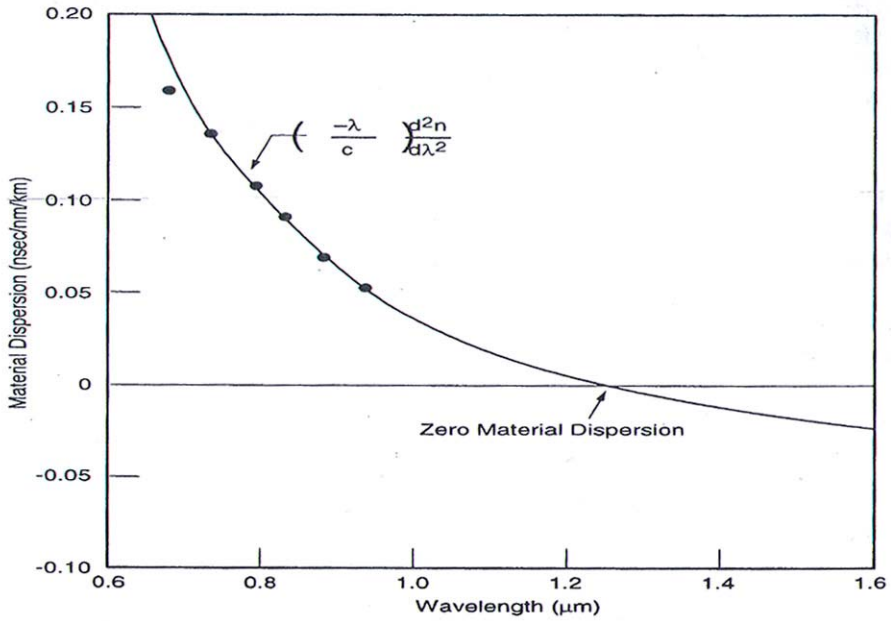

Fig 3.10 Typical plot for the material dispersion for silica glass fiber

The spectral spread of coherent light sources (laser) is small and the effects of material dispersion can be low. However, silica glass offers one other attractive feature that at 1.3 μm, the material dispersion crosses the zero value and the optical attenuation is low (0.5 db/km, a low enough value, though not the least). For this reason, many light wave systems are built with component around a nominal wavelength of 1.3 μm.

It is possible to design single mode fibers in which the waveguide propagation effects can counter the material dispersion effects. The net effect is that the frequency of net zero dispersion is shifted. Also single mode fibers with uniformly low dispersion effects over a significant band of wavelength can be fabricated. This type of fiber design permits the concept of multiplexing numerous channels over pre-assigned optical wavelengths through the same fiber, thus leading to wavelength division multiplexing of the wavelength parameter through the fiber with low dispersion of the pulses in the many wavelengths bands.

As the transmission capabilities are pushed higher and higher, the optical properties other than transmission loss become increasingly important for the fiber. Representative of these properties are the dispersion (chromatic and polarization) effects and scattering (stimulated Raman, stimulated Brillouin, cross-phase modulation and four photon mixing). These limitations affect the various optical systems differently and each system needs to be simulated, studied and experimentally verified.

3.6 More Secure Information Exchange using antisqueeze light

Tatsuya Tomara and Masashi Ban from the Hitachi Advanced Research Laboratory in Japan recently found that more secure optical communication could be achieved by using a "antisqueezed" light [28].

Antisqueezing is one side effect of a process call squeezing. Light is made up of basic units called photons. A photon will allow either its position or its momentum to be measured with high precession, but not both. This limitation is known as Heisenberg Uncertainty principle.

Squeezed light is defined by fluctuation in the precision of the photons' measured position and momentum. When the fluctuation of the measured momentum is squeezed the fluctuation of the measured position must, in accordance with the Heisenberg Uncertainty principle, become inflated or antisqueezed. When squeezed light is transmitted the larger fluctuation (the antisqueezed component) dominates and the squeezed component regresses to the natural fluctuations light experience in vacuum. But the antisqueezed component resists that pull and it is always beyond the vacuum fluctuation, even after loss and amplification. The result is a signal that is far more loss tolerant. Eavesdroppers need loss components of light do their job. But there are few lost pieces in the antisqueezed light.

Tomaru and Ban assumed real light signals that are encrypted prior to transmission with the intended receiver equipped with the proper key to correctly un-encrypt the signal. An eavesdropping receiver would not know this key and it is highly unlikely to guess it. This is a common way to secure a transmission.

3.7 Plastic Optical Fibers (POF)

When we hear about optical fibers it is natural to think about glass fibers. However, only few people in the industry know about the plastic optical fibers. Since the glass fibers have certain advantages, they have dominated the industry, while POFs have remained in the background. Recent development in the industry cut down the barriers of POFs and they are finding a larger market with technology companies worldwide. Today, a new enthusiasm permeates the plastic side of the optical fibers.

Manufacturers form POFs out of plastics materials such as polystyrene, polycarbonates and poly methyl methacrylate (PMMA). These materials have transmission windows in the visible range (520-780nm). However, the loss of light transmitted at these wavelengths is high, ranging from 150 dB/km for PMMA to 1000 dB/km for polystyrene and polycarbonates. These losses often handicap plastic fibers in competing against high quality

glass fibers, which have losses of 0.2 dB/km for a single mode fiber and less than 3 dB/km for multimode fibers.

Hence, plastic fibers have been relegated to short-distances applications, typically of a few hundred meters or less, compared with the hundreds of kilometers for glass. Nonetheless, POFs have found many applications in areas such as industrial controls, automobiles, sensors for detecting high-energy particles, signs, illumination (including lighting works of art museums) and short data links. Basically, POF applications divide into data communication and non-data applications.

3.7.1 Advantages and disadvantages of Plastic Optical Fibers

Certain users find POF systems provide benefits compared to glass fibers, which include:

- Simpler and less expensive components
- Lighter weights
- Operates in the visible range
- Ease in handling due to the larger diameter (20 times that of glass)
- Greater flexibility
- Use of simple and inexpensive test equipments
- Immunity to electromagnetic interferences

There are some disadvantages that researchers and manufacturers are working to overcome. They include:

- High loss during transmission
- A lack of standards
- A lack of awareness among users of how to install and design with POFs
- Limited production, which has kept customers from realizing the full potential of POFs.

The high-loss problem is being addressed with new perfluorinated polymer materials, which have brought losses down to potentially 10 dB/km and European automobile manufacturers have united to solve the production volume issue. The table 3.1 compares the different transmission media, glass, plastic and copper.

	PLASTIC	GLASS	COPPER
Component cost	Potentially low	More expensive	Low
Loss	High-Medium (Short distance)	Medium-low (long distance)	High
Connections	Easy to connect, requires little training or special tools	Take longer, requires special tools and training	Easy to connect
Handling	Easy	Requires training and care	Easy
Flexibility	Flexible	Brittle	Flexible
Wavelength operating range	Visible	Infrared	NA
Numerical aperture	High(0.4)	Low(0.1-0.2)	NA
Bandwidth	High(11Gbps over100m)	Large(40 Gbps)	Limited to 100m at 100Mbps
Test equipment	Low cost	Expensive	High
System cost	Low overall	High	Medium

Table 3.1 Comparison of Plastic Optical Fiber, Glass Optical Fiber and Copper Wire

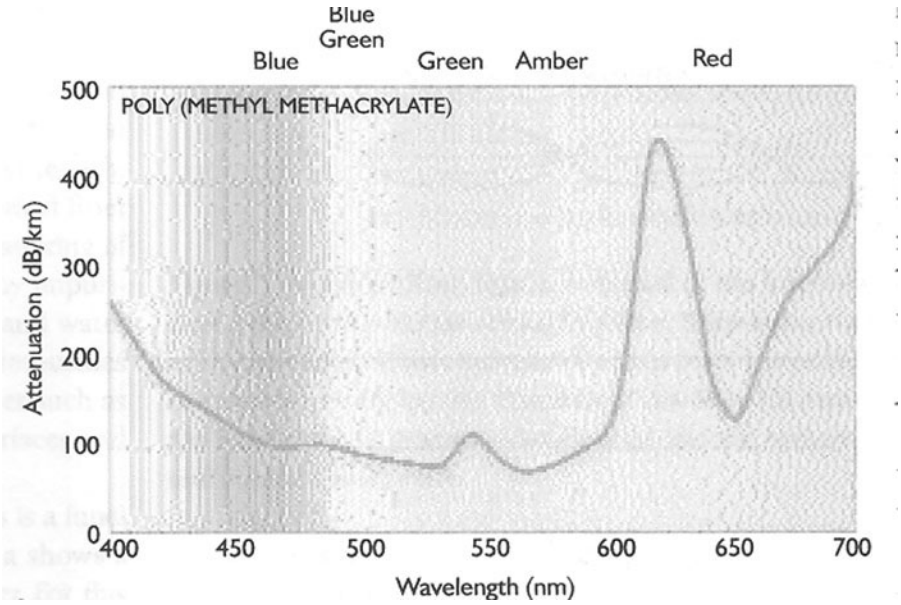

Fig 3.11a Loss curve for PMMA Fiber

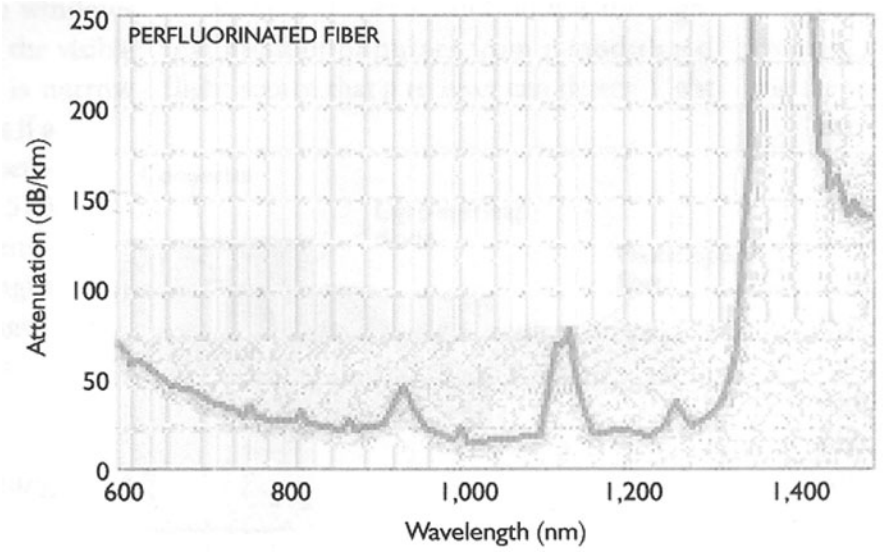

Fig 3.11b Loss curve for Perfluorinated Fiber

Figure 3.11a shows a typical loss curve for a PMMA fiber. For this loss spectrum, the transmission windows are 530, 570 and 650nm all in the

visible range. The window at 650nm is narrow and hence, could cause problems if a 650nm source shifted with temperature. The windows at 530 and 570nm are broader and, thus, less sensitive to shifts in source wavelength resulting from temperature changes. Note that the losses of 125 dB/km at 650nm and of less than 90 dB/km at 530and 570nm limit the use of PMMA plastic fibers for transmitting light to less than 100m.

Newer plastic fibers made from perfluorinated polymers exhibit greater transmission of light over a wider wavelength range. Figure 3.11b shows a typical loss spectrum for a perfluorinated fiber. Compared with loss spectrum of PMMA, perfluorinated polymer fiber has two distinguish features. First, its spectrum ranges 650 to 1300 nm and second, the loss is less than 50 dB/km over this wavelength range. This reduction in loss allows fiber links made from this material of up to several kilometers. Thus, perfluorinated fiber overcomes the distance limitation of PMMA and it can operate using the less expensive components developed for glass optical fibers at 850nm to 1300 nm.

3.7.2 Applications

Market researches project a compound annual growth in POF sales of more than 20% from 2003 through 2006. Unlike glass optical fibers, which are mainly used in telecommunications, POFs have applications in many industries. Thus, a slowdown in the telecommunication field can have a less severe impact.

The two major applications of POFs are in the industrial-controls and automotive fields. Controls remained the biggest and most stable market for the POF industry until year 2005, when sales to automotive companies rose to become the single largest source of revenue for POF markers. The main driver for POF in the industrial controls market is the need for data links that resists electro magnetic interference (EMI) caused by high voltage and high current devices such as arc welders and high voltage apparatuses such as X-ray machines and ion-implantation units. Today, the major source of excitement in the POF business lies in the innovative uses of its products by automobile companies.

3.8 Application of Maxwell's Equations to the Fiber environment

Maxwell's theory is based on a set of four equations, known as Maxwell's equations. This set, in differential form (also known as a point from), is:

$$\nabla . \mathbf{D} = \rho_v$$

$$\nabla . \mathbf{B} = 0$$

$$\nabla \times \mathbf{E} = \frac{-\partial \mathbf{B}}{\partial t}$$

$$\nabla \times \mathbf{H} = \mathbf{J} + \frac{\partial \mathbf{B}}{\partial t}$$

where boldface characters denote the vectors and the regular fonts denote the scalars.

- ∇ is defined as $\nabla = \mathbf{e}_x \frac{\partial}{\partial x} + \mathbf{e}_y \frac{\partial}{\partial y} + \mathbf{e}_z \frac{\partial}{\partial z}$
  with $\mathbf{e}_x$, $\mathbf{e}_y$ and $\mathbf{e}_z$ being the unit vectors of the x, y and z axes, respectively, of the Cartesian coordinate system.
- **D** is the electric-flux density or electric displacement(C/m^2). The electric-flux density is related to the electric-field intensity, E, through the permittivity, ε, of the medium. The formula is $\mathbf{D} = \varepsilon \mathbf{E}$

- **B** is the magnetic-flux density (H/m). The magnetic-flux density is related to the magnetic field intensity, H, through the permeability, μ , of the medium. The formula is $\mathbf{B} = \mu\mathbf{H}$
- **E** (V/m) is the electric-field intensity, defined as the force, **F**, produced by the electric field per unit charge, q, so that $\mathbf{F} = q.\mathbf{E}$
- **J** is the current density (A/m^2). The relationship between J and E can be explain by using the formula $\mathbf{J} = \sigma\ \mathbf{E}$, where σ is the conductivity of the medium.
- **H** is the magnetic field intensity (A/m).

Let's consider the physical meaning of Maxwell's equations. The first equation $\nabla .\ \mathbf{D} = \rho_v$ represents Gauss's law. Let's take the volume integral from both sides of the equation:

$$\int_v \nabla .\ \mathbf{D}\ dv = \int_v \rho_v\ dv \qquad 3.1$$

The right hand side is simply the charge, Q, bounded by the volume v and the left hand side can be transformed by using the divergence theorem:

$$\int_v \nabla .\ \mathbf{D}\ dv = \int_s \mathbf{D}\ ds$$

Thus we get the Maxwell's first equation in integral form:

$$\int_s \mathbf{D}\ d\mathbf{s} = Q$$

Maxwell's second equation:

$$\nabla . \mathbf{B} = 0$$

If we use the same technique as in previous case, we get

$$\int_s \mathbf{B}\, d\mathbf{s} = 0$$

Equation for Fiber Optic simulation from Maxwell's third equation:

$\nabla \times \mathbf{E} = \frac{-\partial \mathbf{B}}{\partial t}$ represents Faraday's law or the law of electromagnetic induction. Let's take the surface integral from both parts of the equation:

$$\int_s \nabla \times \mathbf{E}\, d\mathbf{s} = \int_s \left(\frac{-\partial \mathbf{B}}{\partial t}\right) d\mathbf{s}$$

Left side can be rewritten by using Stroke's theorem in the following form:

$$\int_s \nabla \times \mathbf{E}\, d\mathbf{s} = \int_L \mathbf{E}\, d\mathbf{l}$$

where $d\mathbf{l}$ is the vector differential length. The right hand side can be rewritten in the following form:

$$\int_s \left(-\partial \mathbf{B}/\partial t\right) d\mathbf{s} = -d/dt \int_s \mathbf{B}\, d\mathbf{s}$$

where the partial derivative is replaced by the derivative, since the integration of magnetic flux density over the surface eliminates the space dependence. By definition, integral $\int_s \mathbf{B}\, d\mathbf{s}$ is the magnetic flux**, ψ.**

Thus we arrive at the integral form of Maxwell's third equation:

$$\int_L \mathbf{E}\, d\mathbf{l} = -d\psi/dt$$

The fourth Maxwell's equation:

$$\nabla \times \mathbf{H} = \mathbf{J} + \frac{\partial \mathbf{B}}{\partial t}$$

shows where a time varying magnetic field comes from. The vortex source of a time varying magnetic field is the time-changing density of conduction and displacement currents. There are two sources here **J**(t), which is the conduction current density(A/m^2) and $J_d = \partial \mathbf{D}/\partial t$, which is the displacement current density(A/m^2).

To derive the integral form of Maxwell's fourth equation, we take the surface integral from both sides of the equation,

$$\int_s \nabla \times \mathbf{H} \; d\mathbf{s} = \int_s (\mathbf{J} + \partial \mathbf{B}/\partial t) \; d\mathbf{s}$$

we get the left side of the equation in the form: $\int_s \nabla \times \mathbf{H} \; d\mathbf{s} = \int_L H \; d\mathbf{l}$. The closed path, L, bounds the surface, S, through which total current, I passes. The integral $\int_L H \; d\mathbf{l}$ describes the circulation of the magnetic field intensity, **H**, around the closed loop L.

The right side of the equation consists of the sum of two integrals. The first $\int_s \mathbf{J} \; d\mathbf{s}$ is the integral of the current density over the surface, which by definition is the current I(A). The second integral on the right side of the equation , $\int_s \partial \mathbf{B}/\partial t \; d\mathbf{s}$ gives the displacement current, I_d(A). This is the quantity responsible for alternating-current (ac) flow through a capacitor that provides a-c continuity over the closed electrical circuit that includes the

different components. Putting all the integrations together, one can easily obtain Maxwell's fourth equation in integral form:

$$\int_L H \, d\mathbf{l} = \boldsymbol{I} + \boldsymbol{I}_d$$

A guided linearly polarized (LP) mode along the fiber can be represented by the propagation of electric field distribution E(r, ψ) along z. This field distribution or pattern is in the plane normal to the fiber axis and hence depends on r and ψ , but not on z. Further because of the presence of two boundaries, it is characterized by two integers, l and m. The propagating field distribution in an LP mode is therefore given by $E_{lm}(r, \psi)$ and we represent the mode LP_{lm}. Thus an LP_{lm} mode can be described by a traveling wave along z of the form:

$$E_{LP} = E_{lm}(r, \psi)\, e^{j(\omega t - \beta_{lm} Z)}$$

Where E_{LP} is the field of the LP mode and β_{lm} is its propagation constant along z.

Note that, this has transverse electric and transverse magnetic components. In the case of Fiber, it is necessary to keep both components. If we drop electric component then we get conditions for Twisted Wire Pair (TWP).

Now consider that the amplitude of a light signal, which has propagated over length L of fiber, can be expressed as

$$\psi(L, \tau) = \int \phi(\omega)\, A^{1/2}(L, \omega)\, e^{(j\,\omega t - i\,\beta(\omega) L)}\, d\omega$$

where A(L, ω) is the optical power attenuation coefficient of the fiber a,β(ω) is the phase change per unit length for the fiber and ϕ(ω) is the Fourier transform of the modulated light signal at L = 0;

i.e $\phi(\omega) = \int [S^{1/2}(t).\ \psi_0(t)]\ e^{-j\ \omega t}\ dt$

where s(t) is the modulating signal, $\psi_0(t)$ is the light source amplitude before modulation.

If we define the Fourier transforms

$$\phi_0(\omega) = \int \psi_0(t)\ e^{-j\ \omega t}\ dt \quad \text{and}$$

$$F(\omega) = \int S^{1/2}(t).\ e^{-j\ \omega t}\ dt$$

then $\phi(\omega)$ may be written as the convolution

$$\phi(\omega) = \int \phi_0(u).F(\omega-u)\ du$$

Then the ensemble average of the light power may be expressed as

$$\langle |\ \psi\ (L, t)|^2 \rangle = \int\int\int\int \langle \phi_0(u).\ \phi_0^*(v) \rangle F(\omega-u).\ F'(\omega - v).\ A^{1/2}(L, \omega).$$

$$.A^{1/2}(L, \omega').e^{(j\ (\omega-\omega')t\ -i\ \beta(\omega)\ -\ \beta(\omega')L)}\ du\ dv\ d\omega\ d\omega' \qquad 3.2$$

Assuming that the fluctuations in source frequency are a stationary random process, we can write

$$\langle \phi_0(u).\ \phi_0^*(v) \rangle = \int\int \langle \psi_0(t+\tau).\ \psi_0^*(t) \rangle .\ e^{-iu(t+\tau)} e^{ivt}\, dt\, d\tau$$

$$= \int\int R(\tau).e^{-iu\tau} e^{-i(u-v)t}\, dt\, d\tau$$

$$= G(u).\ \delta(u-v) \qquad 3.3$$

where $R(\tau)$ is the auto correlation of the light source and $G(u)$ is the source power spectral density.

By plugging (3.3) to (3.2) we get,

$$\langle |\ \psi(L, t)|^2 \rangle = \int\int\int G(u).F(\omega-u).\ F(\omega'-u).\ A^{1/2}(L, \omega).\ A^{1/2}(L, \omega').$$

$$. e^{[i(\omega-\omega')t - i(\beta(\omega) - \beta(\omega'))L)}\, du\, d\omega\, d\omega'$$

A change of variable gives

$$\langle |\ \psi(L, t)|^2 \rangle = \int\int\int G(u).F(\omega').\ F(\omega-\omega').\ A^{1/2}(L, u+\omega').\ A^{1/2}(L, u+\omega'-\omega).$$

$$. e^{[i\omega t - i(\beta(u+\omega') - \beta(u+\omega'-\omega))L)}\, du\, d\omega\, d\omega'$$

if we now assume that the modulation frequency range is small compared with the frequency range of $G(u)$, we may approximate

$$\beta(u+\omega') - \beta(u+\omega'-\omega) \approx \beta(u)\,\omega = \tau(u)\,\omega$$

where $\tau(u)$ is the group dealy per unit length of fiber and

$$A^{1/2}(L, u+\omega')\ A^{1/2}(L, u+\omega'-\omega) \approx A(L, u)$$

Consequently,

$$\langle |\psi(L, t)|^2 \rangle \approx \int\int\int G(u).A(L, u).\ F(\omega).\ F(\omega - \omega').\ e^{[i\,\omega t - i\,\tau(u)\,\omega L)}\, du\, d\omega\, d\omega'$$

$$= \int\int G(u).A(L, u).\ S(\omega).\ e^{[i\,\omega t - i\,\tau(u)\,\omega L)}\, du\, d\omega \qquad 3.4$$

$$\cong \int S(\omega).\ H_c(\omega).\ e^{i\,\omega t}\, d\omega \qquad 3.5$$

where $S(\omega)$ is the Fourier transform of $s(t)$ and $H_c(\omega)$ is the desired power transfer function. Comparison of equations 3.4 and 3.5 shows that

$$H_c(\omega) = \int G(u).A(L, u).\ S(\omega).\ e^{[-i\,\omega L\,\tau(u))}\, du$$

Noting that $G(u)\, du = P(\lambda)\, d\lambda$ where $P(\lambda)$ is the source spectral density as a function of λ and integrating over wavelength rather than frequency, we obtain,

$$H_c(\omega) = \int P(\lambda)\ A(L, \lambda)\ e^{[-i\,\omega L\,\tau(\lambda)]} d\lambda.$$

4.0 Generalized Simulation Methodlology

Techniques for the modelling and analysis of digital communication systems fall into three categories: those based on analytical calculations, those based on time domain Monte Carlo simulations and hybrid approaches based on a combination of simulation and analytical calculations. Analytical calculations are computationally very fast but are limited in their applications because of the necessary assumptions and approximations needed model the physical phenomenon. Time domain simulations are more flexible but Monte Carlo simulations of digital light wave links operating at low error rates require very long input sequences.

In the hybrid approach, Monte Carlo simulations are used to derive estimates of statistical distributions that are not analytically tractable and the simulation derived distribution are combined with other distributions that are derived analytically. Hybrid approcahes have been used prviously to evaluate the performance of satellite and microwave links in which the effects of intersymbol interference and nonlinearities are handled through simulations while the effects of addictive Gaussian noise in the receiver are handled analytically.

FS* simulator[1] is used to do the simulation study of this project. FS* is a high-end simulator that can be used for fiber optic systems as well as plain old copper systems. The most important characteristic of the FS* simulator is that it included a complete vendor database so that we can do more flexible and reliable simulation rather than confined our simulation to generic components. I will modify FS* simulator to handle OTDM systems and new Plastic Optic Fiber systems as well as variable length data pulse simulations.

4.1 Basics of FS* simulator

Like any other system, there are at least five components to make up a direct detection light wave system:

a). The data source and the encoder

b). The photonic device

c). The fiber

d). The photo detector

e). The demodulator

[1] **Originally developed by Professor S.V. Ahamed**

4.2 Sources in the simulation environment

For the simulation studies, it becomes necessary to accurately characterize the performance of each of these components in order to evaluate the overall system performance. Typically, the sources (LEDs in particular) have a slow response. The faster devices will be able to track the encoded signal with little or no lag and the quality of the source is characterized by the time constant in emitting the optical energy into the fiber. Laser devices respond faster, and pulse shape for the optical energy follows the encoded signal more accurately. The second characteristic of the source is indicated by the spread of the wavelength over which the optical energy is distributed.

Generally this is a Gaussian distribution for LEDs represented as

$$S(\lambda) = \frac{1}{\sigma_s \sqrt{2\Pi}} .e^{-(\lambda - \lambda_s)^2 / 2\sigma_s}$$

where $S(\lambda)$ is the energy distribution from the source around the nominal wavelength of λ, λ_s is the nominal wavelength of the source and σ_s is the standard deviation of the device.

The energy distribution exhibits much slower variance for laser sources.

4.3 Photo detector in the Simulation Environment

The detectors also have their respective databases and the characteristic constants are appropriately stored. Detectors generally add electronic noise in the system as a number and distribution of photons gets transformed to the electrons and holes in the semiconductor devices are uncertain. Two types of noises are inherent in photo detectors:

a). the thermal Gaussian noise

b). the impulsive or shot noise that depends upon the power level from the photodiode.

These two types of noises affect both PIN devices and APDs. Mostly in the APDs, the shot noise can become a significant proportion of the total noise. Both of these types of noises get combined in the detectors and are the primary cause of limitation in single mode optical fiber systems.

4.4 The PIN Diode Signal Process

The average number of the electron-hole pairs N_{sig} generated within an interval of time Δt, if the device receives an incident optical power of $P_{inc}(t)$ at a time t is given as

$$N_{sig} = \frac{\eta}{h\nu} . P_{inc}(t). \Delta t$$

where $\eta$the quantum efficiency, h is is the Plank's constant and ν is the optical frequency.

The sum of N_{sig} and the electron-hole created by the dark current in the device, gives rise to the average (total) number of electron-hole pairs N in Δt seconds is given by

$$N = N_{sig} = \frac{\eta}{h\nu} . P_{inc}(t). \Delta t + I_d \Delta t$$

where I_d is the dark current in number of electron hole pairs per second.

The number of electron-hole pairs generated, n is a random time-varying Poissonian process, the mean and variance for this process is N and hence the probability that exactly k pairs are generated in Δt can be written as

$$P(n=k) = \frac{(N)^k . e^{-N}}{k !}$$

The total current *i(t)* for the PIN device is simply the rate of flow of the electron charge (q = ne , where e is the charge per electron) and *i(t)* is written as:

$$i(t) = \frac{n.e}{\Delta t}$$

4.5 The APD Diode Signal Process

For the APD, the device current can be modeled as

$$i(t) = \frac{e}{\Delta t} \sum_{t=1}^{n} g_l$$

where g_l is the number of resulting electron-hole pairs (i.e. secondary plus the primary pairs) for every primary pair 'n' in Δt.

4.6 Fiber in the simulation environment

The basic equation that is instrumental in the simulation is the transfer function of a single mode fiber. It assumes two slightly different expressions based upon the

a). the electric field intensity model

or

b). the power intensity model.

If the light source is coherent and the information is communicated by modulating the wavelength or phase of the encoded signal, then laser or single (very narrow) wavelength devices are used as local oscillators.

On the other hand, if the information is communicated by modulating the intensity of the light of an LED, for instance, then it is the power over an entire spectrum of wavelengths that becomes crucial.

4.7 Electric Intensity Model

For the single mode optical fiber, the assumption that it can be represented as a flat band pass filter with a flat amplitude response and linear group delay (within the bandwidth of the data) is justified, because of the very narrow data bandwidth with respect to the absolute frequency.

The group delay is determined from the usual equation for the chromatic dispersion in the fiber and can be written as:

$$\frac{d\tau}{d\nu} = \frac{d\tau}{d\lambda} \cdot \frac{d\lambda}{d\nu}$$

$$= \left\{\frac{-1}{l} \cdot \frac{d\tau}{d\lambda}\right\} \left\{\frac{\lambda^2}{c}\right\} l$$

and the chromatic dispersion $D(\lambda)$ is defined as

$$D(\lambda) = = \left\{\frac{-1}{l} \cdot \frac{d\tau}{d\lambda}\right\}$$

The fiber length is l, the operating wavelength is λ, the optical frequency is ν and the velocity of light is c.

When the optical carrier frequency ν_c is present, the group delay in the fiber can be written as:

$$\tau(\nu) = \tau(\nu_c) + (\nu - \nu_c) \frac{d\lambda}{d\nu}\Bigg|_{\nu = \nu_c}$$

The associated phase for this or any function is given by

$$\phi(v) = 2\Pi \int \tau(v')\, dv'$$

$$\phi(v) = 2\Pi\, v\, \tau(v_c) + 2\Pi \left\{ \frac{(v - v_c)^2}{2} - \frac{v_c^2}{2} \right\} \left. \frac{d\tau}{dv} \right|_{v=v_c}$$

The transfer function of the equivalent model of the low pass single mode can now be evaluated as :

$$H(f) = e^{-j\,\phi(f)} = e^{-j\,\alpha f} = e^{-j \left\{ \alpha\, B^2 [\, f / B]^2 \right\}}$$

with B being the bit rate and

$$\alpha = \Pi\, D\, (\lambda)\, \frac{\lambda^2}{c}\, l \quad \text{and}$$

$$f = v - v_c$$

since only the chromatic dispersion is considered , the constant phase term and phase terms linear with respect to f are not included since they do not introduce any distortion in the received signal.

4.8 Power Intensity Model

The basic equation that is instrumental for this mode of operation in the simulation is the transfer function. For a single mode fiber, it can be written in a simplified form as

$$H(f) = \int_{-\infty}^{+\infty} s(\lambda) \, . \, L(\lambda) . \, e^{-j\omega . T(\lambda) . l} . d\lambda$$

where λ - wavelength

ω - $2\Pi f$

$s(\lambda)$ - optical source spectrum as a function of λ

$L(\lambda)$ - attenuation of the entire fiber as a function of λ

$T(\lambda)$ - group delay of the fiber(per unit length) as a function of λ.

and l - fiber length

The group delay of the fiber is sometimes called the anti derivative of the dispersion characteristic. In silicon fibers, the chromatic dispersion characteristic has been documented as

$$\frac{dT(\lambda)}{d\lambda} = \frac{S}{c} \, . \, \frac{\lambda - \lambda_0}{\lambda^2}$$

where S – a dimensionless constant

c - velocity of light

λ_0 - zero-dispersion wavelength

In elaborate simulation facilities, imperfections of the devices are accurately modeled in the databases and the influence of the device limitations can be accurately predicted.

4.9 Simulation Process

The computer aided design procedure can be divided into three phases of interaction with the designer.

The first phase consists of defining the system configuration. The components are assembled by a set of interactive graphic routines. These routines explain the designer all types of components available in the model library.

The second phase dealing with the simulation of the system, the user is actively informed of status simulation procedures and any errors resulting from user inputs or data base access are posted. Recoverable errors are tackled by the system and unrecoverable errors terminate the simulation procedure.

The final phase permits display (and generation of the hard copy) of the system performance. This phase also operates in an interactive mode. The system offers the designer to see the time domain results as wave shapes at any of the nodes in the fiber optic network.

5.0 Simulation Platform

The rapid pace in the research and development of improved and economical fiber cables devices and systems technology has resulted in large-scale deployment of lightwave communication systems. Early lightwave communication systems utilized multimode fibers which allowed only limited information bandwidth and repeater spacing. As technology advanced, emphasis shifted away from multi-mode lightwave systems, infavor of the higher bandwidths and lower losses aavailable with single-mode systems. This growth has increased the range of potential applications and led to lightwave systems being used more and more in highly compettitive commercial applications. As a result, lightwave system engineers require more detailed information on the possible tradeoffs available when designing or deploying a systems. Analytical methods alone are becoming insufficient because of many necessary simplifying assumptions. The lightwave system designers often forced to evaluate design alternatives by constructing prototypes; an approach which can be costly, especially in a research or early design phase.

In his paper [4], Duff presented models and analysis methods for computer-aided design of digital lightwave systems. Duff's approach was based primarily on analytical approximations to computer performance

measures such as error rates, eye diagrmas and power penalties. In contrast, the approach presented here is based on detailed simulation models for functional blocks in lightwave communication links. Computer simulation of digital lightwave systems is an alternative to both hardware evaluation and pure analytical methods of anlysis. An important advantage of computer simulation is the flexibility available to the designer. Simulation packages such as SYSTID [5] offer the user the capability to study the effects various parameters have on total link performance via bit error rate (BER) estimates, eye diagrams, spectral plots, time plots, etc. In general, computer simulation invloves performing a series of transformations on a data structure(i.e,a signal) and analyzing the effects of these transformations using the performance measures mentioned above, The transformations are between and within the time and frequency domains and model the behavior of cascaded or single components in the system being simulated.

Modeling lighwave system functional blocks and using these in a semi-analytic simulation framework are discussed in this section. Lightwave systems are ideally suited for the semi-analytic approach. The effects of intersymbol interference (ISI) introduced by the Optical source and the fiber, in addition to the quantum noise introduce by the photodetector are simulated. Thermal noise (assumed to be white Gaussian)

enters the simulation only in the receiver which is downstream of any no-linearities introduced by the optical source or photodetector. Hence the effects of thermal noise are handled analytically. Typically , short PN sequences (on the order of hundreds of bits) can be used to evaluate the effects of the nongaussian degradations, which greately reduce the computer time required as compared to the brute-force approach.

The contents of chapter 5 are divided into three sections. Section 5.1 is a brief discussion of the SYSTID simulation package. Section 5.2 presents the models for the lightwave functional blocks. Models discussed in this section are the single-mode optical fiber models featuring versions which allow tabular input of fiber parameters and a choice between time domain or frequency domain signal processing. A PIN diode model and two BER estimator models are also discussed.

5.1 The SYSTID simulation Package

The SYSTID simulation package (developed originally by the Hughes Aircraft Corporation) is a powerful tool for analysing and designing communication systems[5]. SYSTID features a flexible topology format with an input language which corresponds closely to systems level block diagrams. This minimizes the amount of time a user spends translating the block diagrams of the system under analyis into the simulation source

program. Although the user can easily construct new blocks, the SYSTID model library contains many commonly used functional blocks such as signal generators, filters, modems and source encoders. Results of simulations are analyzed using the SYSTID postprocessor called RIP. RIP is a menu driven with large number of commands available such as spectral plots, time plots, eye diagrams, histograms, correlations, covariance etc. To decrease the amount of time a user spends answering questions in a given menu, standard default values are provided when possible.

The structure of SYSTID makes it easy for the user to construct and use models which require tabular data input. This feature was used in the single-mode fiber models to allow laboratory hardware measurements to be used in simulating the fiber, as discussed in Section 5.2.

5.2 Modelling Functional Blocks in a Lightwave Communication Link

5.2.1 Optical Source

Depending upon the application, optical sources under consideration for lightwave communication systems are either semiconductor light emitting diodes(LED) or laser diodes . Both types of optical sources tend to degrade the input bit stream, although incoherant LEDs are more well behaved (and therefore easier to model) than semi-coherant laser sources. Lasers, however, are capable of provising higher values of launched optical

power and are widely used in long distance single-mode fiber systems. LEDs are finding increasing application with single mode fibers for the shorter distance distribution plant[1].

The spectrum of the optical sources plays an imporatnt role in determining the effects of dispersion on a single mode fiber communication system. When using one of the four single mode fiber models discussed below, the user can either input an arbritrary source spectral density curve in tabular form, or supply the needed parameters to speicfy a built-in Gaussian approximation to the source spectrum. If the source spectrum were very narrow, it could be approximated as an impulse and effects of the single-mode fiber could be handled analytically. This is not a realistic assumption, however, simulation techniques are required to evaluate the effects of a non-ideal source spectrum on system performance .

5.2.1.1 Single Mode Fiber

The baseband transfer function of a single mode fiber can be modelled by the following equation [1]:

$$H(f) = \int^{\infty} S(\lambda)L(\lambda)e^{-j\omega LT(\lambda)}\, d\lambda \qquad 5.1$$

Where ω - $2\Pi f$

L – fiber length

$S(\lambda)$ – Optical source spectrum vs wavelength

$L(\lambda)$ – 1 /(fiber loss) vs Wavelength

$T(\lambda)$ – fiber group delay vs. Wavelength

The two major physical chracteristics which influence the performance of the single-mode fiber are fiber loss and chromatoc dispersion. In eq. (5.1), $L(\lambda)$ is the reciprocal of loss(gain) as a fucntion of wavelength. The fiber group delay term, $T(\lambda)$, is actually the antiderivative of the dispersion charcteristic. The degrading effects of chromatic dispersion are realted to the spectral purity of the optical source.

6.0 Simulation Methodology

As we discussed before application of Plastic Optical Fiber (POF) in telecommunication is limited due to high attenuation. In my research I will explore the facts that can be used to improve SNR.

Even though, FS* simulator has given promising results for WDM systems, there are no built-in components to do the simulation with OTDM or Plastic Optical Fibers (POF). My contribution is to modify and use facilities in FS* to do POF simulations as well as OTDM simulations. In addition, I will also investigate

(a) Range and characteristics of plastic optical fiber for local area networks (LANs),

(b) Effects of channel cross talk in WDM erbium doped fibers,

(c) Effects of pulse width on signal to noise ratio,

(d) Effects of temperature sensitivity on plastic optical fibers. In the simulations, the parameter S_0 is adjusted to reflect temperature changes.

(e) Effect of noisy LEDs and lasers sources on FO data transmission systems.

7.0 Actual Simulation

The computer aided design process involves simulation (see fig 7.1). The man machine feedback occurs when the designer defines the system and studies the simulated results to evaluate system performance. System optimization is carried out by the iterative procedure of readjusting the input parameters until a satisfactory design is negotiated.

The simulation software consists of four major segments as depicted in fig 7.2. These segments correspond to the four functions discussed earlier. The entire simulation process consists of providing enough information for the system as follows: *(a)* defining the configuration of the light wave system, *(b)* selecting the components of the system from vendor database, *(c)* approving the final configuration and components selection, and *(d)* defining which of the parameters need to be displayed.

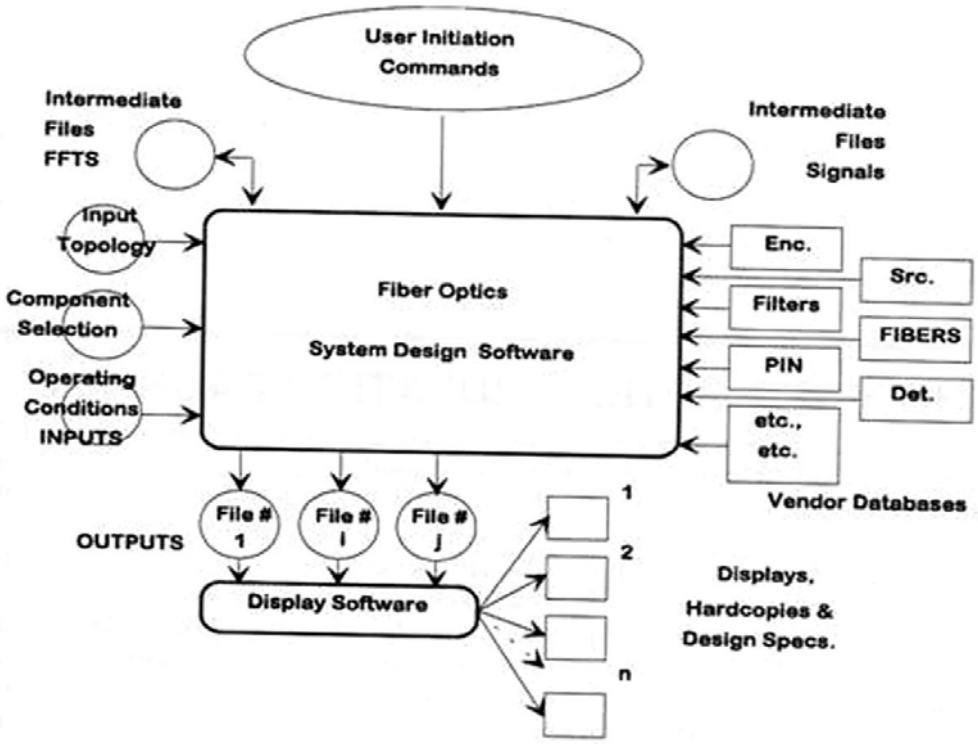

Fig 7.1 Software Organization for the Design of Light wave Systems

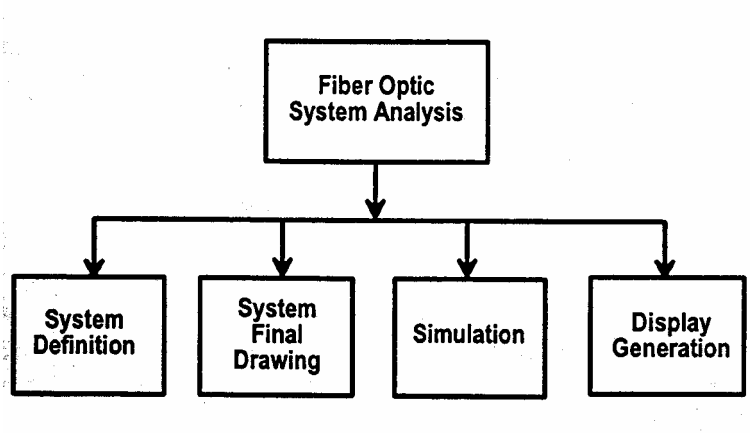

Fig 7.2 Software segments for the light wave Design System

Graphics is used extensively to facilitate the user interface. Accordingly, the following four subsections present the four phases (a) through (d) listed above. At the user's request, hard copies are generated during the entire CAD procedure for user records. This run data may also be

made an integral part of the design procedure, which is a finite step in the overall design procedure. The system is also capable of keeping personalized records of the individual users such that preferred and successful designs may be reused. Highly successful designs may be moved into a common knowledge base of the designers at user's request.

7.1 System Configuration

The input function and the output of the software segment is depicted in figure 7.3

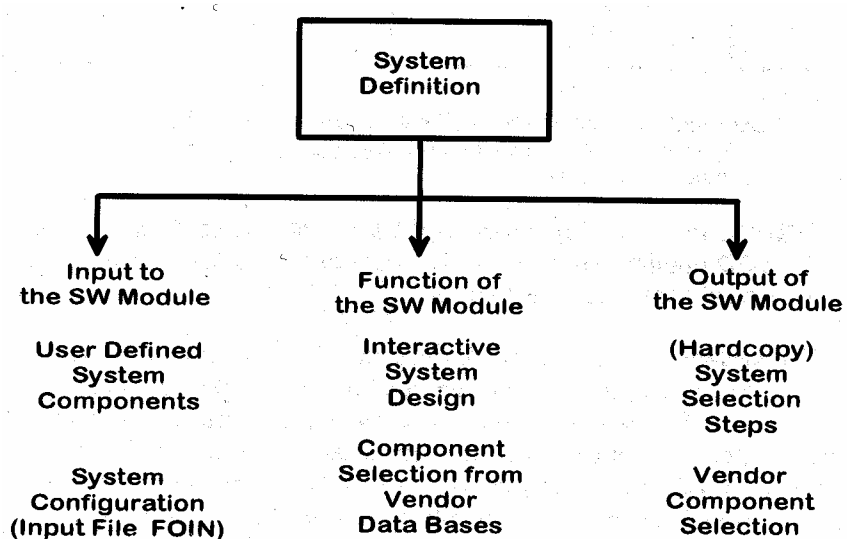

Fig 7.3 User Definition of the Light wave System

At the entry to the CAD software platform, the user defines the number of nodes and components, the generic names of the components is selected and the interconnection between the generic components. For simplicity, only simulation from a serially connected system are presented,

even though multiple optical taps can be incorporated and their performance be evaluated.

The system generates a block diagram of the system that the user has defined. At present, the user has the capability to select components from the any number of generic components (encoders, sources, fibers, filters, PIN diodes, detectors, optical couplers, optical taps, optical signal splitters, etc) commonly used in optical systems. Next, it scans the vender databases to offer the user particular components by vender serial numbers. In figure 7.4 the major vendor for each generic component is displayed.

Light wave design system step 1

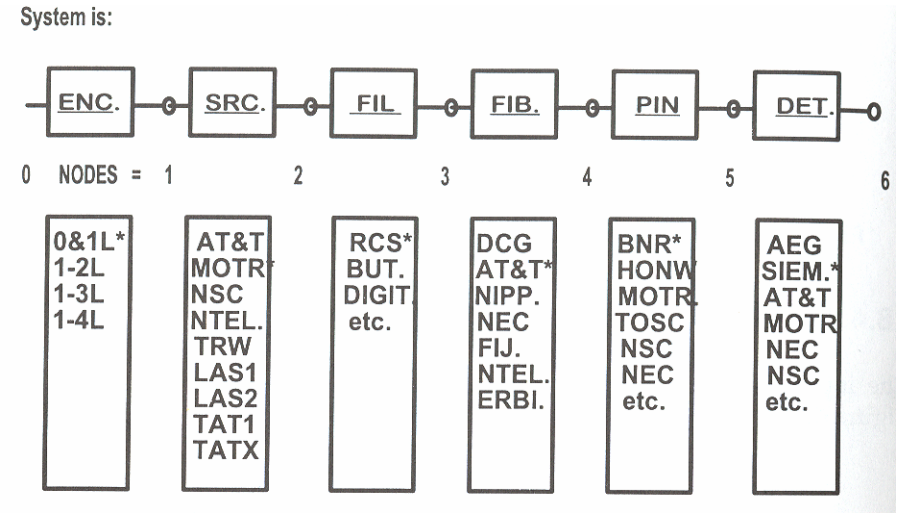

Fig 7.4 Configuration and component selection procedure in the CAD family

7.2 Component Selection

Component selection is also facilitated by graphic routines. The user selects the components (note that the asterisk sign in fig 7.4) in an interactive mode as the component menu is offered to the user. These selected components are tagged by the system and a user defined system configuration is redrawn (fig 7.5) with the appropriate components placed in the block diagram.

System Response to Step 1

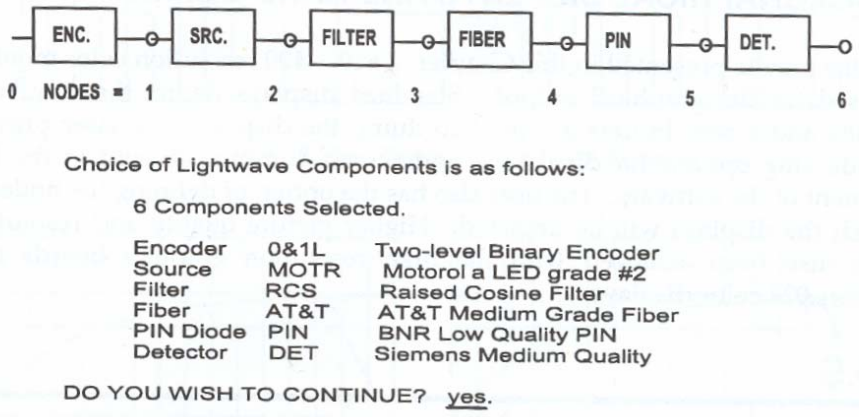

Fig 7.5 System Response and Verification

The user reaffirms the configuration and components that constitute the simulation to follow. After validation, the component identification is stored away for the simulation run. The system generates ample updates throughout the simulation process and uses an intricate file management methodology to provide the user with the necessary information.

8.0 Simulation Results

8. 1 Wave shapes and eye diagrams

8.1.1 General Results

a). Simulation results for 100km and 160 MB/s system

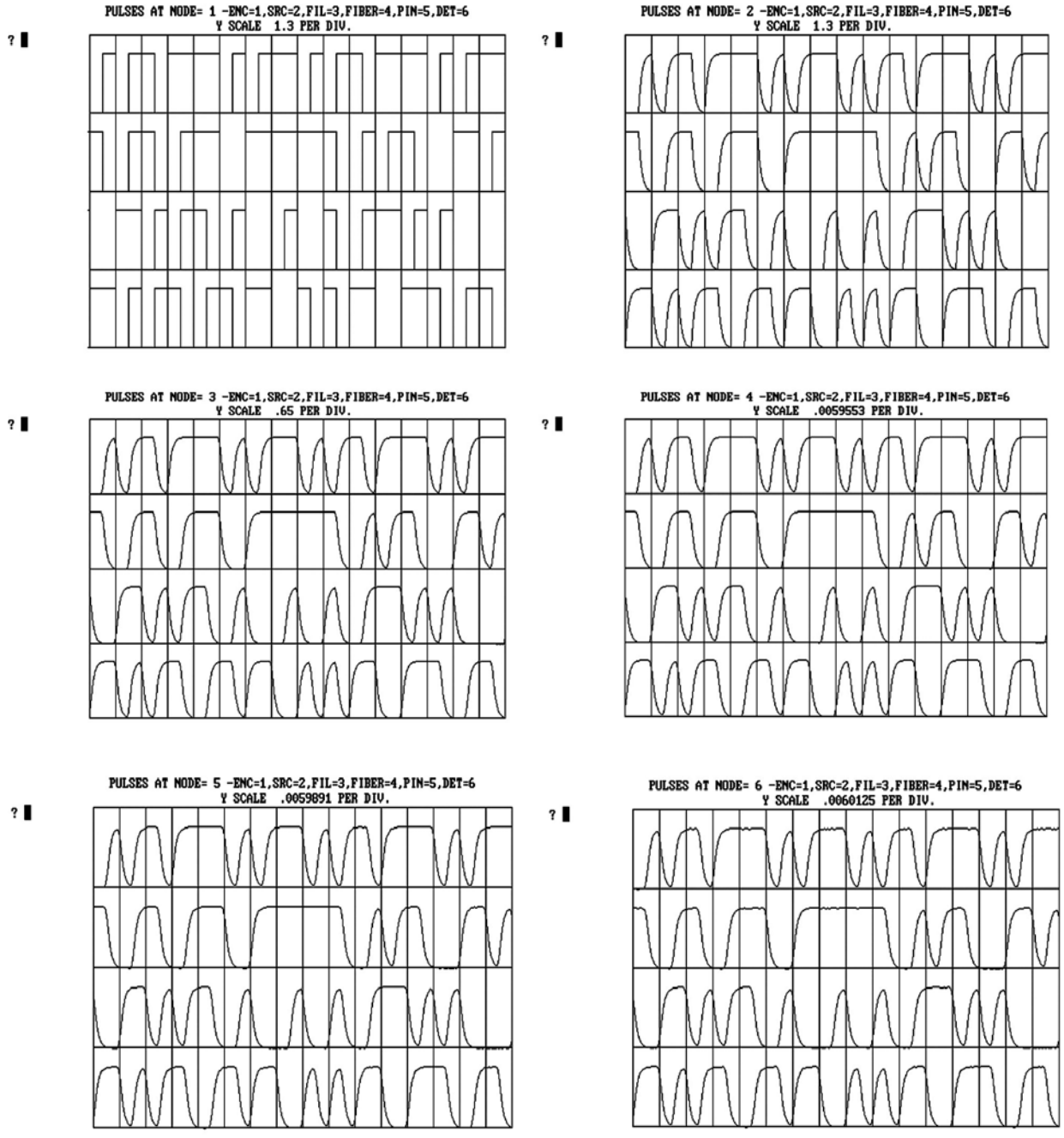

Fig 8.1 Pulse shapes at different nodes

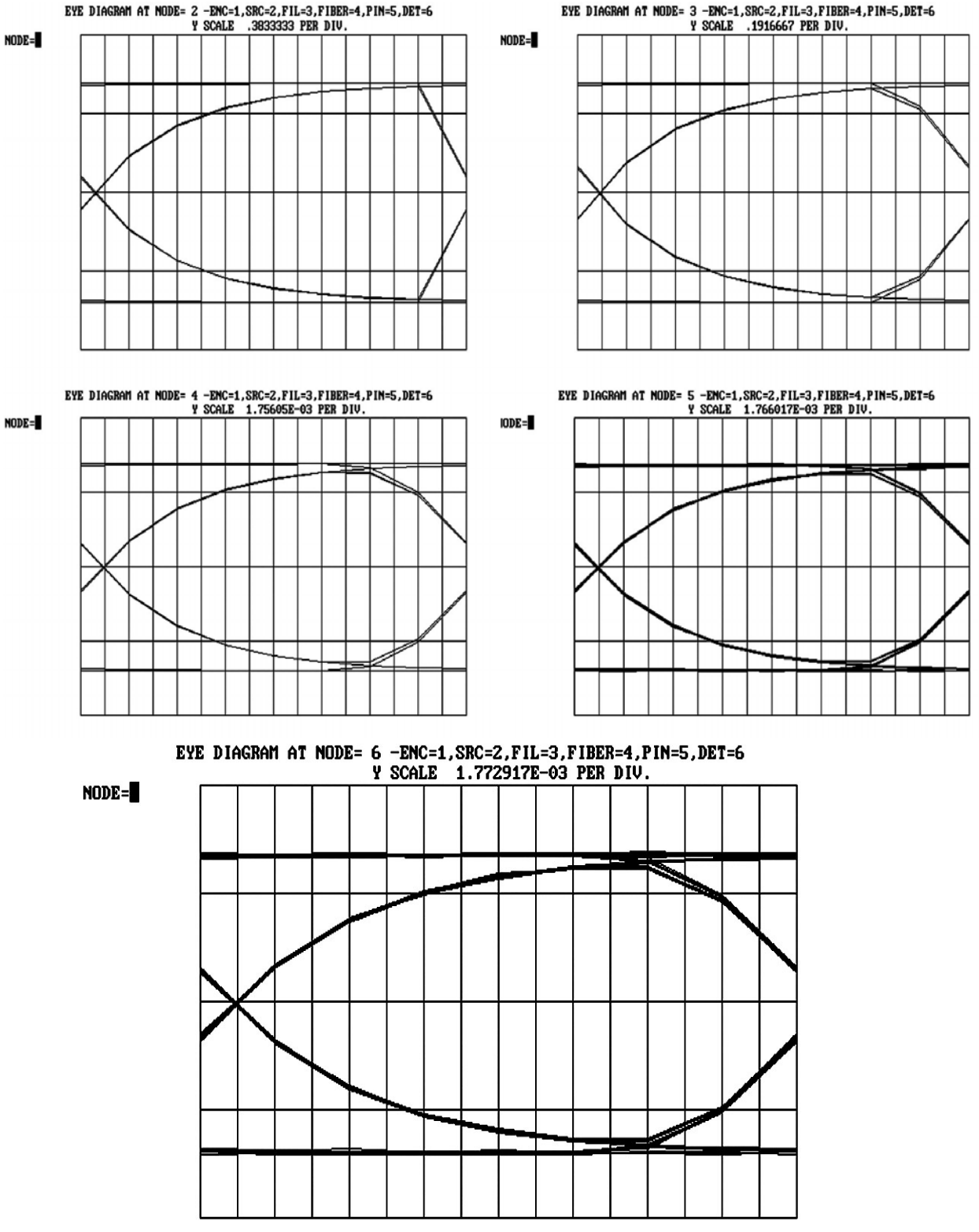

Fig 8.2 Eye diagrams at different nodes

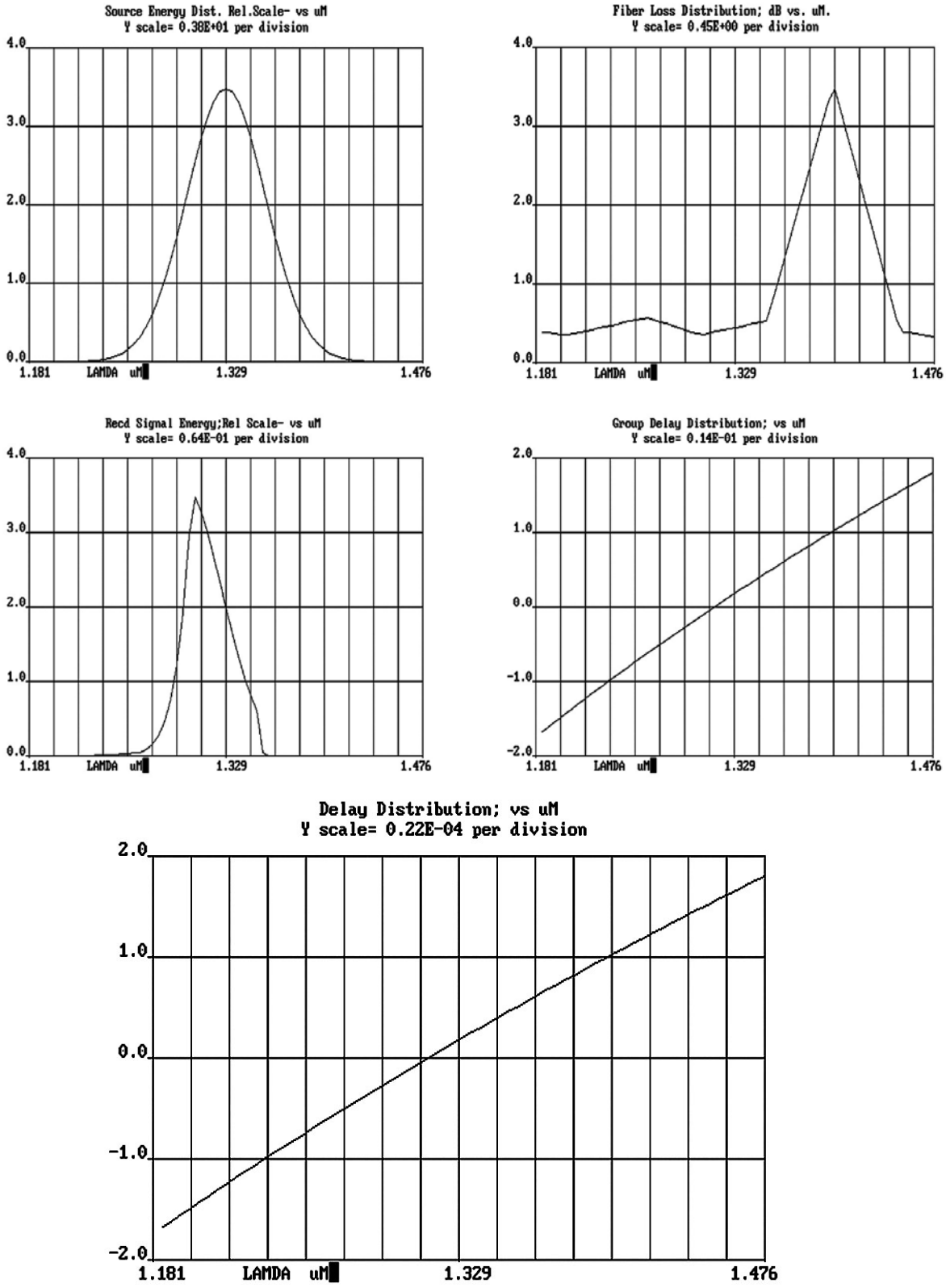

Fig 8.3 Source energy distribution, fiber loss distribution, received signal energy, group delay distribution and delay distribution.

b) Simulation results for 100km and 320 MB/s system

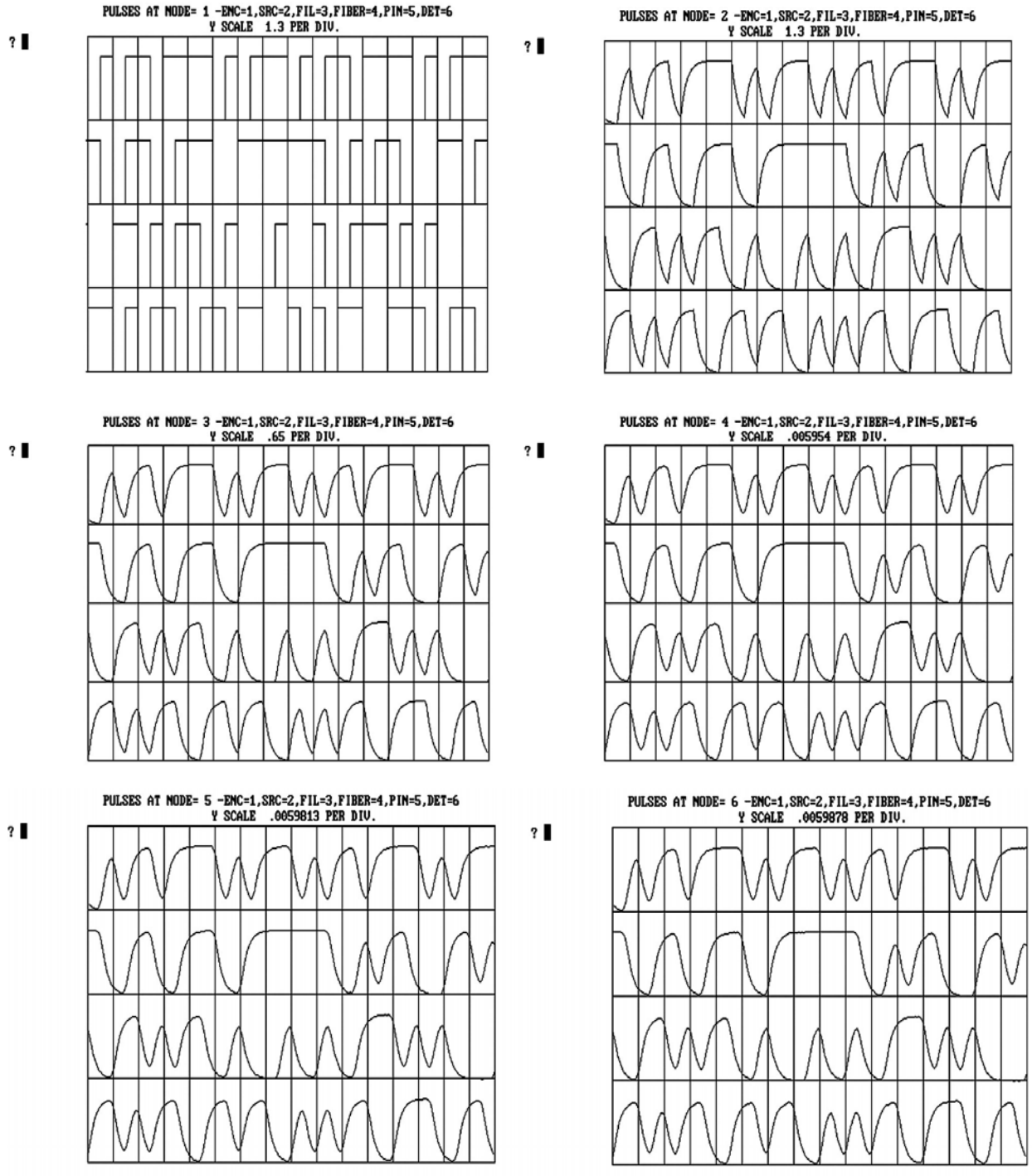

Fig 8.4 Pulse shapes at different nodes

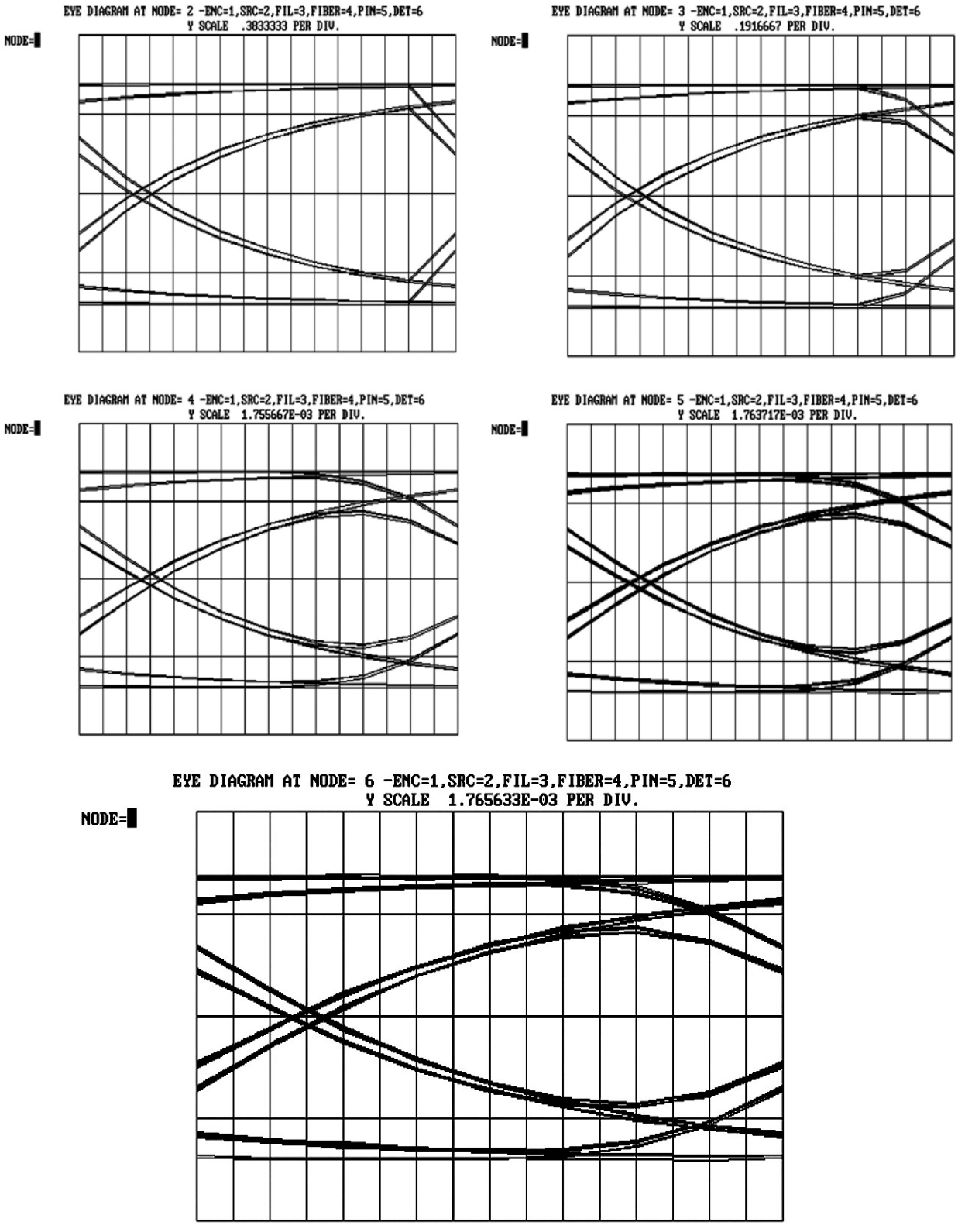

Fig 8.5 Eye diagrams at different nodes

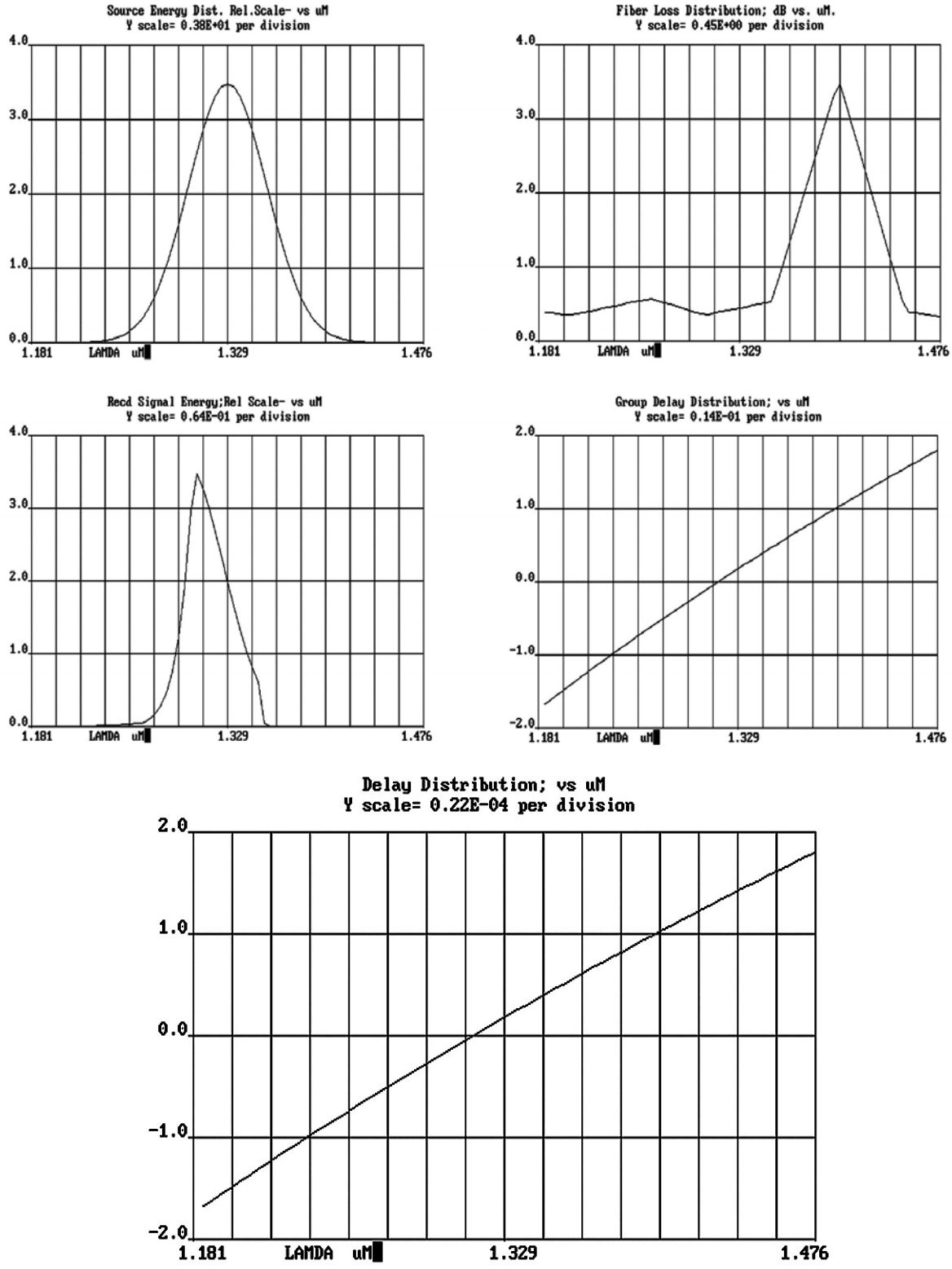

Fig 8.6 Source energy distribution, fiber loss distribution, received signal energy, group delay distribution and delay distribution.

8.1.2 Effects of Noisy LEDs

a). Simulation results for system with Noisy LED sources (fiber length 100 km, the rate is 160 Mb/s and the wave length is 1.329μm).

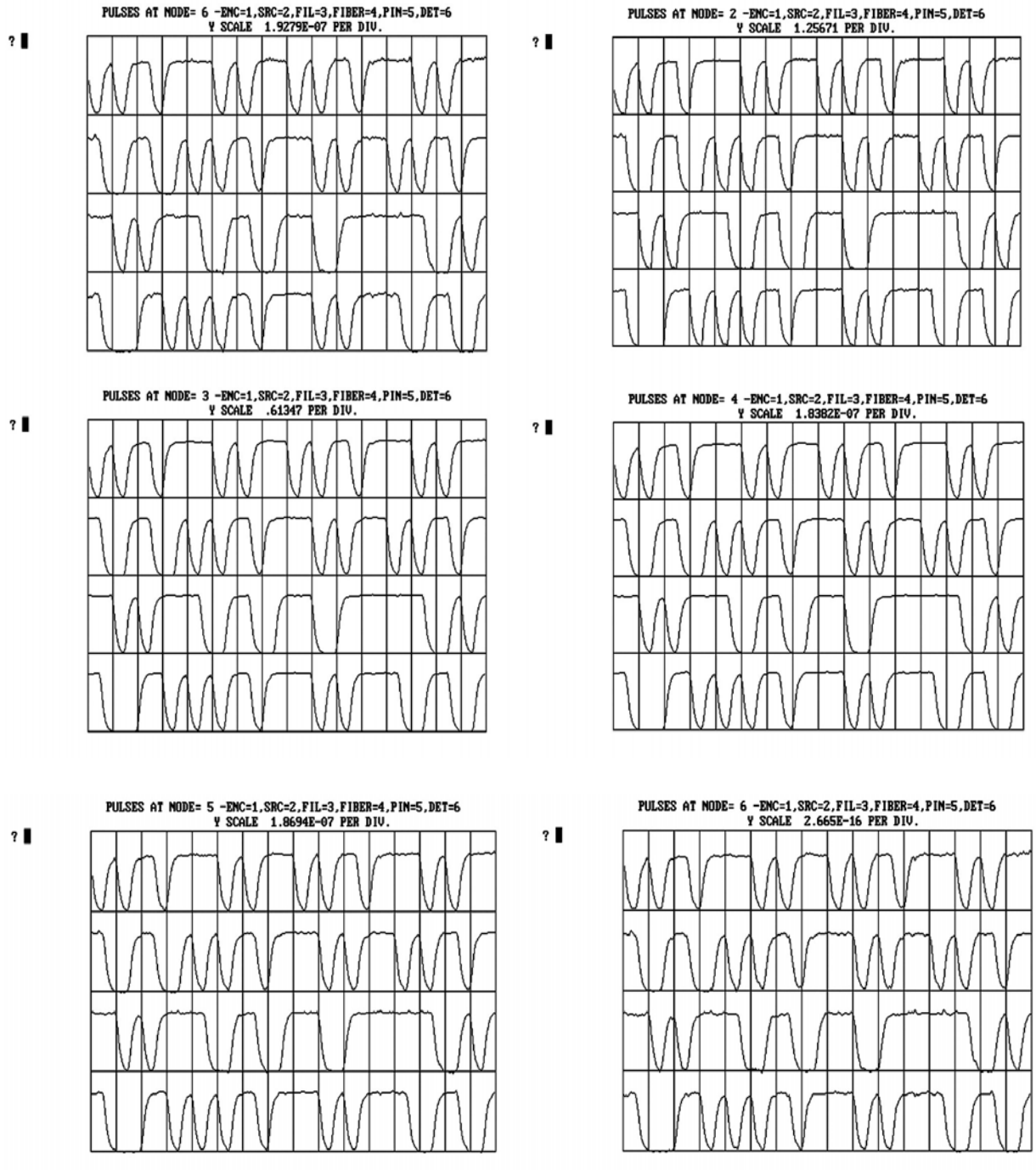

Fig 8.7 Pulse shapes at different nodes

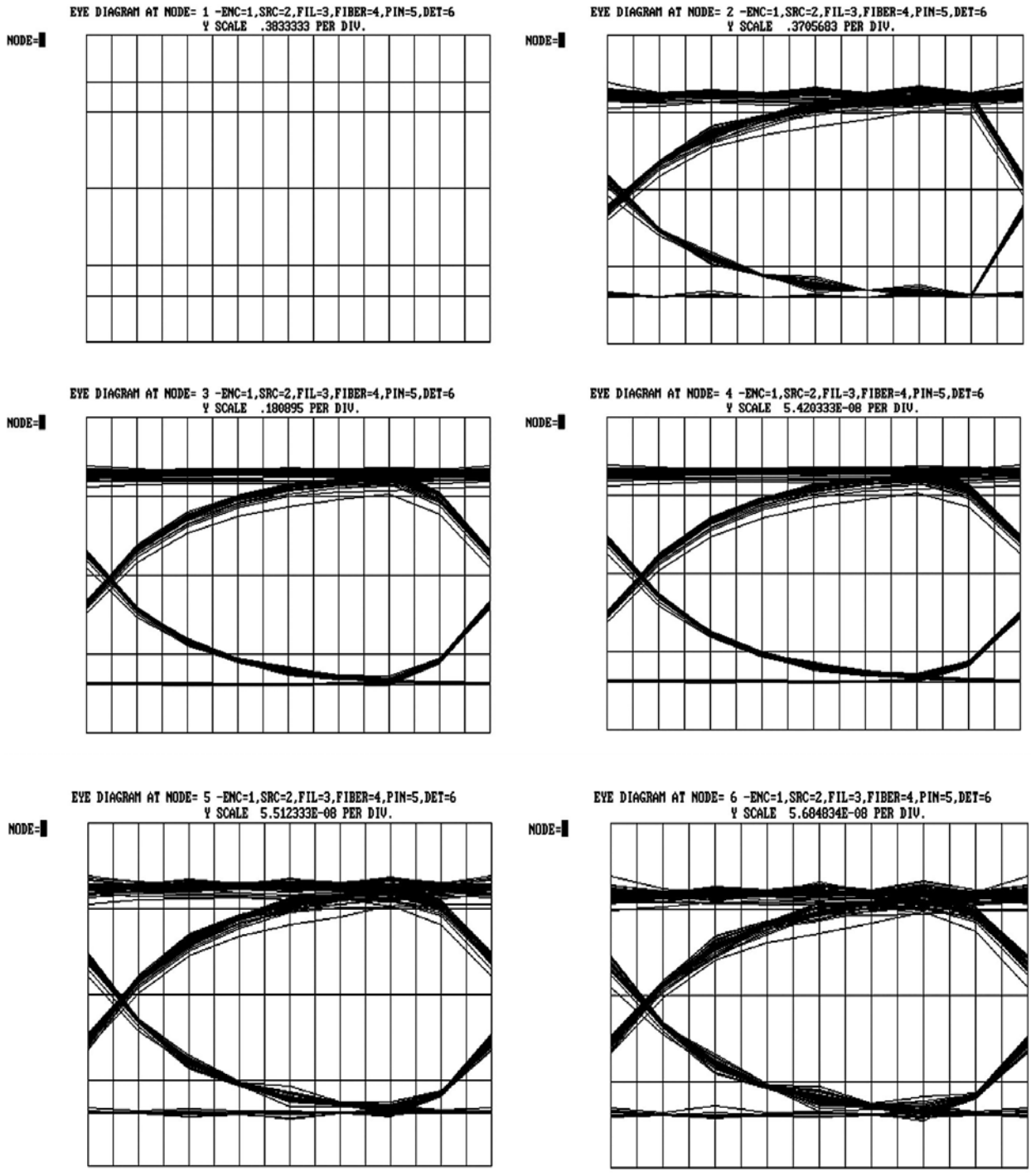

Fig 8.8 Eye diagrams at different nodes

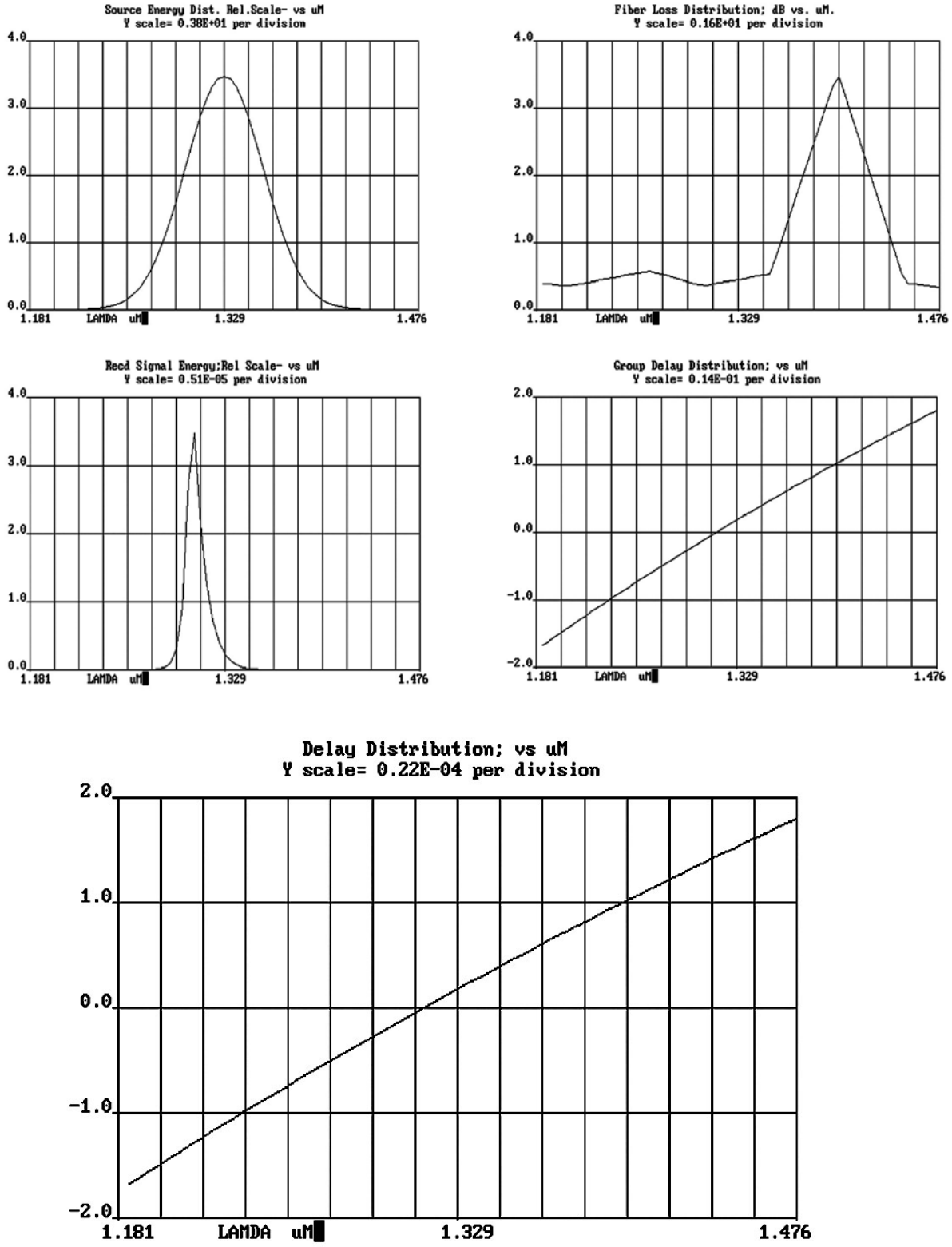

Fig 8.9 Source energy distribution, fiber loss distribution, received signal energy, group delay distribution.

b) Simulation results for system with Noisy LED sources (fiber length 250 km, the rate is 160 Mb/s and the wave length is 1.329μm).

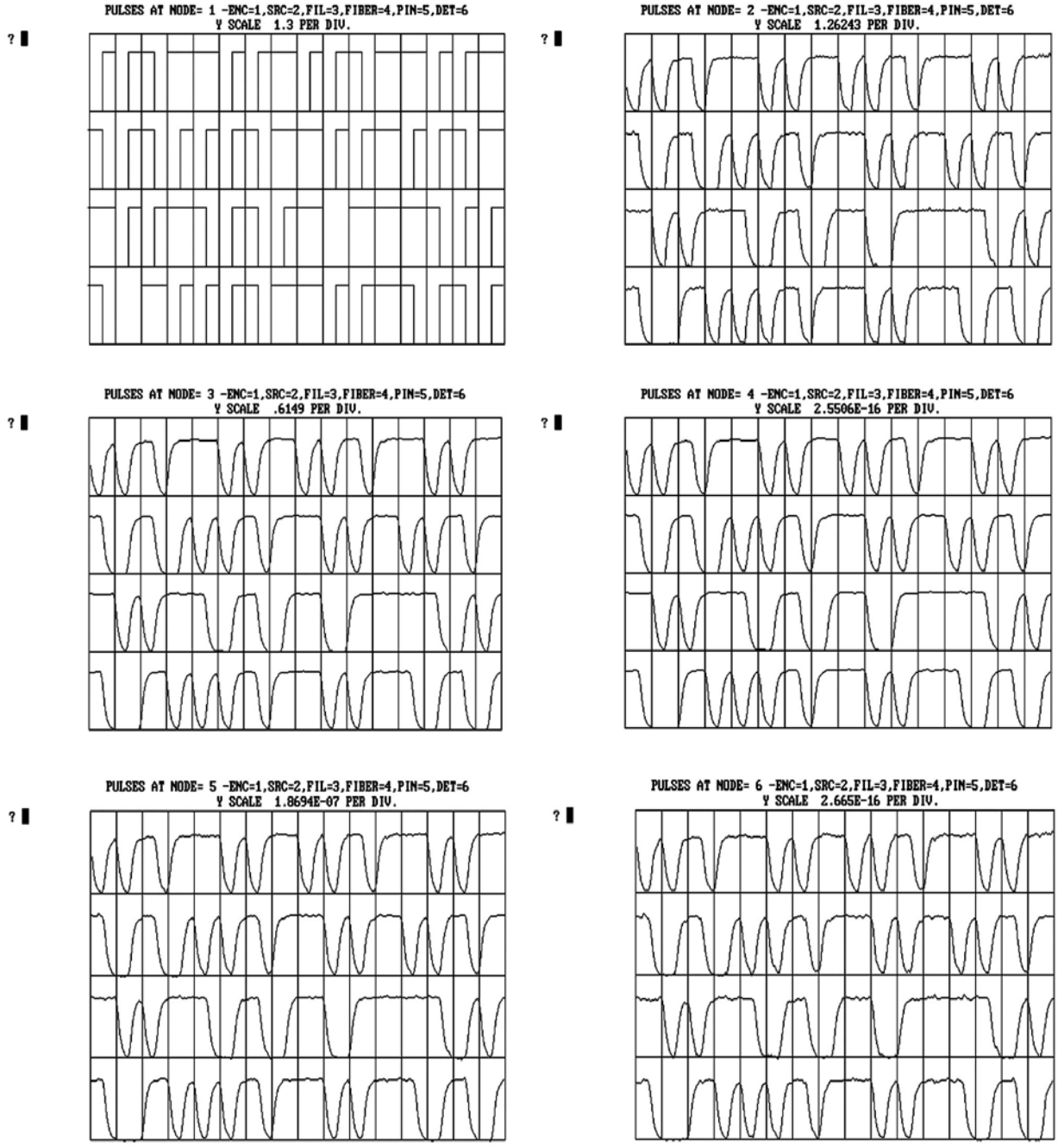

Fig 8.10 Pulse shapes at different nodes

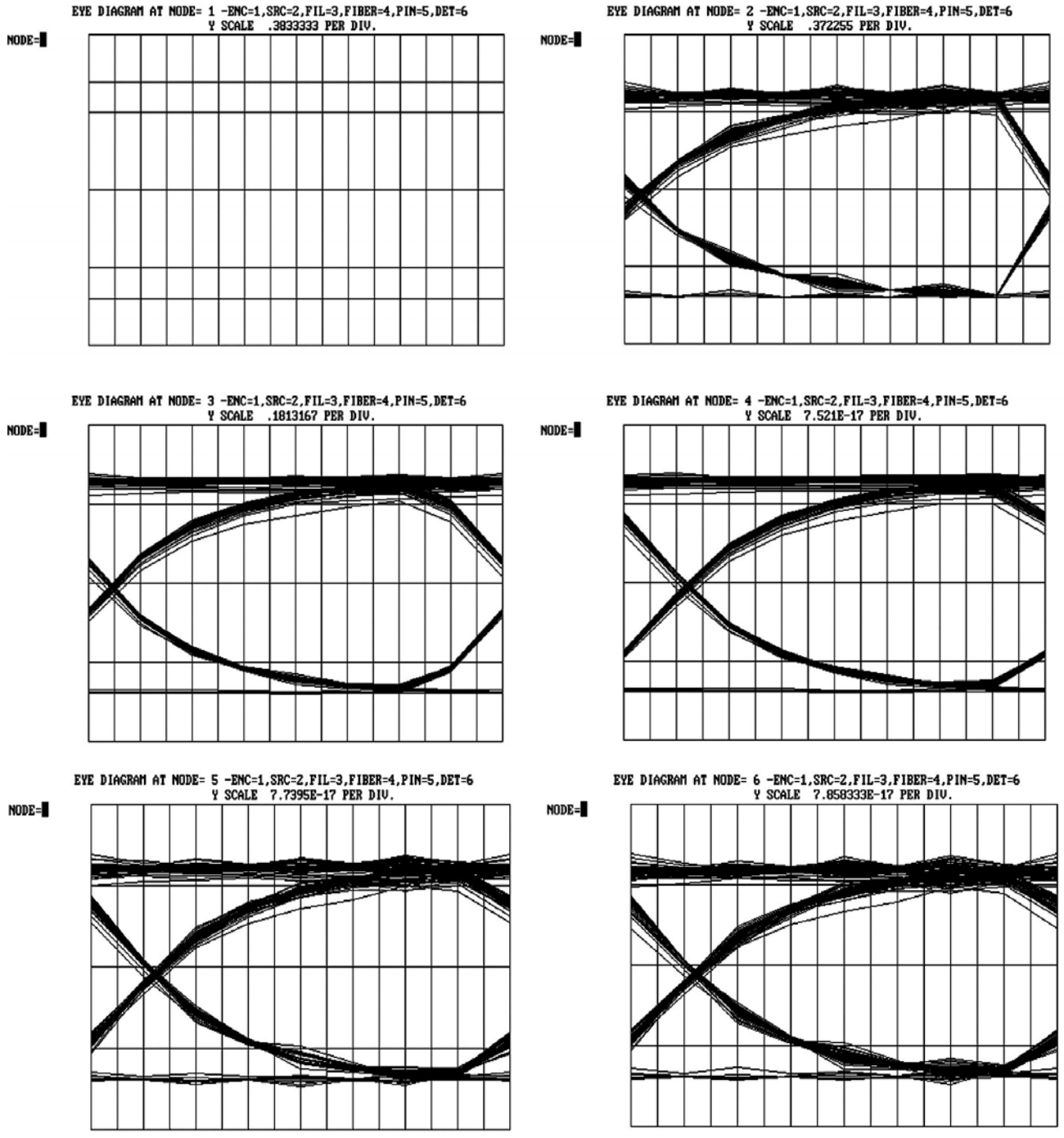

Fig 8.11 Eye diagrams at different nodes

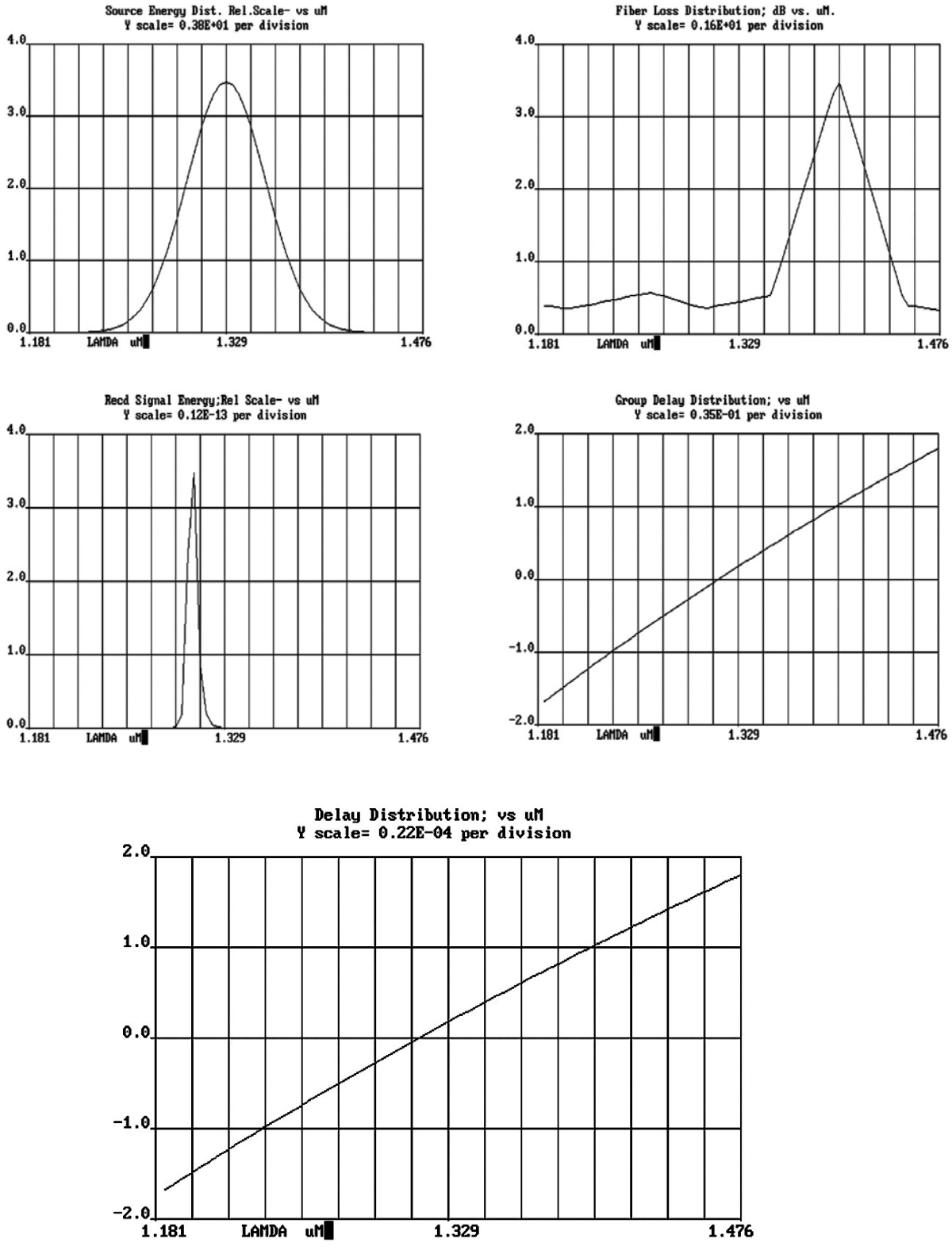

Fig 8.12 Source energy distribution, fiber loss distribution, received signal energy, group delay distribution and delay distribution.

8.1.3 WDM systems

a). Simulation results for WDM system with Laser sources and grade 1 quality components. (fiber length is 100km, the rate is 160 Mb/s and the wave length is 1.329μm).

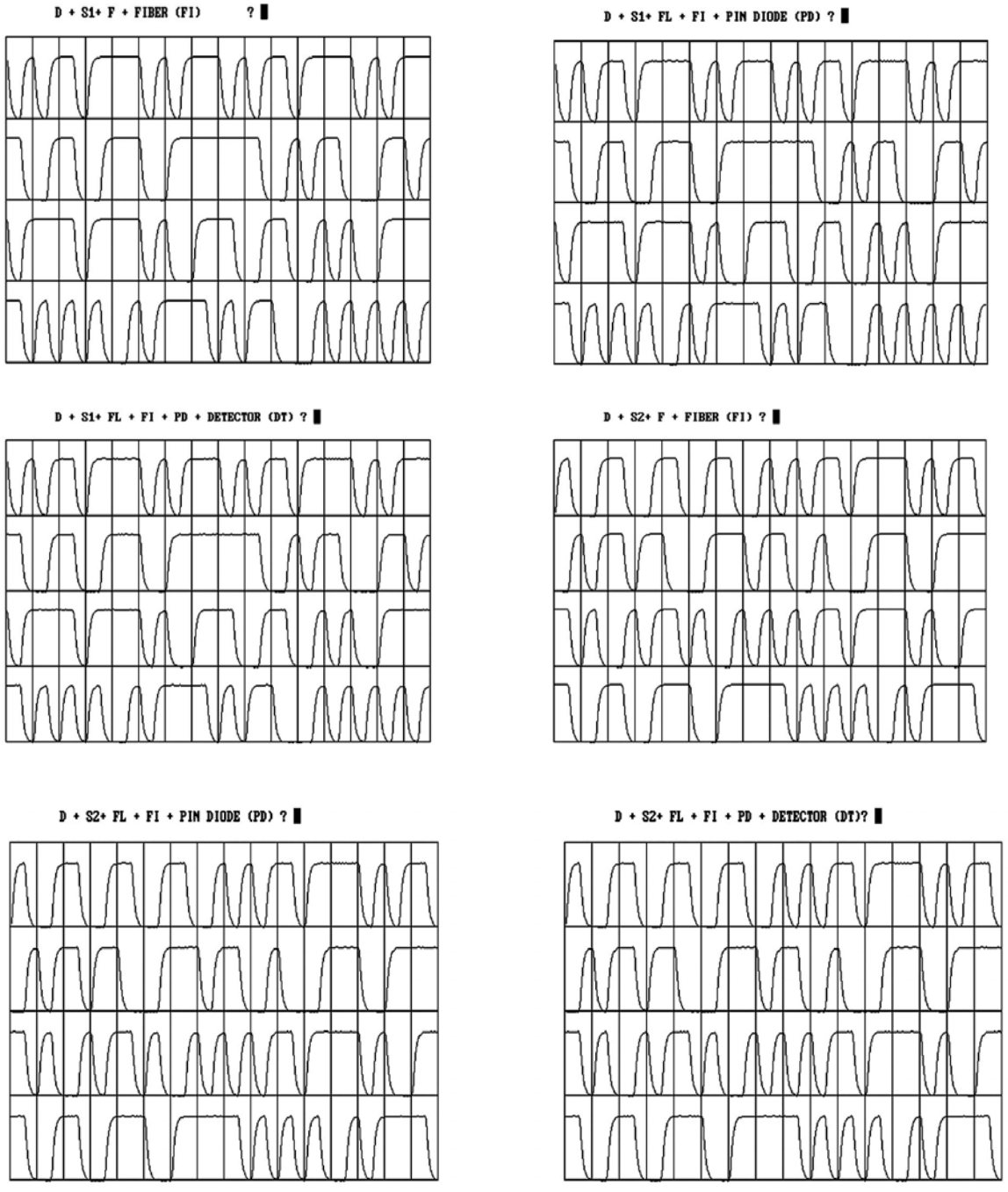

Fig 8.13 Pulse shapes at different nodes

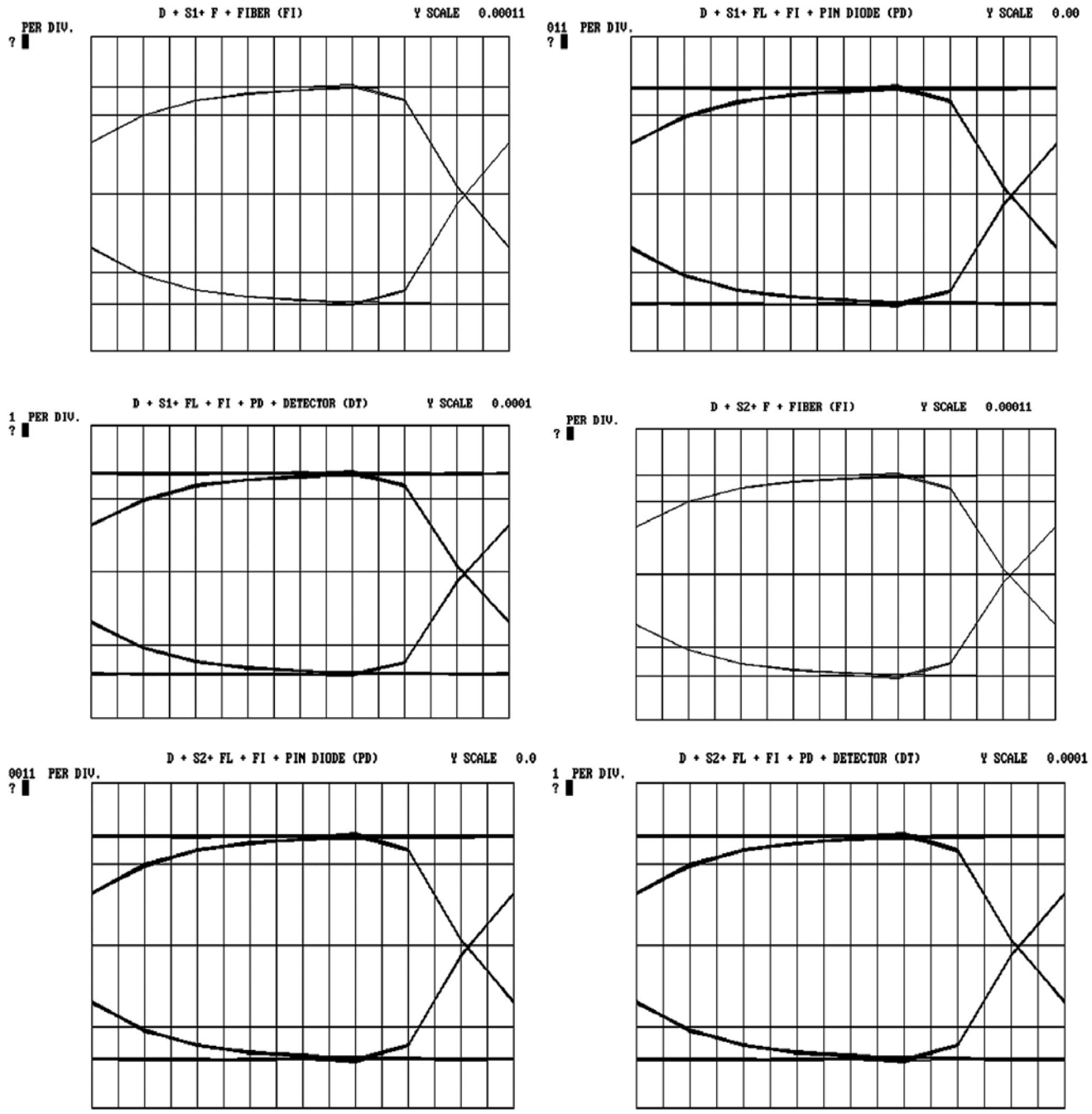

Fig 8.14 Eye diagrams for sources 1 and 2 at different nodes

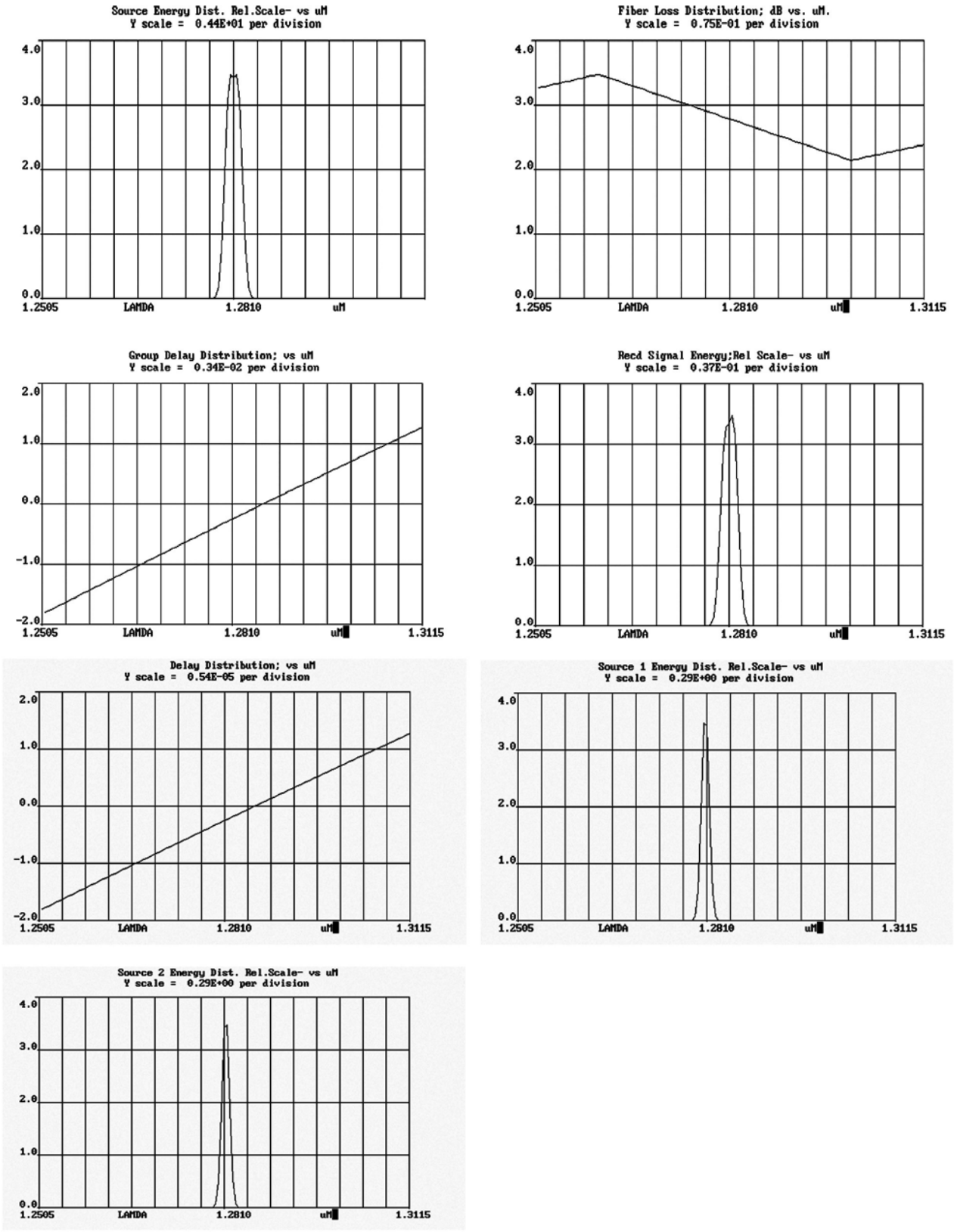

Fig 8.15 Source energy distribution, fiber loss distribution, group delay distribution, received signal energy, delay distribution, sources 1 and 2 energy distributions.

b) Simulation results for WDM system with Laser sources and grade 1 quality components. (fiber length is 200km, the rate is 160 Mb/s and the wave length is 1.329μm).

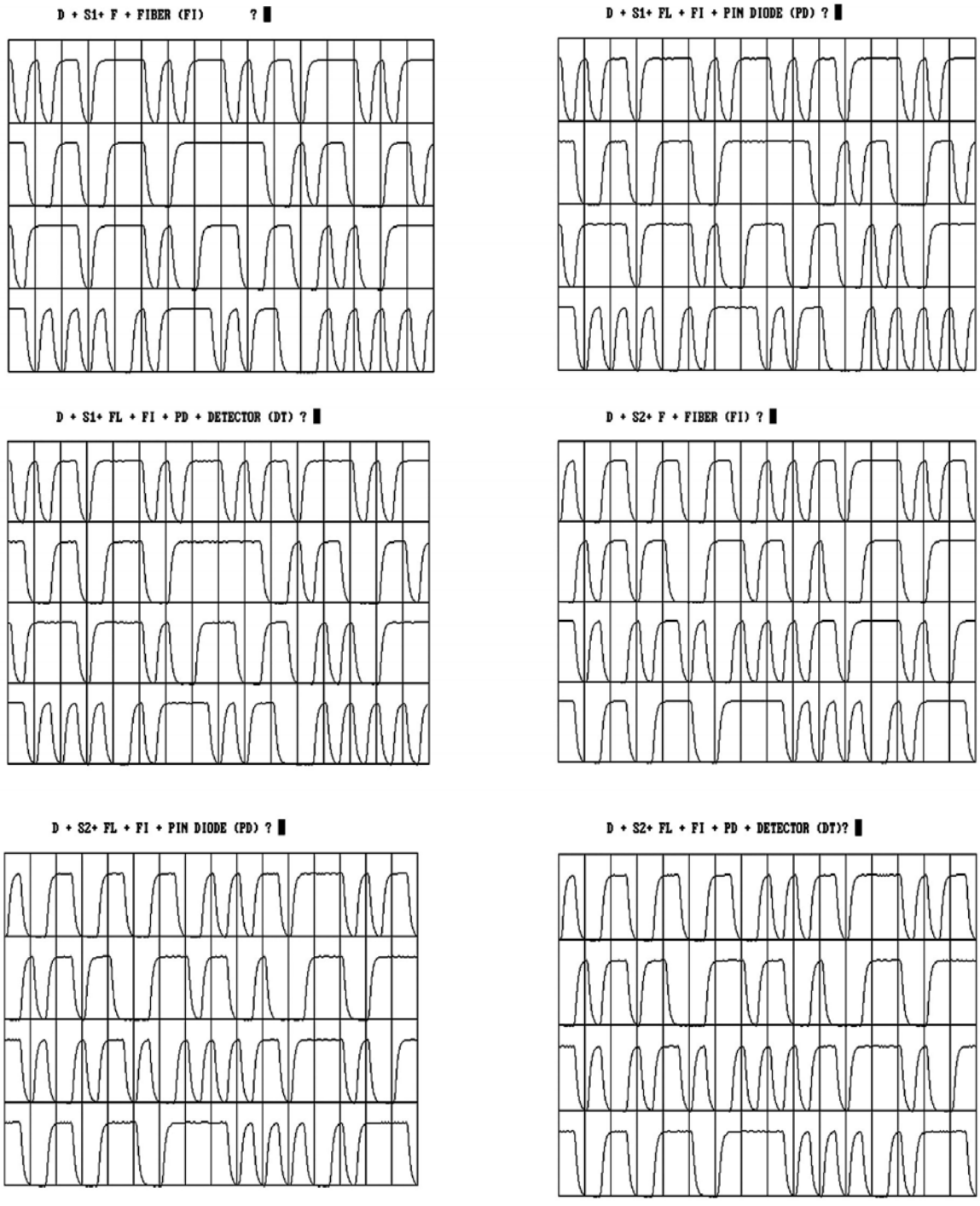

Fig 8.16 Pulse shapes at different nodes

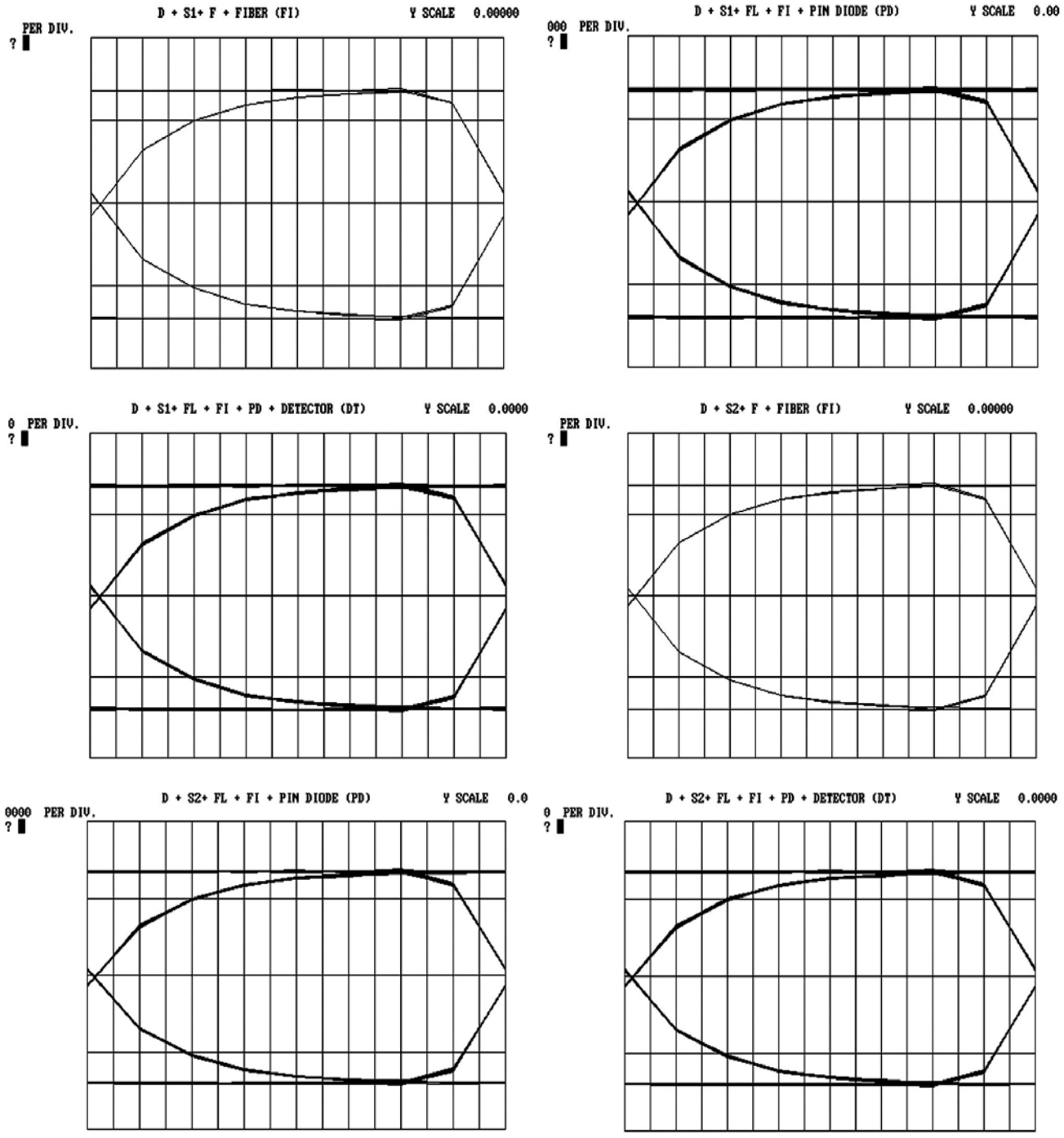

Fig 8.17 Eye diagrams at different nodes

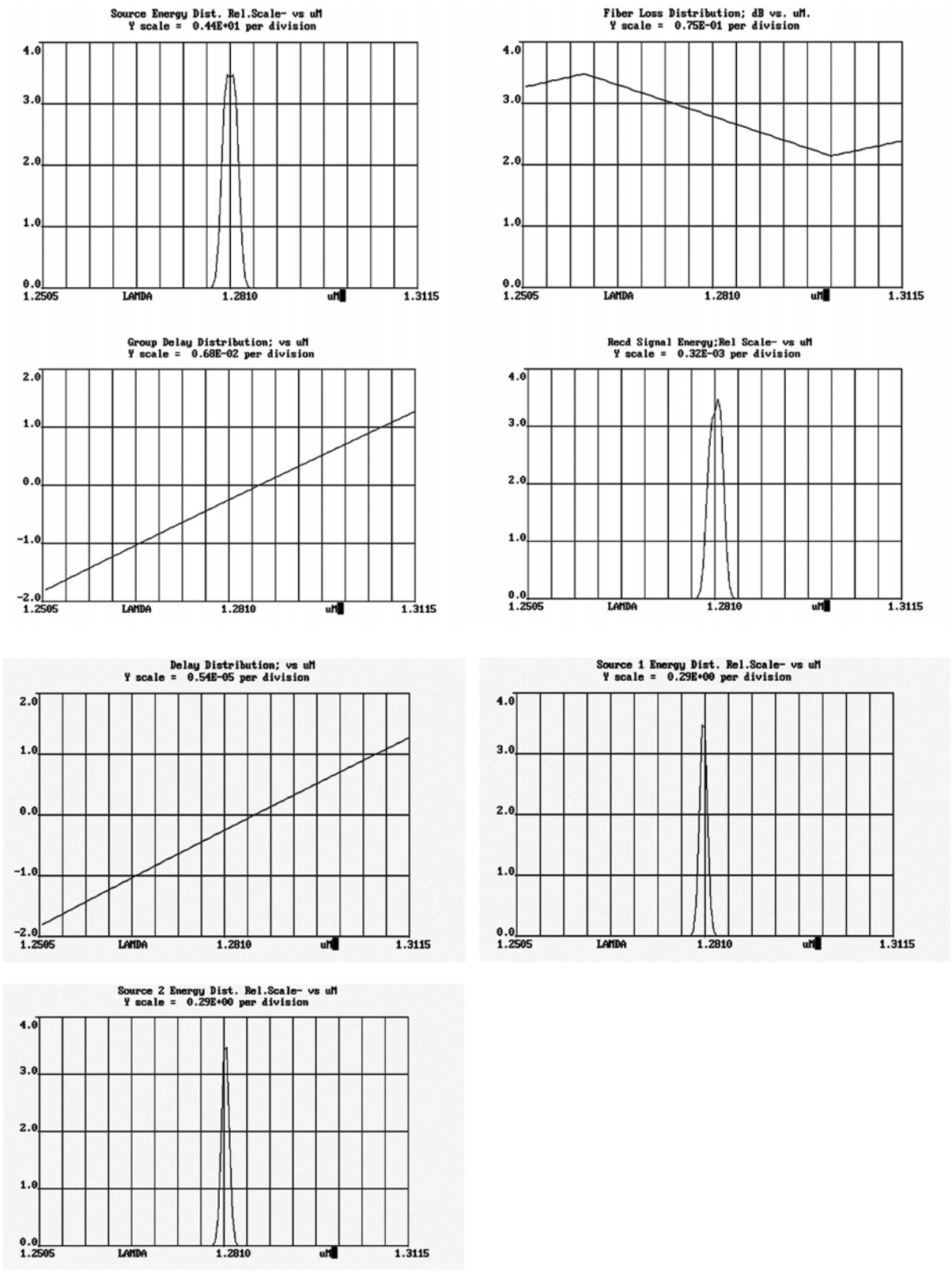

Fig 8.18 Source energy distribution, fiber loss distribution, group delay distribution, received signal energy, delay distribution, sources 1 and 2 energy distributions

c) Simulation results for WDM system with grade 1 components and LED's (fiber length is 200km, rate is 160 Mb/s and the wavelength is 1.329μm).

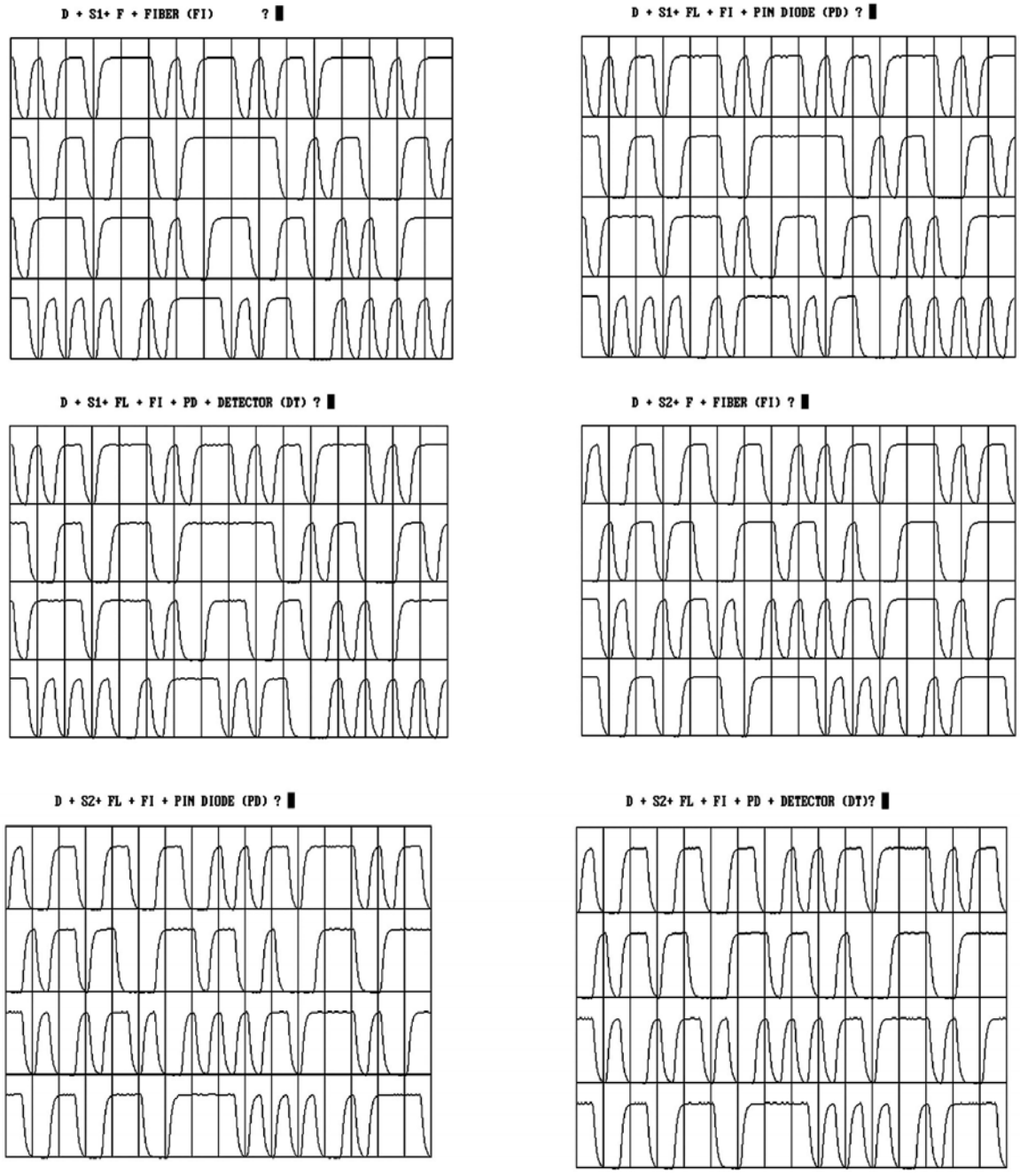

Fig 8.19 Data pulse shapes at different nodes

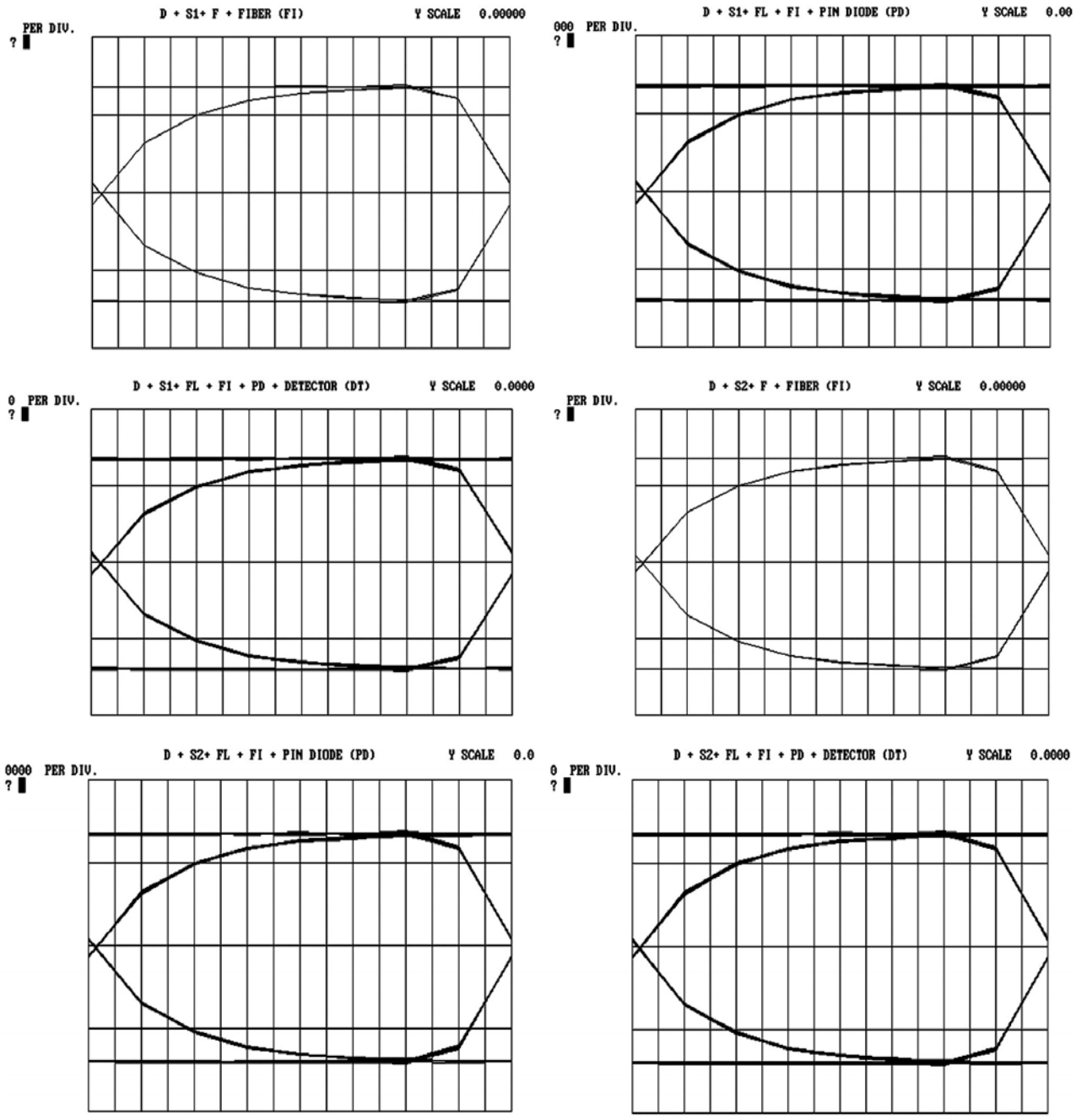

Fig 8.20 Eye diagrams at different nodes.

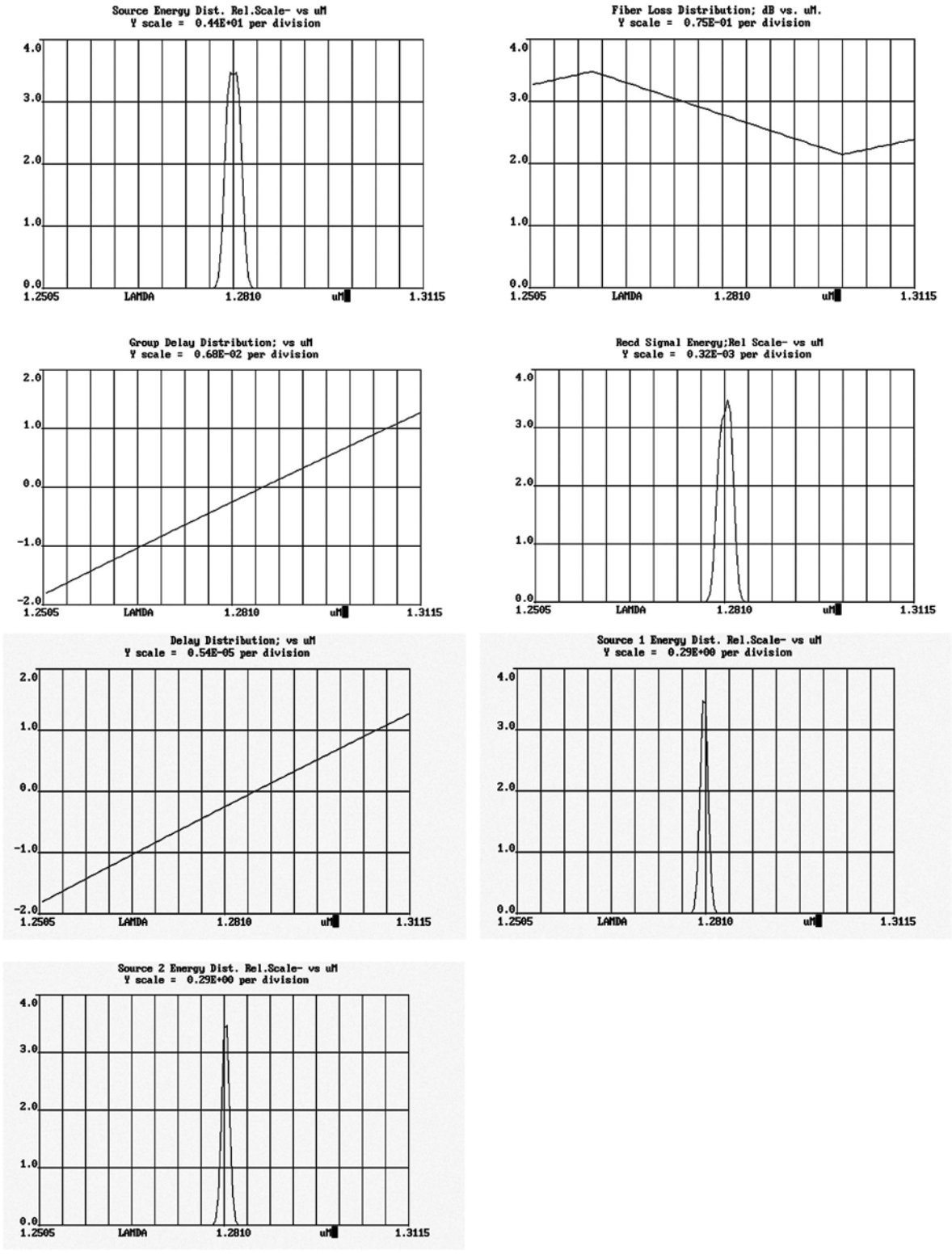

Fig 8.21 Source energy distribution**,** fiber loss distribution, group delay distribution, received signal energy, delay distribution and sources 1 and 2 energy distributions.

d). Simulation results for WDM system with LED's and Grade 5 components (fiber length is 100 km, rate is 160 Mb/s and the wavelength is 1.329μm).

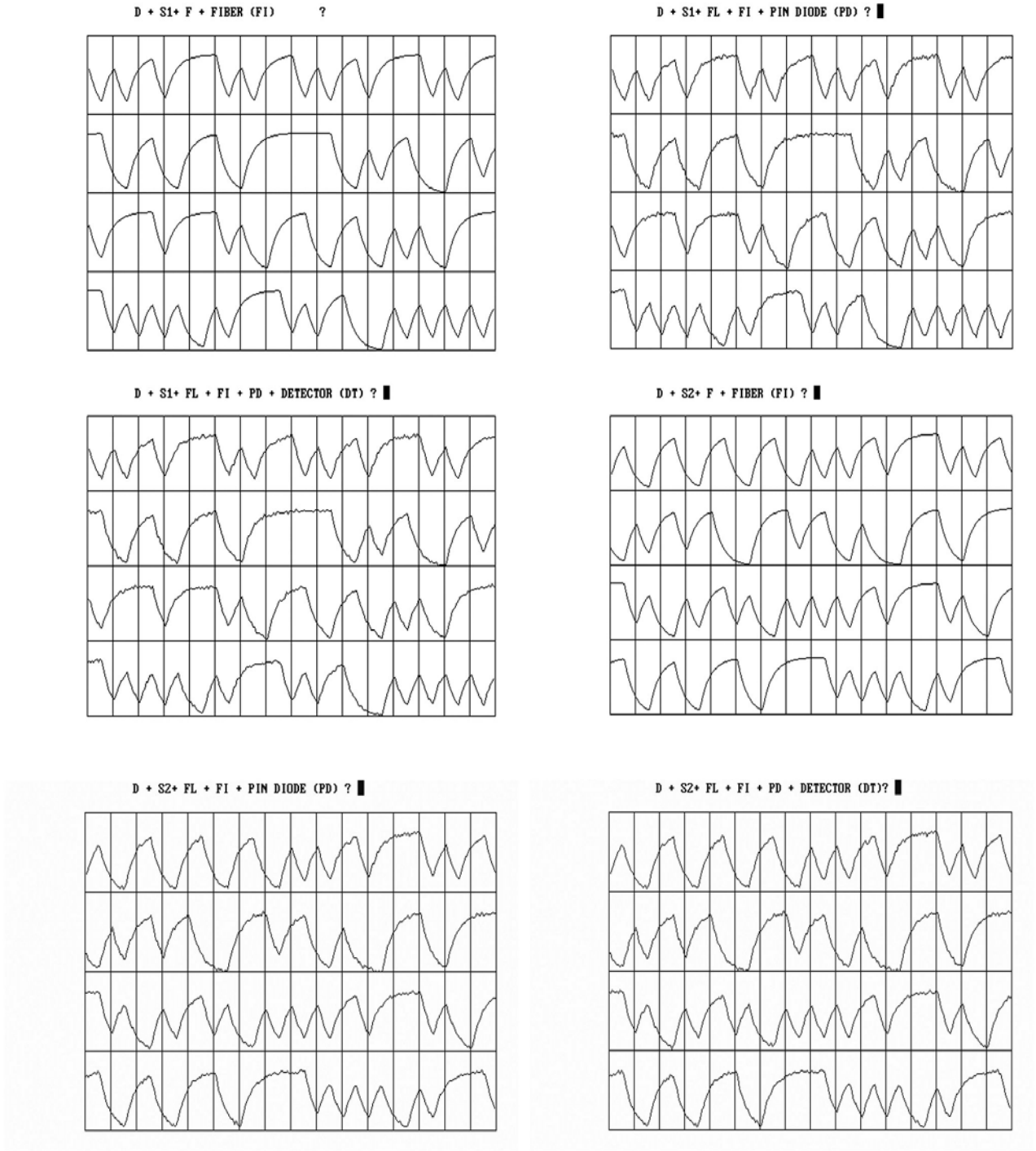

Fig 8.22 Pulse shapes at different nodes

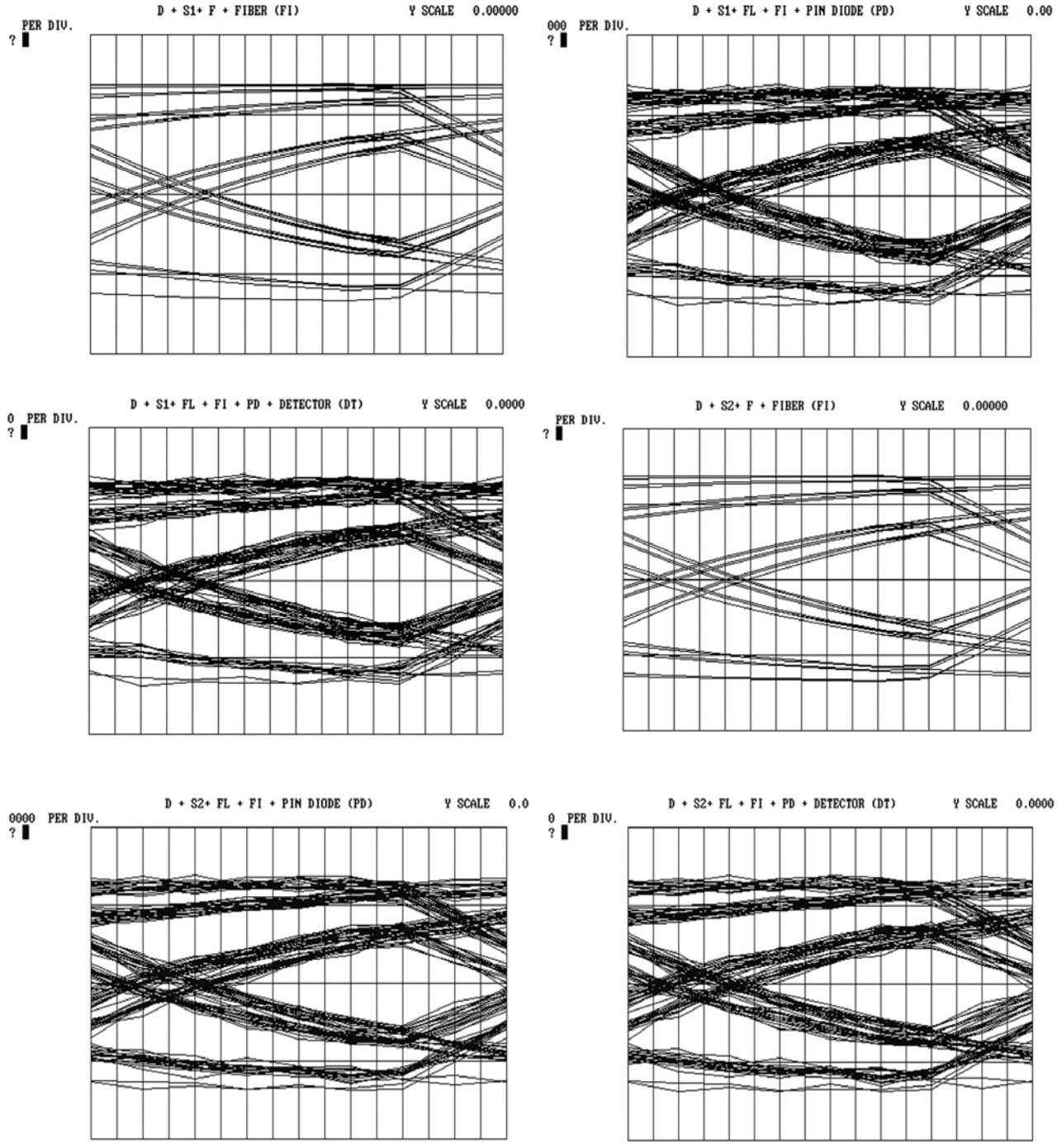

Fig 8.23 Eye diagrams at different nodes

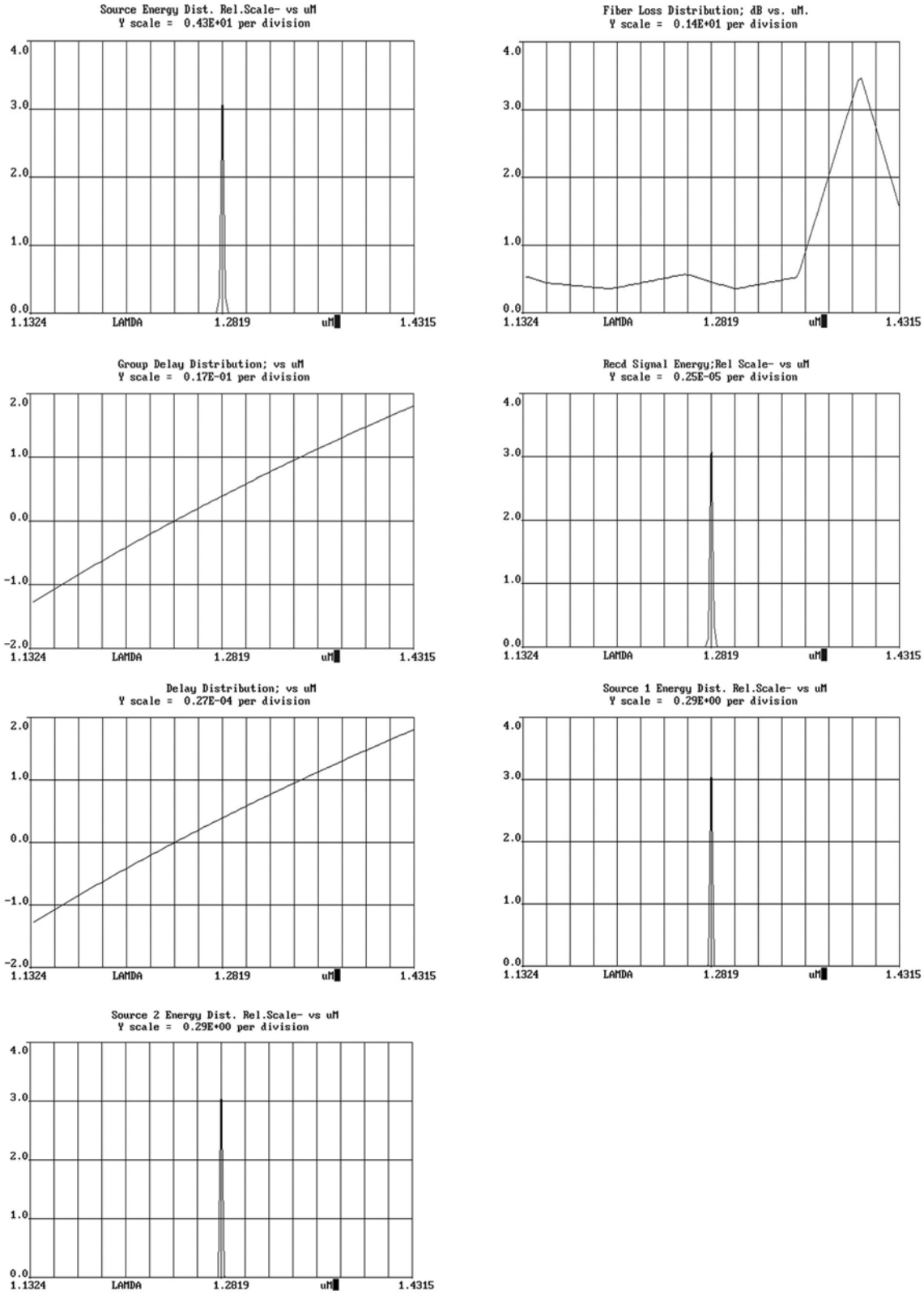

Fig 8.24 Source energy distribution, fiber loss distribution, group delay distribution, received signal energy ,delay distribution, Source 1 & source 2 energy distributions.

8.1.4 Erbium Doped Fiber simulation

a) Simulation results for Erbium doped fiber system with 0% leakage. Fiber length is 100 km and the rate is 160 MB/s.

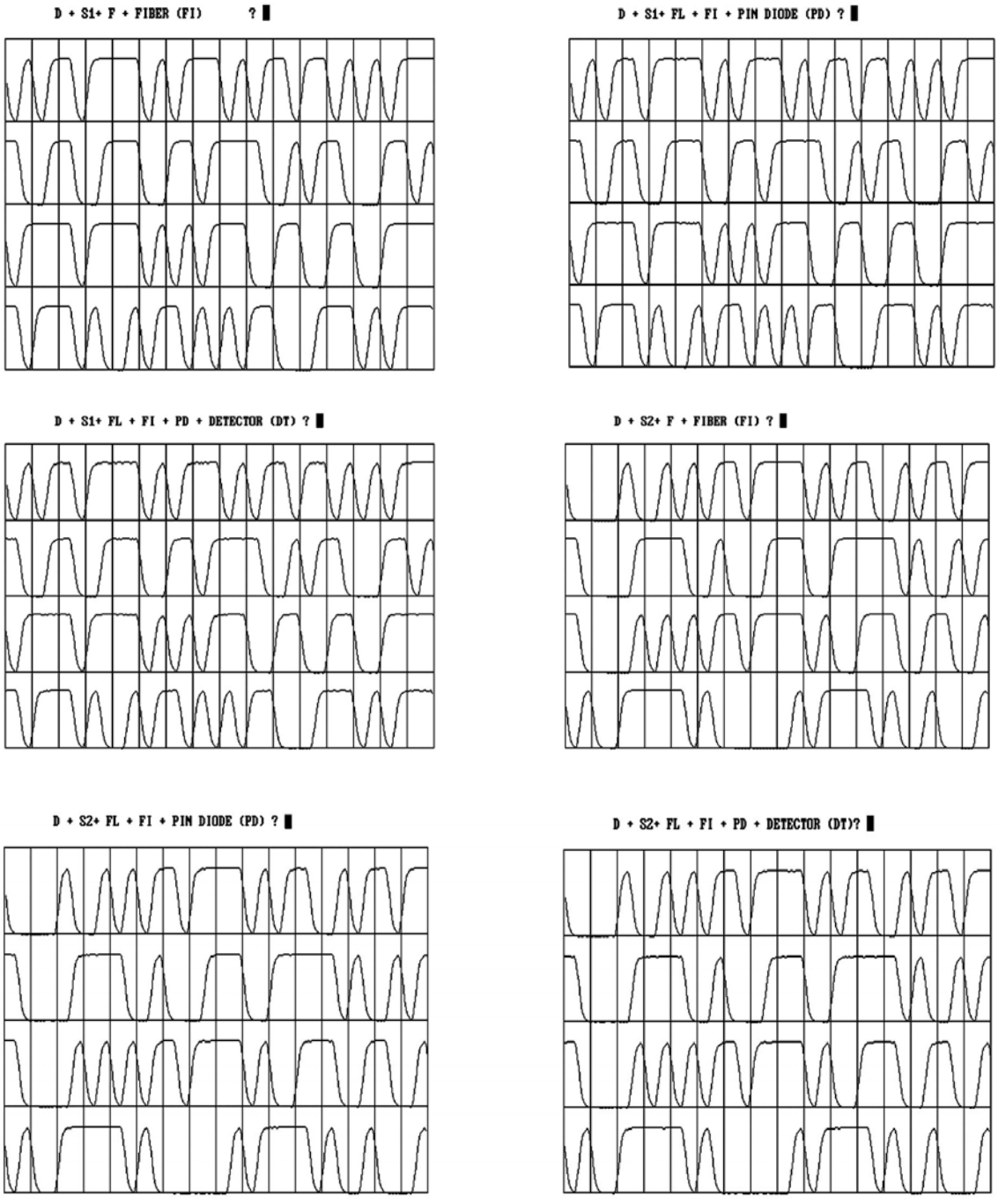

Fig 8.25 Pulse shapes at different nodes

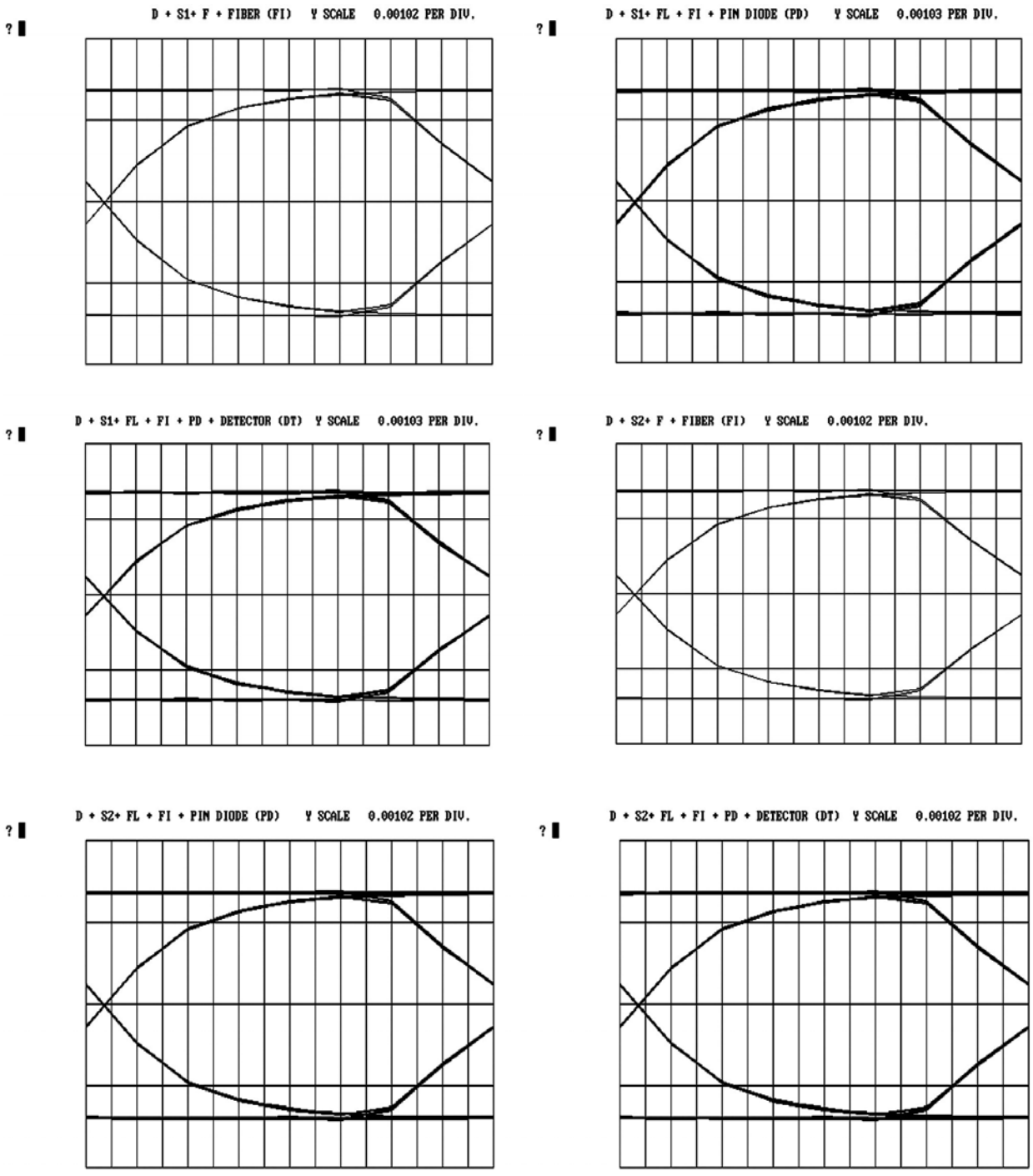

Fig 8.26 Eye diagrams at different nodes

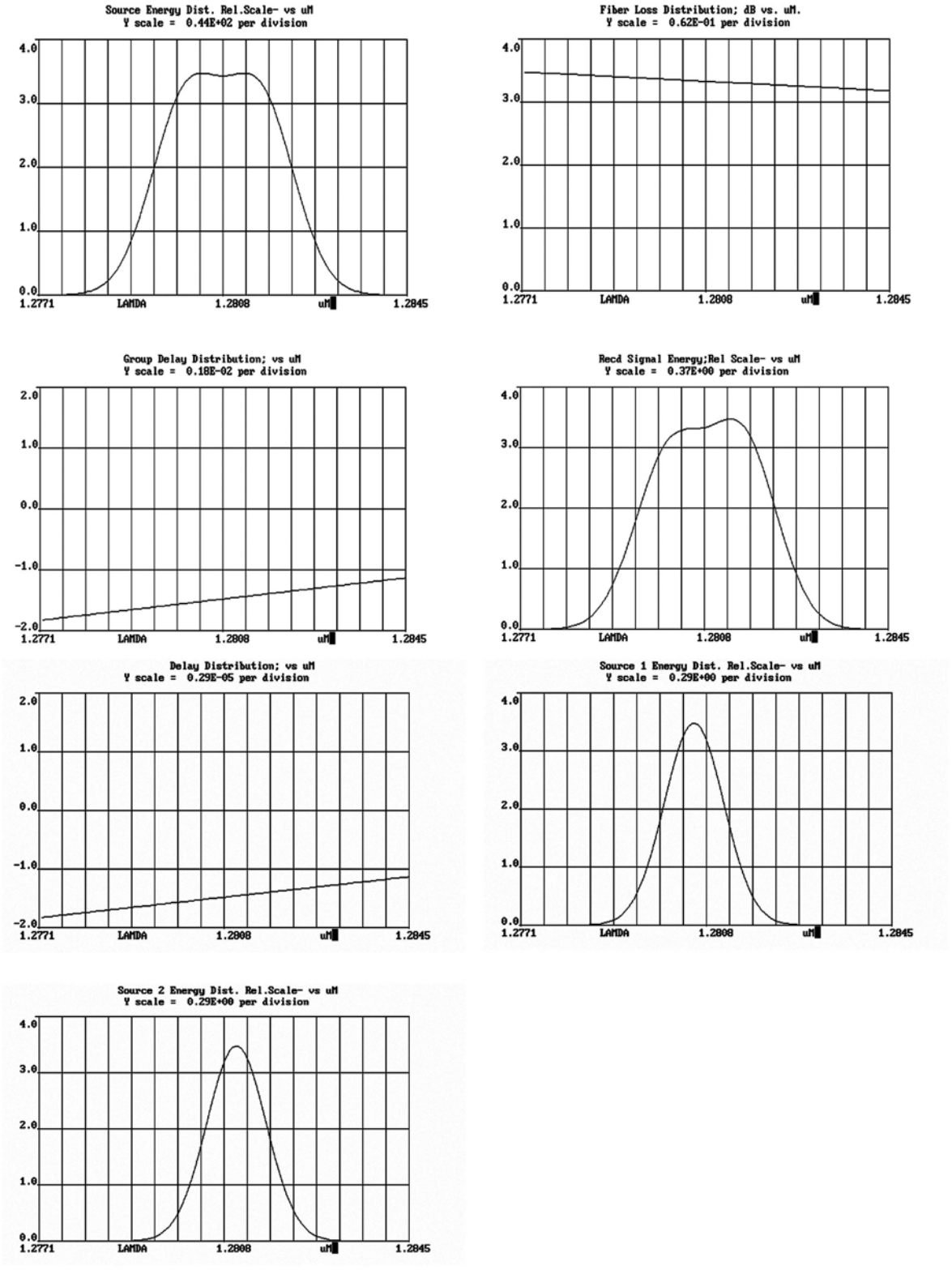

Fig 8.27 Source energy distribution, fiber loss distribution, group delay distribution, received signal energy, delay distribution, sources 1 and 2 energy distributions.

b) Simulation results for Erbium doped fiber system with 1% leakage. Fiber length is 100 km and the rate is 160 MB/s.

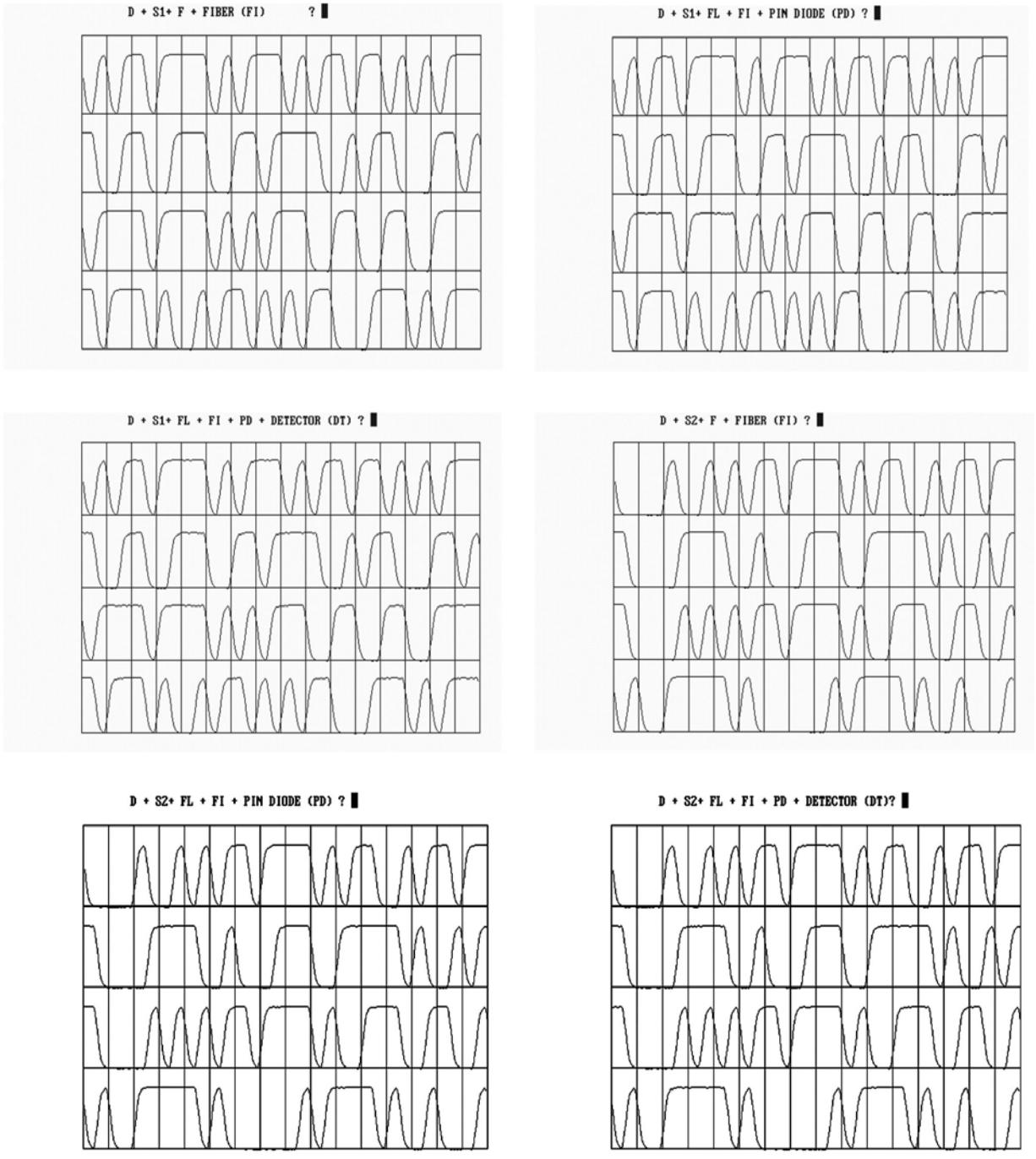

Fig 8.28 Pulse shapes at different nodes

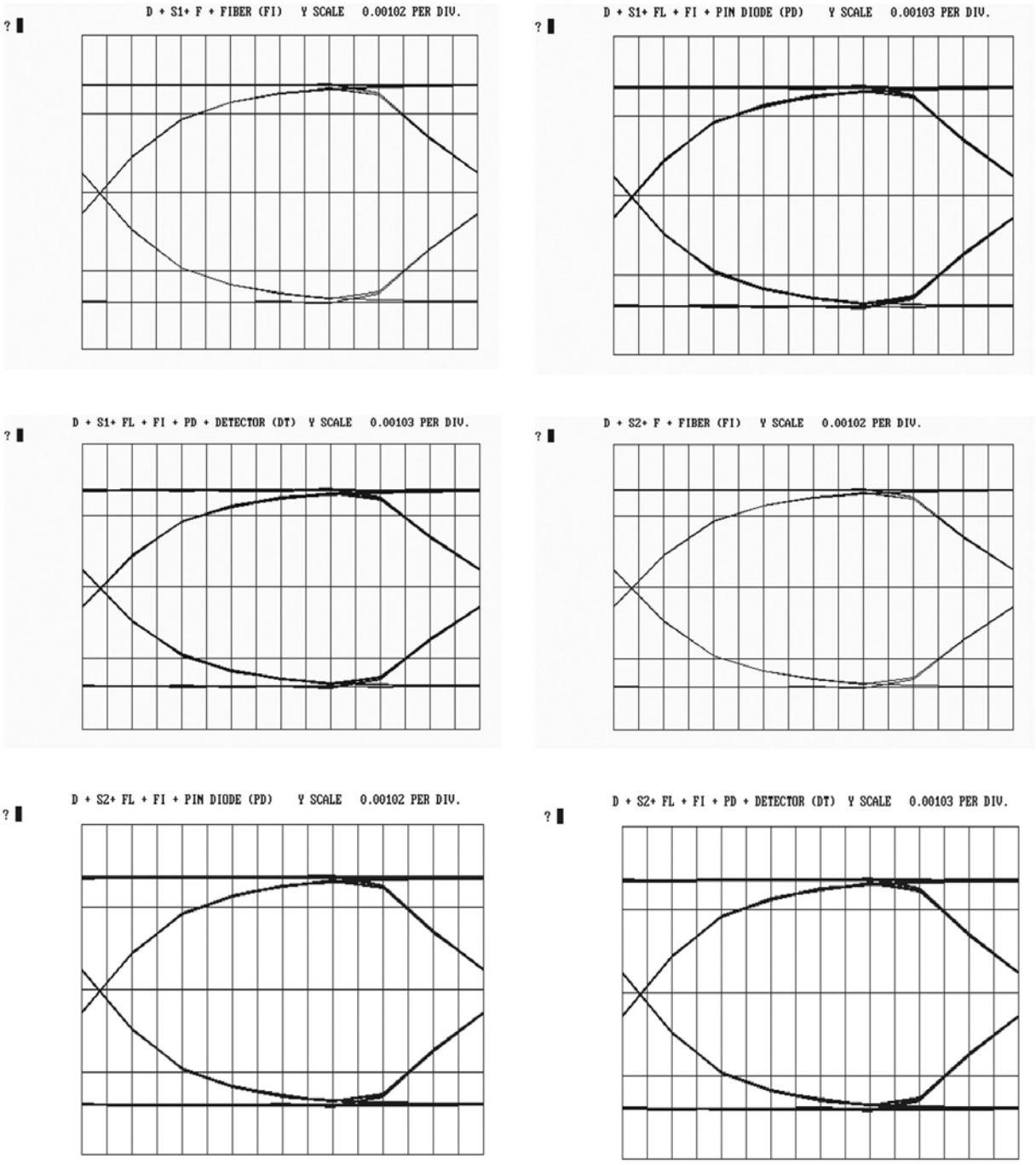

Fig 8.29 Eye diagrams at different nodes

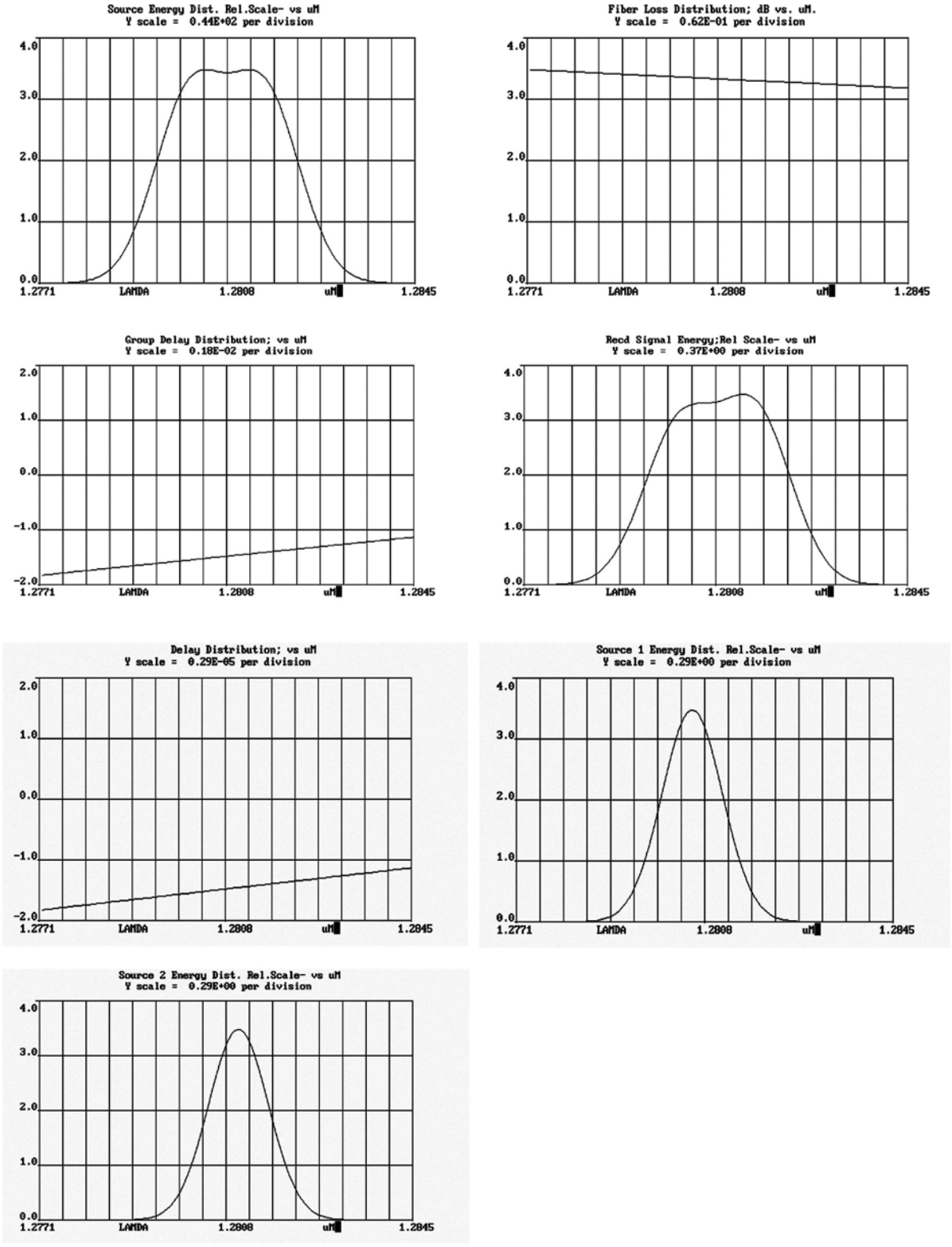

Fig 8.30 Source energy distribution, fiber loss distribution, group delay distribution, received signal energy, delay distribution, sources 1 and 2 energy distributions.

c) Simulation results for Erbium doped fiber system with 3% leakage. Fiber length is 100 km and the rate is 160 MB/s.

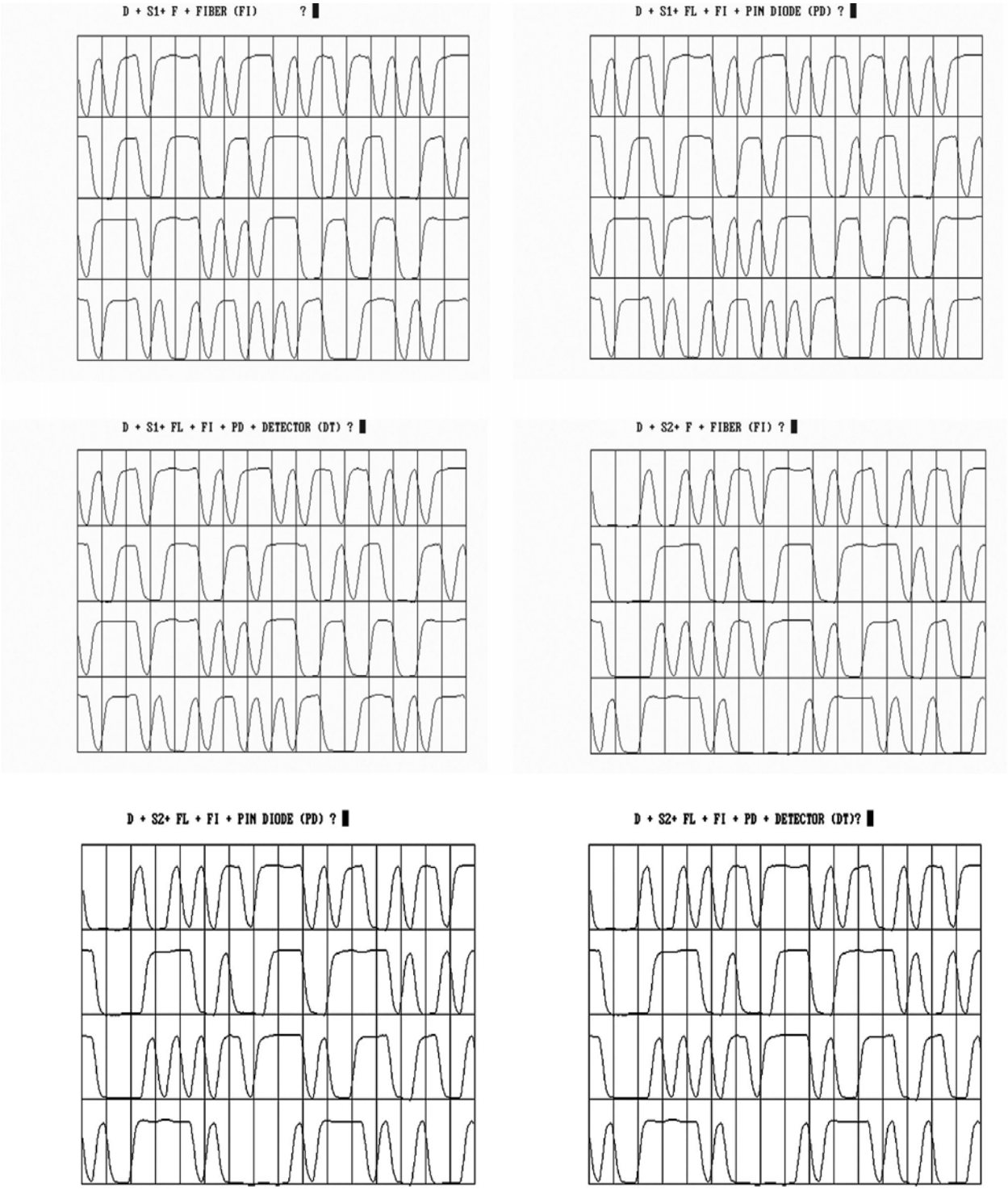

Fig 8.31 Pulse shapes at different nodes

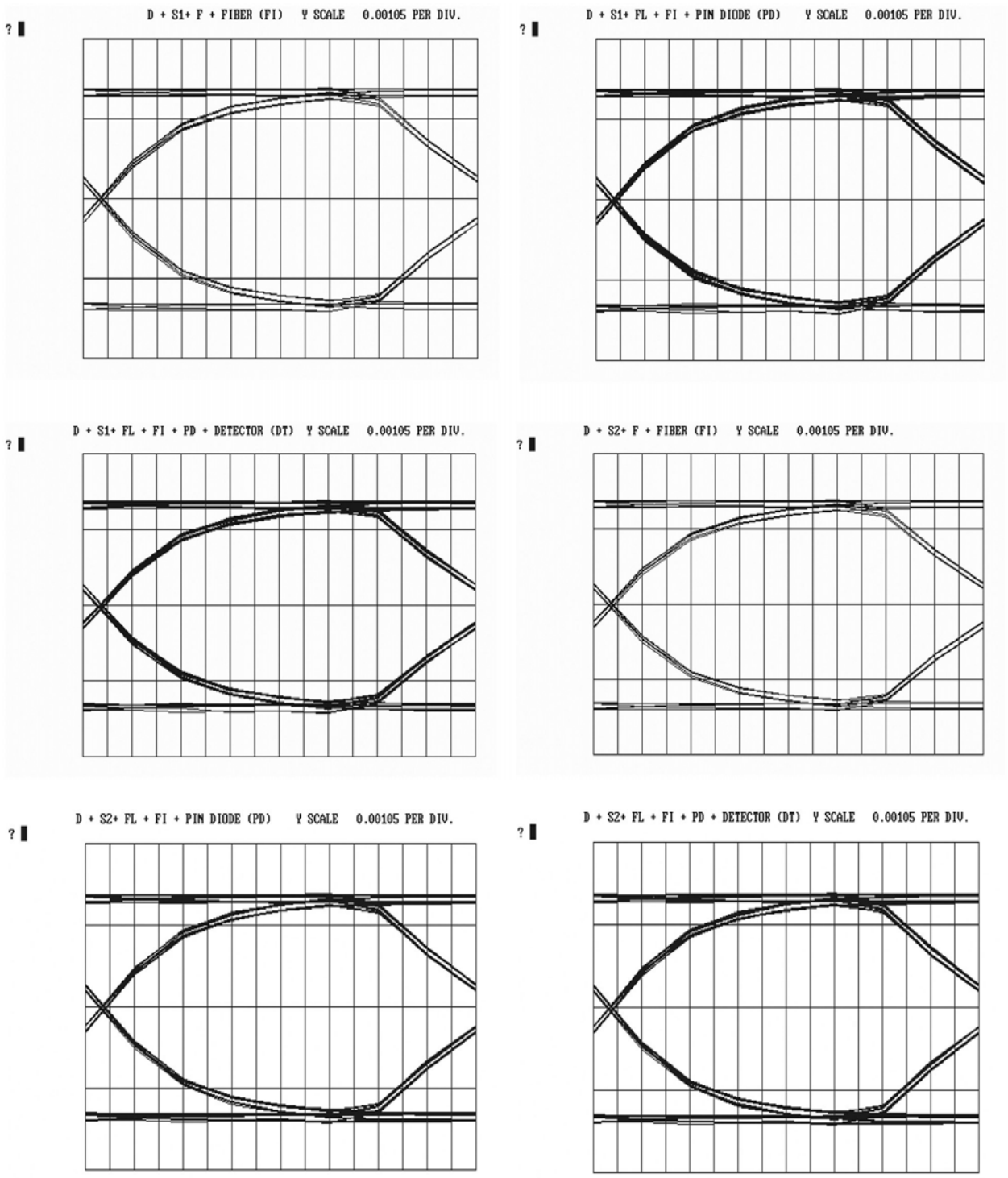

Fig 8.32 Eye diagrams at different nodes

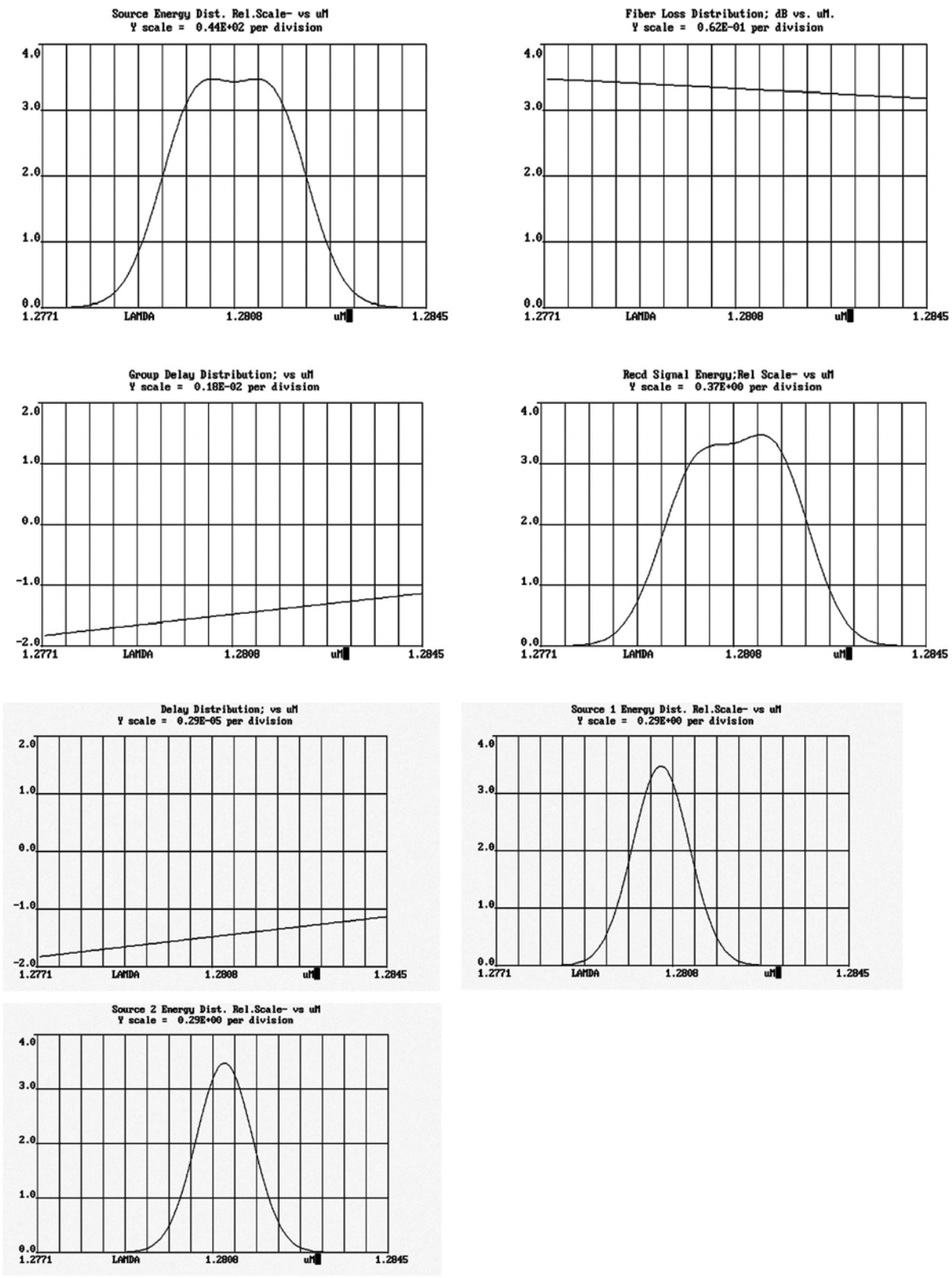

Fig 8.33 Source energy distribution**,** fiber loss distribution**,** group delay distribution, received signal energy, delay distribution ,sources 1 and 2 energy distributions

8.1.5 OTDM Systems

a) Simulation results for OTDM system with grade 1 components. Fiber length is 35 km and the rate is 320 Mb/s.

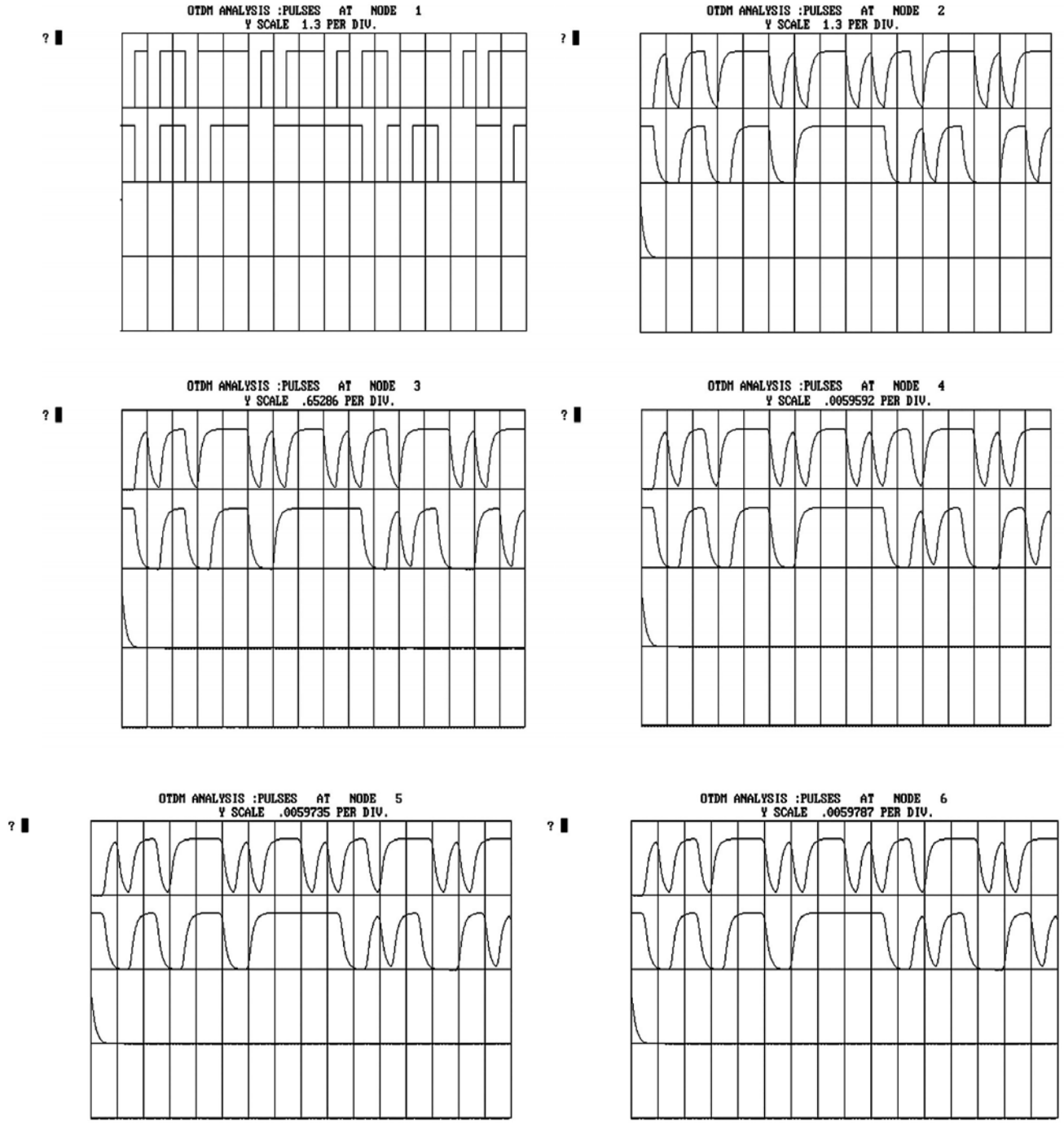

Fig 8.34 Pulse shapes at different nodes.

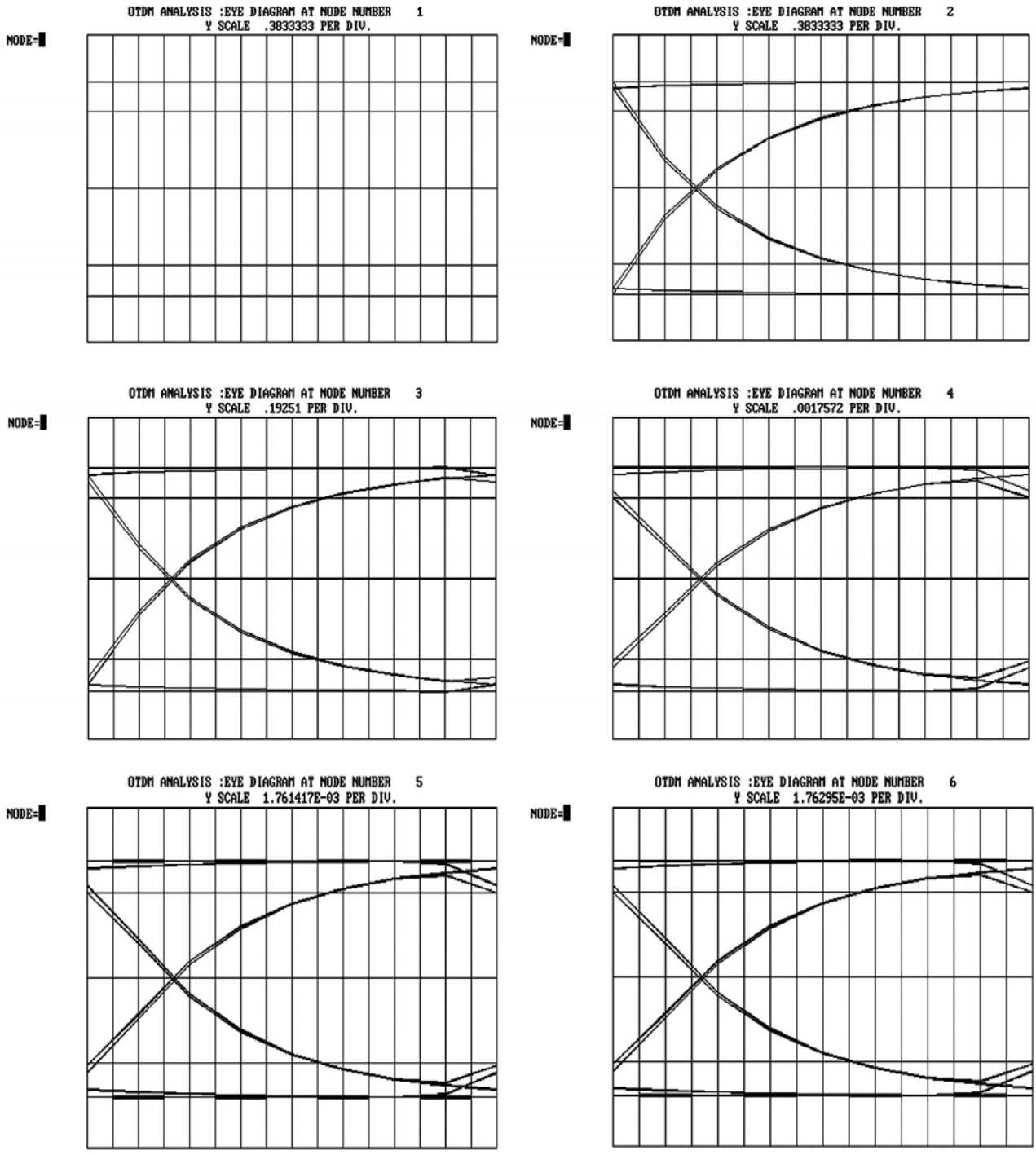

Fig 8.35 Eye diagrams at different nodes.

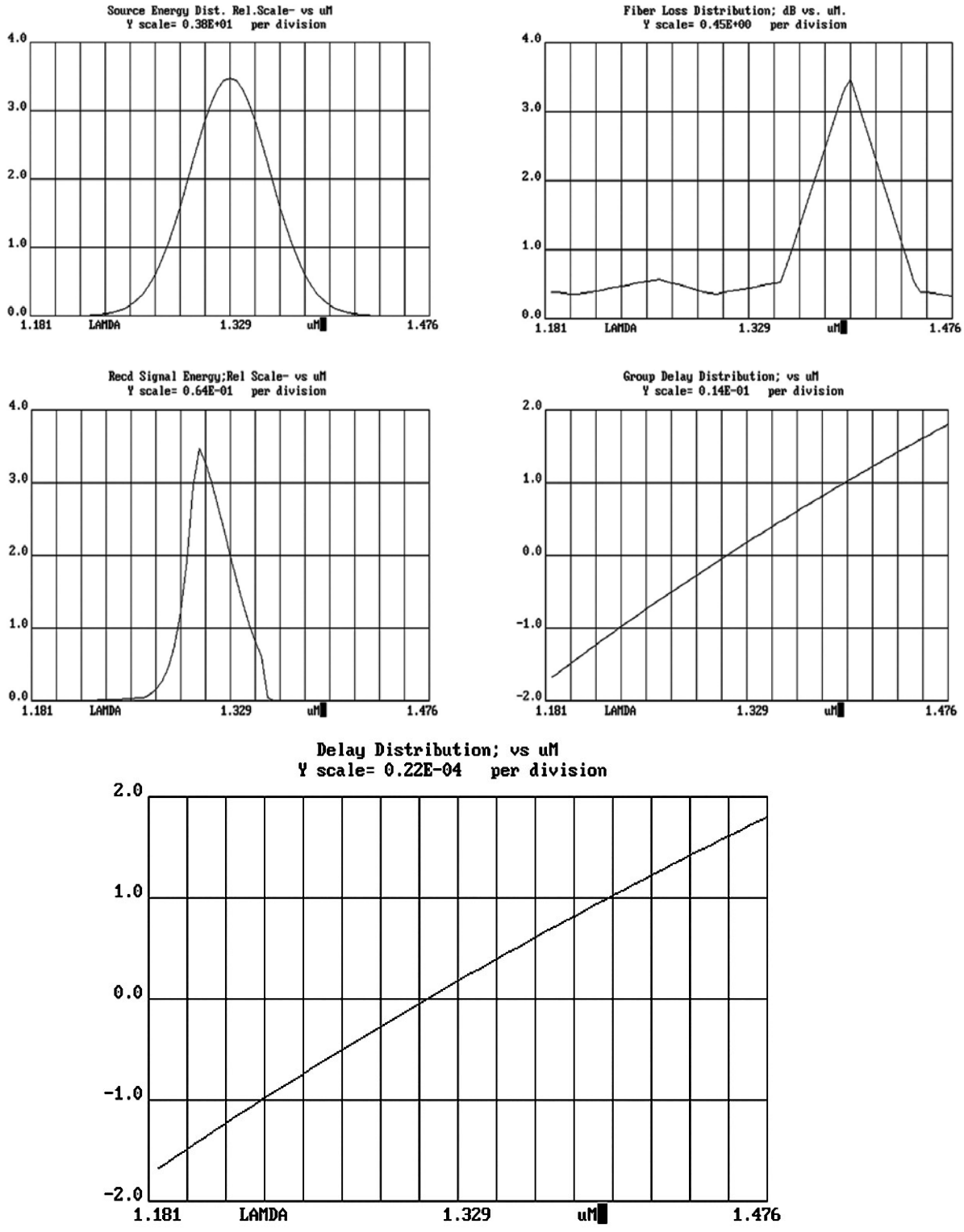

Fig 8.36 Source energy distribution, fiber loss distribution, received signal energy , group delay distribution and delay distribution.

b). Simulation results for OTDM system with grade1 components. Fiber length is 100 km. and the rate 320 Mb/s.

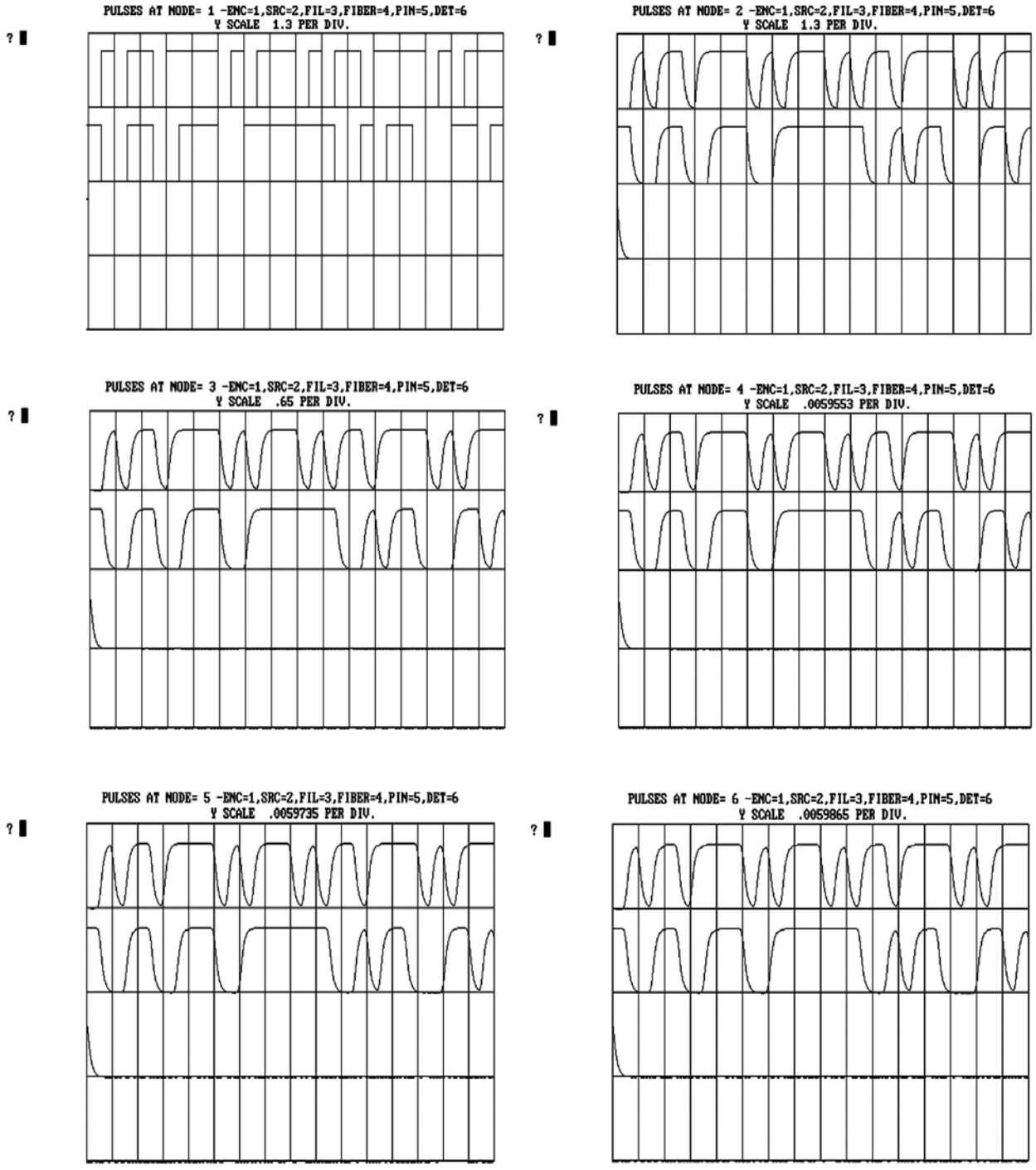

Fig 8.37 Pulse shapes at different nodes

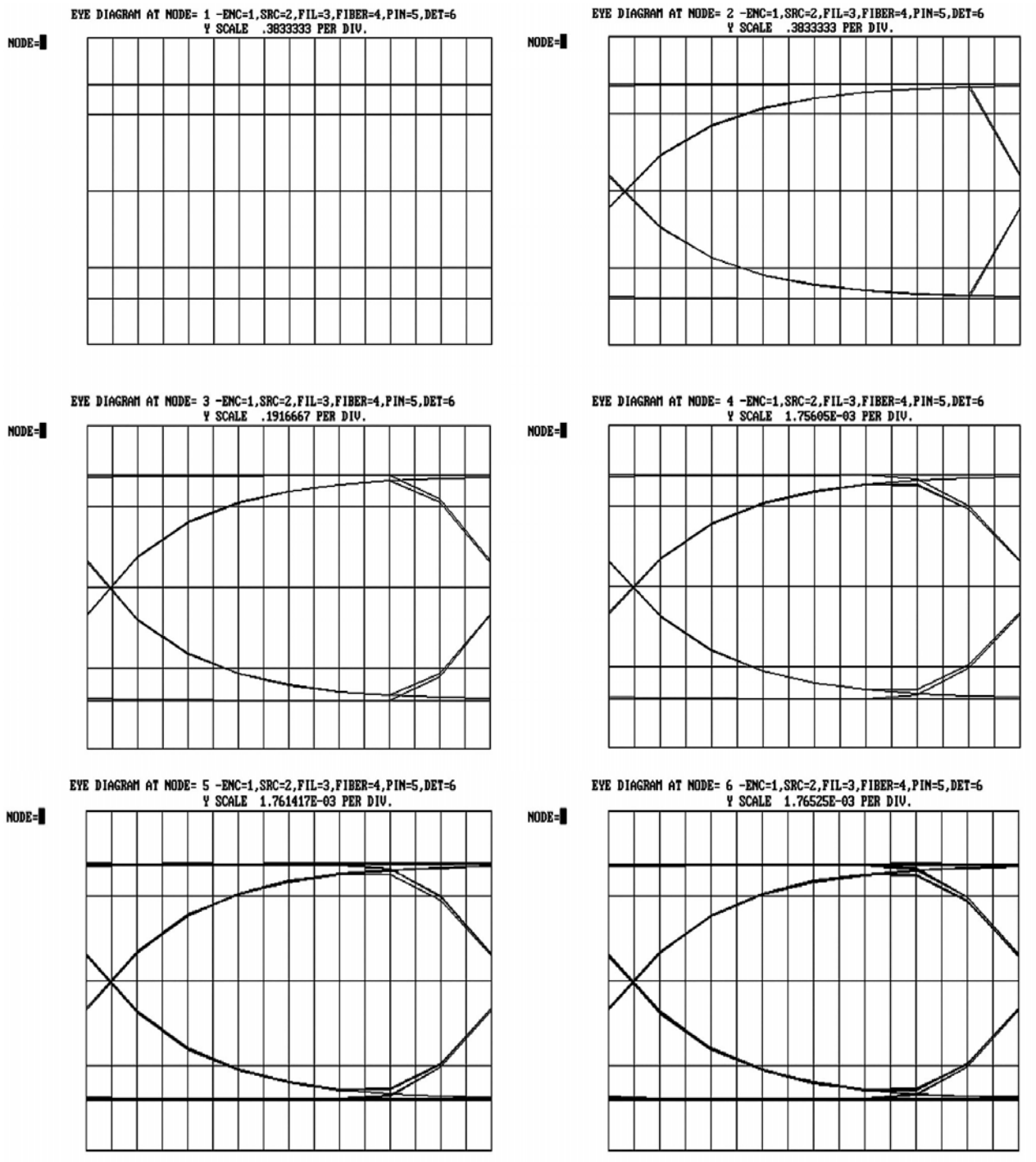

Fig 8.38 Eye diagram at different nodes

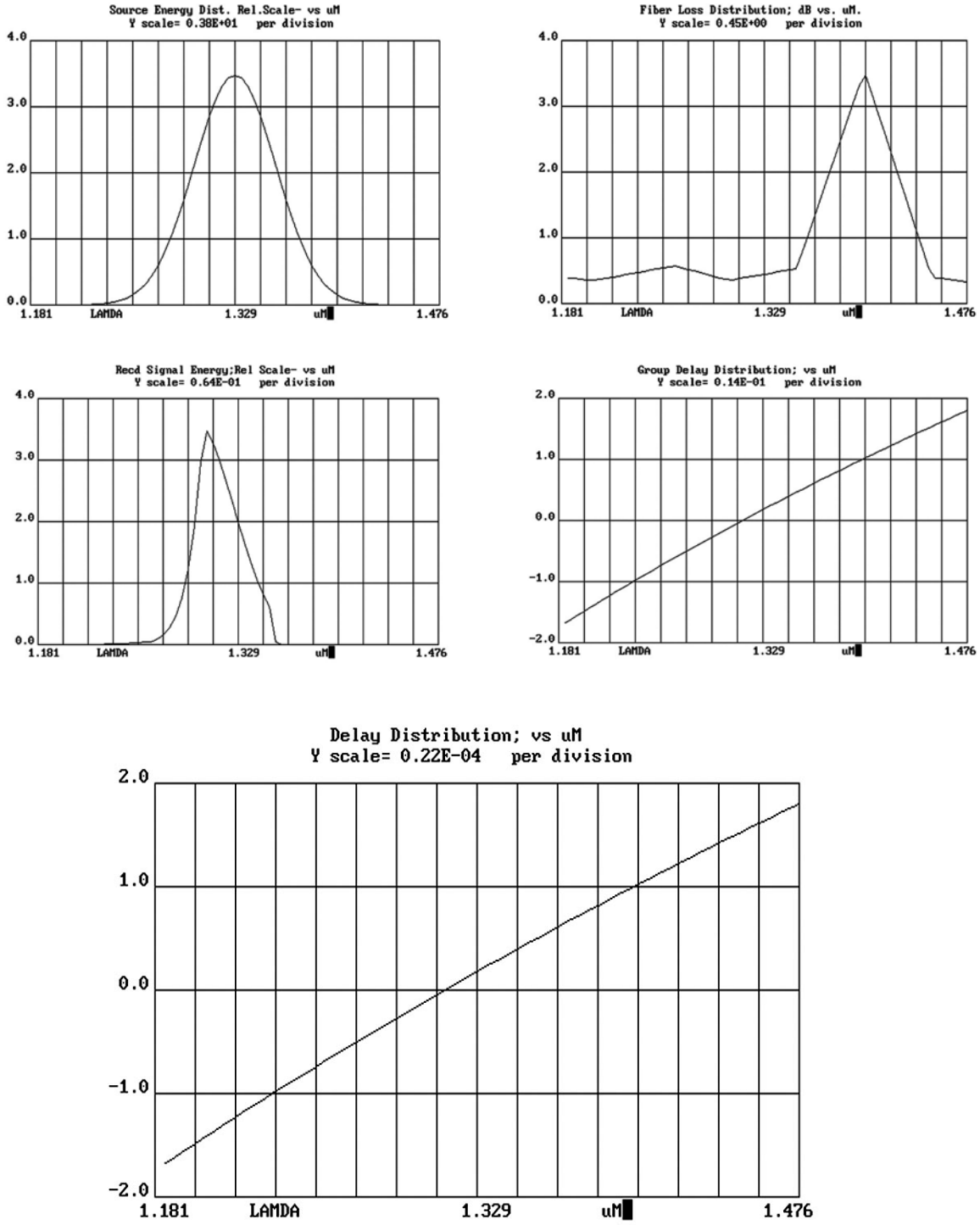

Fig 8.39 Source energy distribution, fiber loss distribution, received signal energy, group delay distribution and delay distribution graphs.

c) Simulation results for OTDM system with grade 3 components. Fiber length is 35 km and the rate is 320 Mb/s.

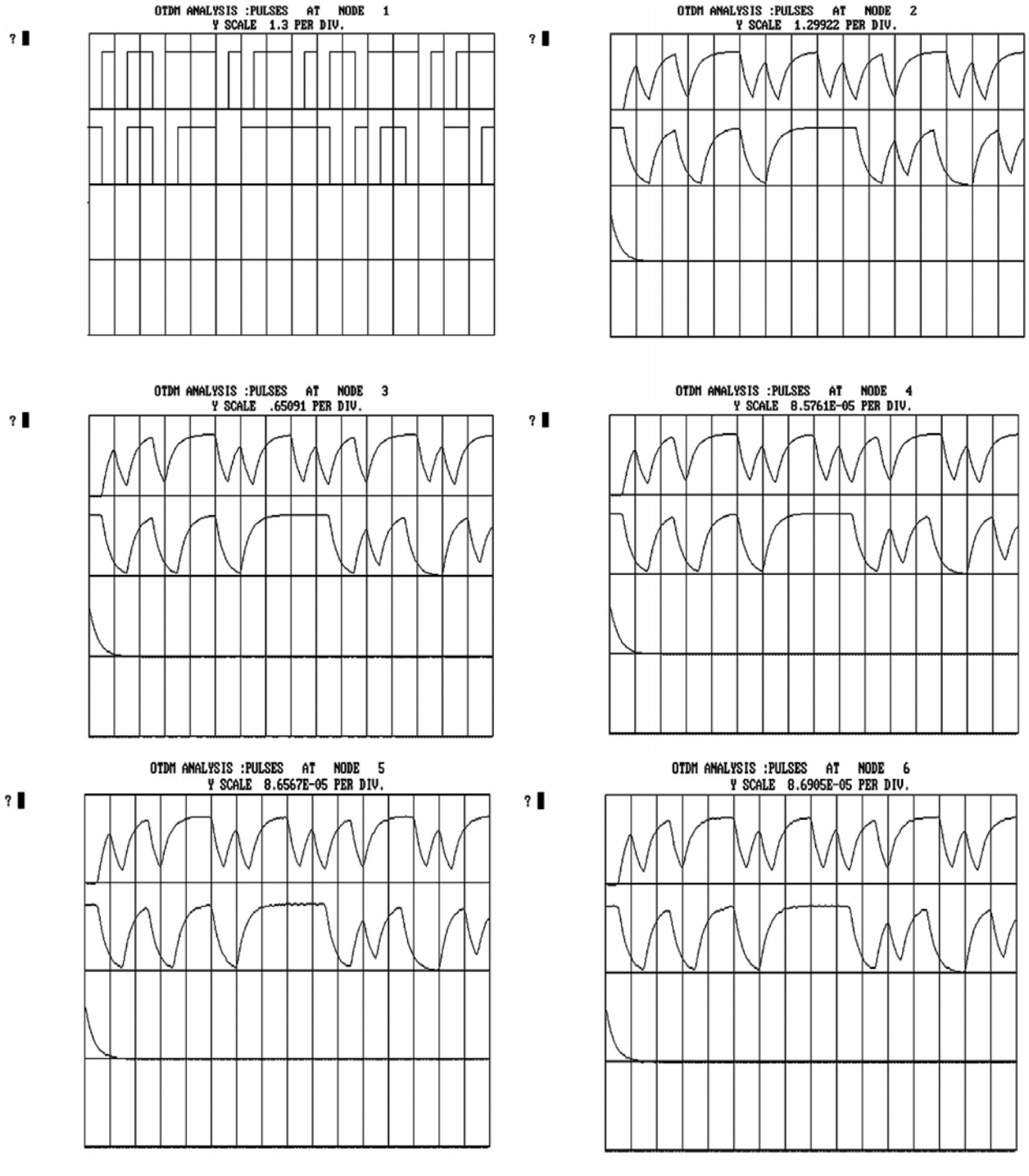

Fig 8.40 Pulse shapes at different nodes.

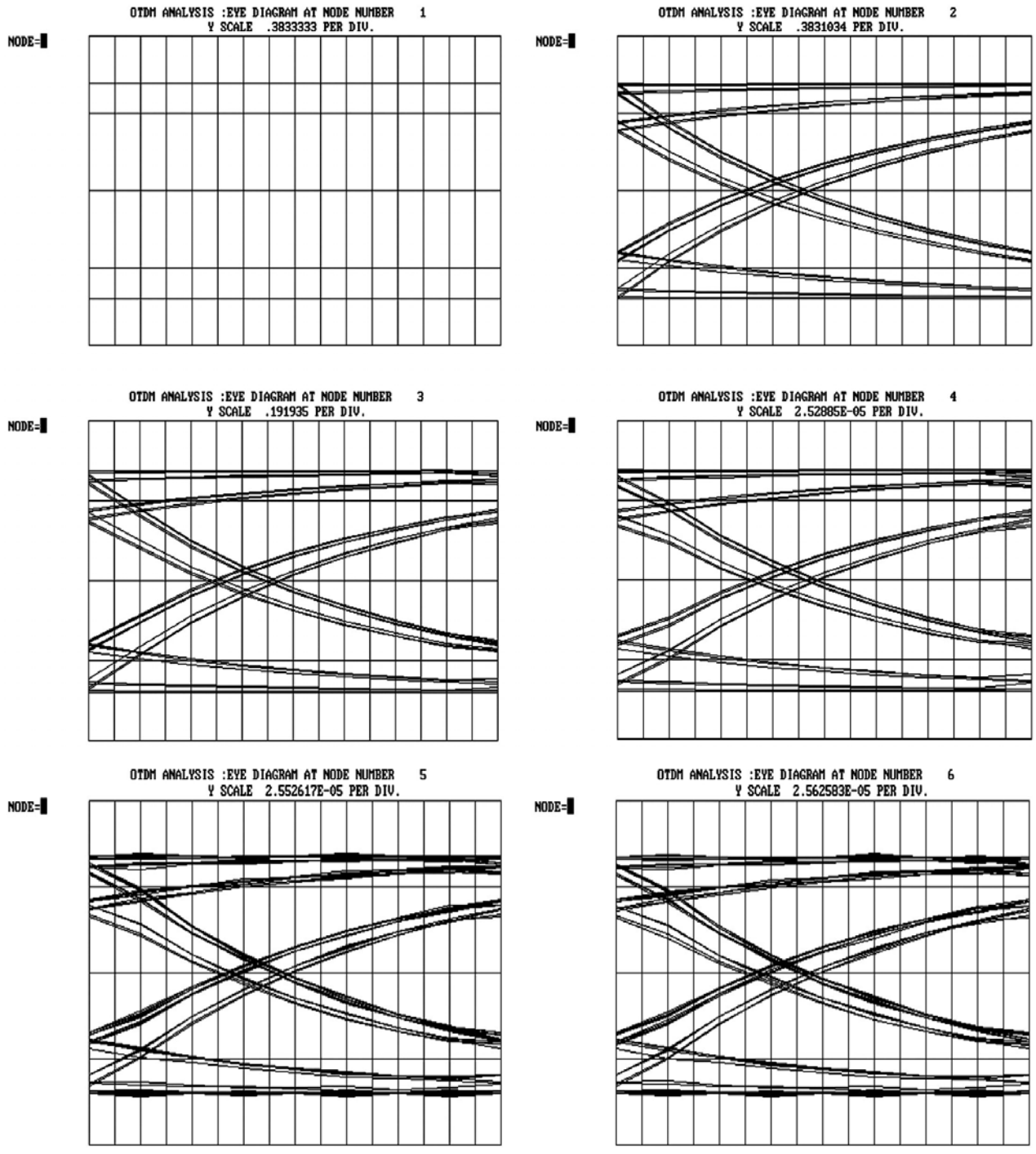

Fig 8.41 Eye diagrams at different nodes

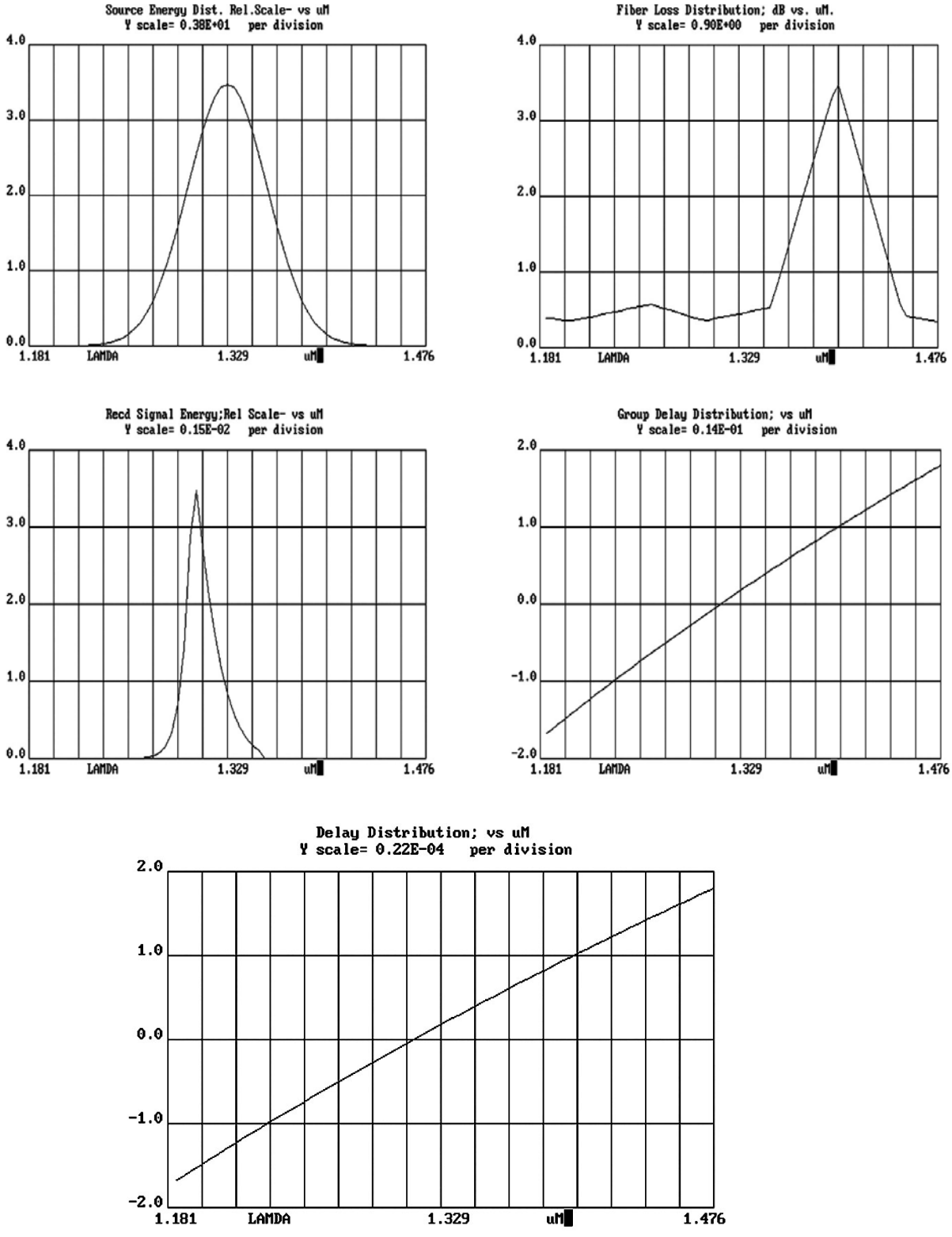

Fig 8.42 Source energy distribution, fiber loss distribution, received signal energy , group delay distribution and delay distribution for OTDM system.

d) Simulation results for OTDM system with grade 3 components. Fiber length is 100 km and the rate is 320 Mb/s.

Fig. 8.43 Pulse shapes at different nodes

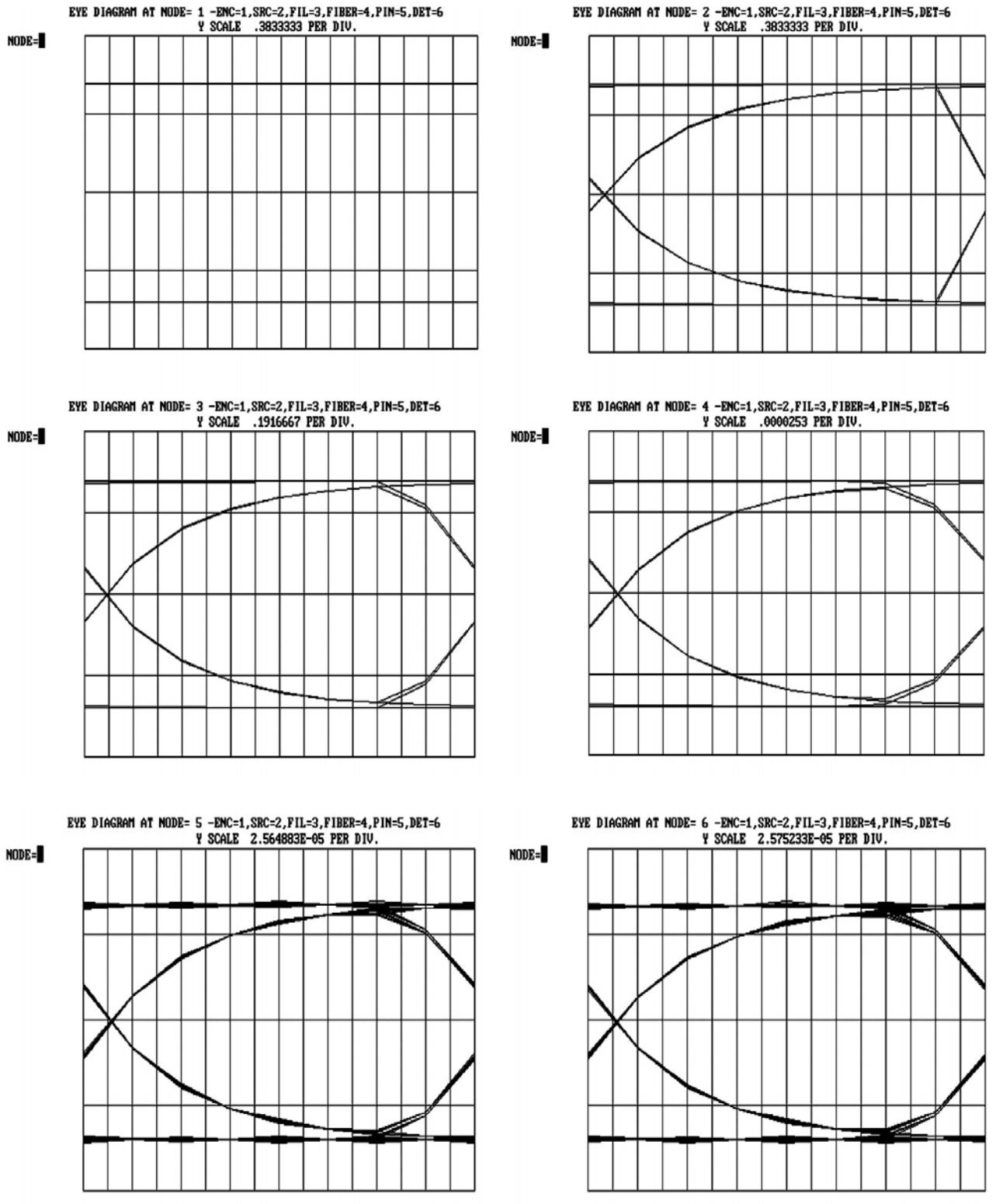

Fig. 8.44 Eye diagrams at different nodes

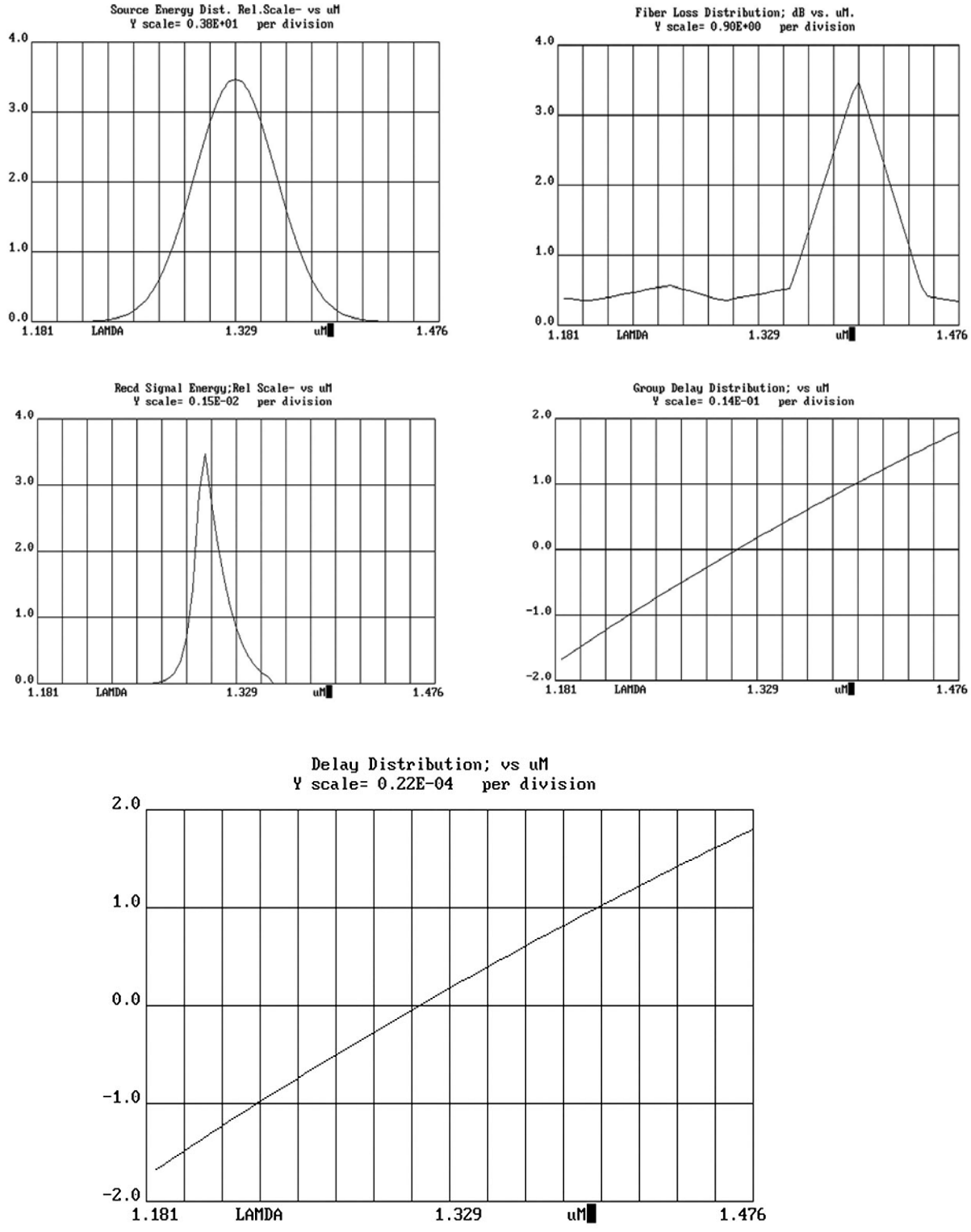

Fig 8.45 Source energy distribution, fiber loss distribution, received signal energy , group delay distribution and delay distribution.

e) Simulation results for OTDM system with Grade 5 components. Fiber length is 100 km and the rate is 320 Mb/s.

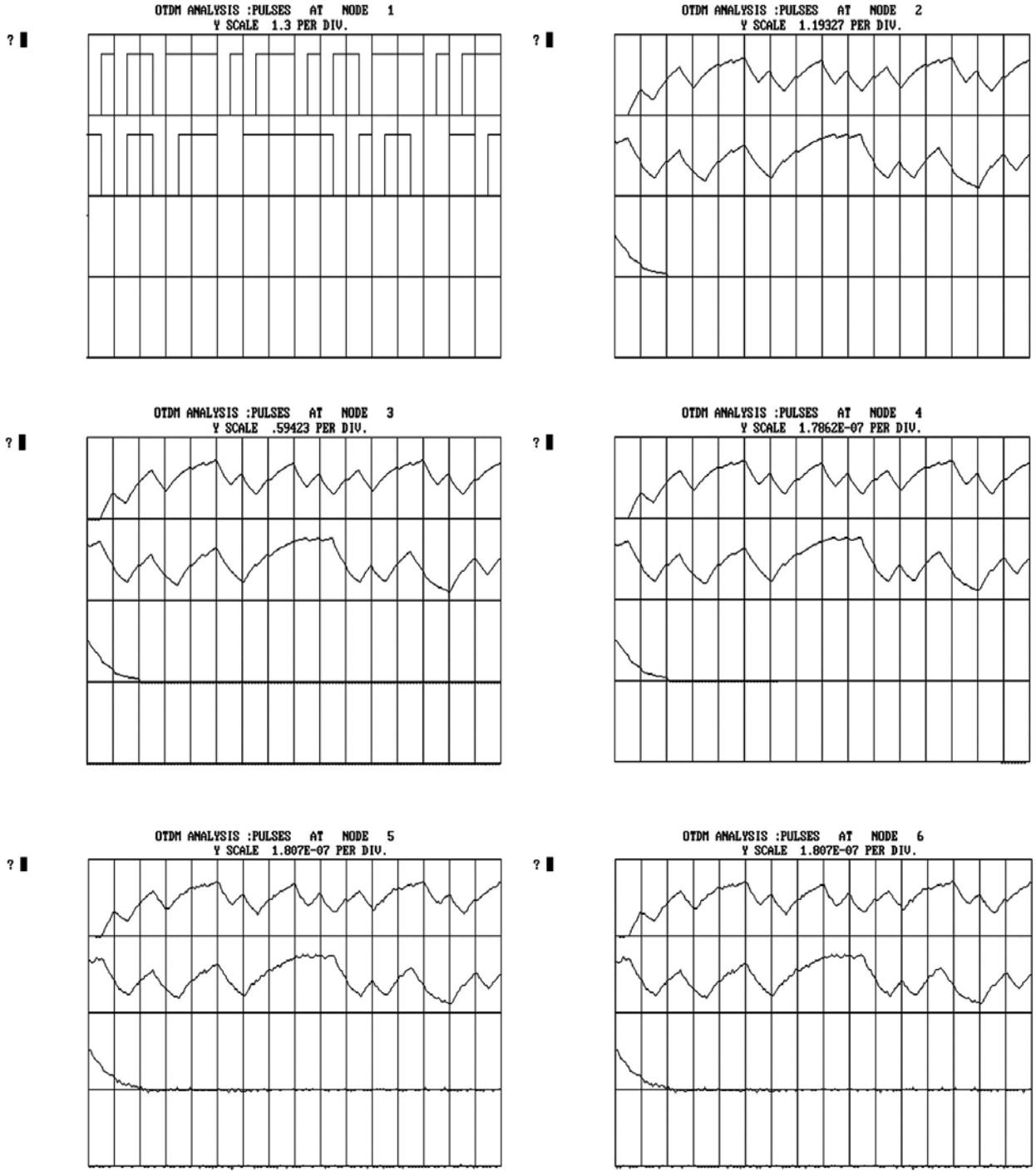

Fig 8.46 Data pulses at different nodes .

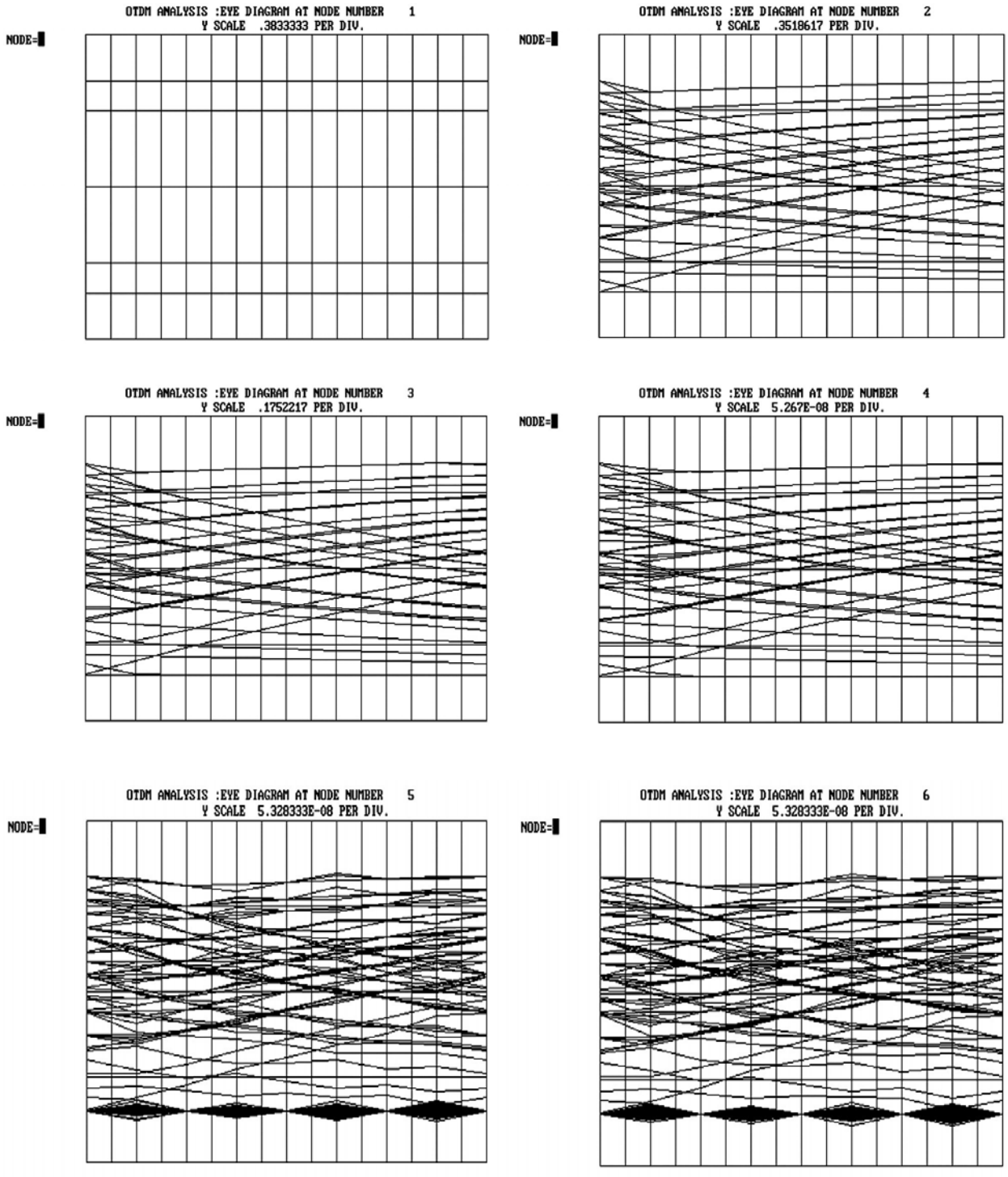

Fig 8.47 Eye diagrams at different nodes

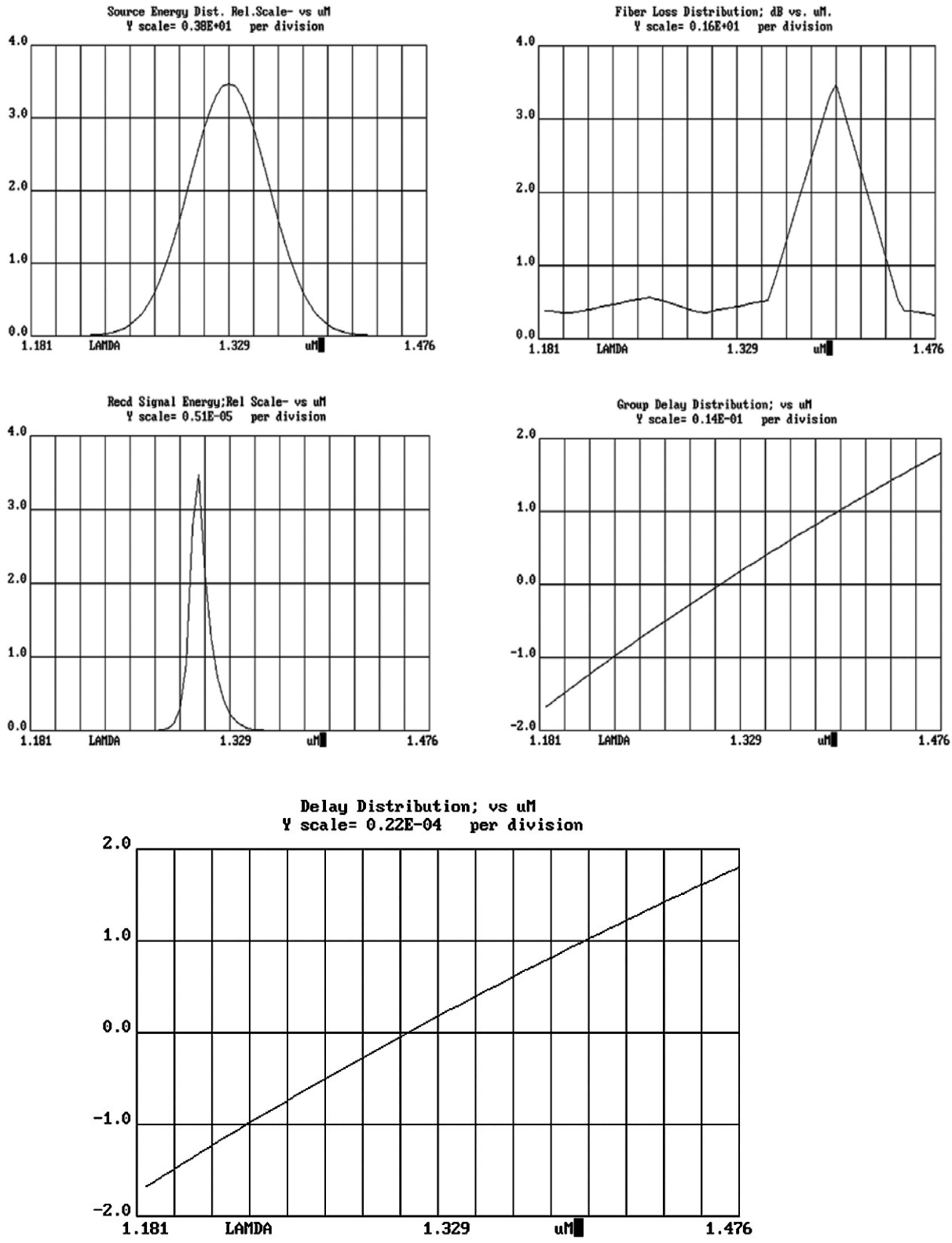

Fig 8.48 Source energy distribution, fiber loss distribution, received signal energy, group delay distribution and delay distribution.

8.1.6 Effects of Half-Width Pulses

a) Effects of half width pulses: Fiber length is 100 km and the rate is 160 Mb/s

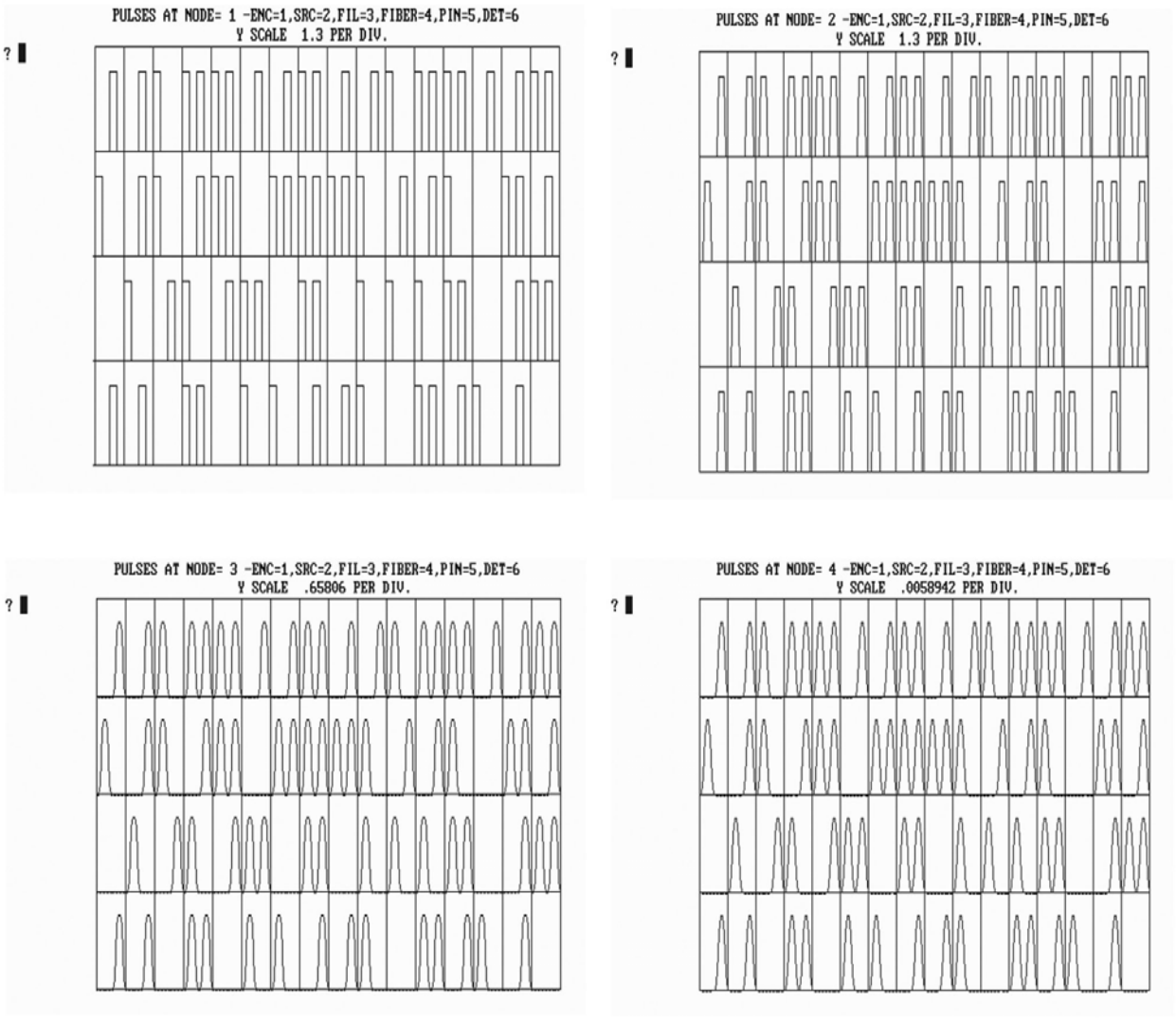

Fig 8.49 Pulse shapes at different nodes

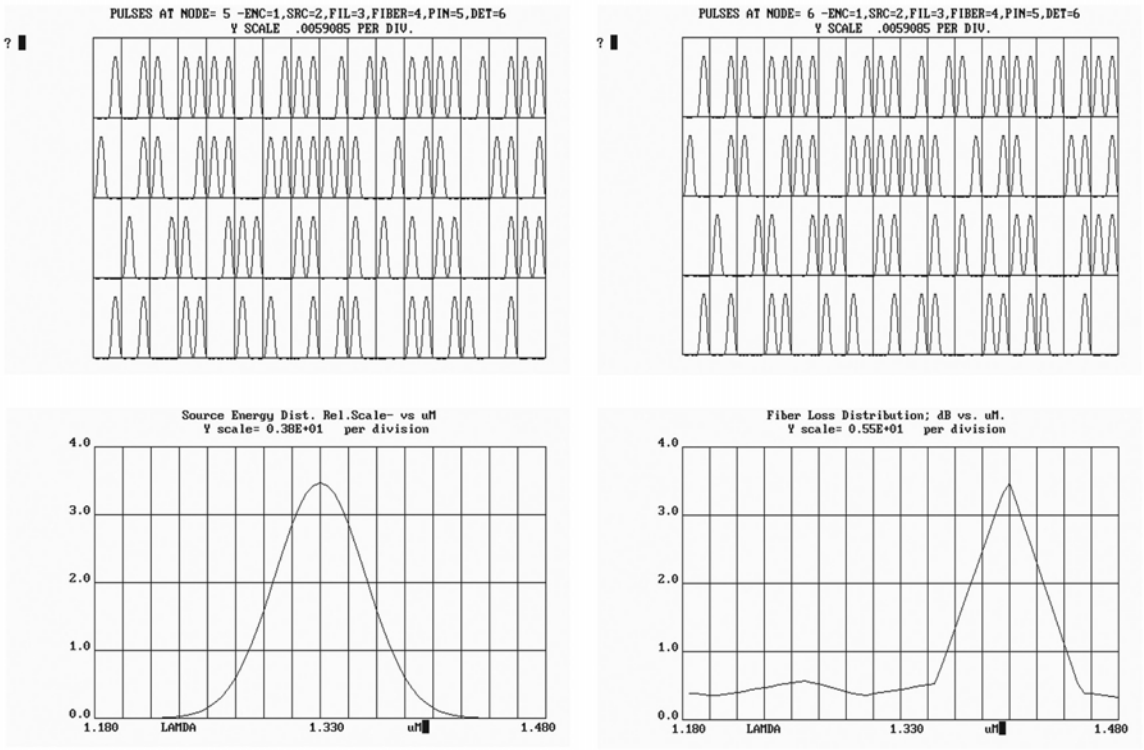

Fig 8.50 Pulse shapes at node 5 and 6, source energy distribution, fiber loss distribution

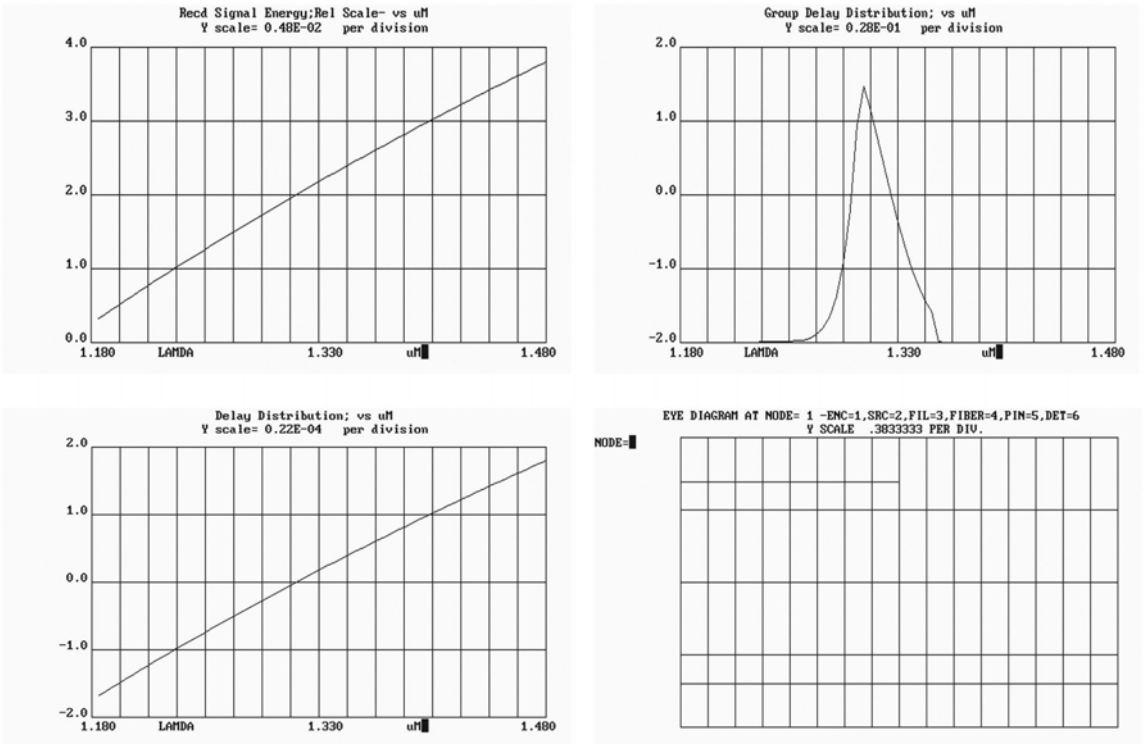

Fig 8.51 Received signal energy, group delay distribution, delay distribution and eye diagram at node1

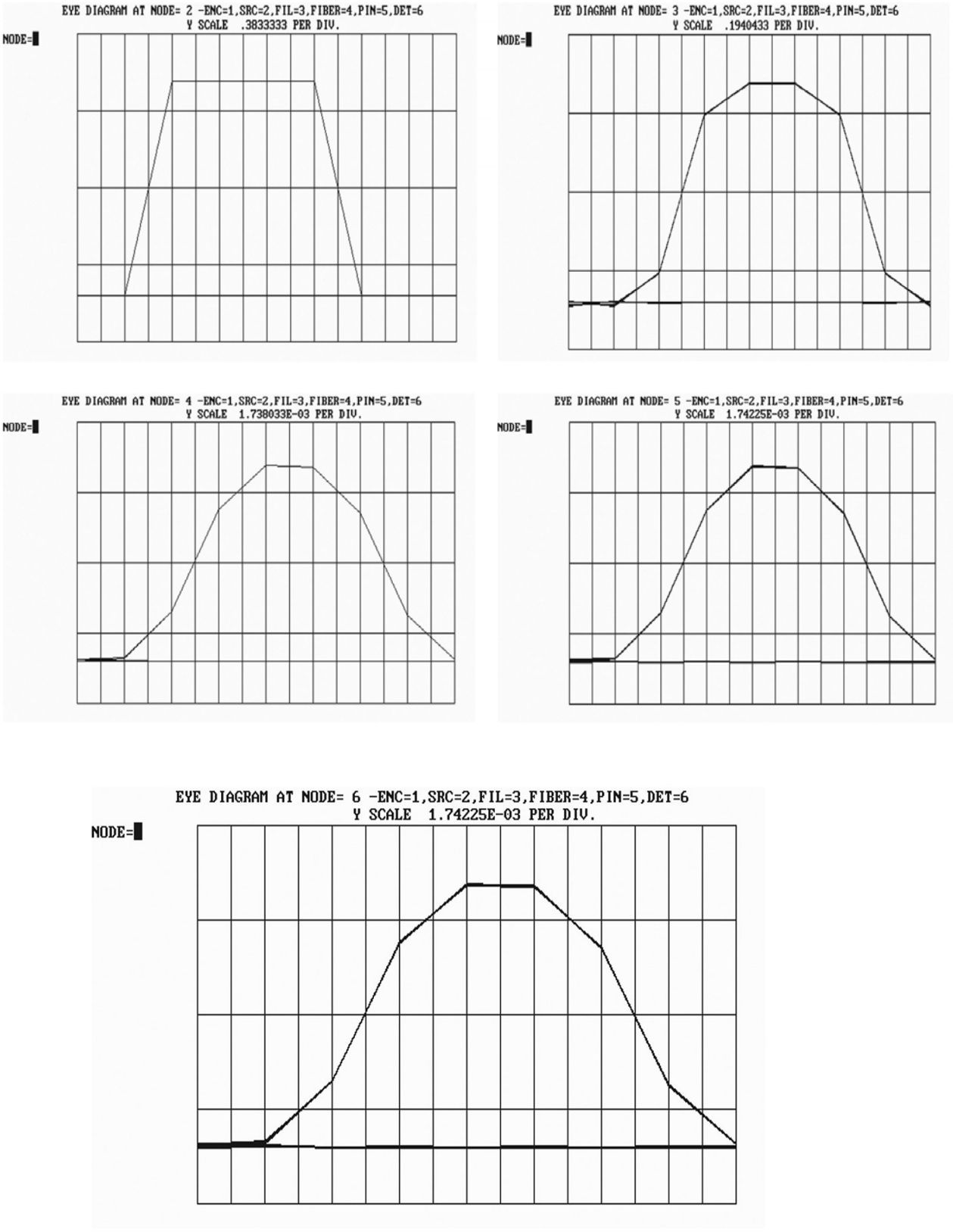

Fig 8.52 Eye diagrams at different nodes

b) Effects of half width pulses: Fiber length is 100 km and the rate is 320 Mb/s

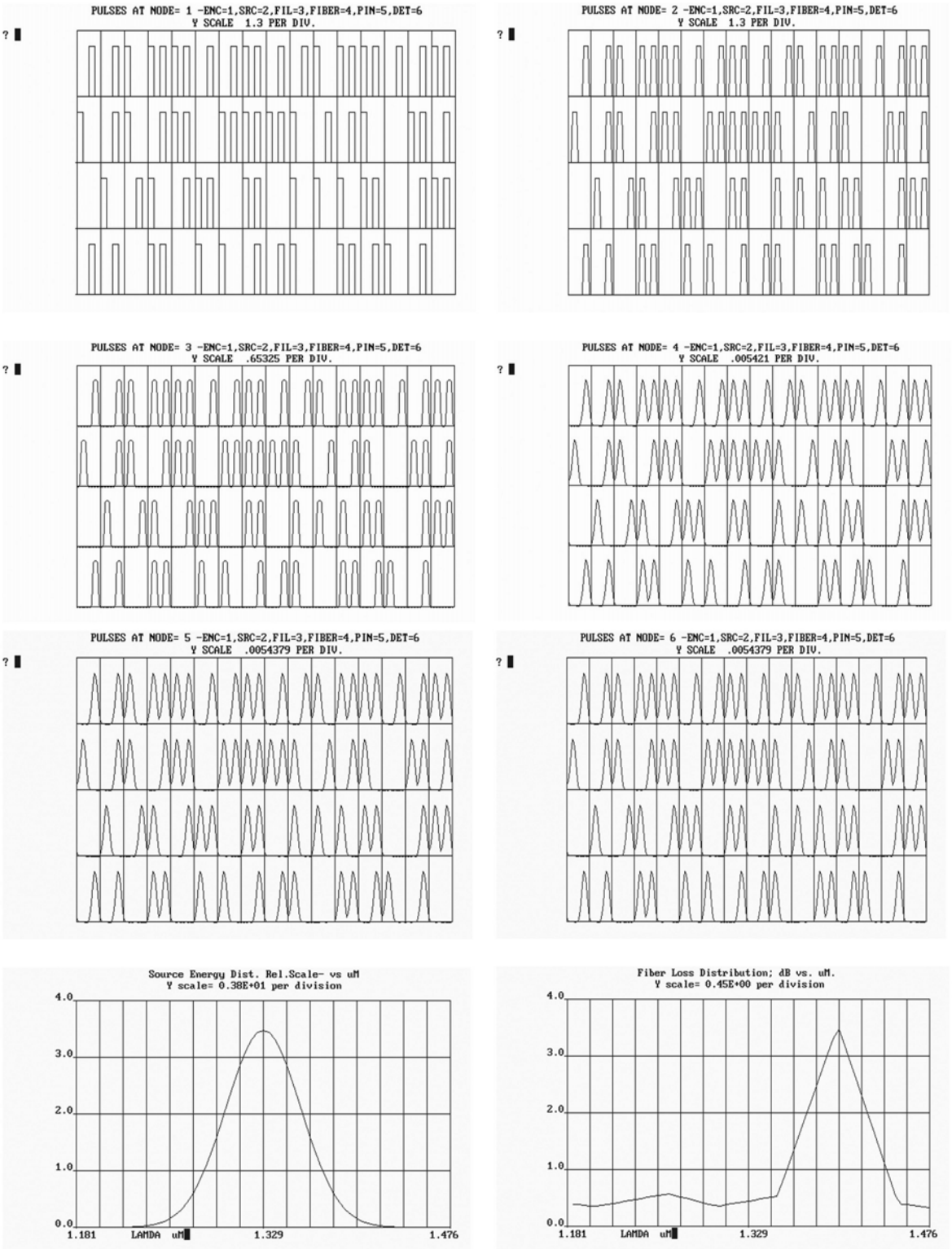

Fig 8.53 Pulse shapes at different nodes, source energy distribution and fiber loss distribution

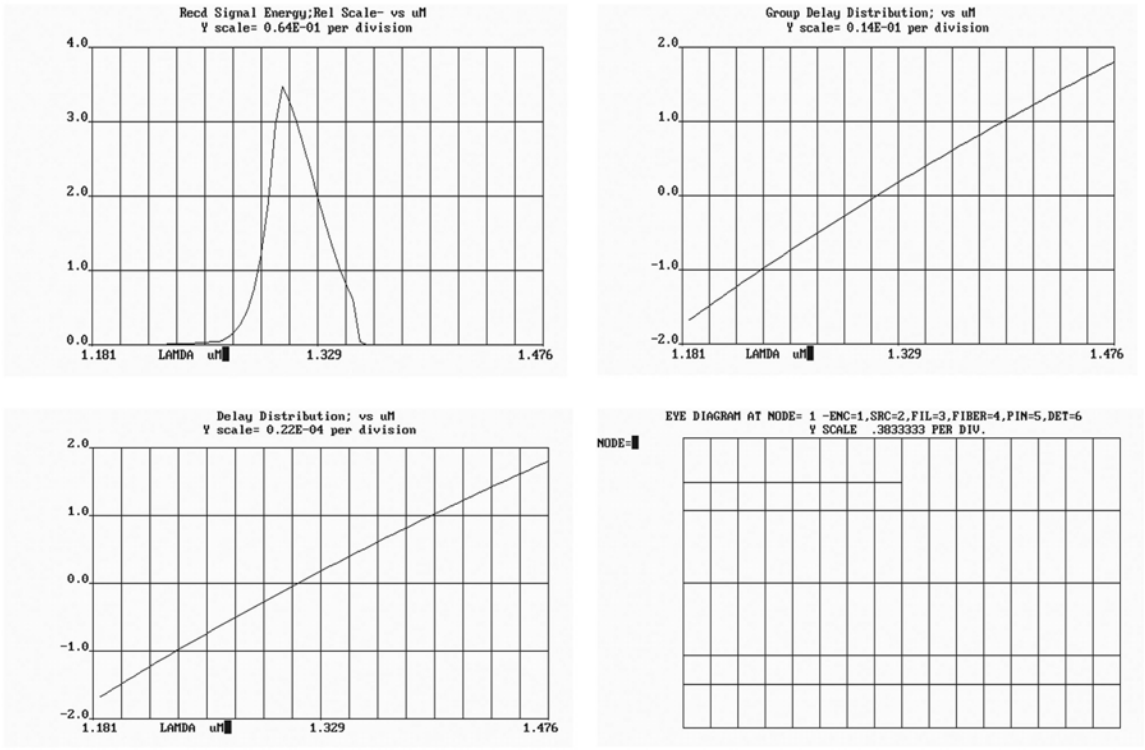

Fig 8.54 Received signal energy, group delay distribution, delay distribution and eye diagram at node1

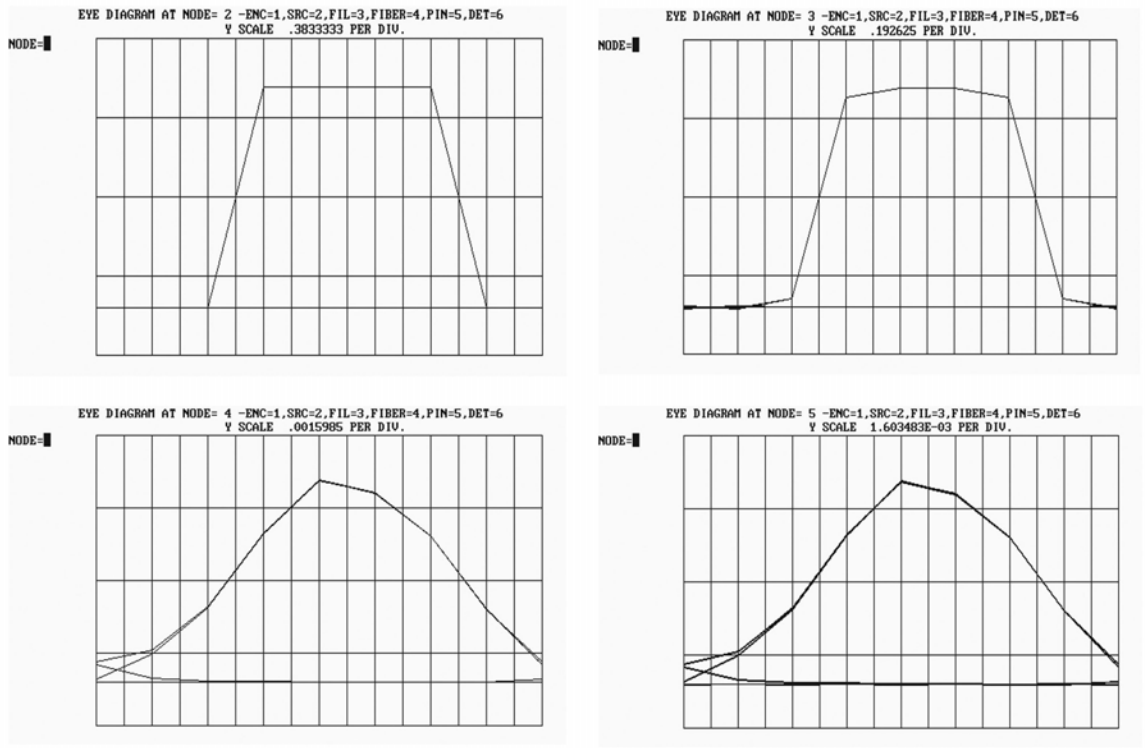

Fig 8.55 Eye diagrams at different nodes

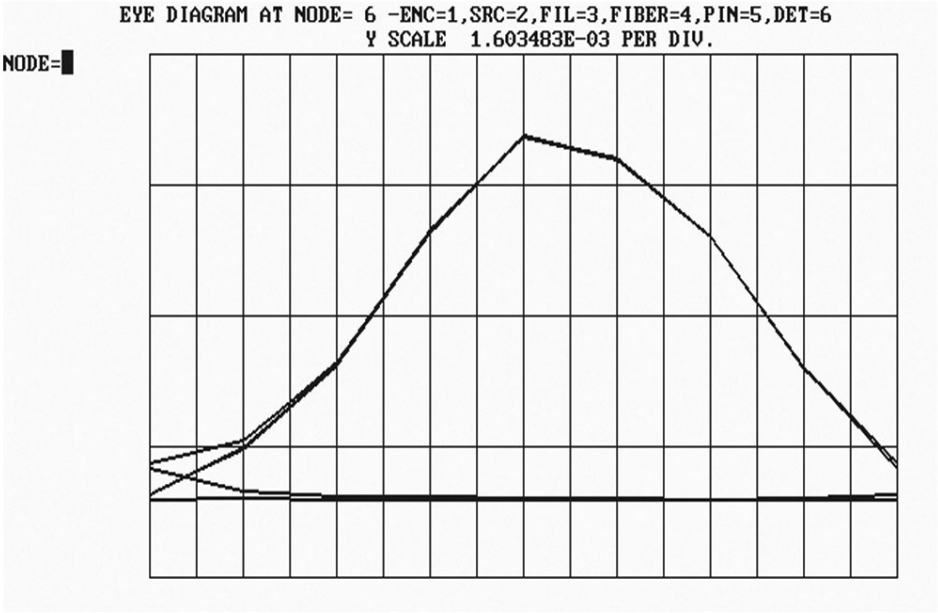

Fig 8.56 Eye diagram at node6

c). Effects of half width pulses : Fiber length is 200 km, and the rate is 320 Mb/s

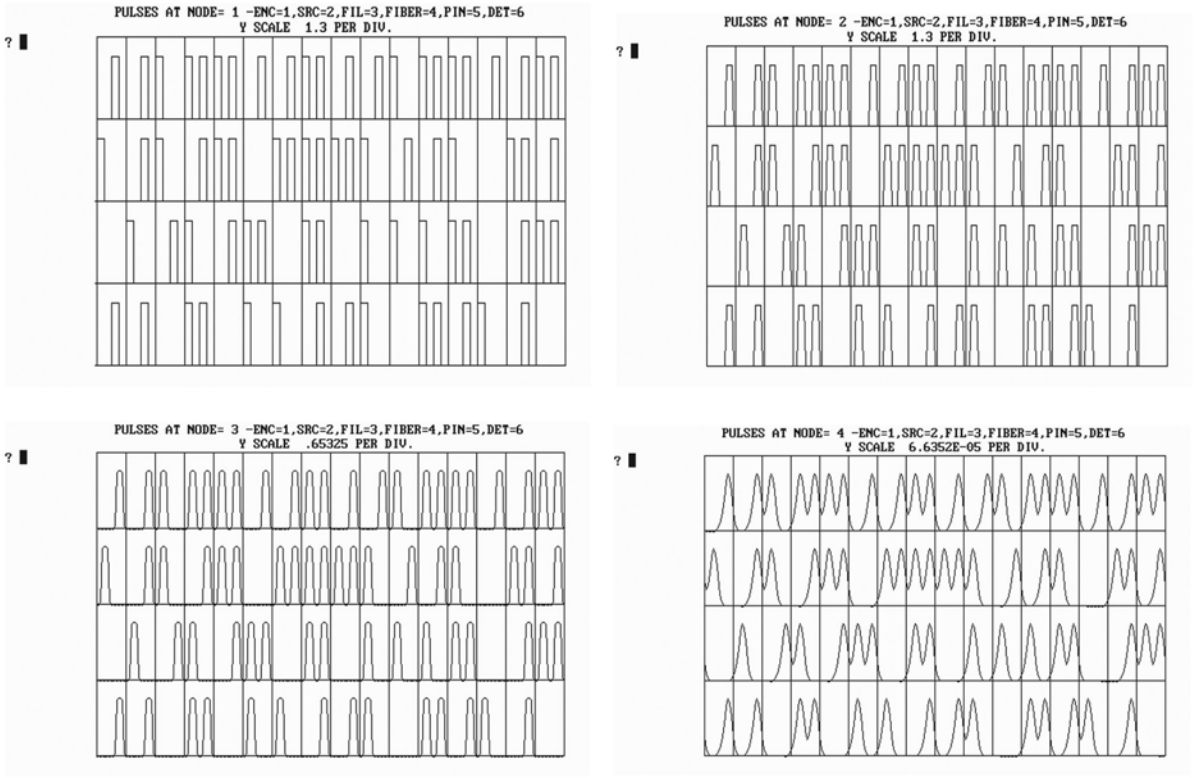

Fig 8.57 Data pulses at different nodes

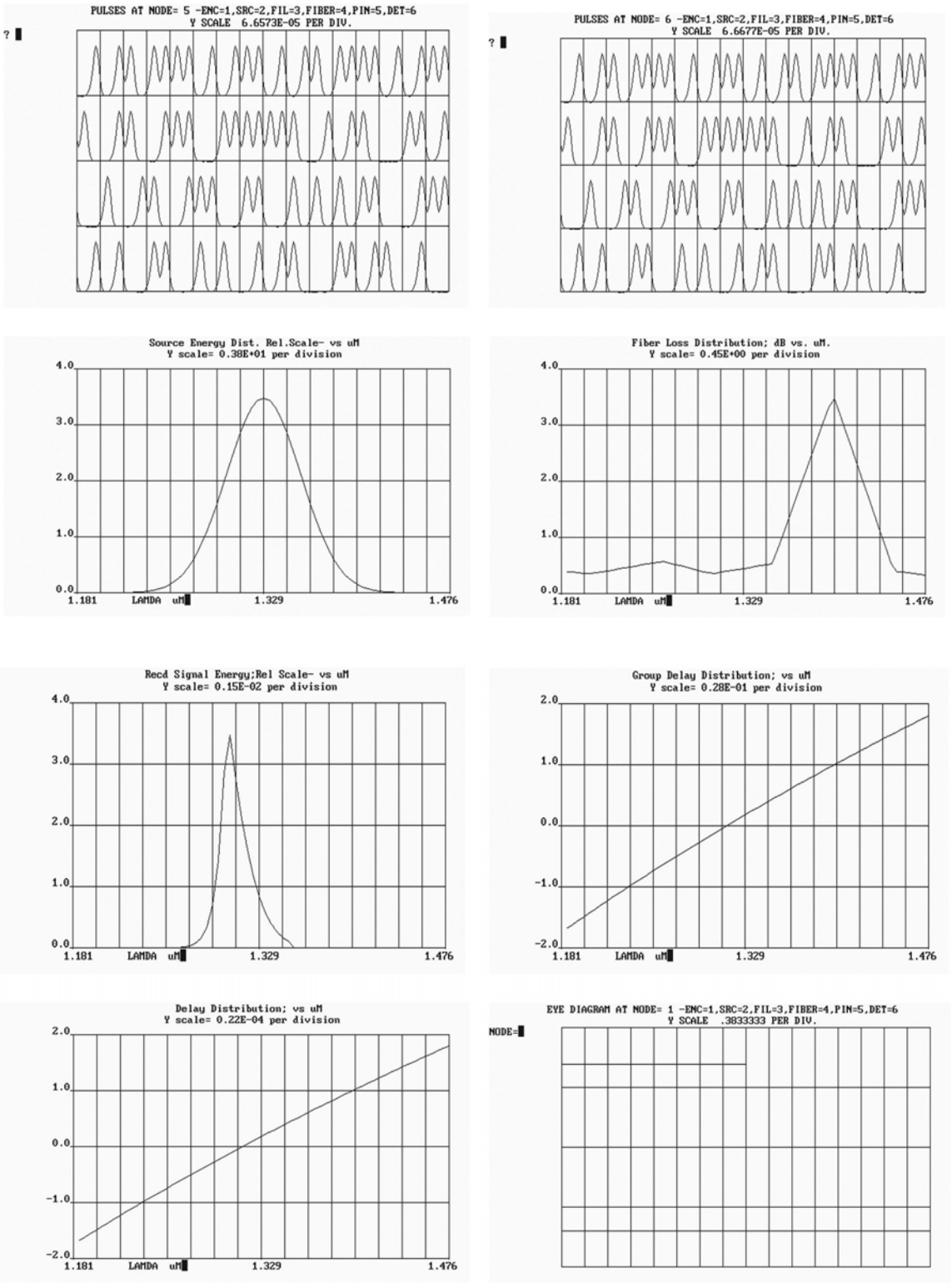

Fig 8.58 Pulse shapes at nodes 5 and 6, Source energy distribution and fiber loss distribution , received signal energy, group delay distribution, delay distribution and eye diagram at node1

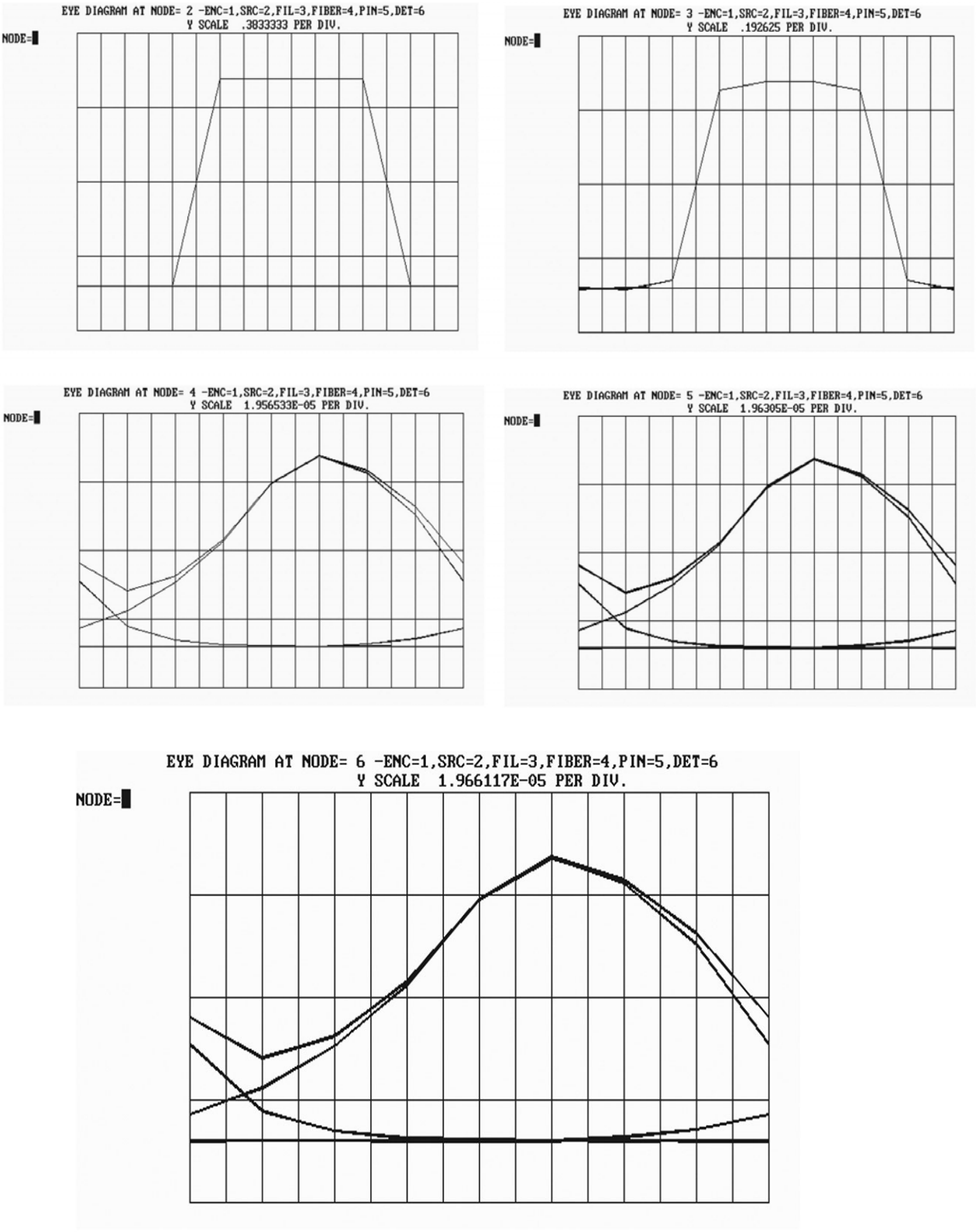

Fig 8.59 Eye diagrams at different nodes

d) Effects of half width pulses: Fiber length is 100 km, and the rate is 640 Mb/s

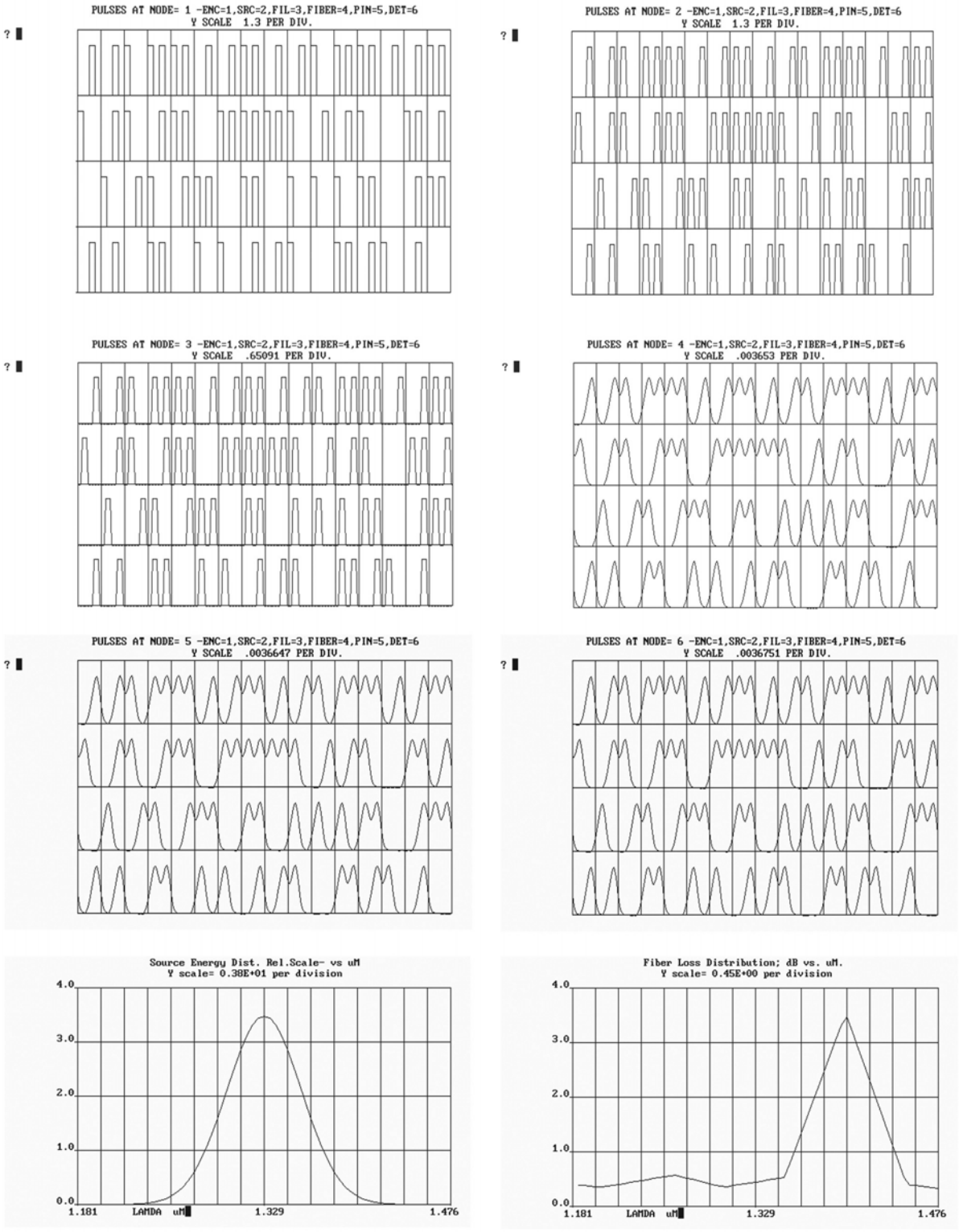

Fig 8.60 Pulse shapes at different nodes, source energy and fiber loss distributions

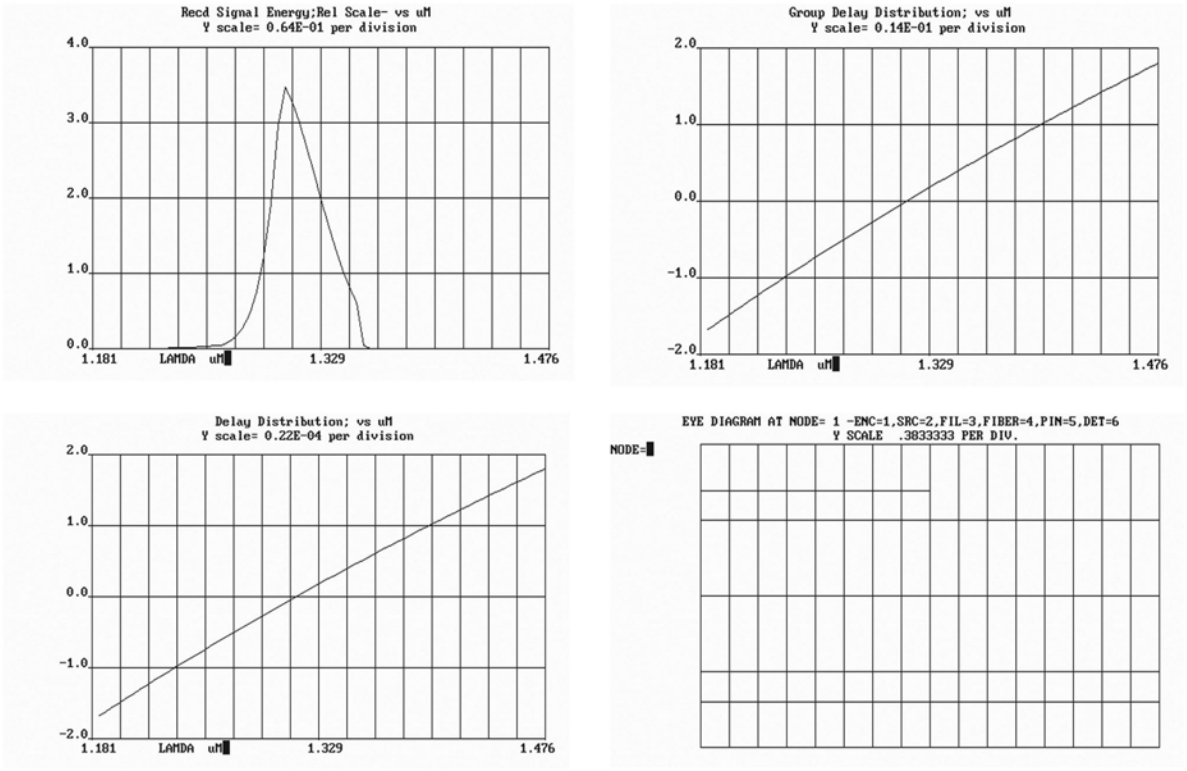

Fig 8.61 Received signal energy, group delay distribution, delay distribution and eye diagram at node1

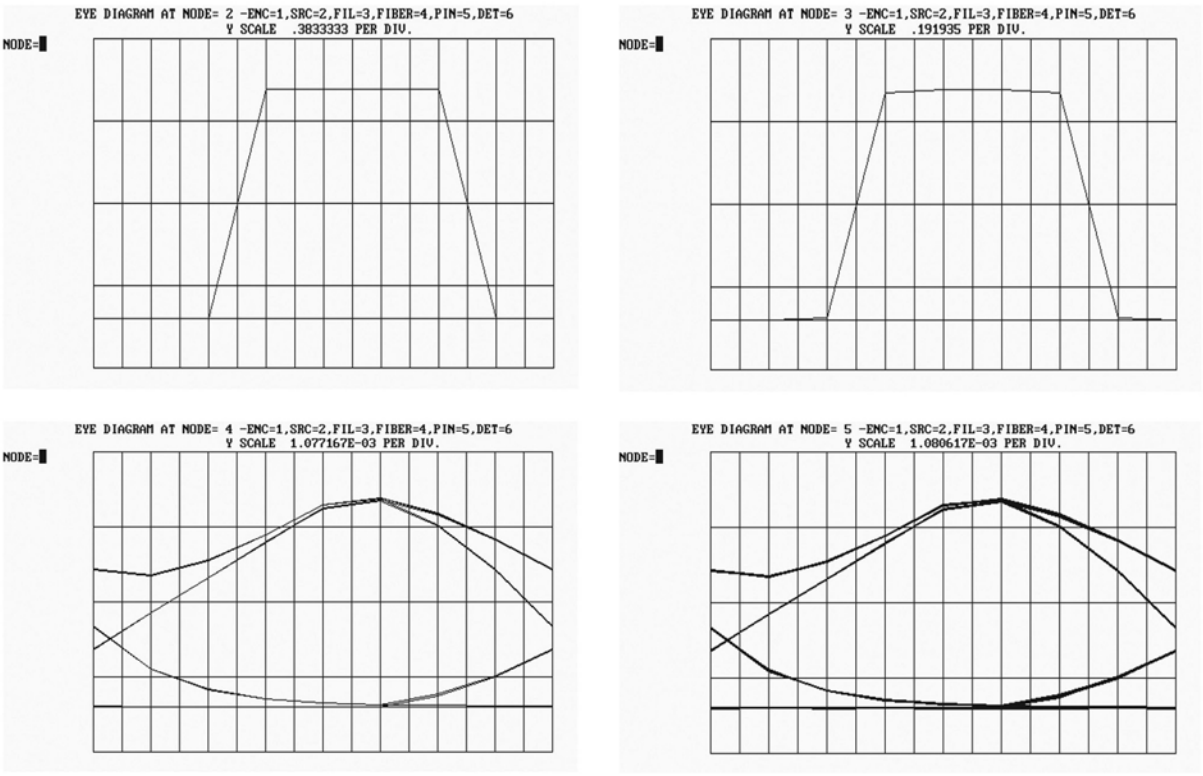

Fig 8.62 Eye diagrams at different nodes

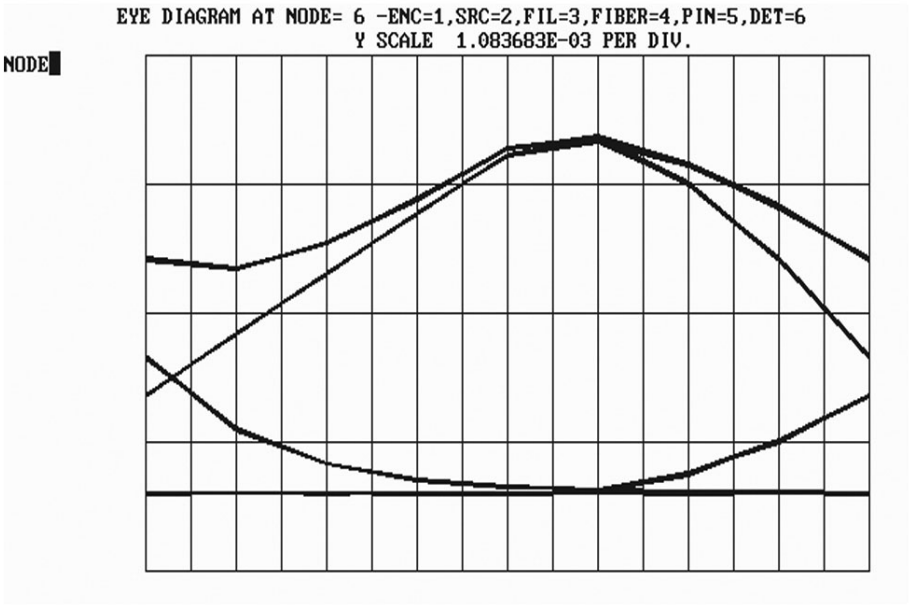

Fig 8.63 Eye diagrams at node 6

e) Effects of half width pulses: Fiber length is 100 km, and the rate is 1000 Mb/s

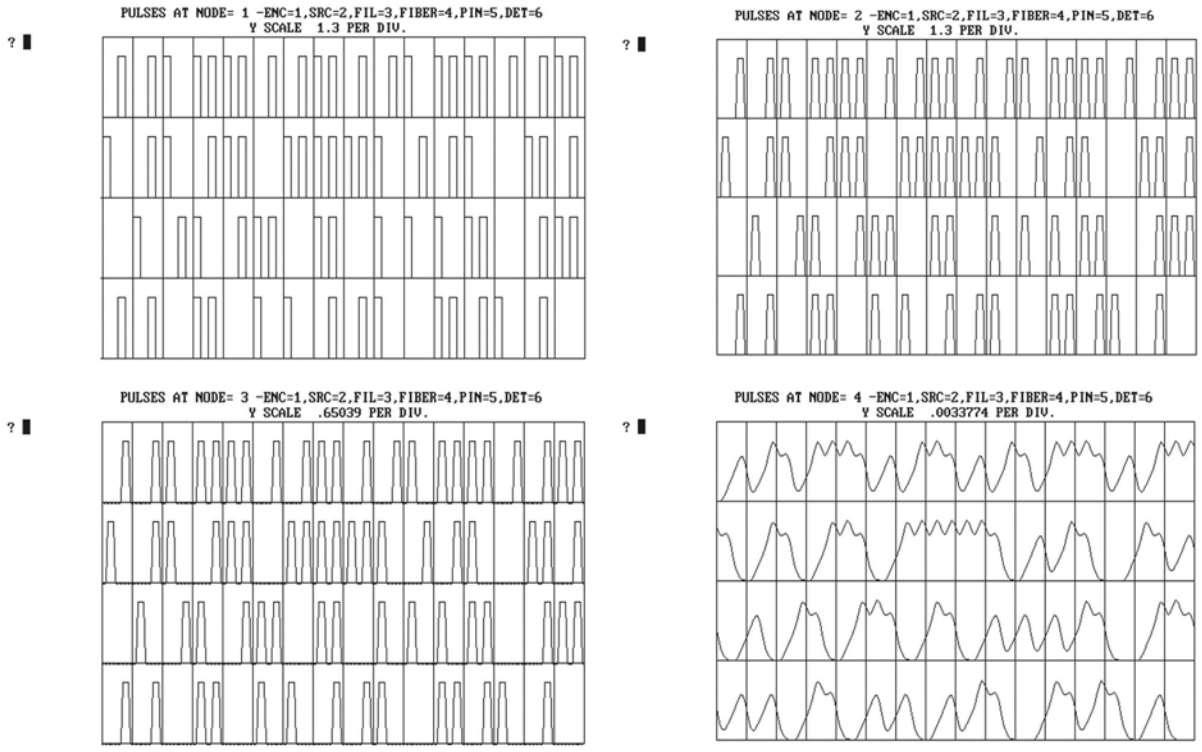

Fig 8.64 Pulse shapes at different nodes

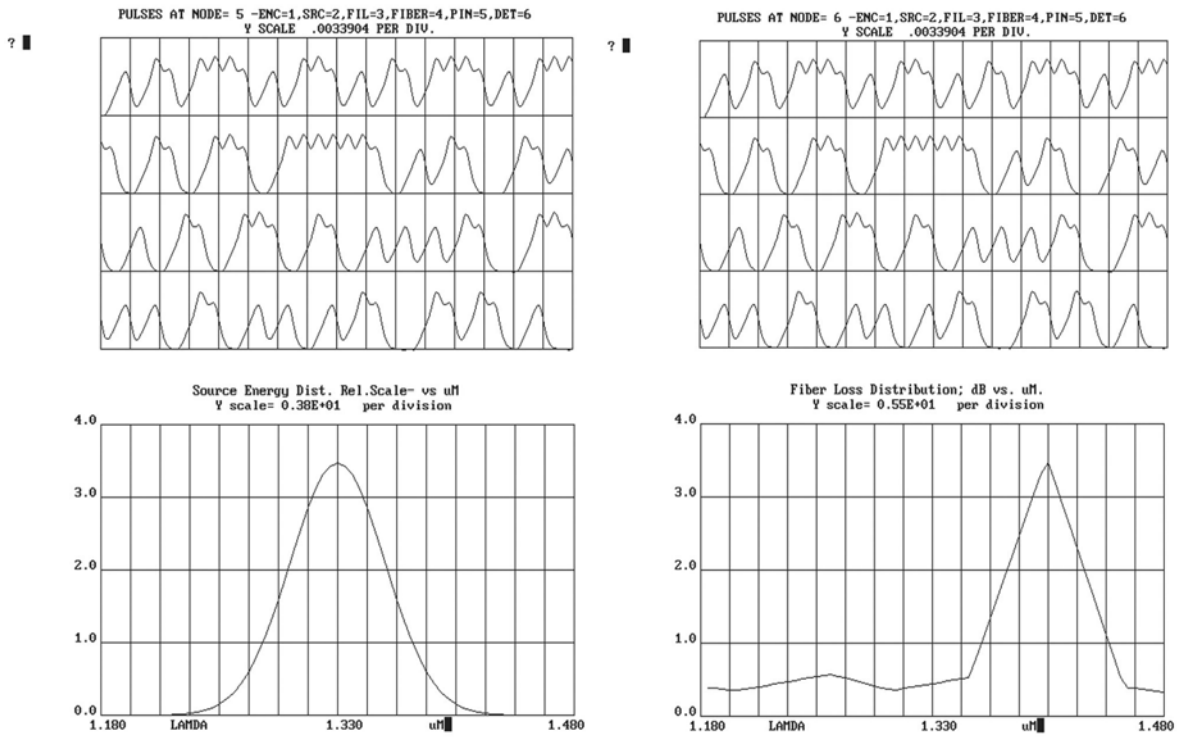

Fig 8.65 Pulse shapes at nodes 5 and 6, source delay and fiber loss distributions

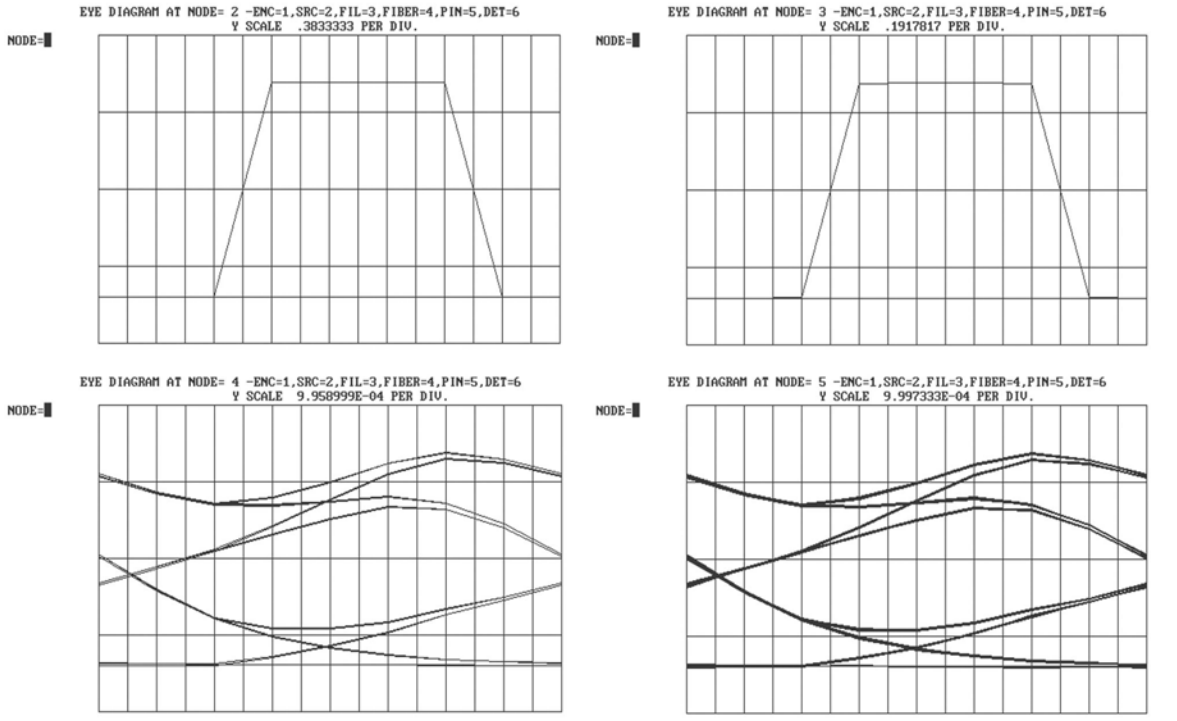

Fig 8.66 Eye diagrams at different nodes

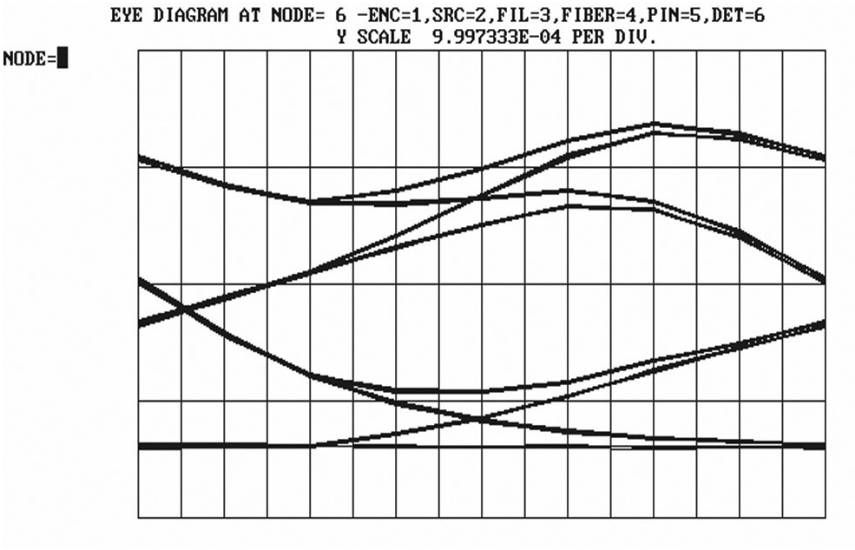

Fig 8.67 Eye diagrams at node 6

8.1.6 **Effects of Quarter-Width Pulses (**Every factor remains the same as in half width case)

a) Fiber length 100 km and the rate 1000 MB/s

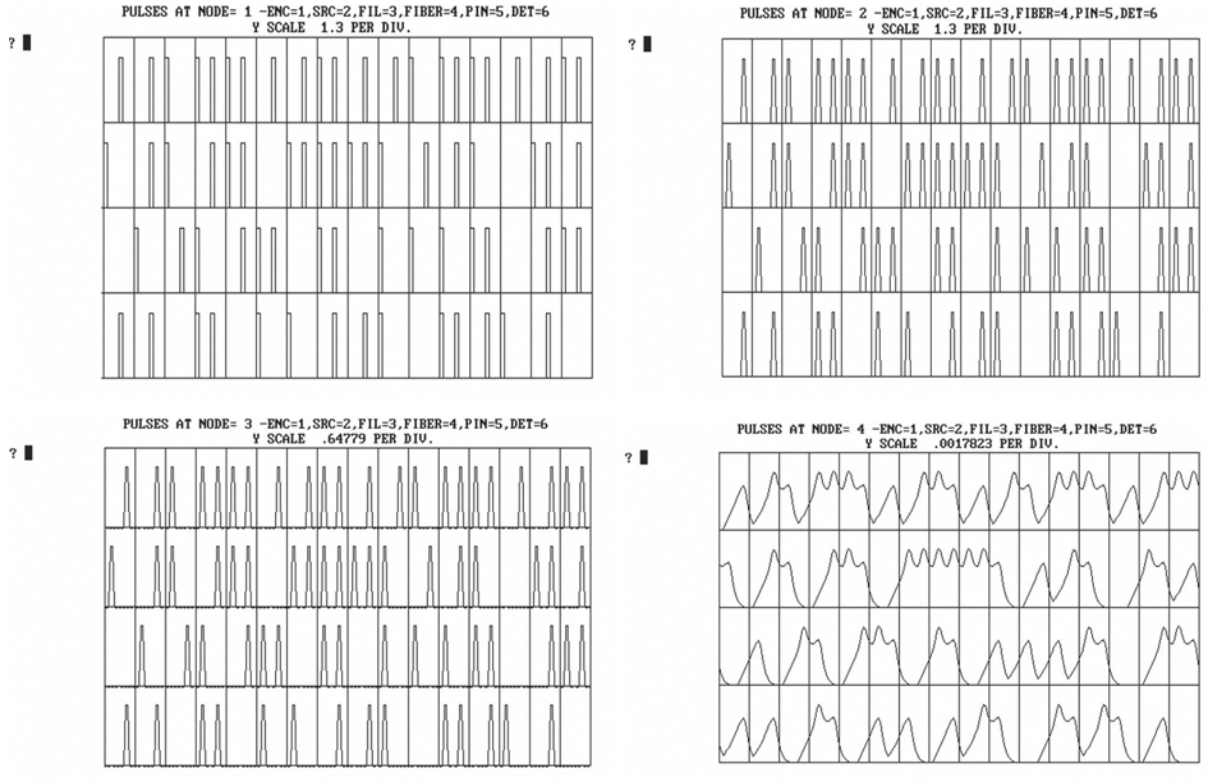

Fig 8.68 Data pulses at different nodes

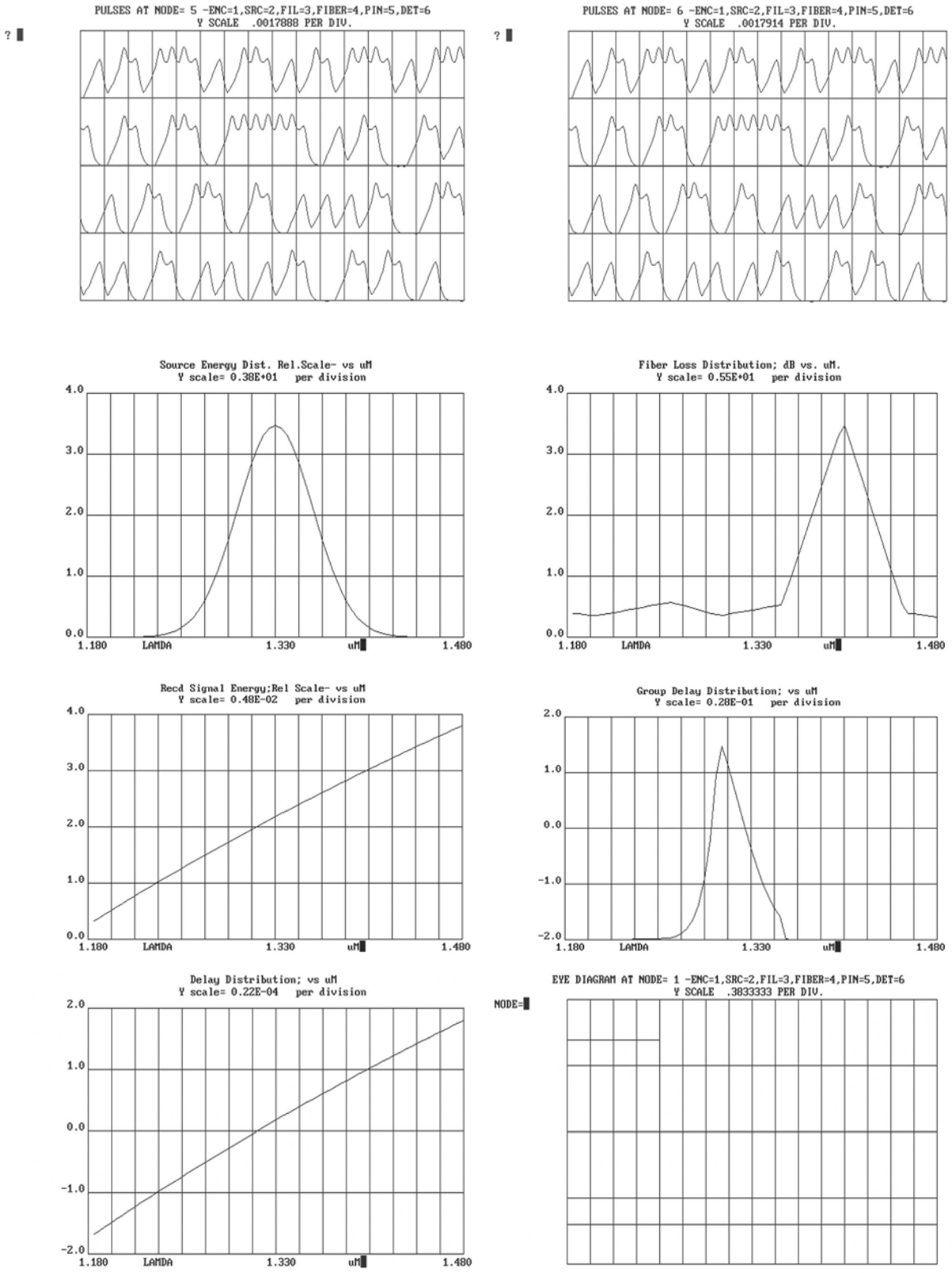

Fig 8.69 Pulse shapes at nodes 5 & 6, source energy distribution, fiber loss distribution Received signal energy, group & delay distributions and eye diagram at node1

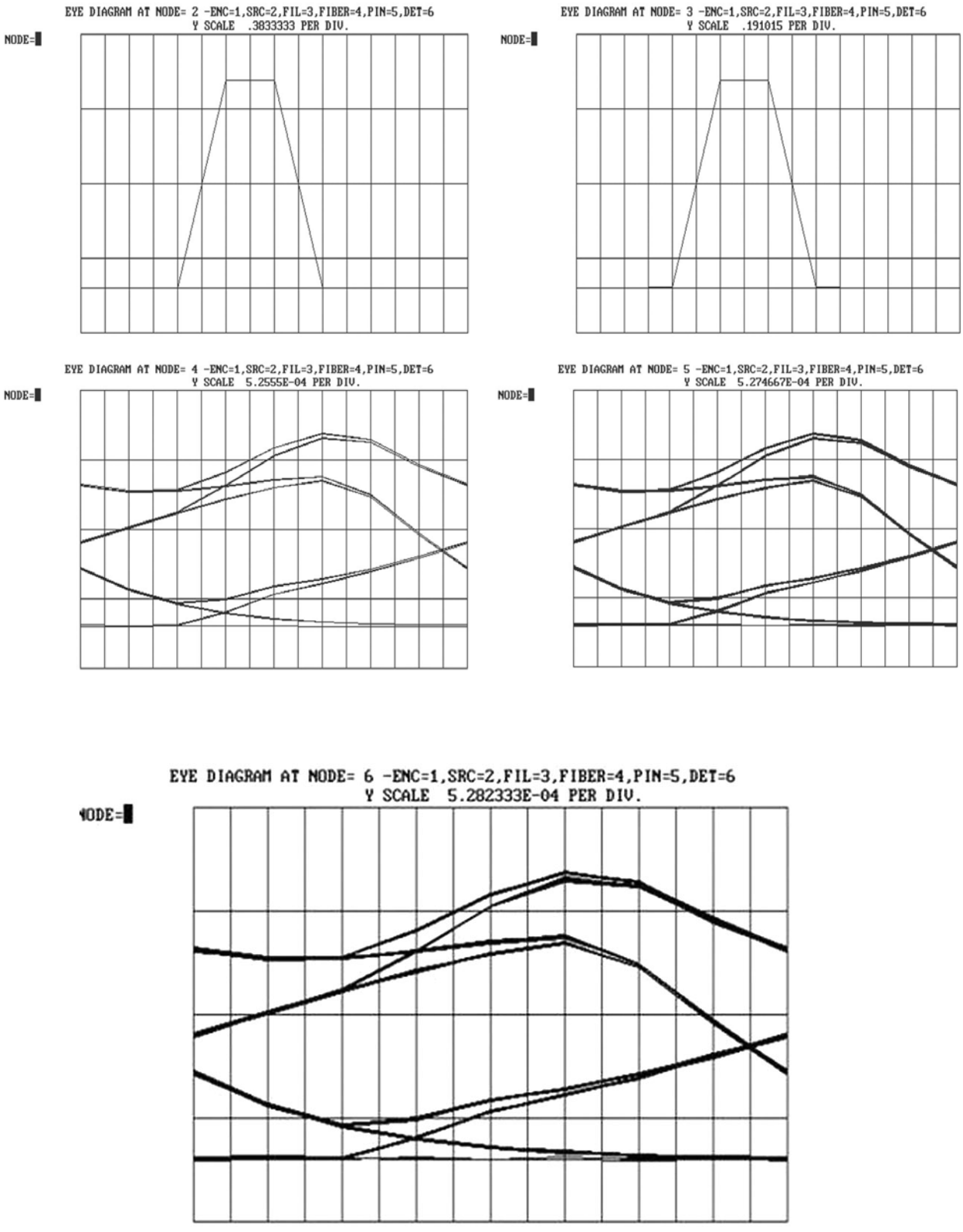

Fig 8.70 Eye diagram at different nodes

b) Effects of Quarter-Width Pulses: Fiber length is 100 km and the rate is 160 MB/s

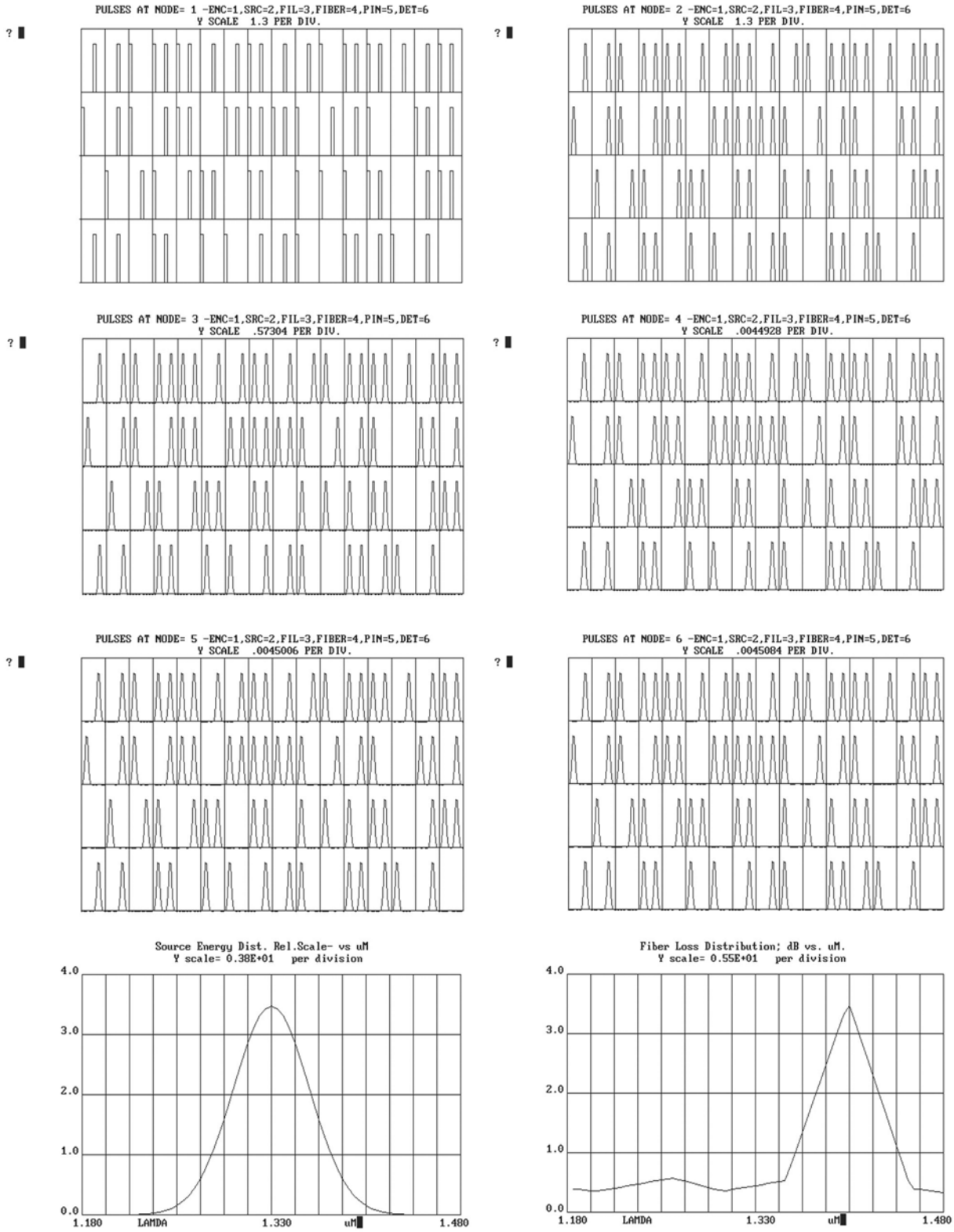

Fig 8.71 Pulse shapes at different nodes, source energy and fiber loss distributions

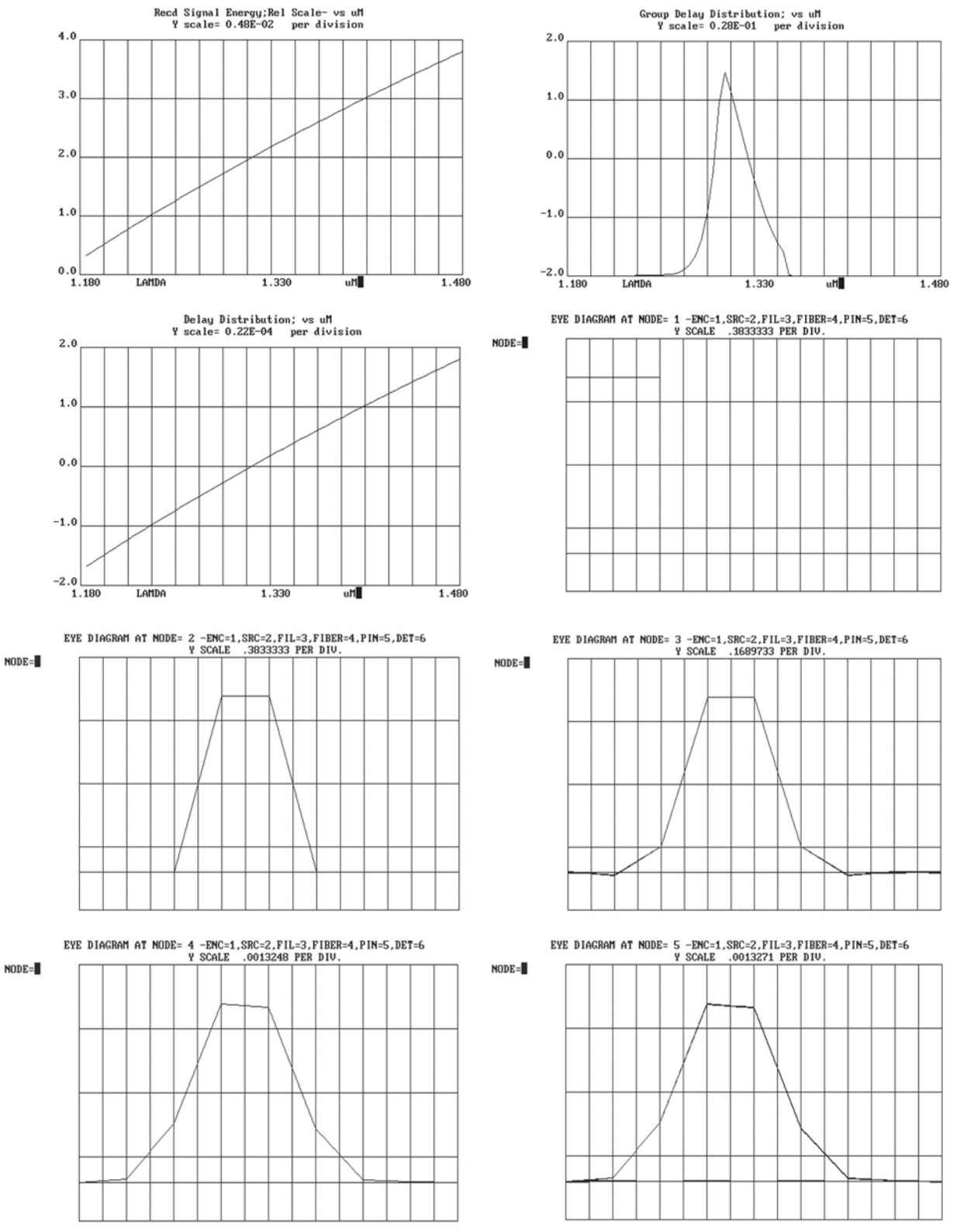

Fig 8.72 Received signal energy, group delay distribution, delay distribution, and eye diagrams at different nodes

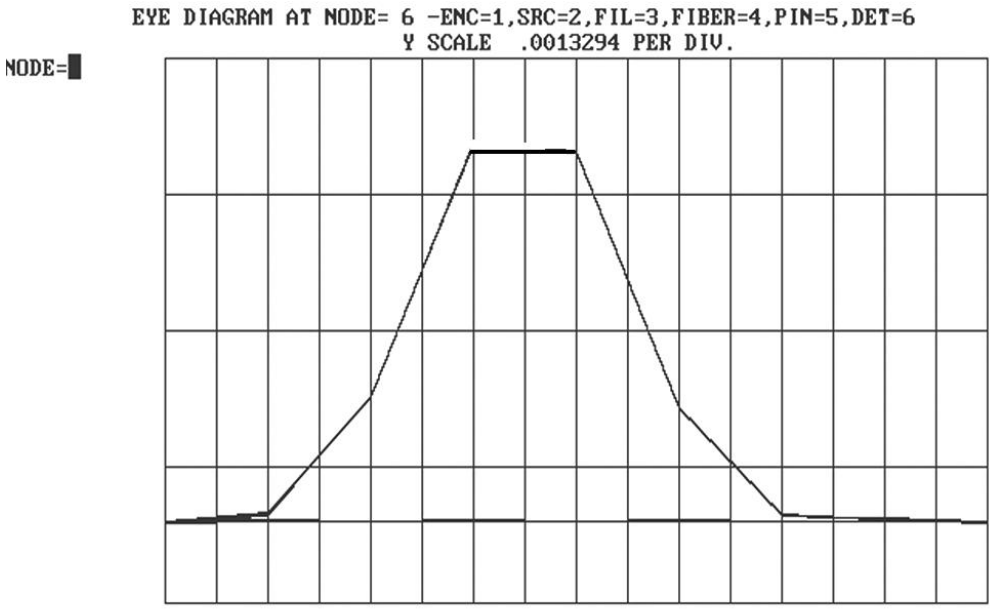

Fig 8.73 Eye diagram at node 6.

c) Effects of Quarter-Width Pulses **:**Fiber length is 100 km and the rate is 320 MB/s

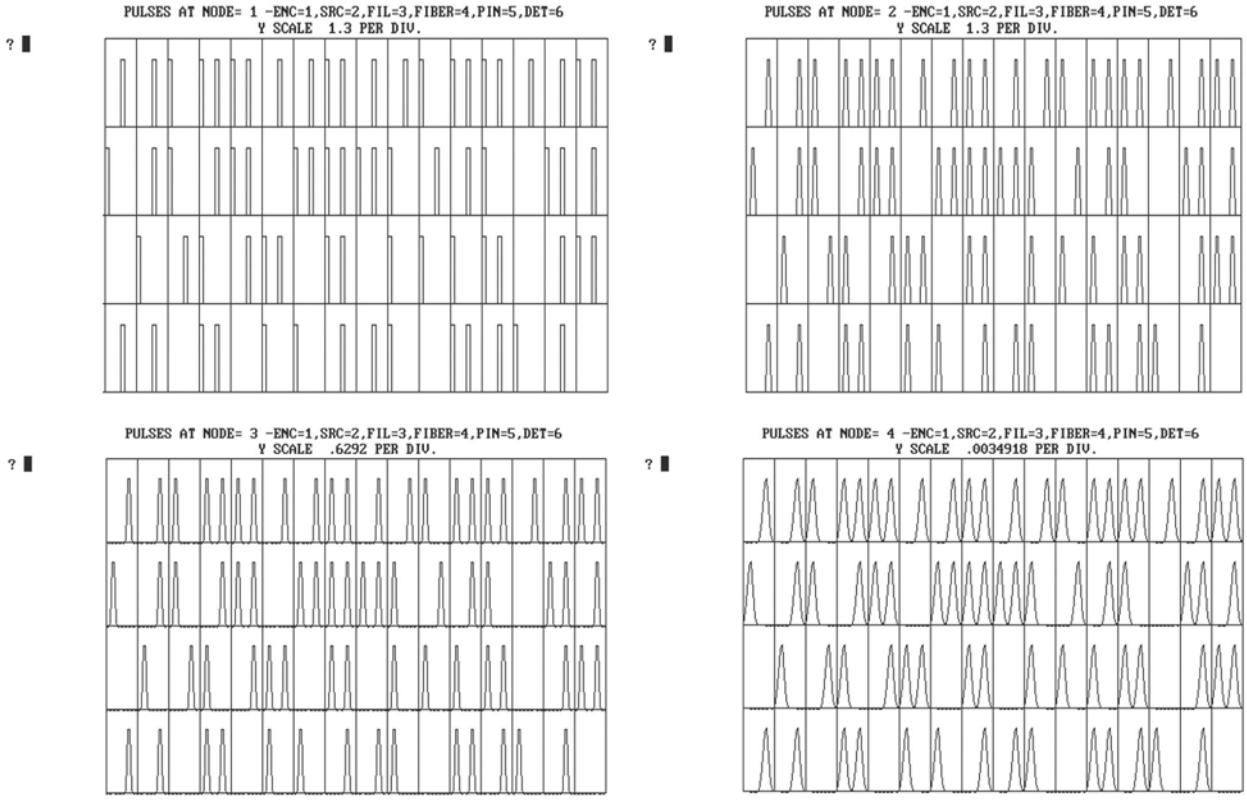

Fig 8.74 Data pulses at different nodes.

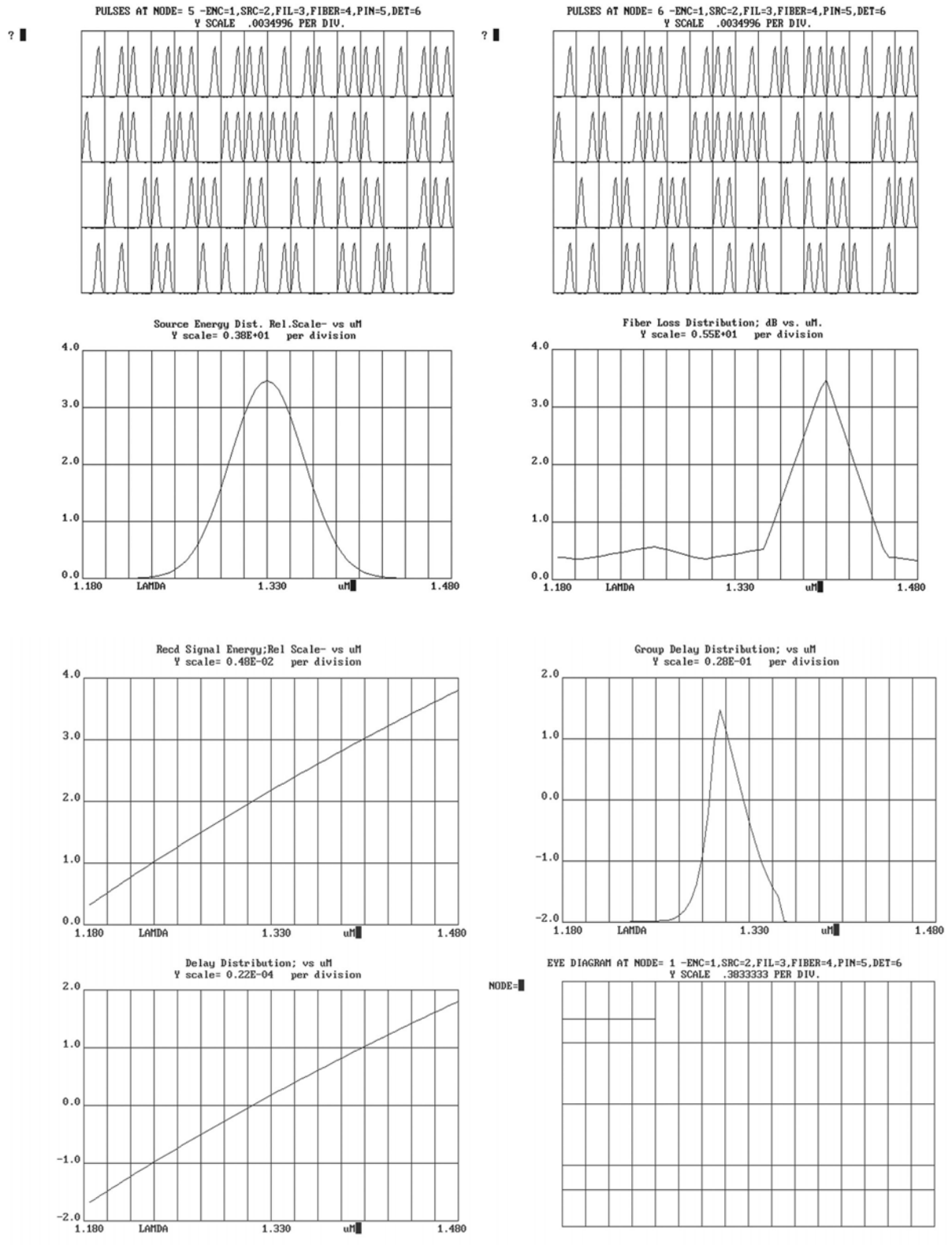

Fig 8.75 Data pulses at nodes 5 and 6, source energy distribution and fiber loss distribution**,** received signal energy, group delay distribution, delay distribution and eye diagram at node 1.

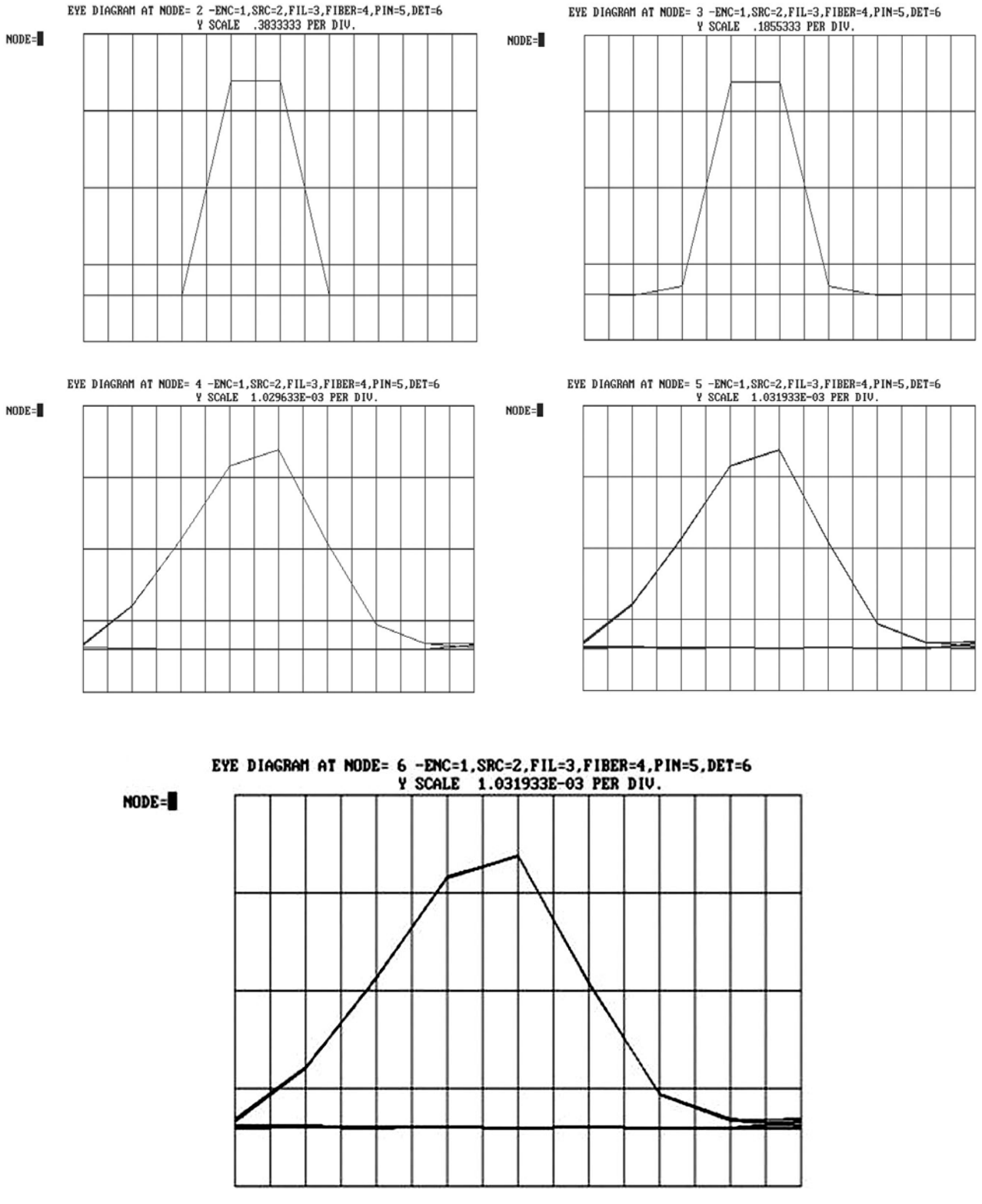

8.76 Eye diagram at different nodes

d) Effects of Quarter-Width Pulses**:** Fiber length is 100 km and the rate is 640 MB/s

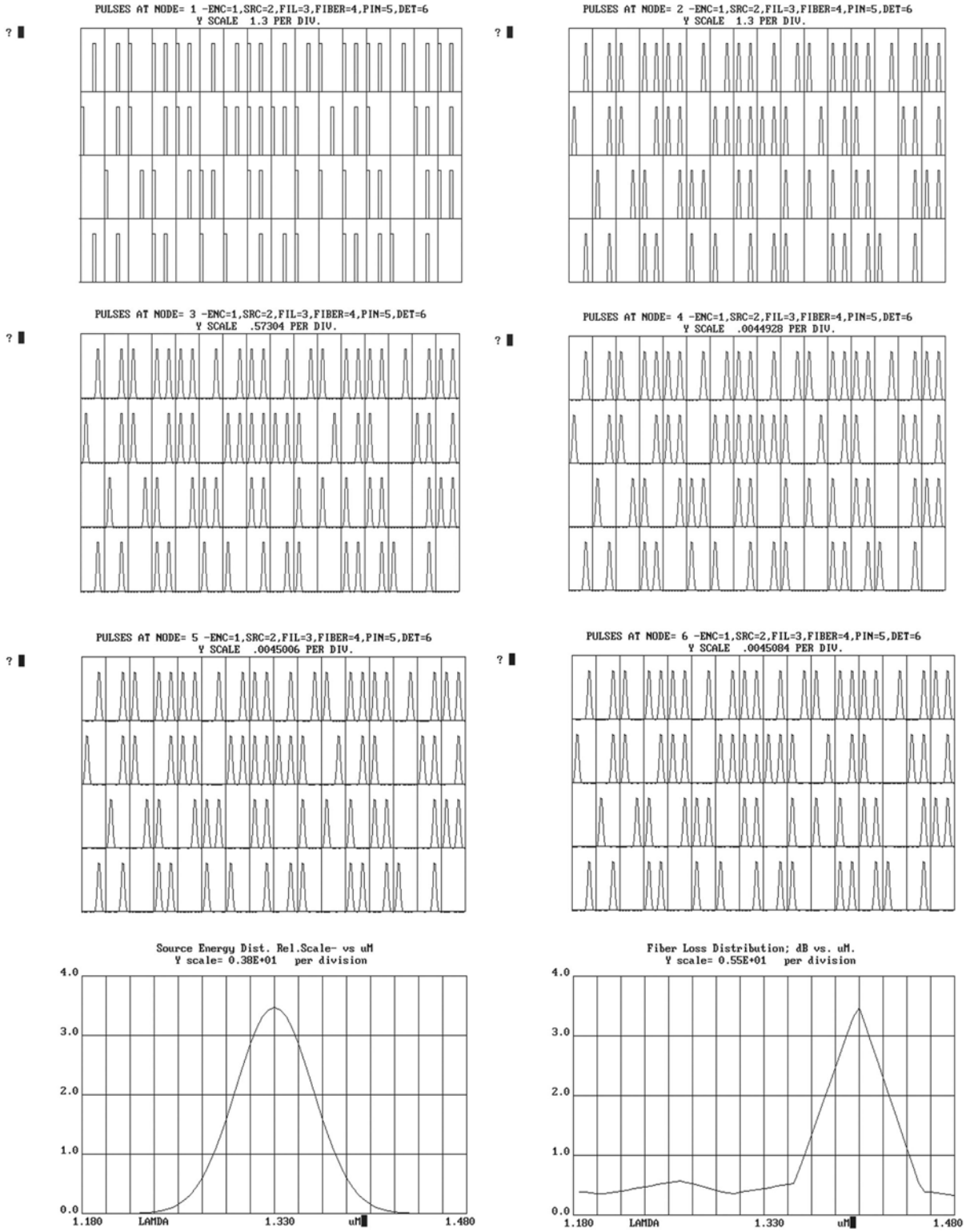

Fig 8.77 Pulse shapes at different nodes, source energy and fiber loss distributions

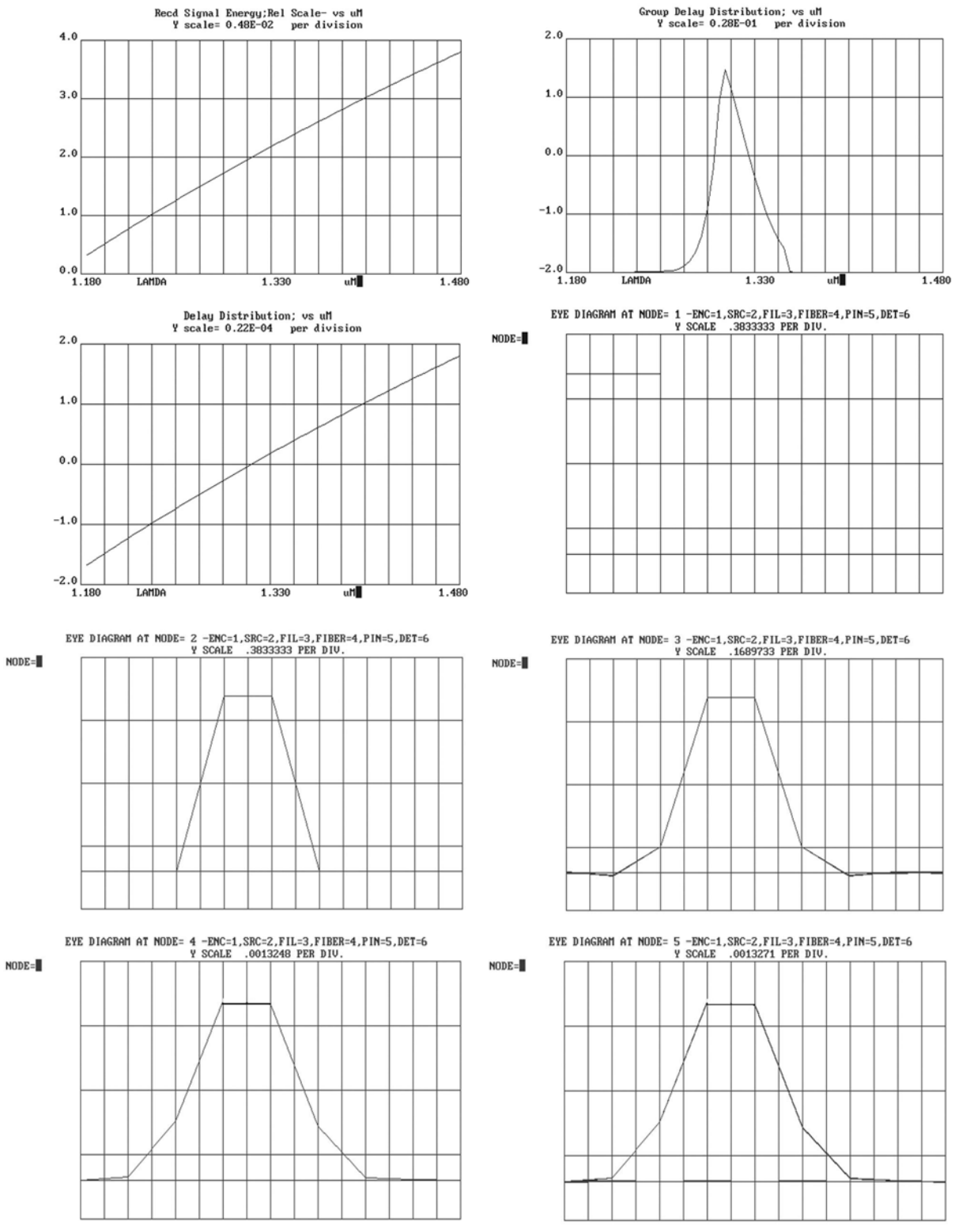

Fig 8.78 Received signal energy, group delay distribution, delay distribution and eye diagram at different nodes

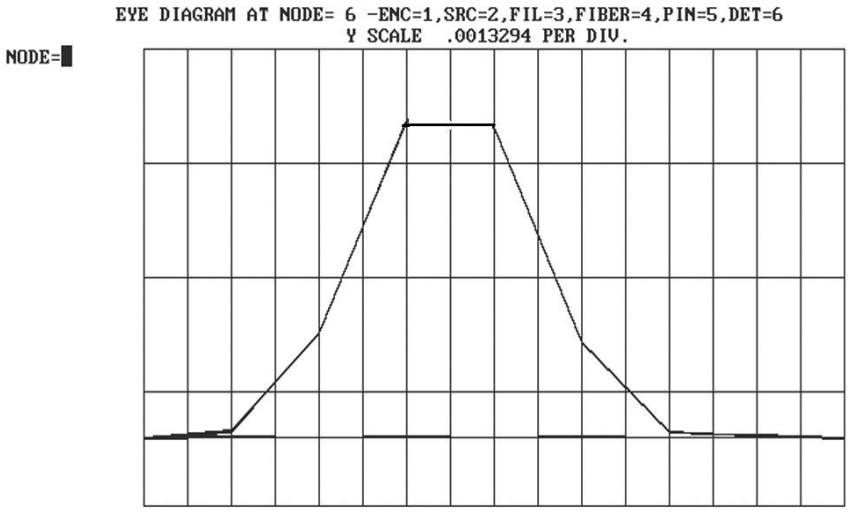

Fig 8.79 Eye diagram at node 6

d) Effects of Quarter-Width Pulses**:** Fiber length is 200 km and the rate is 160 MB/s

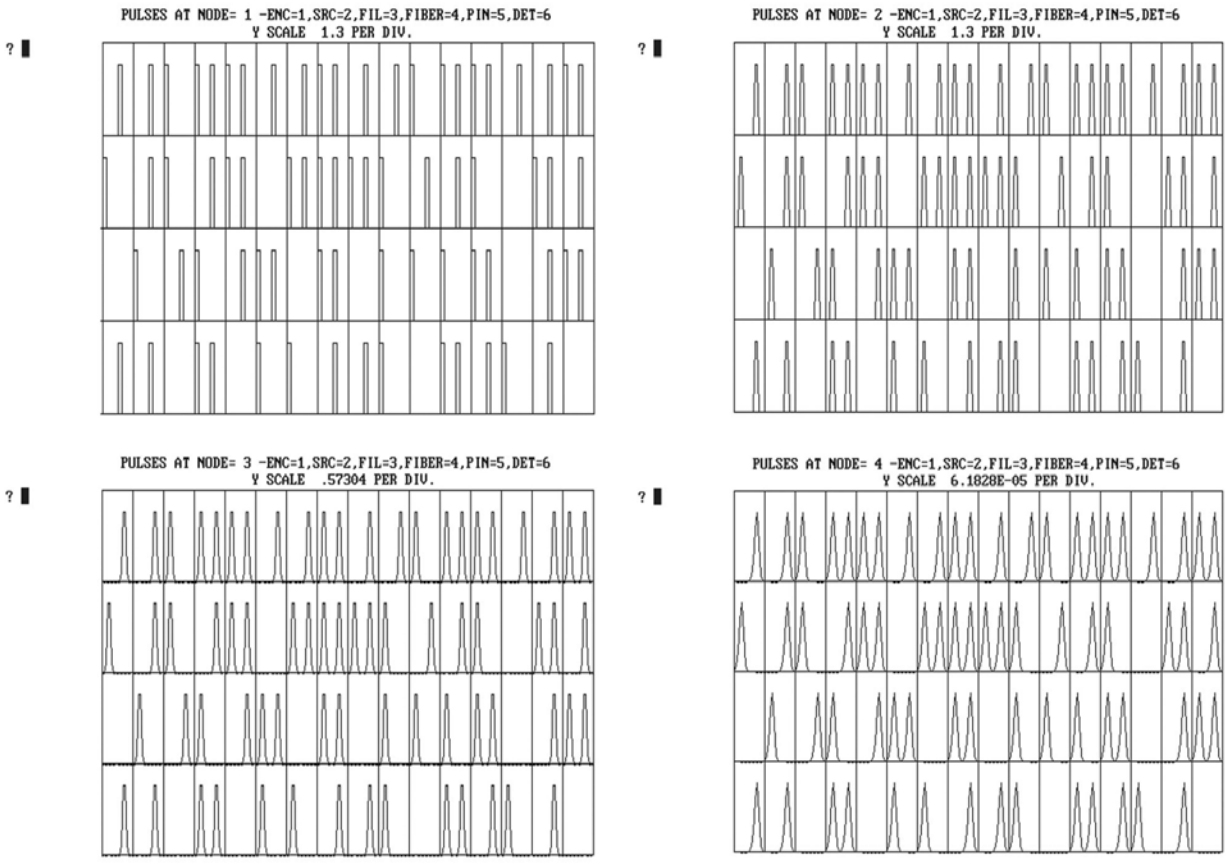

Fig 8.80 Pulse shapes at different nodes

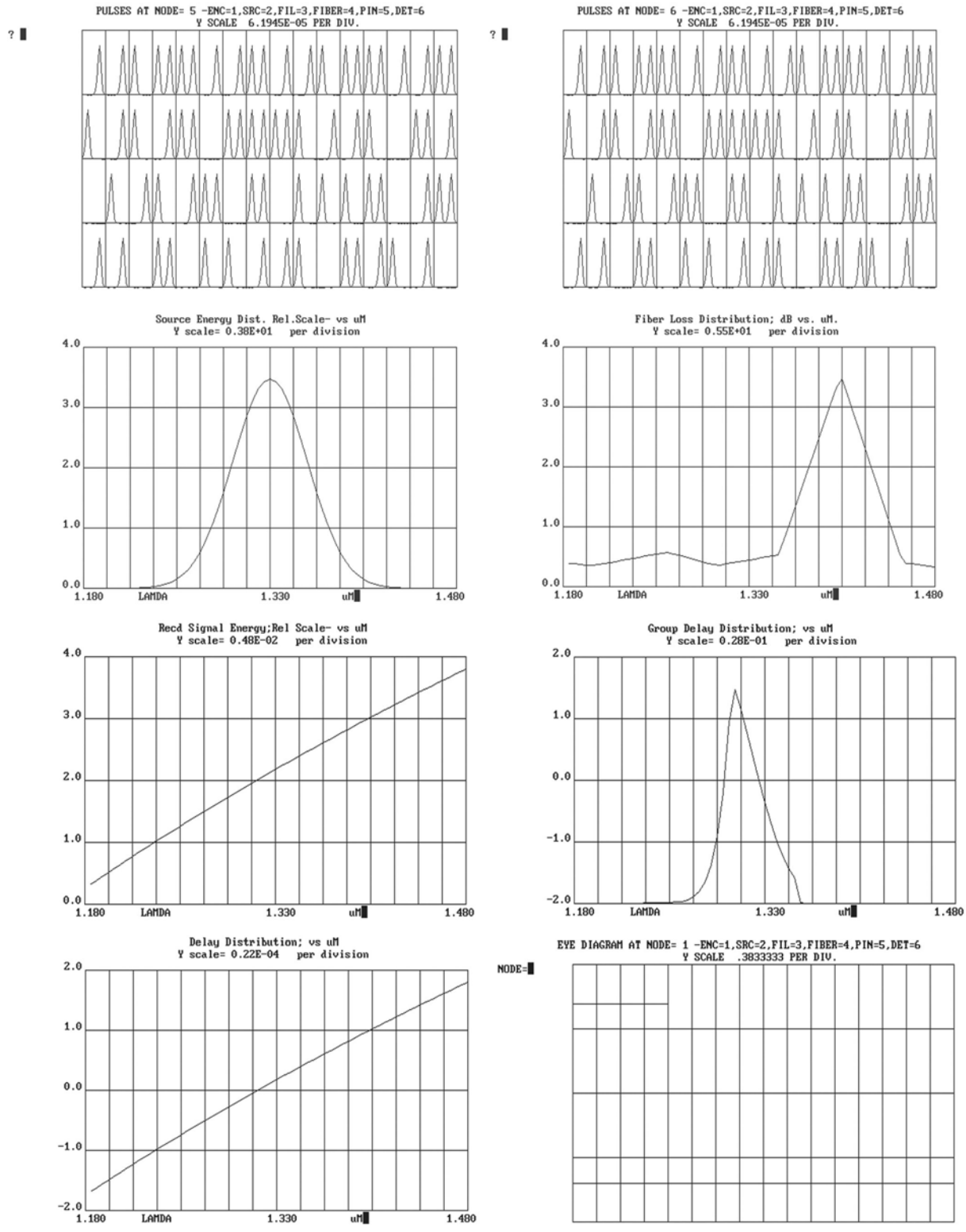

Fig 8.81 Data pulses at nodes 5 and 6, source energy distribution and fiber loss distribution**,** received signal energy, group delay distribution, delay distribution and eye diagram at node1.

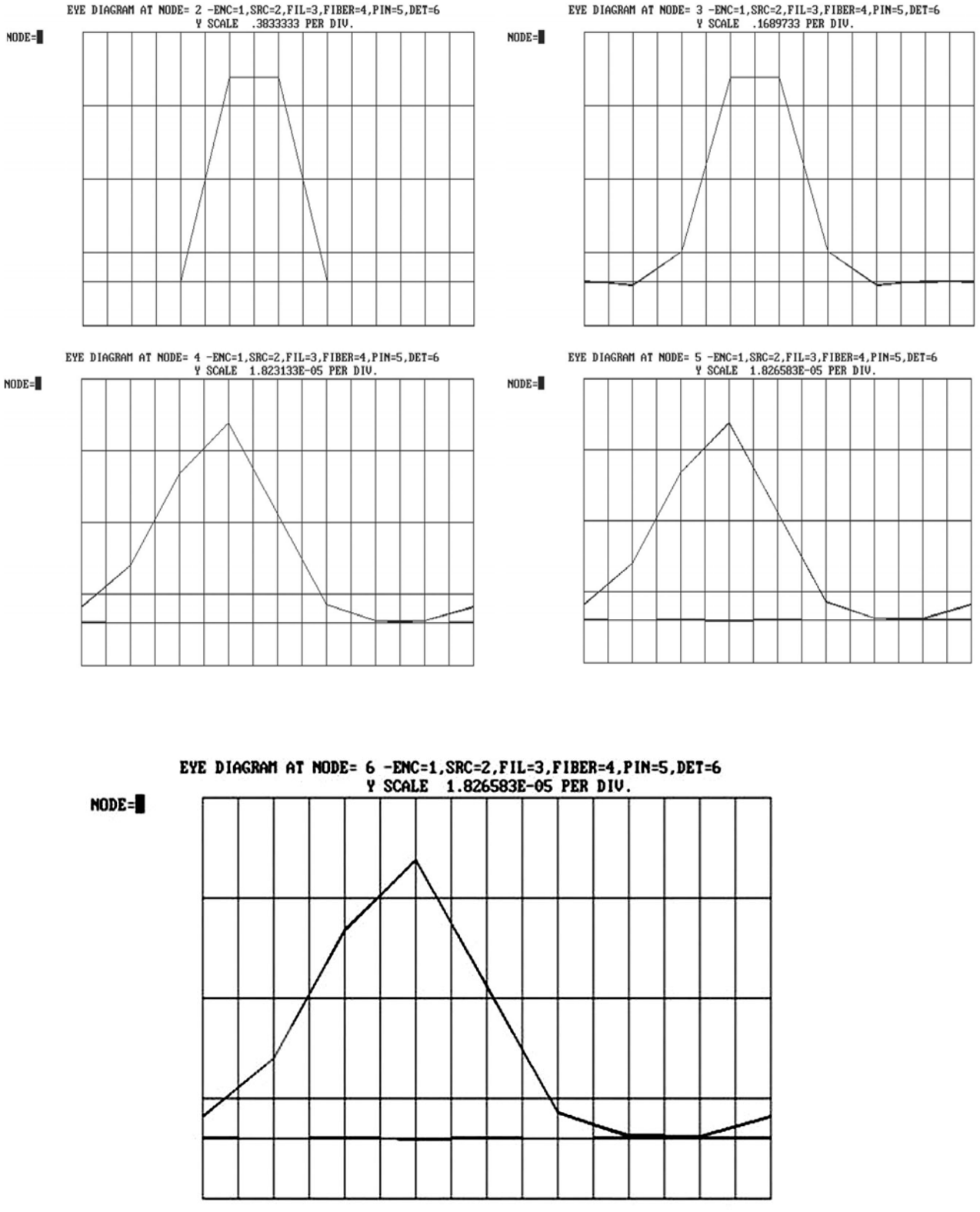

Fig 8.82 Eye diagrams at different nodes

f) Effects of Quarter-Width Pulses**:** Fiber length is 200 km and the rate is 320 MB/s

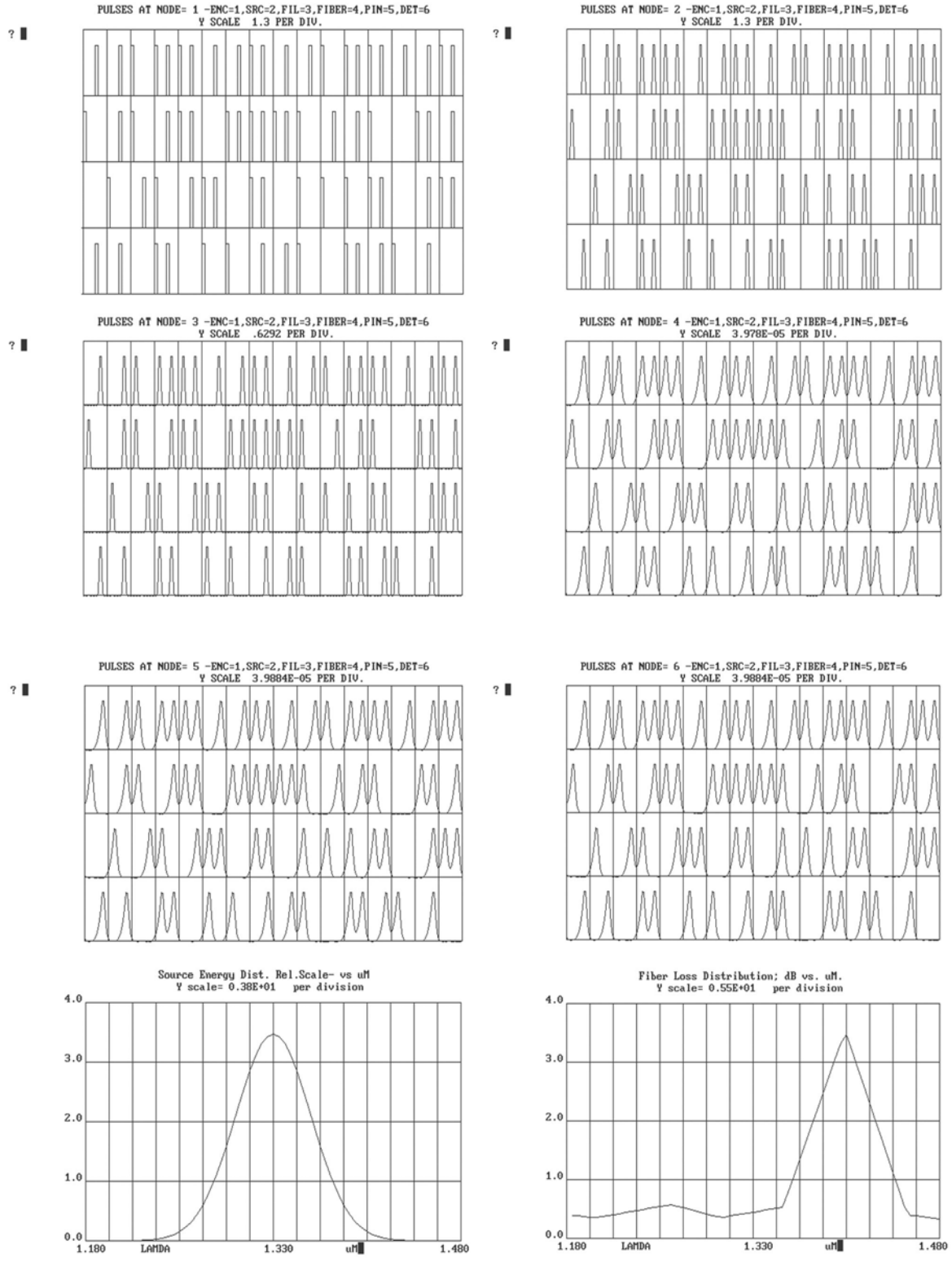

Fig 8.83 Data pulses at different nodes, source energy and fiber loss distributions

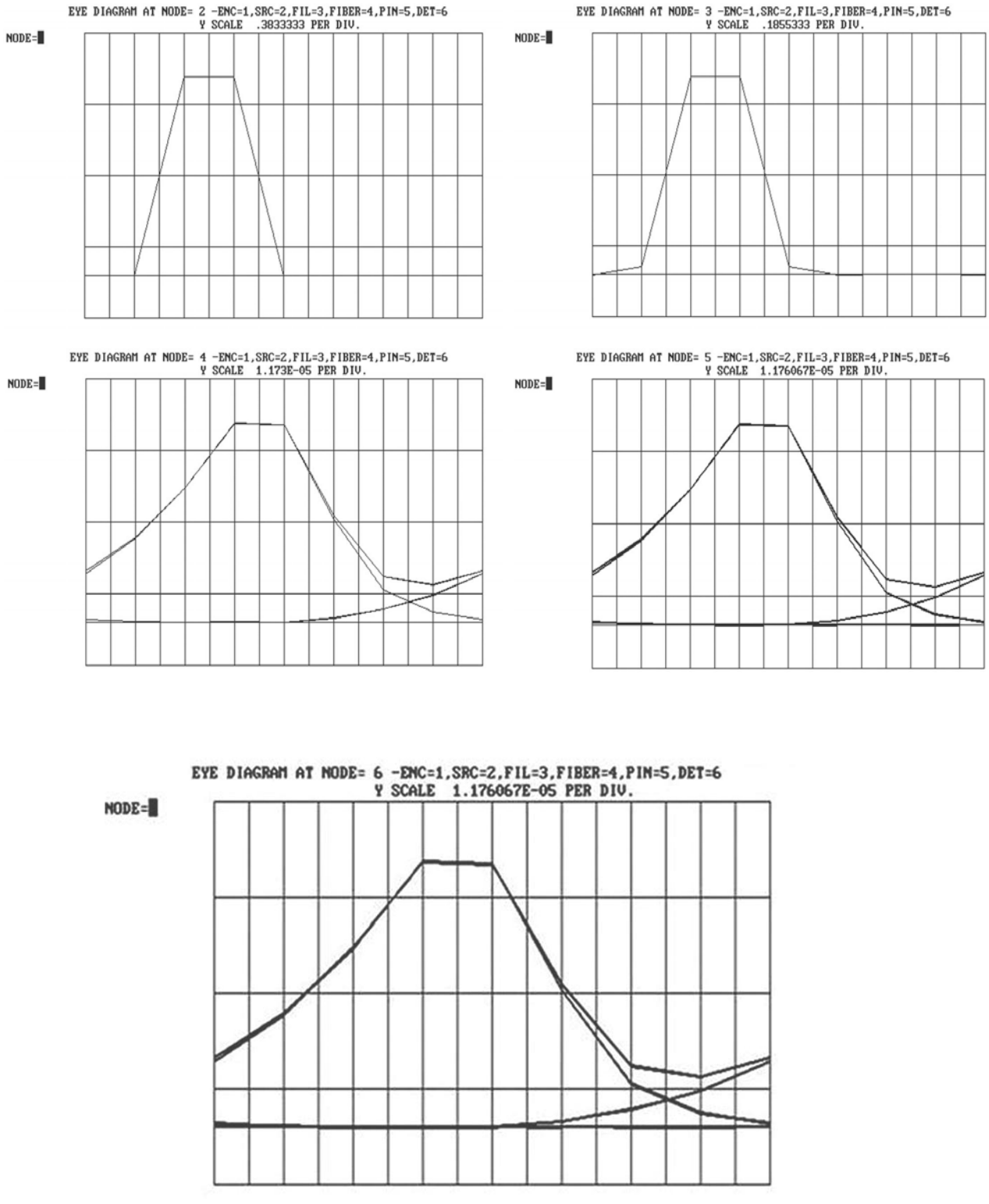

Fig 8.84 Eye diagrams at different nodes

8.1.8 Plastic Fiber Simulation

a). Poly Methyl Meth-Acrylate fiber with the Length 50m and the rate 1GB/s

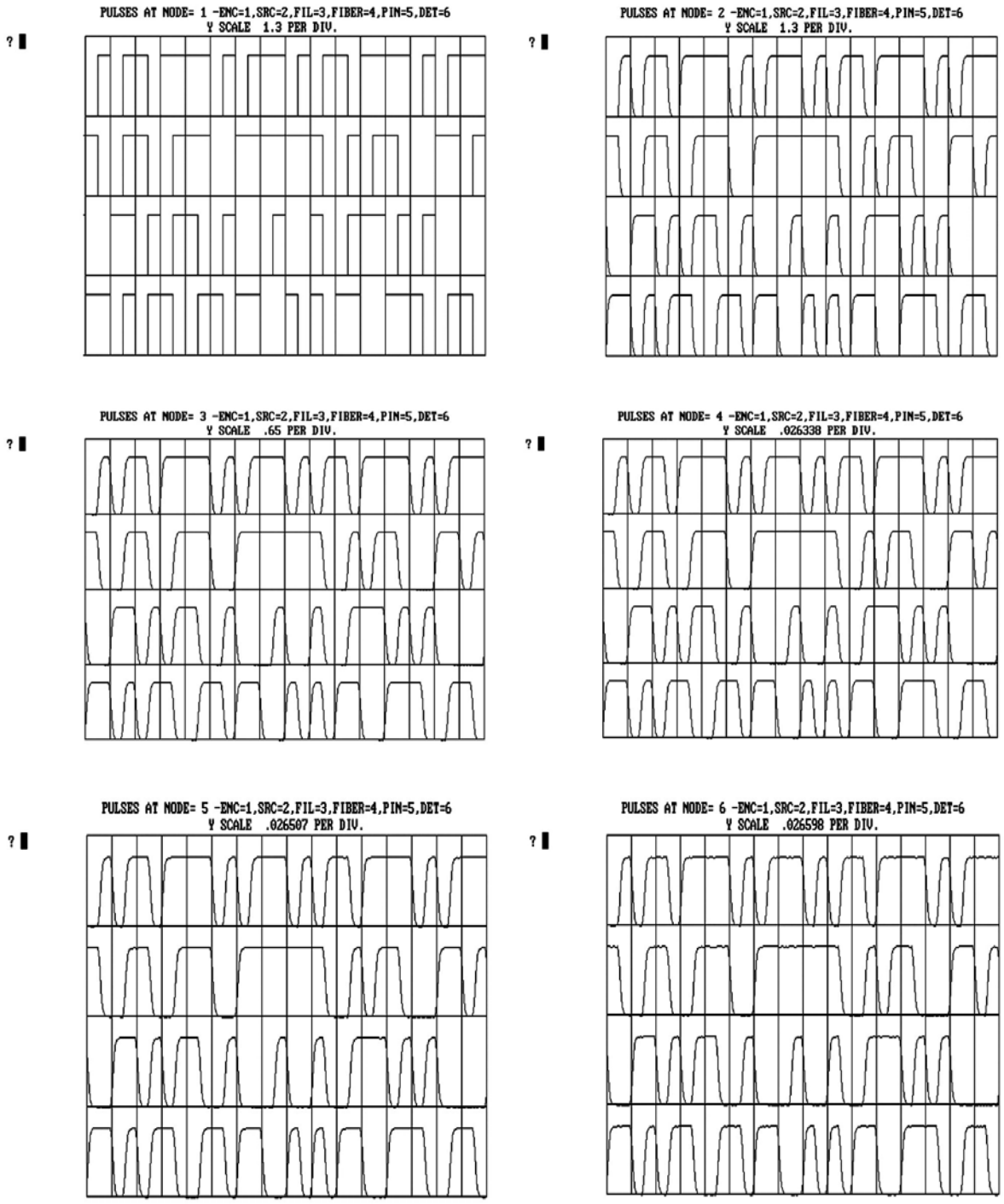

Fig 8.85 Pulse shapes at different nodes

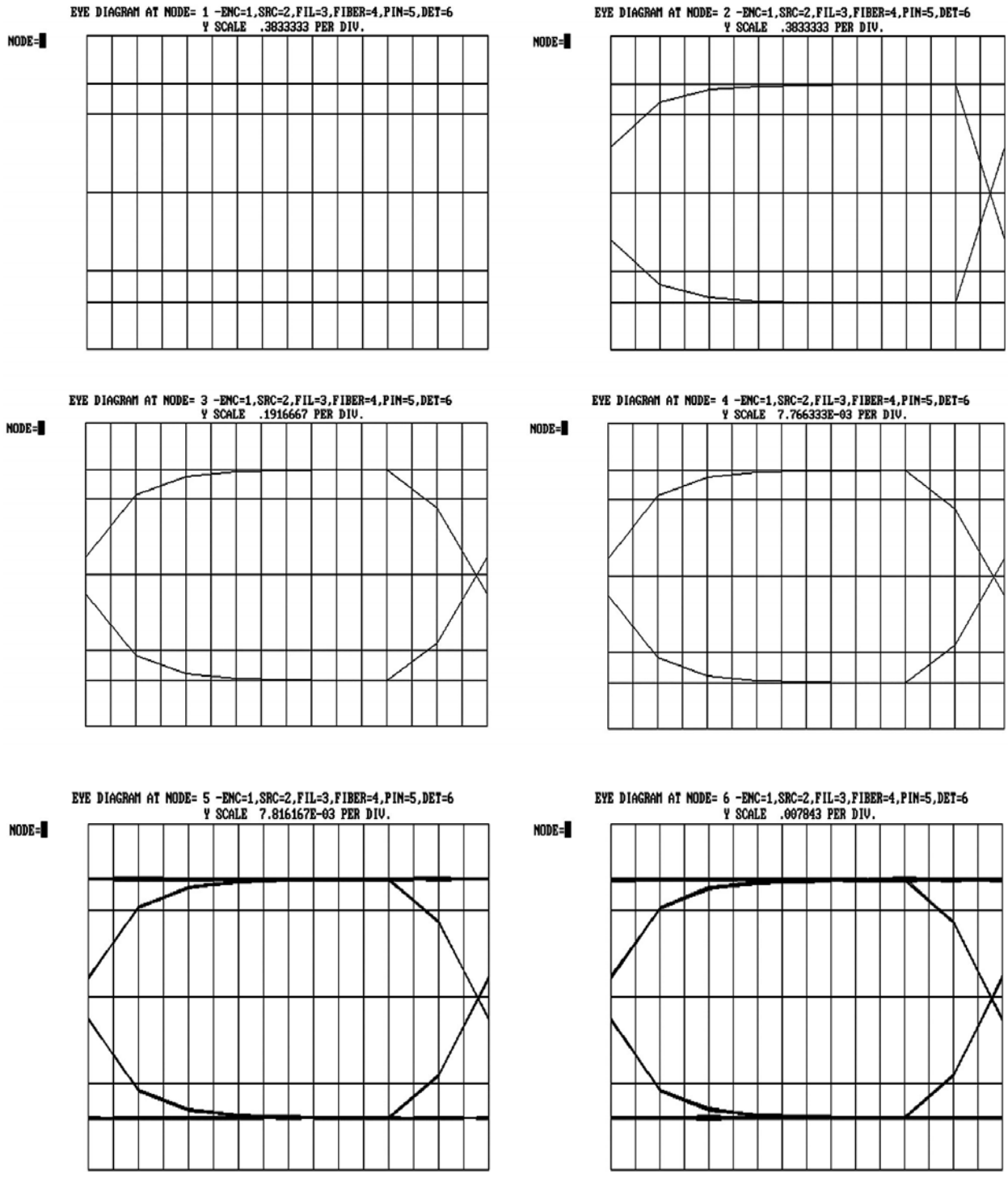

Fig 8.86 Eye diagrams at different nodes

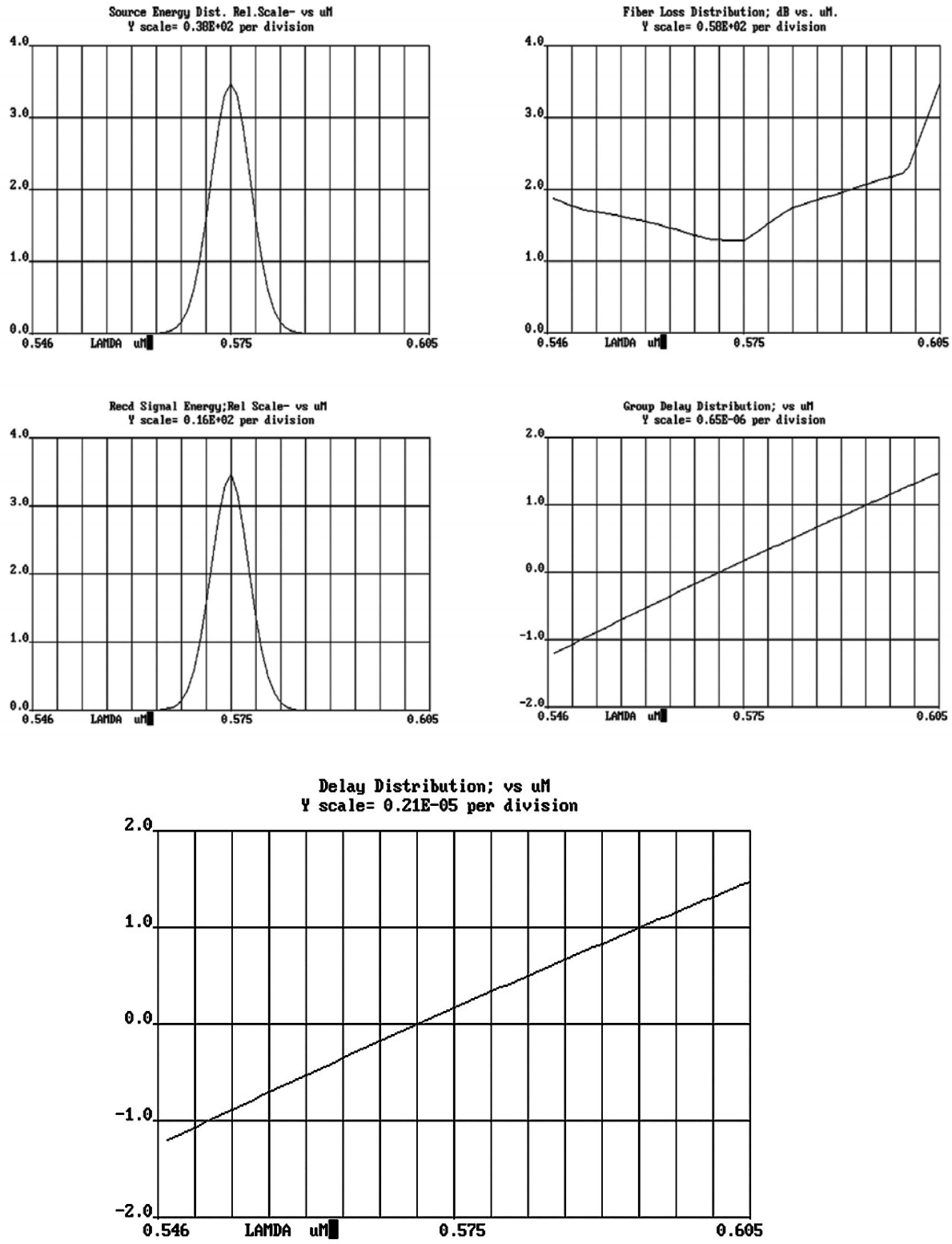

Fig 8.87 Source energy distribution, fiber loss distribution, received signal energy, group delay distribution and delay distribution.

b) Plastic Fiber : Length is 100 m and the rate is 2 GB/s

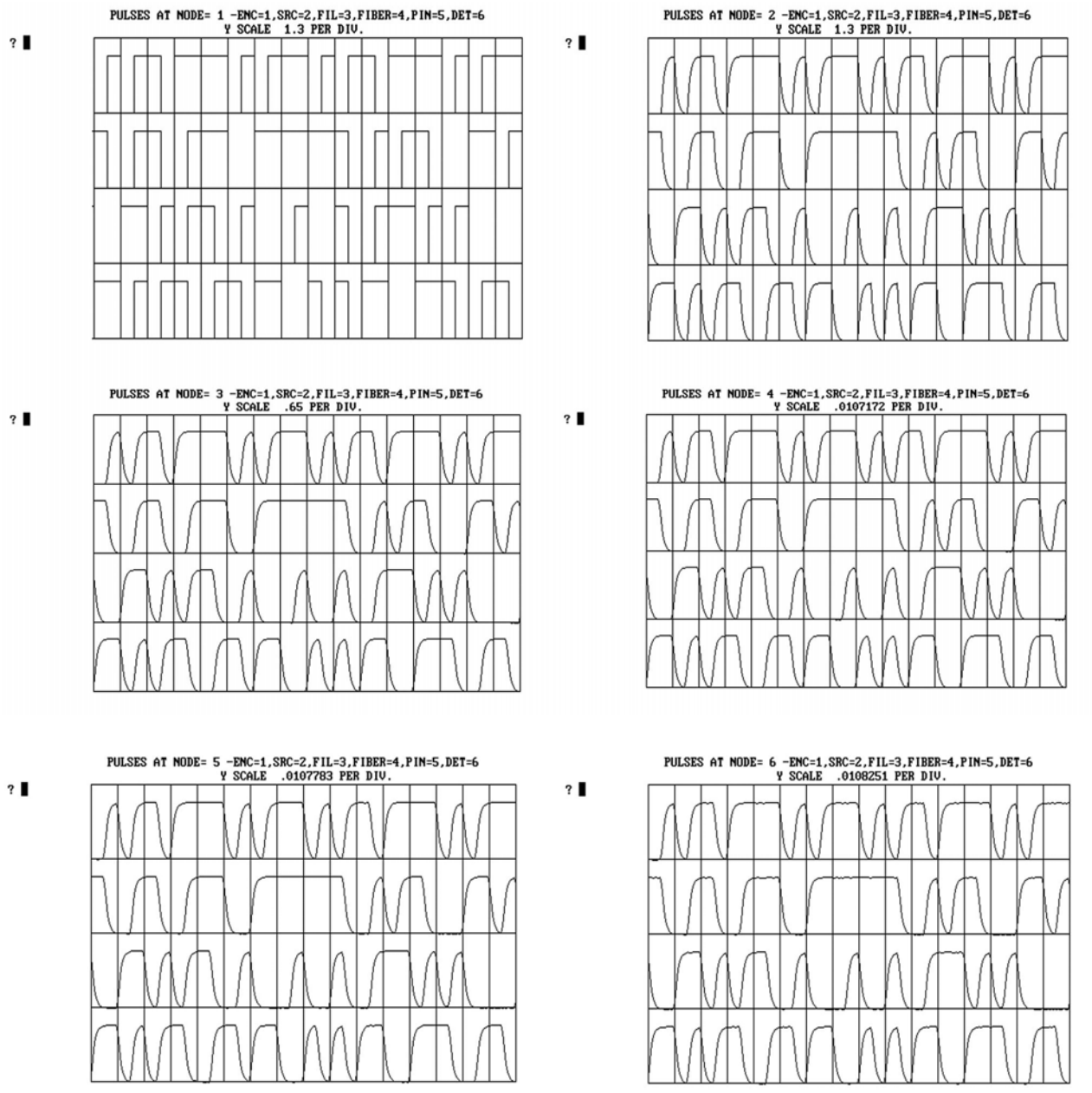

Fig 8.88 Pulse shapes at different nodes

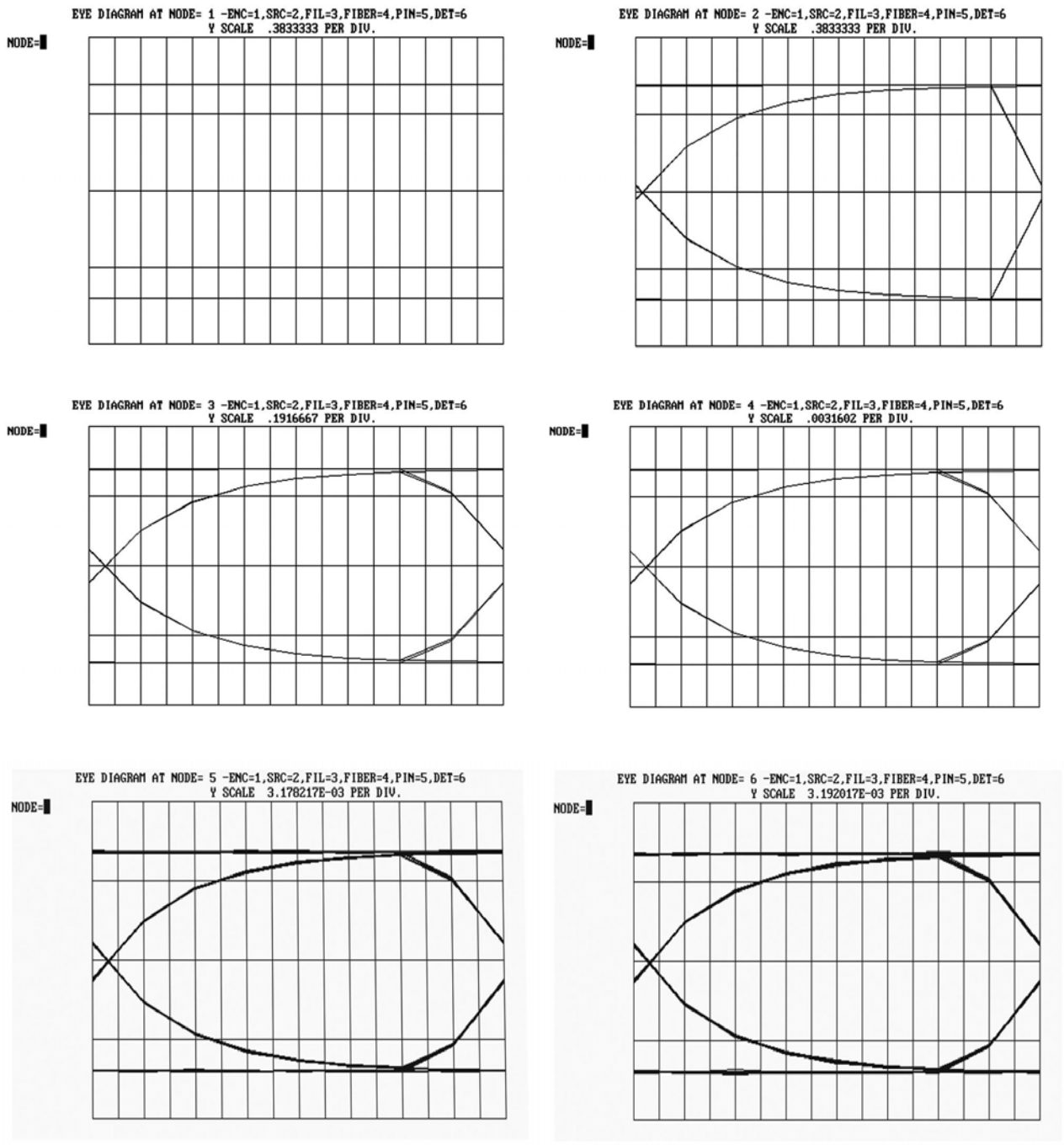

Fig 8.89 Eye diagrams at different nodes

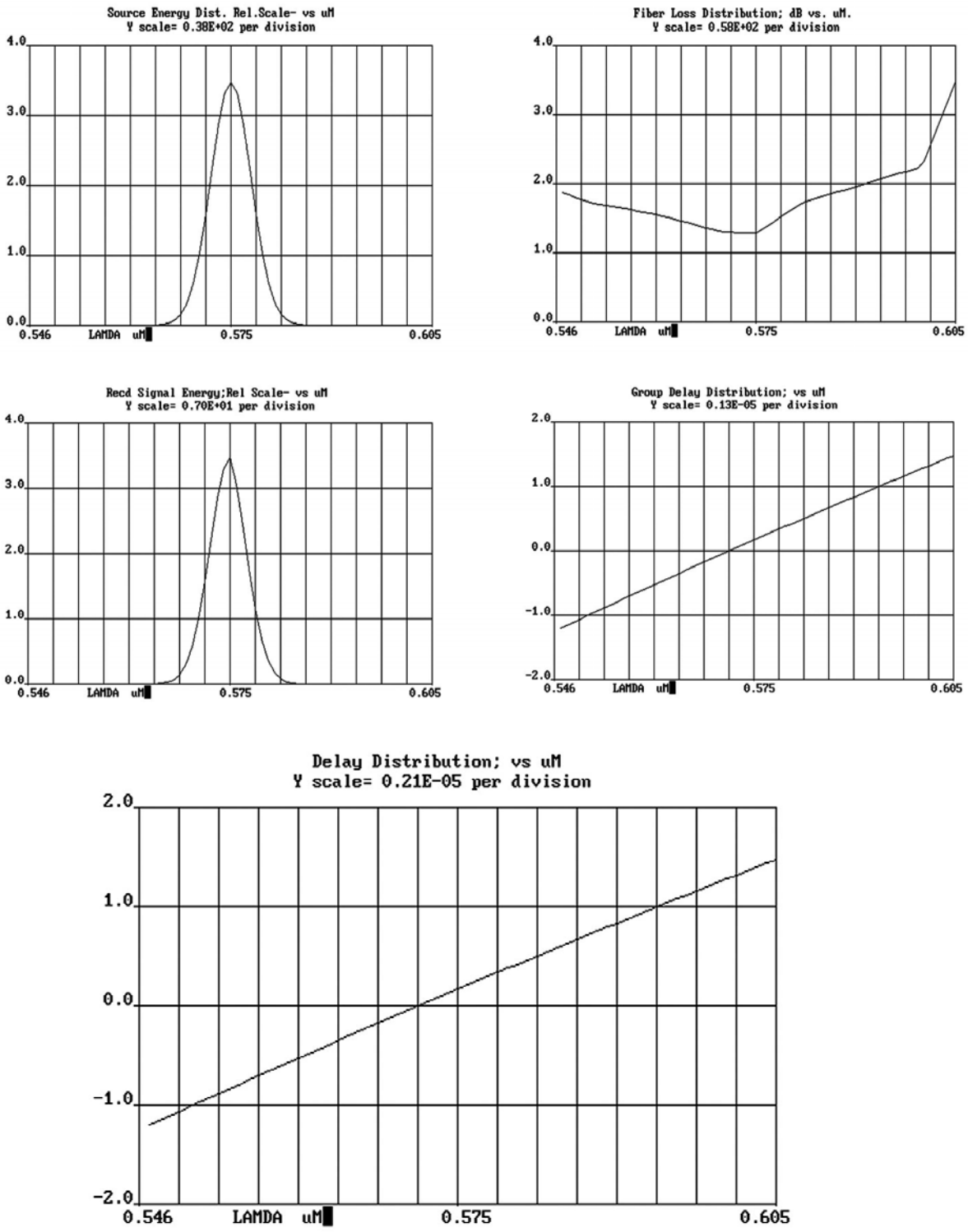

Fig 8.90 Source energy distribution, fiber loss distribution, received signal energy, group delay distribution and delay distribution

8.1.9 Plastic Fiber Simulation with half width pulses

a). Length is 50 m and the rate is 1GB/s

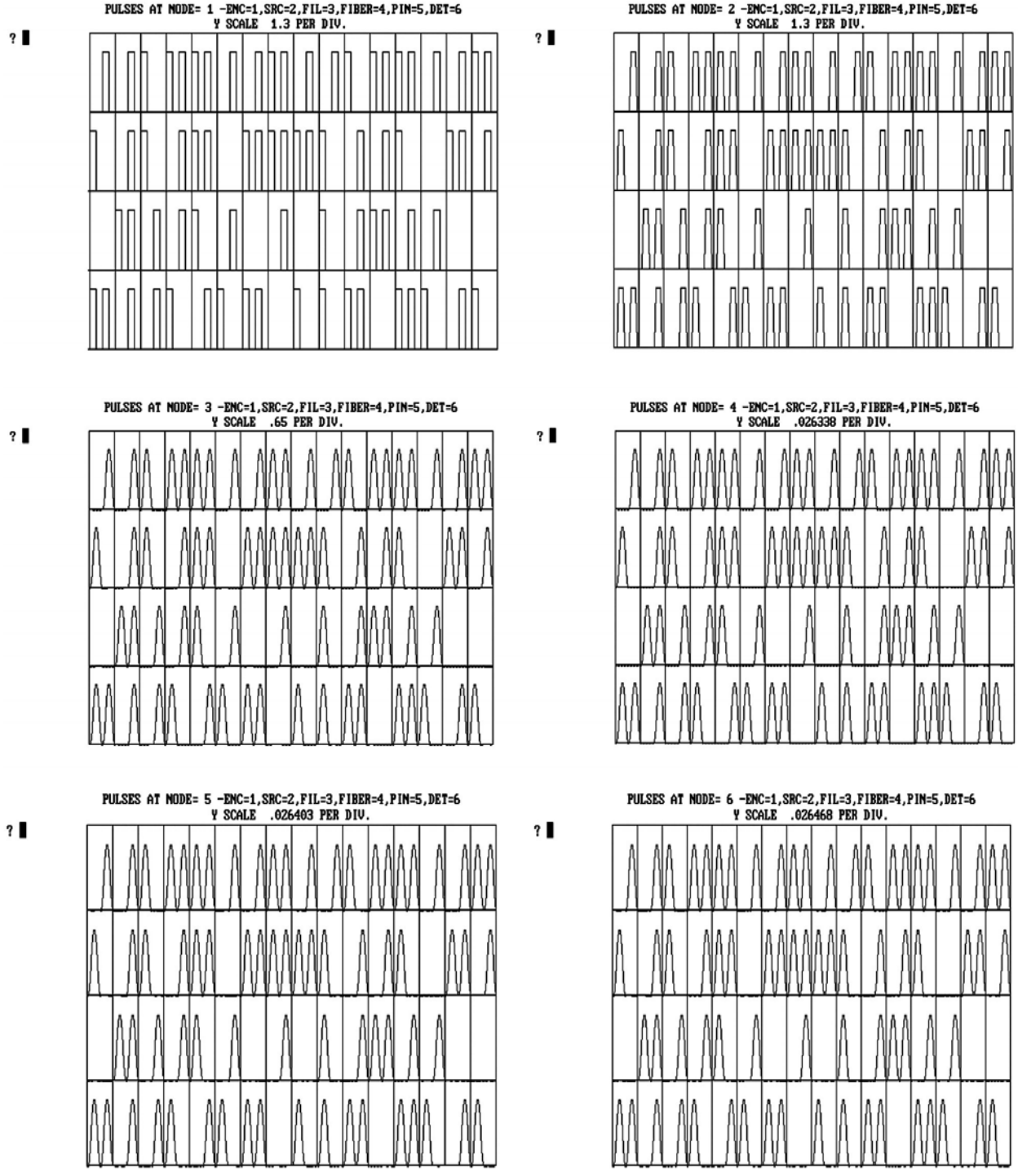

Fig 8.91 Pulse shapes at different nodes

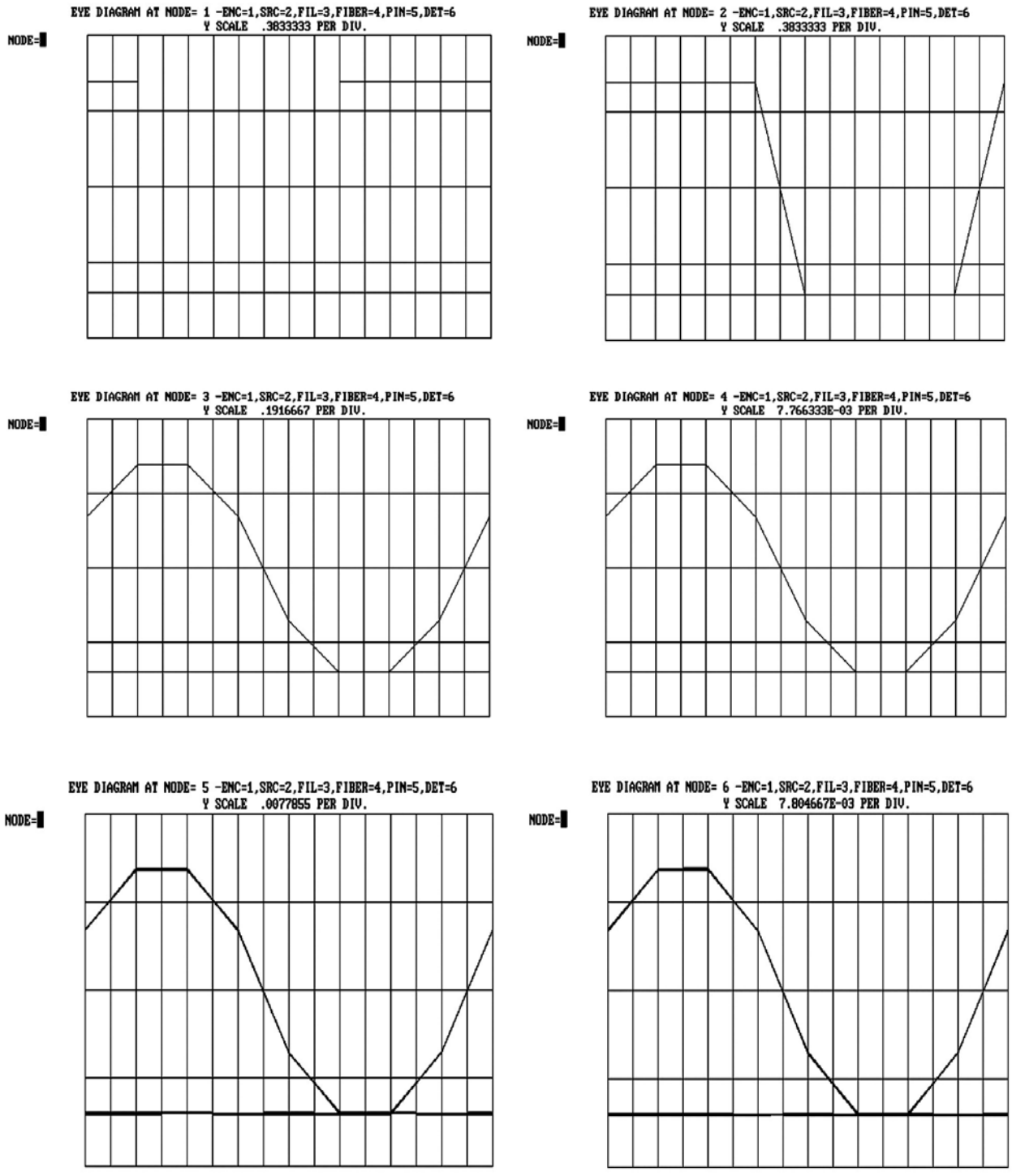

Fig 8.92 Eye diagrams at different nodes

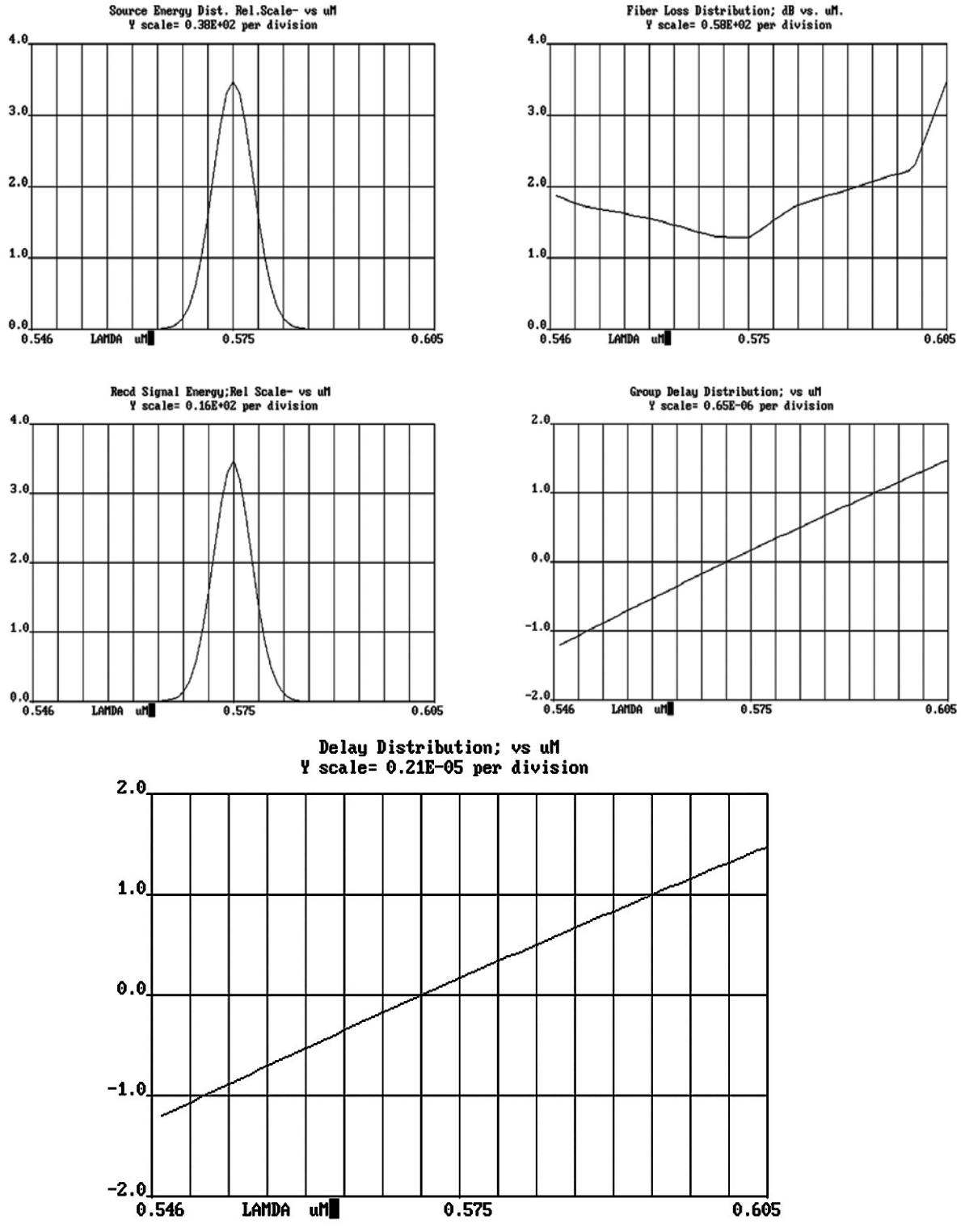

Fig 8.93 Source energy distribution, fiber loss distribution, received signal energy, group delay distribution and delay distribution

b) Plastic Fiber with Half width pulses: length is 100m and the rate is 5 Gb/s

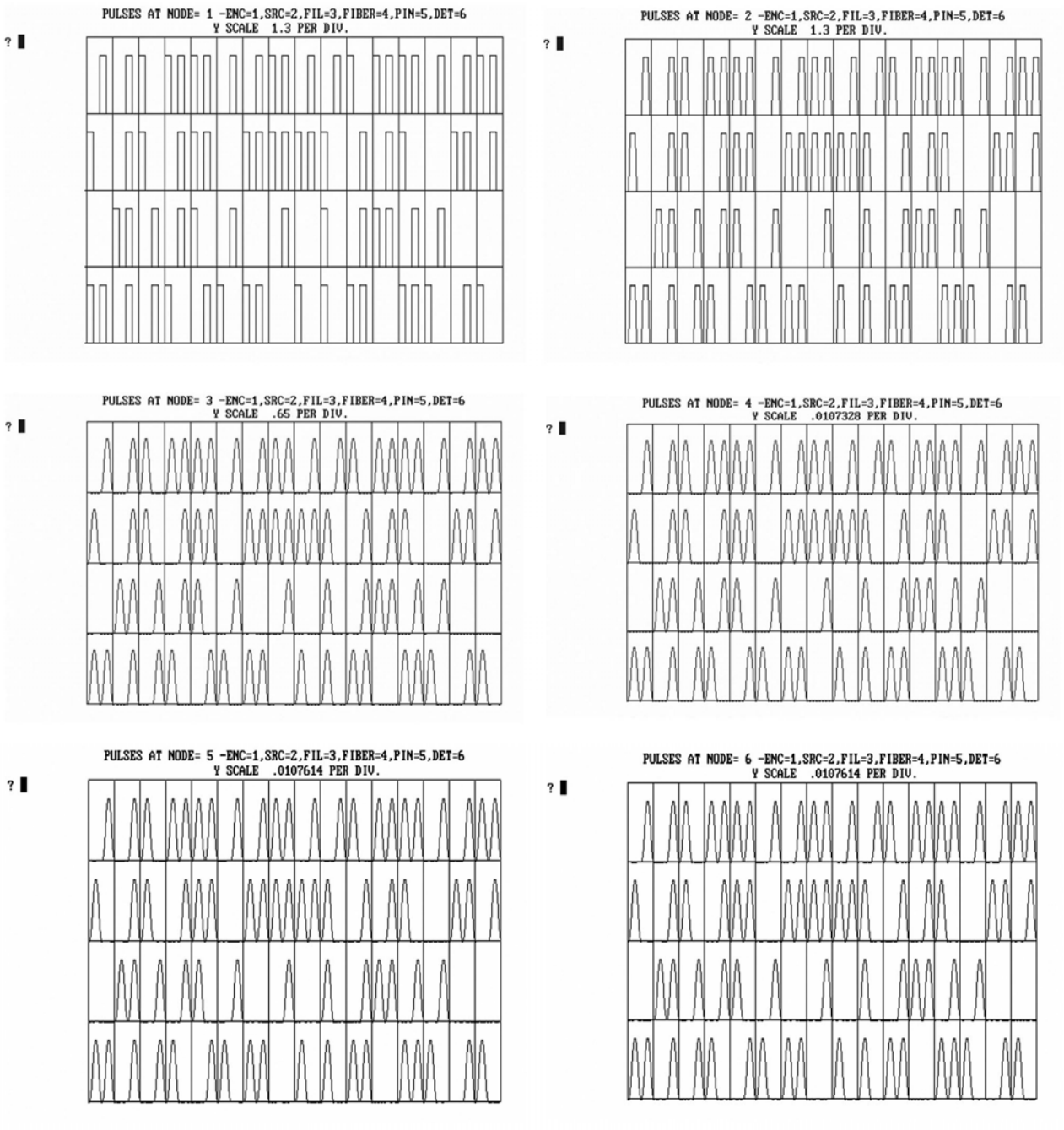

Fig 8.94 Pulse shapes at different nodes

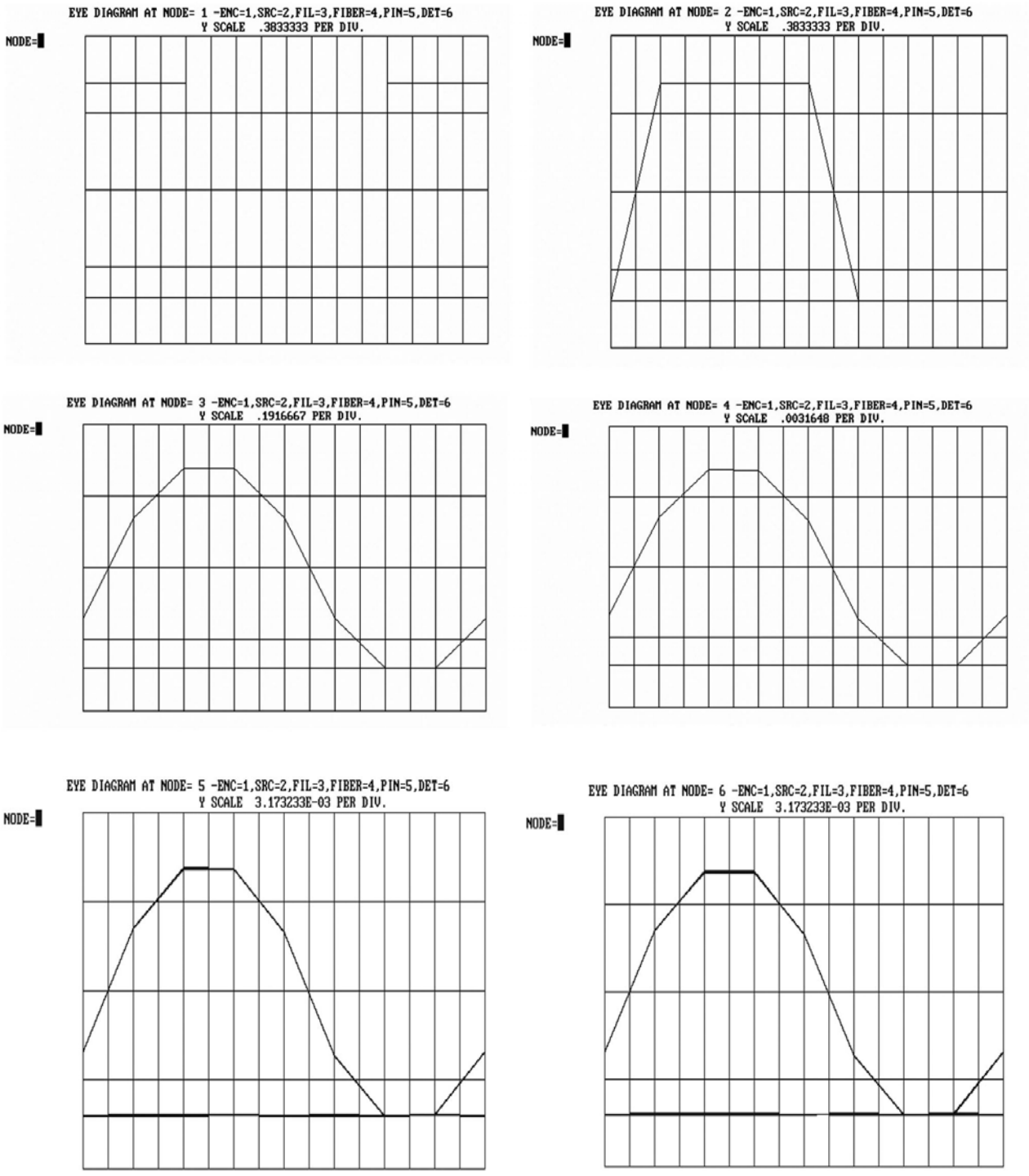

Fig 8.95 Eye diagrams at different nodes

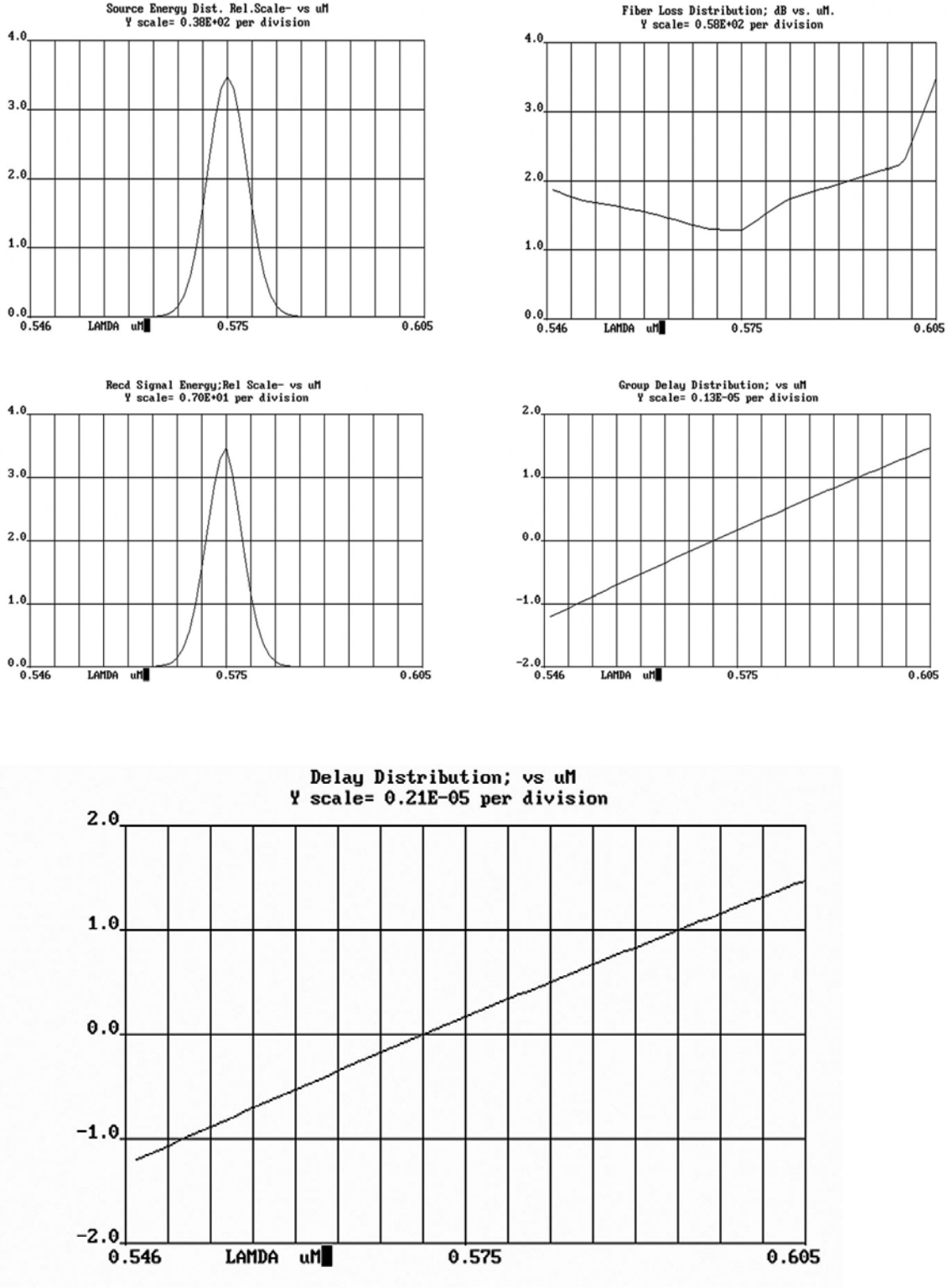

Fig 8.96 Source energy distribution, fiber loss distribution, received signal energy, group delay distribution and delay distribution.

8. 2 Comparison of simulation results with the experimental results

1. a) **Gimlett's experimental results[29]** (wave length= 1529nm, length=7.4 km and bit rate is 90 Mb/s)

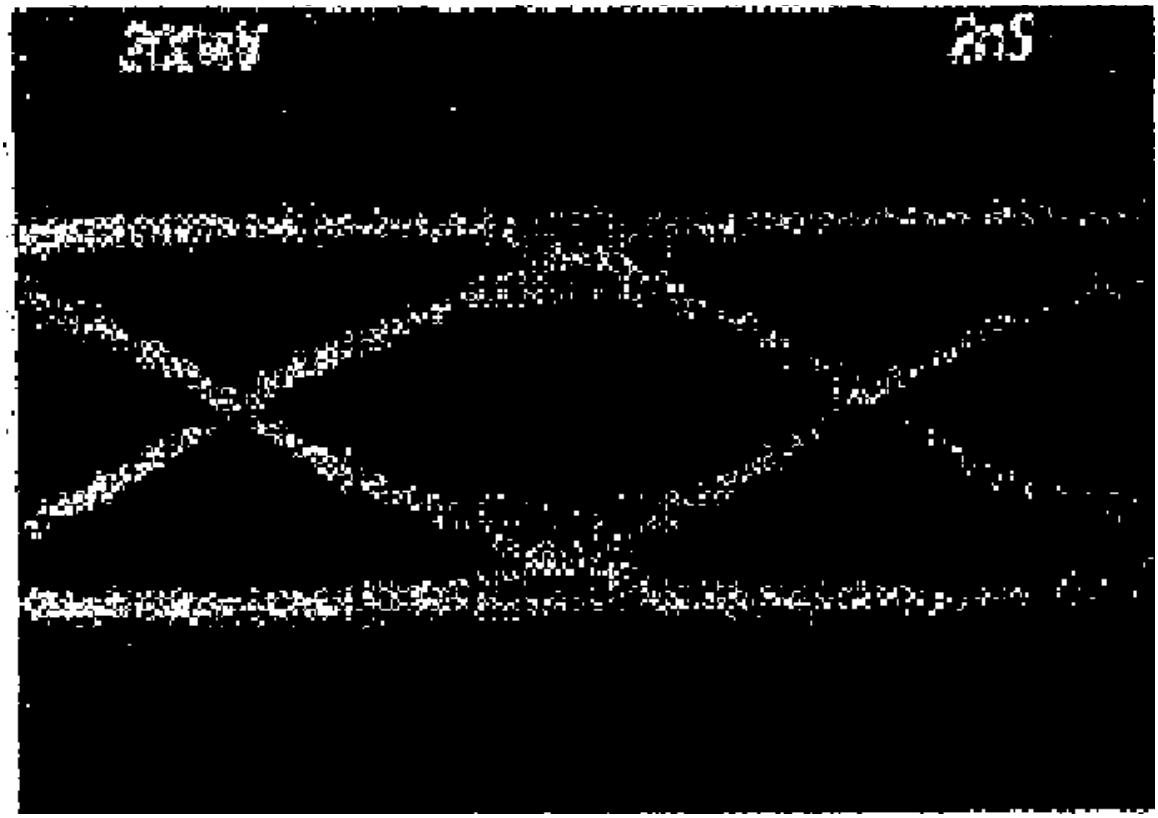

Fig 8.97 Gimlett's Experimental result for wave length 1529nm, fiber length 7.4 km and the bit rate 90 Mb/s

Horizontal Computation		Vertical Computation	
Horizontal eye opening	= 74mm	Vertical eye opening	= 26 mm
Total span of the pulse	= 83 mm	Noise(top)	=12.5mm
Ratio	= 74/83	Noise (bottom)	= 14mm
	=0.89	Total noise	= 26.5 mm
		Eye Opening ratio	= 26/52.5 = 0.495

1 b) Eye diagram obtained using modified FS* model (wave length= 1529nm, length=7.4 km and bit rate is 90 Mb/s)

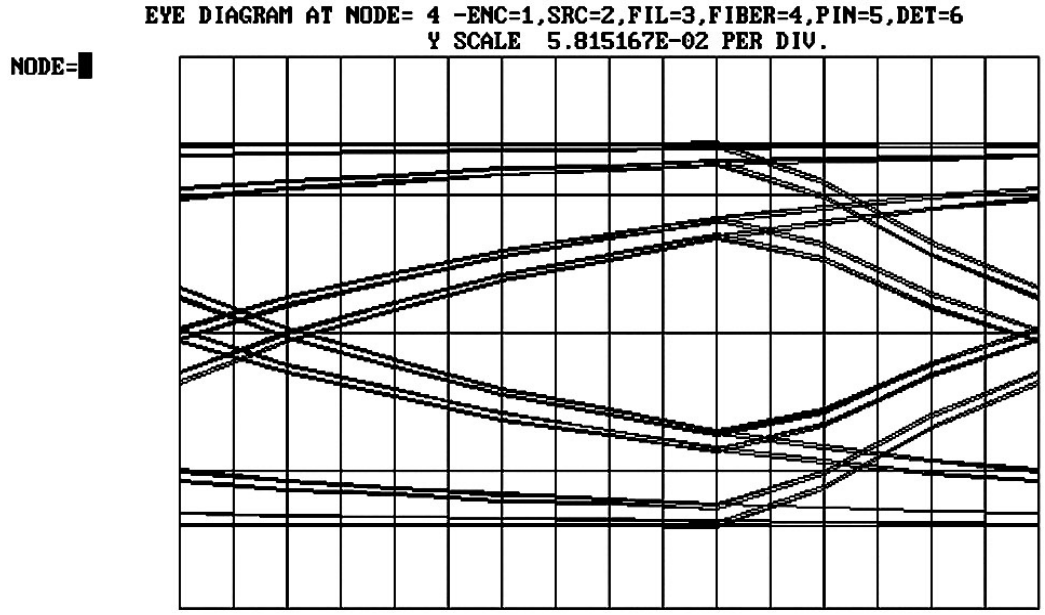

Fig 8.98 Simulation result for wave length 1529nm, fiber length 7.4 km and the bit rate 90 Mb/s

Horizontal Computation		Vertical Computation	
Horizontal eye opening	= 100 mm	Vertical eye opening	= 25 mm
Total span of the pulse	= 121 mm	Noise(top)	=13 mm
Ratio	= 100/121	Noise (bottom)	=12 mm
	=0.83	Total noise	= 25 mm
		Eye opening ratio	= 25/50=0.5

Results of 1 a) and 1 b) reveal that the experimental results and the simulation results are matched.

2 a) Gimlett's experimental results[29] (wave length= 1281 nm, length=32 km and bit rate is 140 Mb/s)

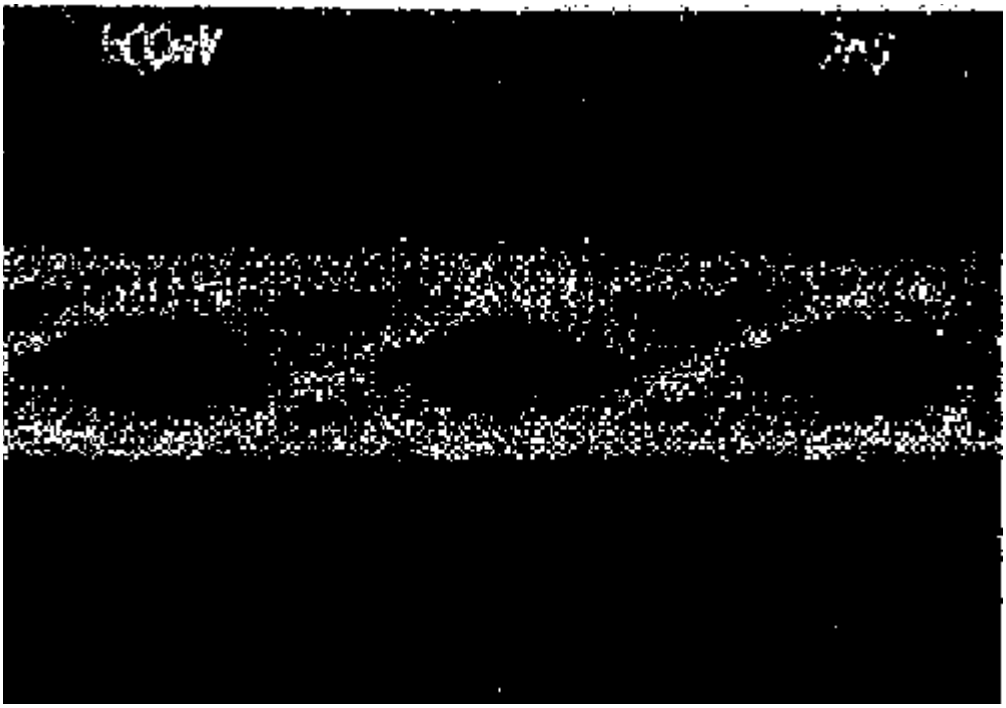

Fig 8.99 Gimlett's Experimental result for wave length 1281nm, length 32 km and the bit rate 140 Mb/s

Horizontal Computation		Vertical Computation	
Horizontal eye opening	= 36mm	Vertical eye opening	= 14mm
Total span of the pulse	= 46 mm	Noise(top)	=6 mm
Ratio	= 36/46	Noise (bottom)	=7 mm
	=0.78	Total noise	= 13 mm
		Eye opening ratio	= 14/27=0.52

2 b) Eye diagram obtained using modified FS* model

(wave length= 1281 nm, length=32 km and bit rate is 140 Mb/s)

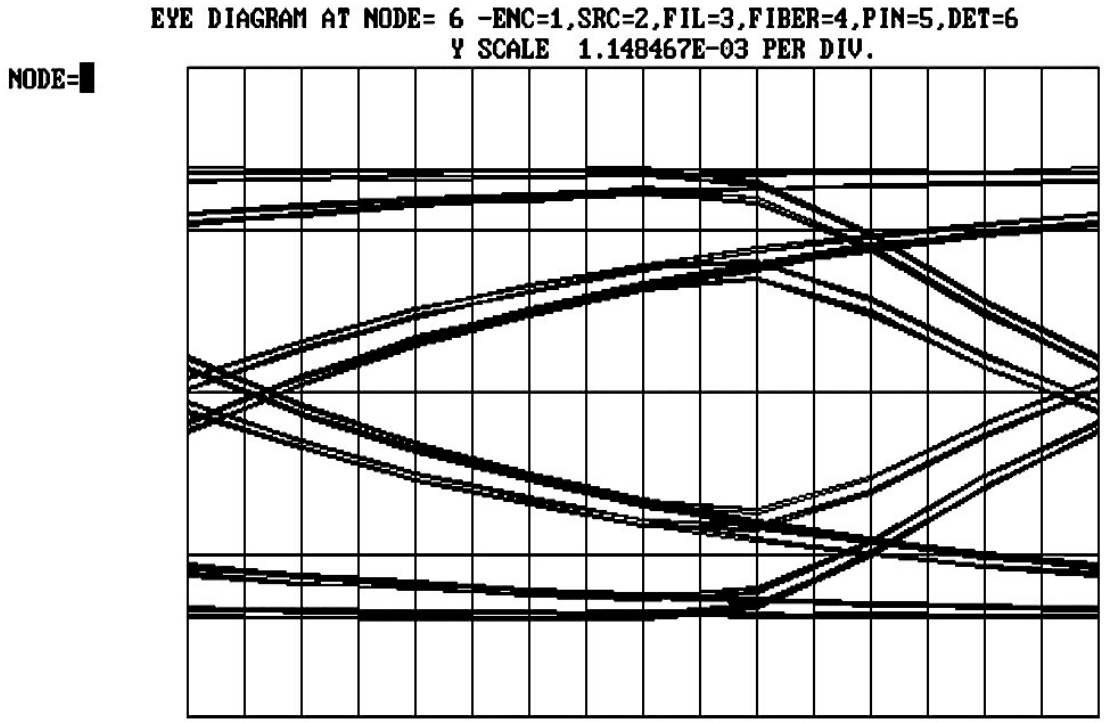

Fig 8.100 Simulation result for wave length 1281nm, length 32 km and the bit rate 140 Mb/s

Horizontal Computation		Vertical Computation	
Horizontal eye opening	= 101 mm	Vertical eye opening	= 31 mm
Total span of the pulse	= 130 mm	Noise(top)	=15.0 mm
Ratio	= 101/130	Noise (bottom)	=14.0 mm
	=0.776	Total noise	= 29.0 mm
		Eye opening ratio	= 31/60=0.516

Results of 2 a) and 2 b) reveal that the experimental results and the simulation results are matched.

3 a) **Linke's experimental results [30]** (wave length= 1550 nm, length=100 km and bit rate is 1 Gb/s)

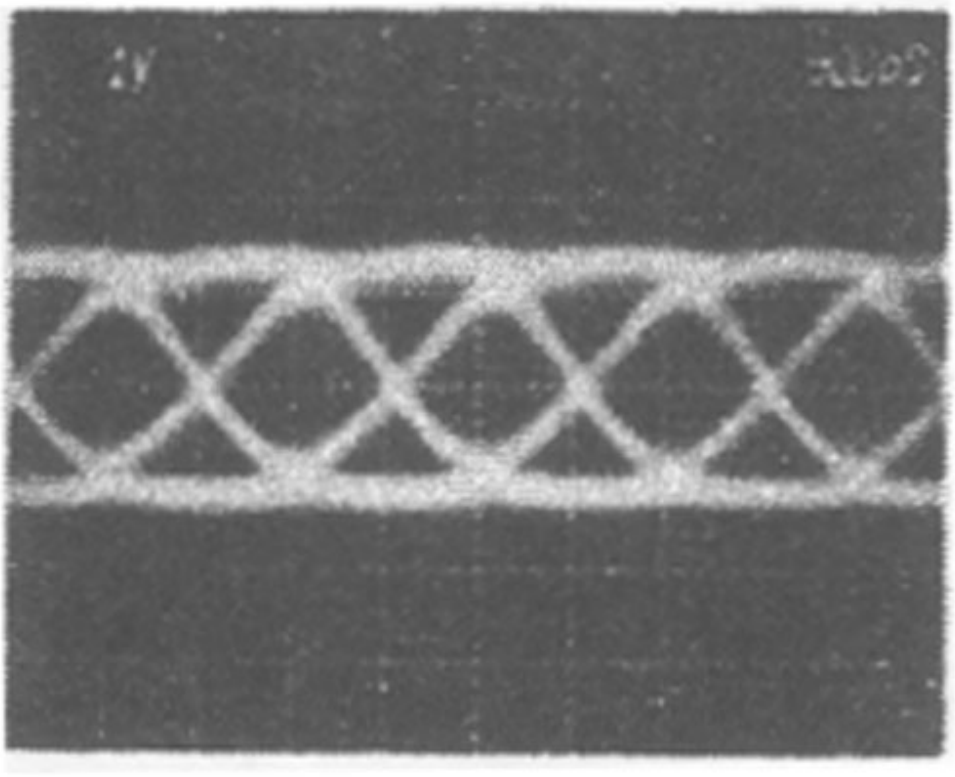

Fig 8.101 Linke's Experimental result for wave length 1550nm, length 100 km and the bit rate 1Gb/s

Horizontal Computation		Vertical Computation	
Horizontal eye opening	= 22 mm	Vertical eye opening	= 18 mm
Total span of the pulse	= 26 mm	Noise(top)	=8 mm
Ratio	= 22/26	Noise (bottom)	=7 mm
	=0.85*	Eye opening ratio	= 18/33=0.545

* Note : Experimental results include considerable amount of timing jitter that comes because of the poor timing recovery circuits. The simulation results do not have errors due to timing recovery.

3 b) Eye diagram obtained using modified FS* model (wave length= 1550 nm, length=100 km and bit rate is 1 Gb/s)

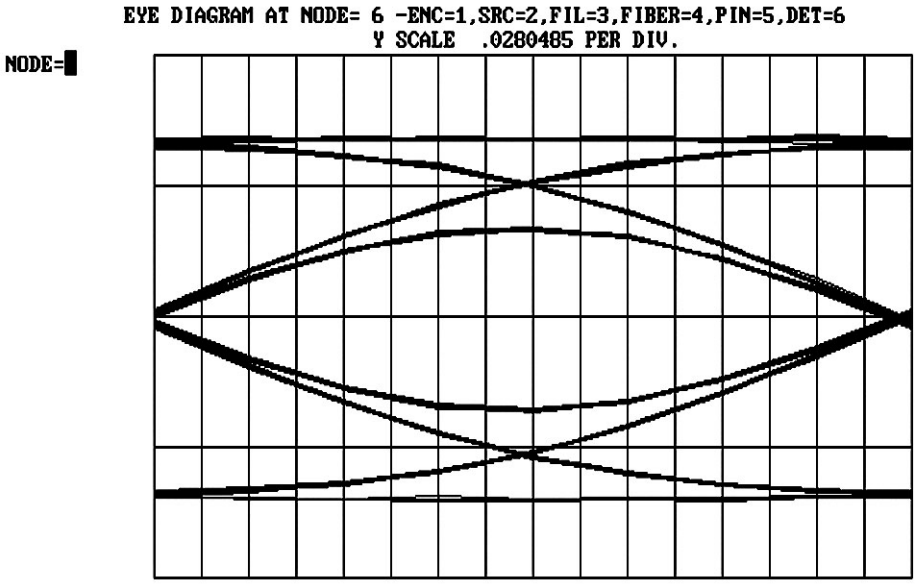

Fig 8.102 Simulation result for wave length 1550 nm, length 100 km and the bit rate 1 Gb/s

Horizontal Computation		Vertical Computation	
Horizontal eye opening	= 97 mm	Vertical eye opening	= 23 mm
Total span of the pulse	= 100 mm	Noise(top)	=12 mm
Ratio	= 97/100	Noise (bottom)	=11 mm
	=0.97	Total noise	= 23 mm
		Eye opening ratio	= 23/46=0.5

.

Results for vertical computation of 3 a) and b) reveal that the experimental results and the simulation results are matched.

3 c) **Linke's experimental results [30]**(wave length= 1550 nm, length=100 km and bit rate is 1.5 Gb/s)

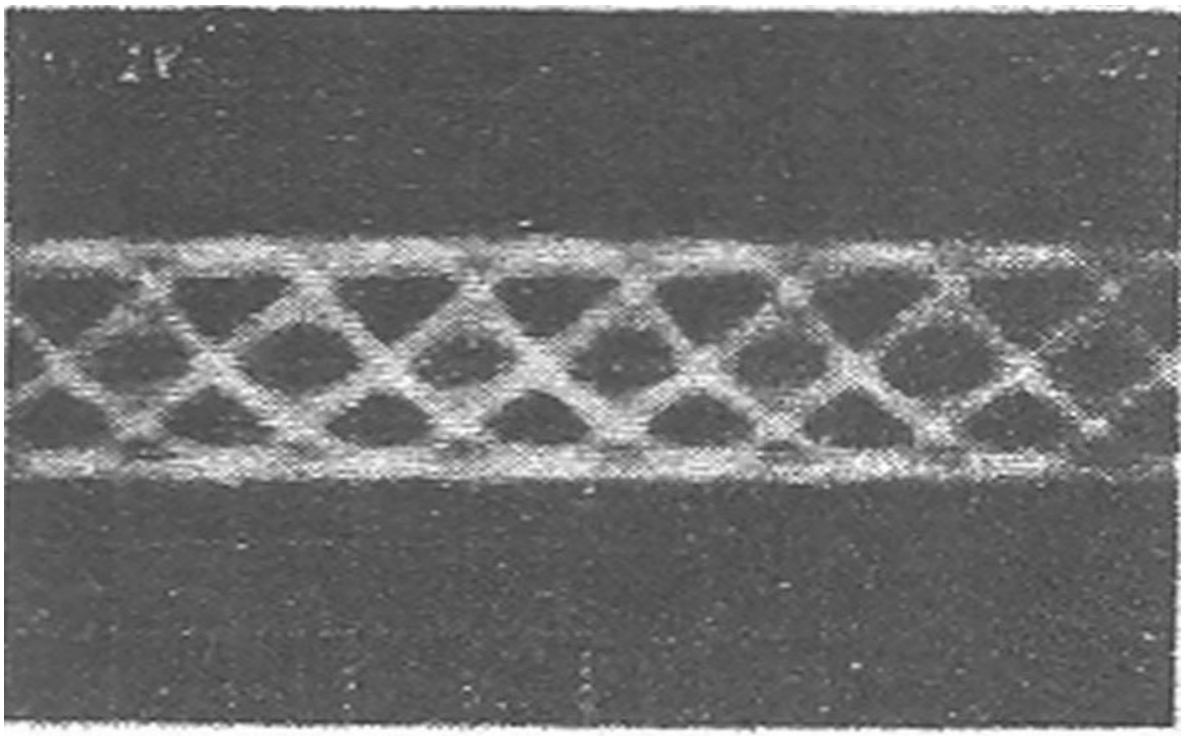

Fig 8.103 Experimental result for wave length 1550 nm, length 100 km and the bit rate 1.5 Gb/s

Horizontal Computation		Vertical Computation	
Horizontal eye opening	= 16 mm	Vertical eye opening	= 9mm
Total span of the pulse	= 23 mm	Noise(top)	=11 mm
Ratio	= 16/23	Noise (bottom)	=11 mm
	=0.69*	Eye opening ratio	= 22/31=0.36

* Note : Experimental results include considerable amount of timing jitter that comes because of the poor timing recovery circuits. The simulation results do not have errors due to timing recovery.

3 d) Eye diagram obtained using modified FS* model

(wave length= 1550 nm, length=100 km and bit rate is 1.5 Gb/s)

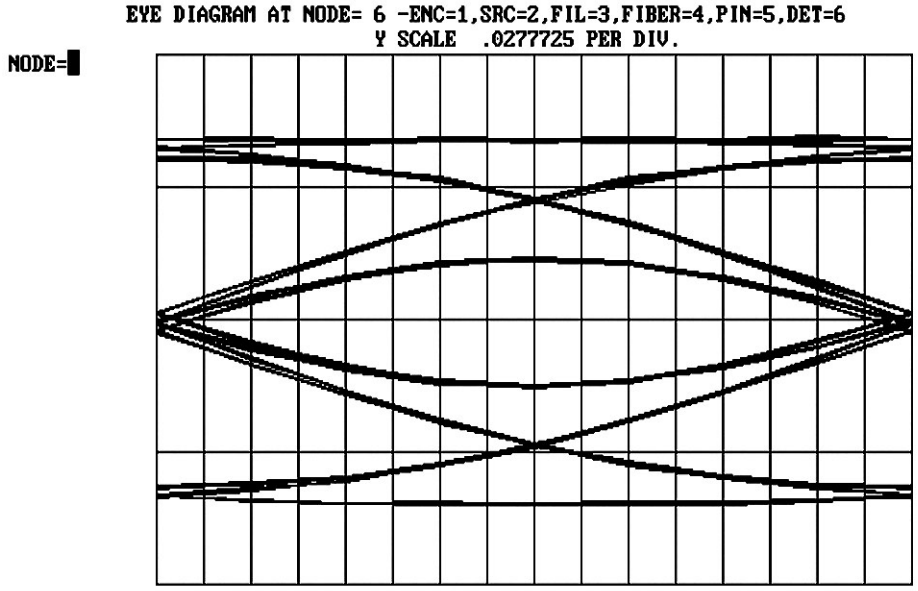

Fig 8.104 Simulation result for wave length 1550 nm, length 100 km and the bit rate 1.5 Gb/s

Horizontal Computation		Vertical Computation	
Horizontal eye opening	= 85 mm	Vertical eye opening	= 16 mm
Total span of the pulse	= 105 mm	Noise(top)	=16 mm
Ratio	= 85/105	Noise (bottom)	=17 mm
	=0.80	Total noise	= 33 mm
		Eye opening ratio	= 16/49=0.33

Results for vertical computation of 3c) and d) reveal that the experimental results and the simulation results are matched.

8. 3 Critical Examination of Results and SNR performance in dB.

8.3.1 Glass Fiber with Grade 1 fiber Components (wave length= 1.329mm) General Analysis

Fiber Length(km)	**Rate (Mb/s)**	Signal to Noise Ratio (SNR) in dB					
		Enc.	Src. (Laser)	Fil. **(Gr1)**	Fib. **(Gr1)**	Pin**.** **(Gr1)**	Det. **(Gr1)**
100	160	394	31.75	26.17	20.64	19.23	19.23
150	160	394	31.75	26.17	19.30	18.12	18.12
100	320	394	10.77	7.30	3.50	3.48	3.53
250	160	394	31.75	26.17	16.75	15.6**3**	15.63

Table 8.1

8.3.2 Effects of Noisy LED's (Wave length= 1.329mm) with different Lightwave System Components

Fiber Length(km)	Rate (Mb/s)	Signal to Noise Ratio (SNR) in dB					
		Enc.	Src. (LED)	Fil. **(**Gr 1)	Fib. (Gr 1)	Pin. (Gr 1)	Det. (Gr 1)
100	160	394	17.37	14.22	13.77	11.68	11.68
250	160	394	17.37	14.22	13.06	12.45	12.45
100	80	394	19.50	17.00	17.20	16.50	16.50
Fiber Length(km)	Rate (Mb/s)	Enc.	Src. (LED)	Fil. (Gr 3)	Fib (Gr 6)	Pin (Gr 4)	Det. (Gr 4)
100	160	394	16.24	15.03	12.67	12.34	12.31
250	160	394	11.00	8.74	5.86	5.75	5.46

Table 8.2

8.3.3 WDM Analysis (Comparison of Lasers sources and LED sources) with grade 1 lightwave system components. Wavelength is 1.329μm.

Fiber Length (km)	**Rate** (Mb/s)	**Signal to Noise Ratio (SNR) in dB**					
		SRC1 (Laser)			**SRC2 (Laser)**		
		Fib. (Gr1)	Pin. (Gr1)	Det. (Gr1)	Fib. (Gr1)	Pin. (Gr1)	Det. (Gr1)
100	160	32.40	28.47	27.19	32.38	27.96	28.11
200	160	32.37	28.32	28.44	32.45	28.17	28.51
400	160	32.16	27.58	26.93	32.53	29.52	29.03
Fiber Length (km)	**Rate** (Mb/s)	**Signal to Noise Ratio (SNR) in dB**					
		SRC1 (LED)			**SRC2 (LED)**		
100	160	16.24	15.03	12.67	12.34	12.31	12.51
200	160	16.21	15.03	11.14	10.83	10.83	10.91
400	160	16.20	15.01	10.23	10.06	9.60	9.81

Table 8.3

8.3.4 Erbium Doped Fiber and Cross-talk between WDM Channels.

Fiber Length (km)	**Rate** (Mb/s)	**Signal to Noise Ratio (SNR) in dB**							
		Channel number	Enc (Gr1)	Src. (laser)	Fil. (Gr1)	Fib. (Gr1)	Pin. (Gr1)	Det. (Gr1)	Leakage between waves
100	160	1	39	42.78	32.28	4.68	4.21	4.15	Too high 3%
		2	40	42.78	32.27	4.65	4.36	4.38	
100	160	1	39	42.78	32.28	26.16	24.72	24.40	Very Low 1%
		2	40	42.78	32.27	26.14	24.47	23.85	
100	160	1	39	42.76	32.28	26.53	24.71	24.32	0%
		2	40	42.78	32.27	26.52	24.55	24.01	

Table 8.4

8.3.5 Effects of Half-Width Pulses

Fiber Length (km)	**Rate** (Mb/s)	**Signal to Noise Ratio (SNR) in dB**						
		Enc.	Src.	Fil.	Fib.	Pin.	Det.	Comments (eye diagram)
100	160	394	394	51.39	63.59	42.25	42.25	Very Good
100	320	394	51.39	58.89	63.58	38.71	38.71	Very Good
200	320	394	394	58.94	49.43	36.89	34.56	O.K
100	640	394	394	70.59	32.69	29.46	27.86	Not good
100	1000	394	394	72.39	3.29	2.92	2.93	Unacceptable

Table 8.5

8.3.6 Effects of ¾ Wide Pulses **(**Every other factor remains the same as in half width case**)**

Fiber Length (km)	**Rate** (Mb/s)	**Signal to Noise Ratio (SNR) in dB**						
		Enc.	Src.	Fil.	Fib.	Pin.	Det.	Comments
100	160	394	394	46.05	58.09	38.55	38.35	Good
100	320	394	394	53.23	58.00	38.01	38.01	Good
100	640	394	394	63.67	23.45	21.77	20.97	Not Good
100	1000	394	394	72.14	1.108	0.879	0.776	Poor
200	160	394	394	46.05	58.27	38.18	38.18	Good
200	320	394	394	53.21	34.79	29.66	28.31	Not Good

Table 8.6

8.3.7 Effects of Quarter-Width Pulses **(**Every factor remains the same as in half width case)

Fiber Length (km)	**Rate** (Mb/s)	**Signal to Noise Ratio (SNR) in dB**						
		Enc.	Src.	Fil.	Fib.	Pin.	Det.	Comment
100	160	394	394	56.70	69.72	44.40	44.42	Good
100	320	394	394	63.79	68.58	42.37	42.37	Good
100	640	394	394	83.73	34.55	31.08	29.81	Too Narrow
100	1000	394	394	31.45	5.45	5.11	5.11	Poor
200	160	394	394	56.70	67.52	44.04	44.04	Good
200	320	394	394	63.79	50.46	38.94	36.94	Good

Table 8.7

8.3.8 Plastic Fiber Simulation

a) Plastic Fiber Simulation(Poly Methyl Meth-Acrylate, Wave length is 0.575μm)

Fiber Length (m)	**Rate** (Gb/s)	**Signal to Noise Ratio (SNR) in dB**						
		Enc. (Gr 1)	Src. (Laser)	Fil. (Gr 1)	Fib. (Gr 1)	Pin. (Gr 1)	Det. (Gr 1)	Comment
50	1.0	394	86.86	67.35	61.88	36.27	35.20	Good
50	1.25	394	63.93	52.52	51.30	35.20	33.22	Good
50	1.50	394	51.77	43.21	42.40	33.24	31.04	Good
50	1.75	394	43.55	36.21	35.29	30.38	28.73	Good
50	2.0	394	37.32	30.92	30.73	27.30	26.00	Not good
50	2.25	394	32.39	26.72	24.25	23.37	23.37	Not good
50	2.5	394	28.40	23.26	23.20	21.66	20.88	Not good
100	1.0	394	86.86	67.30	62.40	36.40	35.30	Good
100	1.25	394	63.93	52.52	51.45	35.39	33.37	Good
100	1.5	394	51.77	43.21	42.69	33.24	31.03	Good
100	1.75	394	43.55	36.21	36.02	30.37	28.68	Good
100	2.0	394	37.32	30.92	30.79	27.23	26.01	Not good
100	2.25	394	32.39	26.72	26.66	24.31	23.36	Not good
100	2.5	394	28.40	23.26	23.20	21.65	20.89	Not good

Table 8.8

b) Plastic Fiber Simulation with a half width pulse

(Poly Methyl Meth-Acrylate, Wave length is 0.575μm, perfect laser source)

Fiber Length (m)	Rate (Gb/s)	Signal to Noise Ratio (SNR) in dB						
		Encoder (Gr 1)	Source (Laser)	Filter (Gr 1)	Fiber (PMMA)	Pin. (Gr 1)	Det. (Gr 1)	Comments Gr1 is the best in current database
50	1.0	394	394	135	129.8	40.17	40.12	Good
50	1.25	394	394	135	132.0	40.17	40.12	Good
50	2.0	394	394	135	131.6	40.17	40.17	Good
100	1.0	394	394	135	129.9	40.38	40.23	Acceptable
100	2.0	394	394	135	129.9	40.38	40.23	Acceptable
100	2.5	394	394	135	128.1	40.38	40.23	Acceptable
100	5.0	394	394	135	124.9	40.40	40.20	Acceptable
500	1.0	394	394	135	126.1	40.39	40.28	Acceptable
500	5.0	394	394	135	139.9	40.29	40.26	Acceptable
500	10.0	394	394	135	146.0	40.39	40.28	Low Signal(LS) Acceptable
1000	1.0	394	394	135	124.5	40.56	40.18	(LS) Acceptable
1000	2.0	394	394	135	130.2	40.55	40.18	(LS) Acceptable
1000	5.0	394	394	135	62.50	40.14	40.23	(LS) Acceptable
5000*	1.0	394	394	135	71.80	40.60	40.53	Very low signal
5000*	5.0	394	394	135	85.57	40.58	39.98	Very low signal
5000*	10.0	394	394	135	64.29	40.57	40.57	Very low signal

Table 8.9

***** The optical signal strength gets low as the fiber length is increased. The noise level in the receiver and the sensitivity of the timing recovery systems will influence the SNRs and the actual bit-error-rate(BER) in the POFs. Generally it is necessary that the data is recovered before the integrated power due to all interference(s) start to approach a given percentage level of the received power. The exact value of the percentage ratio depends on the BER requirement from the system.

At very high rates the SNR at the output of 500m fiber is higher than at the end of the fiber. We suspect that this is because the fiber acts as a filter in its own right and it can smooth out the sharpness at the peak of the received optical energy. The SNR computations become somewhat unpredictable when the value is over 120dB.

8.3.9 a) Effects of Changing the Fiber Constant S_0 (Glass Fiber Simulation with a half width pulse (Worst Case), wave length is 1.329 μm)

Length /km	Rate (MB/s)	S_0	Signal to Noise Ratio (SNR) / dB						
			Enc. (Gr.1)	Src. (Laser)	Fil. (Gr.1)	Fib. (Gr. 1)	Pin (Gr.1)	Det. (Gr. 1)	S_0
100	320	0.12	394	394	61.19	27.05	24.36	24.36	Poor
100	320	0.10	394	394	61.19	42.38	34.55	32.64	Optimum
100	320	0.09	394	394	61.19	38.87	32.64	31.45	Very Good
100	320	0.11	394	394	61.19	32.24	28.05	28.05	Poor

Table 8.10

8.3.9 b) Effects of Changing the Fiber Constant S_0 (Plastic Fiber Simulation with a half width pulse (Worst Case)**,** Poly-Methyl Meth-Acrylate, Wave length is 0.575μm)

Length /km	Rate (GB/s)	S_0	Signal to Noise Ratio (SNR) in dB						
			Enc. (Gr.1)	Src. (Laser)	Fil. (Gr.1)	Fib. (Gr. 1)	Pin (Gr.1)	Det. (Gr. 1)	S_0
5	10.0	0.09	394	394	135	64.29	40.57	40.57	
5	10.0	0.12	394	394	135	62.58	40.51	40.51	
5	10.0	0.10	394	394	135	77.68	42.48	40.48	Optimum

Table 8.11

9.0 Conclusion

9.1 General conclusions

1. I have developed a glass and plastic fiber optic generalized simulation platform. For an example, this simulation package can be used to simulate inter wavelength cross talk and it is a new technique. Such a simulation has not been reported in literature.
2. For WDM system, high quality filter at the transmitter end is essential to improve the SNR in the eye diagram.
3. Use of best quality fiber and good filters at the receiver end is essential to improve the Signal to Noise Ratio (SNR).
4. Updating of vendor database from time to time is also essential.
5. Performance of fiber optic system can be greatly improved by using half width pulses. In the case of pulse width, half width pulse gives you the excellent results (SNR is 63 dB vs. 32dB for 100km, 160MB/s systems for TAT, submarine applications). Other improvements are presented in chapter 8.

9.2 Specific Contributions

The Specific contributions of this research are:

1. With this Fiber Optic simulation platform, we can explore almost all the limitation of plastic fiber optics.
2. Right now plastic fiber applications are limited to auto and airline industry. From these simulations I found that plastic optic fibers can be used for LANS as they exist in tall buildings and small campus networks. (SNR for 5km, 10GB/s system is 38.44dB.)
3. Half width pulse simulations applicable to glass fibers as well as plastic fibers. This methodology is generic.
4. We can adjust the composition of fiber (using S_0) to get best SNR depending on the application.
5. Noisy lasers do not materially degrade the SNR in the plastic optical fiber.

I have found that the Fiber Simulator used in the dissertation, is more generic and powerful than simulators such as OPNET for research and applications.

10.0 APPENDIX

10.1 Fast Fourier Transformation used in the simulation program [1]

We can represent a periodic signal as an infinite sum of sine wave components. Fourier transform is the most useful tool in the case of analysis of non-periodic signals. The Fourier transform is more general in placation than the Fourier series. The primary motivation for using the Fourier series or the Fourier transform is to obtain the spectrum of a given signal, which describes the frequency content of the signal. In effect, this transformation provides an alternative method of viewing the signal that is often more reveling than the original description of the signal as a function of time.

10.1.1 Fourier series

Let g_p (t) denote a periodic signal with period T_0. By using a Fourier series expansion of this signal, we are able to resolve the signal into an infinite sum of sine and cosine terms. This expansion may be expressed in the form:

$$g_p(t) = a_0 + 2 \sum_{n=1}^{\infty} \left[a_n \cos \left(\frac{2\Pi nt}{T_0} \right) + b_n \sin \left(\frac{2\Pi nt}{T_0} \right) \right] \qquad \text{A.1}$$

where the coefficients a_n and b_n represent the unknown amplitude of the cosine and sine terms, respectively . The quantity n / T_0 represents the n^{th} harmonic of the fundamental frequency $f_0 = 1/ T_0$. Each of the cosine and

sine functions in the equation 1 is called a basis function. These basis functions form an orthogonal set over the interval T_0 in that they satisfy the following set of relations:

$$\int_{-T_0/2}^{T_0/2} \cos\left(\frac{2\Pi mt}{T_0}\right) \cos\left(\frac{2\Pi nt}{T_0}\right) dt = \begin{cases} T_0/2 & m = n \\ 0 & m \neq n \end{cases} \qquad \text{A.2}$$

$$\int_{-T_0/2}^{T_0/2} \cos\left(\frac{2\Pi mt}{T_0}\right) \sin\left(\frac{2\Pi nt}{T_0}\right) dt = 0 \quad \text{for all m and n} \qquad \text{A.3}$$

$$\int_{-T_0/2}^{T_0/2} \sin\left(\frac{2\Pi mt}{T_0}\right) \sin\left(\frac{2\Pi nt}{T_0}\right) dt = \begin{cases} T_0/2 & m = n \\ 0 & m \neq n \end{cases} \qquad \text{A.4}$$

To determine the coefficients a_0 , we investigate both sides of the equation A.1 over a complete period. We thus find that a_0 is the mean value of the periodic signal $g_p(t)$ over one period, as shown by the time average:

$$a_0 = \frac{1}{T_0} \int_{-T_0/2}^{T_0/2} g_p(t)\, dt \qquad \text{A.5}$$

To determine the coefficient a_0 , we multiply the both sides of equations A.1 by the cosine function $\cos(2\Pi nt/ T_0)$ and integrate over the interval $-T_0/2$ to $T_0/2$. Then using equations A.2 and A.3, we find that

$$a_n = \frac{1}{T_0} \int_{-T_0/2}^{T_0/2} g_p(t) \cos\left(\frac{2\pi nt}{T_0}\right) dt \qquad n=1,2,\ldots \qquad \text{A.6}$$

Similarly we find that

$$b_n = \frac{1}{T_0} \int_{-T_0/2}^{T_0/2} g_p(t) \sin\left(\frac{2\pi nt}{T_0}\right) dt \qquad n=1,2,\ldots \qquad \text{A.7}$$

To apply the Fourier series representation of Equation A.1, it is sufficient that inside the interval $-T_0/2 \leq t \leq T_0/2$ the function $g_p(t)$ satisfies the following conditions:

1. The function $g_p(t)$ is single valued.

2. The function $g_p(t)$ has a finite number of discontinuities.

3. The function $g_p(t)$ has a finite number of maxima and minima.

4. The function $g_p(t)$ is absolutely integrable, that is,

$$\int_{-T_0/2}^{T_0/2} \left|g_p(t)\right| dt < \infty$$

where $g_p(t)$ is assumed to be complex valued.

10.1.2 Fast Fourier Transform (FFT) Algorithm

Fast Fourier Transform (FFT) algorithm was developed by R.C. Singleton in 1968 to compute a real and complex Fourier transform [32]. FFT algorithm is used in simulation programs since the algorithm is computationally efficient. For the simpler codes involving one real parameter (such as the real amplitude of an excitation signal and its variation with respect to time), the FFT of a real variable (as opposed to the FFT of a complex variable) will suffice. These simpler FFTs are invariably used for simpler codes such as AMI, Manchester, Block Codes etc. The computation is considerably faster than that for the complex FFTs and significantly faster than that for plain Fourier Transforms.

Consider the following:

$$\alpha_k = \sum_{j=0}^{n-1} x_j \exp(i\, 2\, \Pi jkln) \qquad \text{A.8}$$

for k=0,1,…,n-1 where $\{x_j\}$ and $\{\alpha_k\}$ are both complex valued and i is defined $\sqrt{-1}$. The complex Fourier transform can be expressed as a matrix multiplication:

$$\alpha = T\, x \qquad \text{A.9}$$

where T is an n x n matrix of complex exponential

$$t_{jk} = \exp(i2\, \Pi jk / n) \qquad \text{A.10}$$

The matrix T can be decomposed as

$$T=PF_mF_{m-1}\ldots F_2F_1 \qquad \text{A.11}$$

where F_i is the transform step corresponding to the factor n_i of n and P is a permutation matrix. The matrix F_i has only n_i non-zero elements in each row and column and is partitioned to n/n_i square sub matrices of dimension n_i. The matrices F_i are further factored to yield

$$F_i = R_i\, T_i \qquad \text{A.12}$$

where α_j is a diagonal matrix of rotation factors and T_i can be further partitioned into n / n_i identical square sub matrices (each is a matrix of complex Fourier transform of dimension n_i).

The permutation P is required because the transformed result is in digit reversed order, i.e. The Fourier coefficient α_j with

$$j=j_mn_{m-2}\ldots n_1 + j_2n_1 + j_1 \qquad \text{A.13}$$

is found in location

$$j'=j_1n_2\, n_3\ldots n_m + j_2n_3\, n_4 \ldots\, n_m + \ldots\, j_m \qquad \text{A.14}$$

The permutation can be performed in place by pair interchange if n is factored so that

$$n_i = n_{m-i}$$

for $i < n-i$. In this case, one can count j in natural order and j' in digit reverse order, then exchange α_j if $j < j'$.

The rotation factor R_i following the transform step T_i has diagonal elements

$$r = \exp \left\{ i\, 2 \frac{\Pi}{kk} (j \bmod k) \left[j \bmod \frac{kk}{k} \right] \right\}$$

for $j = 0,1,..., n-1$ where $k = n/ n_1 n_2 \ldots n_i$ and $kk = n_i k$ A.15

and the square brackets [ ] denotes the greatest integer function. The rotation factors multiplying each transform of dimension n_i within T_i have angles

$$0, \Theta, 2\Theta, \ldots (n_i - 1)\Theta$$

where Θ may differ from one transform to another.

10.1.2.1 Decomposition of a Complex Fourier Transform

The complex number $(a_k + i\, b_k)$ can be decomposed as

$$\begin{aligned} a_k + i\, b_k &= \sum_{j=0}^{n-1} (x_j + i\, y_j) \left[\cos(2\Pi j\, k/p) + i \sin(2\Pi j\, k/p)\right. \\ &= x_0 + \sum_{j=1}^{n-1} x_j \cos(2\Pi j\, k/p) \\ &\quad + i \left\{ y_0 + \sum_{j=1}^{n-1} y_j \cos(2\Pi j\, k/p) + \sum_{j=1}^{n-1} x_j \sin(2\Pi j\, k/p) \right\} \\ &= x_0 + \left\{ y_0 + \sum_{j=1}^{(p-1)/2} (x_j + x_{p-j}) \cos(2\Pi j\, k/p) + \sum_{j=1}^{(p-1)/2} (y_j - y_{p-j}) \sin(2\Pi j\, k/p) \right\} \\ &\quad + i \left\{ y_0 + \sum_{j=1}^{(p-1)/2} (y_i + y_{p-j}) \cos(2\Pi j\, k/p) + \sum_{j=1}^{(p-1)/2} (x_j - x_{p-j}) \sin(2\Pi j\, k/p) \right\} \end{aligned} \quad \text{A.16}$$

for k=0, 1,..., p-1.

The remaining Fourier coefficients can be expressed as

$$a_k = a_k^+ - a_k^-$$
$$a_{p-k} = a_k^+ - a_k^-$$
$$b_k = b_k^+ - b_k^-$$
$$b_{p-k} = b_k^+ - b_k^-$$

for k= 1,2,..., (p-1)/2, where

$$a_k^+ = x_0 + \sum_{j=1}^{(p-1)/2} (x_j + x_{p-j}) \cos(2\Pi j\, k/p)$$

$$a_k^- = \sum_{j=1}^{(p-1)/2} (y_j + y_{p-j}) \sin(2\Pi j\, k/p)$$

$$b_k^+ = y_0 + \sum_{j=1}^{(p-1)/2} (y_j + x_{p-j}) \cos(2\Pi j\, k/p)$$

$$b_k^- = \sum_{j=1}^{(p-1)/2} (x_j + x_{p-j}) \sin(2\Pi j\, k/p)$$

Altogether there are 2(p-1) terms in the series to sum, each with (p-1)/2 multiplications, for a total of $(p-1)^2$ real multiplications.

11.0 References

1. Syed V. Ahamed and Victor B. Lawrence
Design and Engineering of Intelligent Communication Systems Kluwer Academic Publishers, 1997.

2. Syed V. Ahamed
Intelligent Internet Knowledge Networks, John Wiley & Sons Inc., 2007.

3. T. Li
Advances in optical fiber communications: A historical perspective
IEEE journal on selected Areas in communications,
Vol. 3, pp 67-75, April 1983.

4. D. G. Duff
Computer-aided design of digital lightwave systems
IEEE journal on selected Areas in communication, Vol Sac-2, No.1, pp 171-185, January 1984

5. M. Fashano, A.L. Strodbeck
Communication systems simulation and analysis with SYSTID,
IEEE journal on selected Areas in communication, pp 8-28,
January 1984

6. A. Elrefai et. al.
Lightwave systems simulation in the time and frequency domain
IEEE journal on selected Areas in communication, Vol Sac-3, January 1984

7. A.A. Bergh
Optical sources for fiber transmission systems
Proceedings of the IEEE, pp 1240-1247, October 1980

8. E.E. Basch, T.G. Brown
Introduction to coherent optical fiber transmission
IEEE communication magazine, vol 23, No 5, pp 23-30, may 1985.

9. P.W. Shumate, J.L. Gimlet, M.Stern, M.B. Romeiser, N. K. Cheung, *Transmission of 140 Mbit/s signals over single-mode fiber using surface and edge emittion1.3 μm LED's,* Electronic letters, June 6, 1985

10. R.G. Smith *Photodetection for fiber transmission systems*, Proceedings of the IEEE, October 1980.

11. M. Fashamo, A. L. Strodtbeck *Communication Systems simulation and analysis with SYSTID* i.b.i.d. January 1984.

12. Rajiv Ramaswami , Kumar N. Sivaranjan *Optical Networks - A Practical Perspective,* Morgan Kaufman Publishers, 1998.

13. Djafar K. Mynbaev, Lowell L. Scheiner *Fiber - Optic Communications Technology*, Prentice Hall, 2001.

14. P.E. Green *The Future of Fiber Optic Computer Networks,* IEEE Computer, 24(9):78-79, September 1991.

15. S.V. Ahamed , V.B. Lawrence *A PC Based CAD environment for Fiber Optic Simulations*, IEEE, 1989

16. A.E. Elrefaie et al. *Computer Simulation of Digital Lightwave links,* IEEE Journal on selected areas in communications, January 1988.

17. R.L. Cruz, G.R. Hill, A.L. Kellner, R. Ramaswami and G.H. Sasaki *Special Issues on High Capacity Optical Transport Networks* IEEE JSAC, 1998.

18. G. R. Hill and P. Diemester *Special Issues on Photonic Networks in Europe*, IEEE Communication Magazine, Volume 35, pages 23-30, April 1997.

19. M.J. O'Mahony
Semi Conductor Laser Amplifier for Future Fiber Systems, IEEE/OSA Journal on Light wave technology, pages 531-544, April 1998.

20. R.I. Laming et al.
Fiber Gratings for Dispersion Compensation, FC 97 Technical Digest, pages 234-235, 1997.

21. K. Bala et al.
WDM Network Economics, Proceedings of National Fiber Optics Engineers Conference, Pages 163-174, 1996.

22. R. Cardwell et al.
WDM Network Economic Sensitivities, Proceedings of National Fiber Optics Engineers Conference, Pages 105-116, 1997.

23. G.B. Redifier
DWDM versus TDM in Metro and Long-Haul Applications
Proceedings of National Fiber Optics Engineers Conference, Pages 117-124, 1997.

24. S.Melle , M. Page
WDM Planning and Deployment Considerations for Optimizing Network evolution, Proceedings of National Fiber Optics Engineers Conference, Pages 137-147, 1997.

25. T. Tomaru, M. Ban
Secure Optical Communication Using Antisqueezing, Physics Rev. A pages 74-80, 2006

26. Paul Polishuk
Plastic Optical Fibers Branch Out, The Industrial Physicist, pages 42-50, May 2006

27. Gimlett J, Nim Cheung
Dispersion Penalty Analysis for LED/Single Mode Fiber Transmission Systems, Journal of Light wave Technology, vol 49, pages 1381-1392, 1986

28. Linke R.A
High Capacity Coherent Lightwave Systems, Journal of Light Wave Technology , vol 6, pages 1750-1769, 1988

29. Singleton R.C
An Algorithm for Computing the Mixed Radix Fast Fourier Transform
IEEE Transaction on Audio and Electroacoustics, vol 17, pages 93-103, 1986